

**SYNTHESIS OF FUNCTIONAL GROUP CONTAINING
CALIX[4]PYRROLES**

**Ph.D. Thesis by
Abdullah AYDOĞAN**

Department : Chemistry

Programme : Chemistry

OCTOBER 2010

**SYNTHESIS OF FUNCTIONAL GROUP CONTAINING
CALIX[4]PYRROLES**

**Ph.D. Thesis by
Abdullah AYDOĞAN
(509032200)**

Date of submission : 30 July 2010

Date of defence examination: 15 October 2010

Supervisor (Chairman) : Prof. Dr. Ahmet AKAR (ITU)
Members of the Examining Committee : Prof. Dr. E. Naciye TALINLI (ITU)
Prof. Dr. Ahmet GÜL (ITU)
Prof. Dr. Selim KÜSEFOĞLU (BU)
Prof. Dr. Mustafa BULUT (MU)

OCTOBER 2010

İSTANBUL TEKNİK ÜNİVERSİTESİ ★ FEN BİLİMLERİ ENSTİTÜSÜ

FONKSİYONEL GRUP İÇEREN KALİKS[4]PİROLLERİN SENTEZİ

**DOKTORA TEZİ
Abdullah AYDOĞAN
(509032200)**

Tezin Enstitüye Verildiği Tarih : 30 Temmuz 2010

Tezin Savunulduğu Tarih : 15 Ekim 2010

**Tez Danışmanı : Prof. Dr. Ahmet AKAR (İTÜ)
Diğer Jüri Üyeleri : Prof. Dr. E. Naciye TALINLI (İTÜ)
Prof. Dr. Ahmet GÜL (İTÜ)
Prof. Dr. Selim KÜSEFOĞLU (BÜ)
Prof. Dr. Mustafa BULUT (MÜ)**

EKİM 2010

FOREWORD

I would like to dedicate this dissertation to my dear lovely son Burak, my wife Hasibe and my parents who are the meanings of my life.

I would like to express my special thanks to my adviser Prof. Dr. Ahmet AKAR from very bottom of my heard. He is not only my adviser but also a person who illuminates my life with his wisdom. Another person that I must present my special thanks is Prof. Dr. Jonathan L. Sessler (The University of Texas at Austin, TX) who offered me the opportunity of working in his lab and recommendations about my study.

Finally, special thanks must be dedicated to my colleagues for their beloved friendships and valuable helps.

October 2010

Abdullah Aydođan

TABLE OF CONTENTS

	<u>Page</u>
FOREWORD	v
TABLE OF CONTENTS	vii
ABREVIATIONS	xi
LIST OF TABLES	xiii
LIST OF FIGURES	xv
SUMMARY	xxiii
ÖZET	xxv
1. INTRODUCTION	1
1.1 Anions	1
1.2 Goal of the Thesis	2
2. CALIX[4]PYRROLES	3
2.1 History of Calix[4]pyrroles	4
2.2 Anion Binding Properties of Calix[4]pyrroles	5
2.3 Theoretical Studies about Calix[4]pyrroles	7
2.4 Synthetic Methods for the Preparation of Calixpyrrole Core Macrocycles	9
2.4.1 One-pot condensation	9
2.4.1.1 Homo-condensation	9
2.4.1.2 Mixed condensation	11
2.4.2 [2+2] Condensation	12
2.4.3 [3+1] Condensation	13
2.5 Modification of Calix[4]pyrrole Core Macrocycle	14
2.5.1 Modification at C-rim	14
2.5.1.1 Lithiation of Octamethylcalix[4]pyrrole	14
2.5.1.2 Bromination of Calix[4]pyrrole	15
2.5.2 Modification at N-rim	16
2.5.2.1 N-alkylation of meso-octaethylcalix[4]pyrrole	16
2.5.2.2 Metallation of octamethylcalix[4]pyrrole	17
2.6 Calixpyrrole Derivatives	18
2.6.1 Derivatization at meso positions	18
2.6.2 Derivatization at C-rim	26
2.7 Applications of Calix[4]pyrrole Derivatives	27
2.7.1 Calix[4]pyrrole-based chromatographic separation systems	28
2.7.2 Calix[4]pyrrole based optical sensors	29
2.7.2.1 Anthracene linked calix[4]pyrroles	30
2.7.2.2 1,3-Indane-based calix[4]pyrroles	31
2.7.2.3 Tetra-TTF calix[4]pyrrole	34
2.7.2.4 Dipyrrolylquinoxaline strapped calix[4]pyrrole	35
2.7.2.5 Chromogenic units attached N-confused calix[4]pyrroles	37
2.7.3 Calix[4]pyrrole based electrochemical sensors	39
2.7.3.1 Ferrocene appended calix[4]pyrroles	39
2.7.3.2 Calix[4]pyrrole modified electrodes	41
2.8 Measurement Methods of Anion Binding Constants	43
2.8.1 Sample preparation	45
2.8.2 NMR spectroscopy	45
2.8.3 Optical methods	46

2.8.3.1 UV-vis spectroscopy	46
2.8.3.2 Fluorescence spectroscopy	47
2.8.4 Isothermal titration calorimetry	48
2.8.5 Job Plots	50
3. EXPERIMENTAL SECTOIN	53
3.1 General	53
3.2 Materials	53
3.3 ITC Titration Studies	53
3.4 Synthesis of Calix[4]pyrroles with Long Alkyl Chains	54
3.4.1 Monoester functional calix[4]pyrrole	54
3.4.2 Monoester octabromocalix[4]pyrrole	54
3.4.3 Monocarboxylic acid functionalized calix[4]pyrrole	55
3.4.4 Octabromomonocarboxylic acid functionalized calix[4]pyrrole	56
3.4.5 Hydrolysis of C-rim modified calix[4]pyrrole	56
3.4.6 Bromination of C-rim modified calix[4]pyrrole	57
3.4.7 Attaching long alkyl chains	57
3.4.7.1 Octadecyl <i>meso</i> -Calix[4]pyrrole carboxylate	57
3.4.7.2 Octadecyloctabromocalix[4]pyrrolyl carboxylate	58
3.4.7.3 Octadecyl 2- β -calix[4]pyrrolyl acetate	58
3.4.7.4 Octadecyl 2- β -heptabromocalix[4]pyrrolyl acetate	59
3.5 Tetrabenzocalix[4]pyrrole	60
3.5.1 Synthesis of 2,3-bis(phenylsulfonyl)bicyclo[2.2.2] oct-2-ene	60
3.5.2 Ethyl 4,7-dihydro-4,7-ethano-2 <i>H</i> -isoindole-1-carboxylate	60
3.5.3 Ethyl 4,7-dihydro-4,7-ethano-2 <i>H</i> -isoindole-1-carboxylic acid	60
3.5.4 Synthesis of 4,7-dihydro-4,7-diethano-2 <i>H</i> -isoindole	61
3.5.5 Synthesis of tetra-bicyclo[2.2.2]-oct-2-ene fused calix[4]pyrrole	61
3.5.6 Tetrabenzocalix[4]pyrrole	62
3.6 Synthesis of Polymers with Pendant Calix[4]pyrroles	63
3.6.1 Mono-hydroxy functionalized calix[4]pyrrole	63
3.6.2 Methacrylate functionalized calix[4]pyrrole	63
3.6.3 Homopolymer of methacryloyl functionalized calix[4]pyrrole	64
3.6.4 Copolymerization of monomer 3.18 and MMA	65
3.6.5 Polymerization of monomer 3.18, monomer 3.21 and MMA	65
3.6.6 Copolymerization of 3.21 and MMA	66
3.6.7 Copolymerization of 3.18 and 3.21	66
3.6.8 Synthesis of control pseudo dimers	67
3.6.8.1 Pseudo dimer I	67
3.6.8.2 3'-Hydroxyphenyl substituted calix[4]pyrrole	68
3.6.8.3 3-(2-Bromoethoxy)phenyl substituted calix[4]pyrrole	69
3.6.8.4 Pseudo dimer II	69
3.7 Synthesis of Dendrimeric Calix[4]pyrroles	70
3.7.1 But-3-yn-1-yl 4-oxopentanoate	70
3.7.2 Alkyn functionalized calixpyrrole	71
3.7.3 Tetra-1-bromopentyl-tetramethylcalix[4]pyrrole	71
3.7.4 Tetraazidocalix[4]pyrrole	72
3.7.5 4'-Hydroxyphenyl functional calix[4]pyrrole	72
3.7.6 Propargyl ether of 4'-hydroxyphenyl functional calix[4]pyrrole	73
3.7.7 Dendrimeric structures	73
3.7.7.1 Dendrimer I	73
3.7.7.2 Dendrimer II	74
3.7.7.3 Dendrimer III	75
3.7.7.4 Dendrimer IV	76
3.8 Supporting of Calix[4]pyrrole on Silica	77
3.8.1 Siloxane functionalized calix[4]pyrrole	77
3.8.2 Modification reactions	77

3.8.3 Synthesis of silica nanoparticles	78
4. RESULTS AND DISCUSSION.....	79
4.1 Calix[4]pyrroles with Long Alkyl Chains.....	81
4.1.1 Synthesis and crystal structures.....	82
4.1.2 Anion binding studies	94
4.1.3 Conclusion	97
4.2 Tetrabenzocalix[4]pyrrole	97
4.3 Polymers with Pendant Calix[4]pyrrole Units	103
4.3.1 Tetrabutylammonium fluoride and chloride extraction studies	104
4.3.1.1 Synthesis of methacryloyl functionalized calix[4]pyrrole	104
4.3.1.2 Synthesis of homopolymer and MMA copolymer	108
4.3.1.3 Extraction Studies.....	110
4.3.2 KCl and KF extraction studies	114
4.3.2.1 Synthesis of calix[4]pyrrole, crown ether, and MMA copolymers	115
4.3.2.2 Synthesis of pseudo dimers.....	117
4.3.2.3 Extraction studies	119
4.4 Dendrimeric Calix[4]pyrroles.....	126
4.4.1 Synthesis of starting materials	128
4.4.2 Synthesis of dendrimeric structures	134
4.5 Supporting of Calix[4]pyrrole on Silica	140
5. CONCLUSIONS	149
REFERENCES	151
APPENDICES	163
CURRICULUM VITAE.....	199

ABREVIATIONS

DCC	: Dicyclohexylcarbodiimide
DCM	: Dichloromethane
DFT	: Density functional theory
DMAP	: 4-Dimethylaminopyridine
DMF	: NN'-Dimethylformamide
DMSO	: Dimethylsulfoxide
DNP	: Dinitrophenyl
EI	: Emission intensity
FAB	: Fast atomic bombardment
FES	: Flame emission spectroscopy
FTIR	: Fourier transform infrared spectroscopy
GPC	: Gel permeation chromatography
HOBt	: Hydroxybenzotriazole
HPLC	: High performance liquid chromatography
HRMS	: High resolution mass spectrometry
ITC	: Isothermal titration calorimetry
LRMS	: Low resolution mass spectrometry
MMA	: Methylmethacrylate
MS	: Mass spectrometry
NBS	: N-Bromosuccinimide
NMR	: Nuclear magnetic resonance
PDI	: Polydispersity index
PMMA	: Poly(methylmethacrylate)
TBA	: Tetrabutylammonium
TBACl	: Tetrabutylammonium chloride
TBAF	: Tetrabutylammonium fluoride
TEOS	: Tetraethoxysilane
TFA	: Trifluoroacetic acid
THF	: Tetrahydrofuran
TLC	: Thin layer chromatography
TMS	: Tetramethyl silane
TTF	: Tetrathiafulvalene

LIST OF TABLES

	<u>Page</u>
Table 2.1 : Stability constants for 2.1 with different anionic substrates (n-Bu ₄ N ⁺ salts) at 25 °C.....	6
Table 2.2 : Energetics of binding of various anions to calix[4]pyrrole 2.1 in dry acetonitrile (<10 ppm H ₂ O) at 30 °C as determined by ITC.....	7
Table 2.3 : Stability constants for 2.1 and 2.3 with anionic substrates in CD ₂ Cl ₂ at 25 °C.....	19
Table 2.4 : Association constants for the formed between compounds 2.31 and 2.32 and fluoride, chloride, and dihydrogen phosphate anions.	20
Table 2.5 : Association constants for the compounds 2.1 , 2.5 , and 2.6 with anionic substrates as determined from ¹ H NMR spectroscopic titrations carried out in acetonitrile- <i>d</i> ₃ (0.5% v/v D ₂ O) at 22 °C.....	21
Table 2.6 : Affinity constants for sensors 2.41–2.43 and anionic substrates as determined in acetonitrile (0.01% v/v water) for sensors 2.41 and 2.42 and acetonitrile–water (96:4, pH 7.0 ± 0.1) for sensor 2.43	24
Table 2.7 : Association constants (<i>K</i> _a , M ⁻¹) of 2.1 and 2.50 for chloride anion (tetrabutylammonium salt) in CH ₃ CN (2% v/v H ₂ O) as obtained from ITC analysis and NMR titrations carried out in the corresponding deuterated solvents at 22 °C.....	26
Table 2.8 : Association constants and Fc/Fc ⁺ redox potentials for compound 2.80 with various anionic guest species.....	40
Table 2.9 : Association constants for compounds 2.78 and 2.79 in DCM and electrochemical parameters obtained from CV measurements.	41
Table 4.1 : Radii differences of typical isoelectronic cations and anions.	79
Table 4.2 : Structural specifications of the compounds prepared for long alkyl chain substituted calix[4]pyrroles.....	94
Table 4.3 : Chloride and acetate anion-binding affinities measured in 1,2-dichloroethane (as the tetrabutylammonium salts) using ITC. Estimated errors are less than 10%.....	95
Table 4.4 : Specifications of polymers 3.19 and 3.20	110
Table 4.5 : Summary of extraction data of 4.3 and 4.4	120
Table 4.6 : Absorbance values (top) and UV-vis spectra (bottom) of standardized dye solutions.	121
Table 4.7 : Emission intensities of standardized solutions of potassium tetrakis(2-thienyl)borate. ^a	123
Table 4.8 : Summary of KF extraction efficiencies. ^a	124
Table 4.9 : Some characterization data of starting materials.....	134
Table 4.10 : Specifications of modified silica gels.....	147

LIST OF FIGURES

	<u>Page</u>
Figure 2.1 : Different oxidation behaviors of 2.1 and 2.2	3
Figure 2.2 : Structures of meso-tetraspirocyclohexyl-calix[4]pyrrole and meso-octaethylcalix[4]pyrrole.	4
Figure 2.3 : Structure of sapphyrin.	5
Figure 2.4 : X-ray crystal structures of calix[4]pyrrole 2.1 in the absence and presence of an anion.	6
Figure 2.5 : Four limiting conformations of representative calix[4]pyrroles.	7
Figure 2.6 : Cone-like halide complexes of 2.1 energy-minimized in the gas phase.	8
Figure 2.7 : Schematic representation of a symmetric homo-condensation.	10
Figure 2.8 : Mixed homo-condensation products.	10
Figure 2.9 : View of the molecular structures of the ethanol adduct of the $\alpha\alpha\alpha\alpha$ isomer of 2.5 in the cone conformation (left) and the acetonitrile adduct of the $\alpha\alpha\alpha\beta$ isomer (methoxy) of 2.6 in the partial cone conformation (right).	11
Figure 2.10 : Synthesis of calix[4]pyrrole monoester 2.7 via mixed condensation.	11
Figure 2.11 : Synthesis of diester functional calix[4]pyrrole 2.8 via mixed condensation.	12
Figure 2.12 : [2+2] Condensation of dipyrromethane containing metalloporphyrin to obtain metalloporphyrin capped calix[4]pyrrole.	12
Figure 2.13 : Synthesis of a cryptand-like calix[4]pyrrole by [3+1] condensation.	13
Figure 2.14 : C-rim modification of octamethylcalix[4]pyrrole.	14
Figure 2.15 : Synthesis of alkynyl functionalized calix[4]pyrrole.	15
Figure 2.16 : Bromination of octamethylcalix[4]pyrrole.	15
Figure 2.17 : N-rim modified meso-octaethylcalix[4]pyrroles.	16
Figure 2.18 : Synthesis of tetrakisruthenocenecalix[4]pyrrole and its copper(II) complex.	17
Figure 2.19 : Structures of calix[4]pyrroles 2.1 , 2.3 , 2.21 , and 2.30	18
Figure 2.20 : Structures of meso-tetraspirocycloalkylcalix[4]pyrroles.	19
Figure 2.21 : Calix[4]pyrroles prepared from acetophenone derivatives and steroidal compounds.	21
Figure 2.22 : Calix[4]pyrroles derivatized at meso-positions.	22
Figure 2.23 : X-Ray crystal structure of the calix[4]pyrrole carboxylate dimer.	23
Figure 2.24 : Structures of second generation sensors 2.41-2.43 . These systems contain dansyl (2.41), lissamine-rhodamine B (2.42), and fluorescein (2.43) moieties as the fluorescent elements, respectively.	24
Figure 2.25 : Schematic representation of the multiple hydrogen bonding interactions that are believed to account for the high phosphate and pyrophosphate affinities observed for sensors 2.41 , 2.42 , and 2.43 respectively.	25
Figure 2.26 : Difunctional calix[4]pyrroles prepared via 2+2 condensation.	25
Figure 2.27 : Synthesis of octamethyloctafluorocalix[4]pyrrole.	26

Figure 2.28 :	Structure of methoxylated tetraspirocyclohexyl calix[4]pyrrole.	27
Figure 2.29 :	Sessler's calix[4]pyrrole modified silica gels.	28
Figure 2.30 :	Zhou's calix[4]pyrrole-modified silica gels.	29
Figure 2.31 :	HPLC separation of amino acids on gel 2.55 column.	29
Figure 2.32 :	Synthesis of anthracene linked calix[4]pyrroles.	30
Figure 2.33 :	Fluorescence spectra of calix[4]pyrrole 2.58 in CH ₂ Cl ₂ showing the changes induced upon the addition of increasing quantities of tetrabutylammonium fluoride.	31
Figure 2.34 :	Synthesis of 1,3-indane based calix[4]pyrroles.	32
Figure 2.35 :	Anion-hydrogen bonding results in partial charge transfer from electron-rich pyrrole to electron-poor indanylidene.	32
Figure 2.36 :	Titration of receptor 2.61 with fluoride and iodide anions.	33
Figure 2.37 :	Synthesis of receptors 2.68 and 2.69	33
Figure 2.38 :	Synthesis of tetra-TTF calix[4]pyrrole.	34
Figure 2.39 :	Absorption spectra of tetra-TTF calixpyrrole under different conditions.	35
Figure 2.40 :	Change in conformation associated with the addition/removal of chloride anion to a CH ₂ Cl ₂ solution of the tetra-TTF calix[4]pyrrole 2.70 and the electron-deficient guest 2.71 (represented by the distorted rectangle).	35
Figure 2.41 :	Synthesis of dipyrrolylquinoxaline strapped calix[4]pyrrole.	36
Figure 2.42 :	¹ H NMR spectral changes of receptor 2.75 seen upon titration with F ⁻ (as its tetrabutylammonium salt) in CD ₃ CN/DMSO- <i>d</i> ₆ (9:1 v/v).	37
Figure 2.43 :	Modification of N-confused calix[4]pyrroles.	38
Figure 2.44 :	Tautomer form of 2.77	38
Figure 2.45 :	Absorption spectra of 2.76 and 2.77 upon addition of fluoride and chloride anions. Insets: Solutions of 2.76 and 2.77 in the absence and presence of anionic species.	39
Figure 2.46 :	Ferrocene appended calix[4]pyrrole derivatives.	39
Figure 2.47 :	Schematic representation of the ferrocene CH and calixpyrrole NH hydrogen-bonding interactions of the receptor 2.80	40
Figure 2.48 :	Calix[4]pyrrole appended α -free pyrrole derivatives.	41
Figure 2.49 :	Electrochemical copolymerization of pyrrole and calix[4]pyrrole appended α -free pyrroles.	42
Figure 2.50 :	Basic schematic illustration of the ITC instrument.	49
Figure 2.51 :	Example of a Job plot.	51
Figure 3.1 :	Synthesis of calix[4]pyrrole based dendrimer I.	74
Figure 3.2 :	Synthesis of calixpyrrole based dendrimer II.	75
Figure 3.3 :	Synthesis of dendrimer III.	75
Figure 3.4 :	Synthesis of dendrimer IV.	76
Figure 4.1 :	Shapes of some anionic species.	80
Figure 4.2 :	Synthesis of n-alkyl ester calix[4]pyrroles over <i>meso</i> positions.	83
Figure 4.3 :	Synthesis of n-alkyl ester calix[4]pyrroles over β positions.	83
Figure 4.4 :	¹ H NMR (CDCl ₃) spectrum of the compound 3.1	84
Figure 4.5 :	View of the mono ester calix[4]pyrrole 3.1 in 3.1a and 3.1b showing the atom labeling scheme. Displacement ellipsoids are scaled to the 50% probability level.	85
Figure 4.6 :	¹ H NMR spectrum of 3.2 recorded in CD ₂ Cl ₂	86
Figure 4.7 :	¹ H NMR spectrum of 3.2 in CD ₂ Cl ₂ recorded at various temperatures. Temperatures: 1 = 27 °C, 2 = 0 °C, 3 = -20 °C, 4 = -40 °C, 5 = -60 °C.	87

Figure 4.8 :	View of 3.2 showing the atom labeling scheme. Displacement ellipsoids are scaled to the 50% probability level. The methyl hydrogen atoms have been removed for clarity. The ethyl group was disordered as shown.	88
Figure 4.9 :	¹ H NMR spectrum of 3.3 recorded in CDCl ₃	89
Figure 4.10 :	¹ H NMR spectrum of 3.4 recorded in CDCl ₃	89
Figure 4.11 :	¹ H NMR spectra of the C-rim modified heptabromocalix[4]pyrrole 3.6 (up) and 2.14 (down).	90
Figure 4.12 :	¹ H NMR spectrum of 3.7	91
Figure 4.13 :	¹ H NMR spectrum of 3.8 recorded in CDCl ₃	92
Figure 4.14 :	¹ H NMR spectrum of 3.9 recorded in CDCl ₃	93
Figure 4.15 :	Structure of 2-heptabromo-β-calix[4]pyrrolyl acetic acid.	93
Figure 4.16 :	¹ H NMR spectrum of 3.10 recorded in CDCl ₃	94
Figure 4.17 :	ITC titration curve obtained from the titration of compound 2.20	96
Figure 4.18 :	Synthesis of 3.11 and 3.12	98
Figure 4.19 :	¹ H NMR spectrum of 3.11 recorded in CDCl ₃ . Empty baselines were removed for clarity.	99
Figure 4.20 :	¹ H NMR spectrum of 3.12 recorded in CDCl ₃	99
Figure 4.21 :	¹ H NMR spectrum of 3.13 recorded in d ₆ -DMSO.	100
Figure 4.22 :	Saponification pathways of 3.12	101
Figure 4.23 :	¹ H NMR spectrum of 3.14 recorded in CDCl ₃	101
Figure 4.24 :	Synthesis of the compound 3.15 and tetrabenzocalix[4]pyrrole (3.16).	102
Figure 4.25 :	¹ H NMR spectra of 3.15 recorded in CDCl ₃	102
Figure 4.26 :	FAB Mass spectrum of 3.16	103
Figure 4.27 :	Synthesis of hydroxymethyl calix[4]pyrrole 3.17	105
Figure 4.28 :	¹ H NMR spectrum of 3.17 recorded in CDCl ₃	105
Figure 4.29 :	View of molecule 3.17 in the atom labeling scheme. Displacement ellipsoids are scaled to the 50% probability level (CCDC 668095).	106
Figure 4.30 :	Synthesis of methacryloyl substituted calix[4]pyrrole.	106
Figure 4.31 :	¹ H NMR spectrum of 3.18 recorded in CDCl ₃	107
Figure 4.32 :	View of 3.18 showing the atom labeling scheme. Displacement ellipsoids are scaled to the 50% probability level.	107
Figure 4.33 :	Structures of the homopolymer and MMA copolymer of 3.18	108
Figure 4.34 :	¹ H NMR spectrum of homopolymer 3.19 recorded in CD ₂ Cl ₂ . Solvent peaks were removed for clarity.	108
Figure 4.35 :	¹ H NMR spectrum of calixpyrrole-MMA copolymer 3.20 recorded in CDCl ₃	109
Figure 4.36 :	Thermogravigram of polymer 3.20 taken under an atmosphere of nitrogen at a scan rate = 10 °C/min.	110
Figure 4.37 :	¹ H NMR spectra of CD ₂ Cl ₂ solutions of (1) octamethylcalix[4]pyrrole (2.1), (2) 2.1 + TBAF (29 mM) and, (3) PMMA (125 mM, based on the repeat unit) + TBAF, (4) polymer 3.20 (effective concentration of the calix[4]pyrrole repeat unit = 6.5 mM), (5) polymer 3.20 + TBAF.	111
Figure 4.38 :	¹ H NMR spectra of CD ₂ Cl ₂ solutions of 3.20 and other control systems.	112
Figure 4.39 :	Structures of calixpyrrole, crown ether monomers and their polymers.	114
Figure 4.40 :	¹ H NMR spectrum of 3.22 recorded in CD ₂ Cl ₂	115
Figure 4.41 :	¹ H NMR spectrum of 3.23 recorded in CD ₂ Cl ₂	116
Figure 4.42 :	¹ H NMR spectrum of 3.24 recorded in CD ₂ Cl ₂	117
Figure 4.43 :	Structures of calix[4]pyrrole – crown ether pseudo dimmers.	117
Figure 4.44 :	Synthesis of pseudo dimer I (3.25).	118

Figure 4.45 :	^1H NMR spectrum of 3.25 recorded in CD_2Cl_2 .	118
Figure 4.46 :	Structures of dyes used in extraction studies.	119
Figure 4.47 :	Aqueous solutions (top layers) of 4.3 (left) and 4.4 (right).	119
Figure 4.48 :	UV-vis spectra of aqueous phases belonging to dye solutions 4.3 (left) and 4.4 (right) exposed to DCM solutions of copolymer 3.22 and the other control systems.	120
Figure 4.49 :	UV-vis spectra of standardized dye solutions of 4.3 (left) and 4.4 (right).	121
Figure 4.50 :	^{19}F NMR spectra of CD_2Cl_2 solutions of copolymers 3.22 (effective [calix[4]pyrrole] = 6.25 mM), 3.20 ([calix[4]pyrrole] = 6.50 mM), and 3.23 (no calix[4]pyrrole) after adding D_2O solutions of KF (3.4 M), shaking the tubes vigorously, and then separating the phases with the aid of centrifugation (10 min).	122
Figure 4.51 :	Structure of copolymer 3.24 .	123
Figure 4.52 :	Plot of NH peak intensities and shifts of copolymer 3.22 in CD_2Cl_2 as recorded by ^1H NMR spectroscopy after exposure to different aqueous KF concentrations.	125
Figure 4.53 :	Catalysed Huisgen 1,3-dipolar cycloaddition.	127
Figure 4.54 :	Proposed outline of species involved in the catalytic cycle.	128
Figure 4.55 :	Synthesis of But-3-yn-1-yl 4-oxopentanoate and its calix[4]pyrrole.	128
Figure 4.56 :	^1H NMR spectrum of 3.29 and 3.30 recorded in CDCl_3 . Solvent residual and water peaks were indicated by a *	129
Figure 4.57 :	FTIR spectra of 3.29 and 3.30 .	130
Figure 4.58 :	Synthesis of 3.33 and 3.34 .	131
Figure 4.59 :	^1H NMR spectrum of 3.33 (down) and 3.34 (up) recorded in CDCl_3 . Solvent residual peaks were indicated by *.	131
Figure 4.60 :	Synthesis of tetra(pentylbromide) (3.31) and tetraazido (3.32) calix[4]pyrroles.	132
Figure 4.61 :	^1H NMR spectra of 3.31 and 3.32 recorded in CDCl_3 .	133
Figure 4.62 :	FTIR spectra of tetrabromo and tetraazido substituted calix[4]pyrroles 3.31 and 3.32 .	133
Figure 4.63 :	Illustration of strategic pathway of obtaining dendrimeric calixpyrrole compounds.	134
Figure 4.64 :	Structure of calixpyrrole based dendrimers 3.35 and 3.36 .	135
Figure 4.65 :	^1H NMR spectrum of the compound 3.35 recorded in CDCl_3 .	135
Figure 4.66 :	FTIR spectra of calixpyrrole based dendrimer 3.35 and its starting materials.	136
Figure 4.67 :	^1H NMR spectrum of the compound 3.36 recorded in CDCl_3 .	136
Figure 4.68 :	FTIR spectra of calixpyrrole based dendrimer 3.36 and its starting materials.	137
Figure 4.69 :	Structures of tripodal dendrimers 3.37 and 3.38 .	137
Figure 4.70 :	^1H NMR spectrum of the compound 3.37 recorded in CDCl_3 .	138
Figure 4.71 :	FTIR spectra of calixpyrrole based dendrimer 3.37 and its starting materials.	139
Figure 4.72 :	^1H NMR spectrum of the compound 3.38 recorded in CDCl_3 .	139
Figure 4.73 :	FTIR spectra of calixpyrrole based dendrimer 3.38 and its starting materials.	140
Figure 4.74 :	Synthesis of siloxane functionalized calix[4]pyrrole 3.39 .	142
Figure 4.75 :	^1H NMR spectrum of siloxane functionalized calix[4]pyrrole 3.39 recorded in CDCl_3 .	142
Figure 4.76 :	View of 3.39 showing the atom labeling scheme.	143
Figure 4.77 :	FTIR spectra of modified and unmodified silica gel 60.	144
Figure 4.78 :	Thermogravigrams of modified and unmodified silica gel 60.	144
Figure 4.79 :	FTIR spectra of modified and unmodified fume silica.	145

Figure 4.80 :	Thermogravigrams of modified and unmodified fume silica.....	145
Figure 4.81 :	FTIR spectra of modified and unmodified SiO ₂ nanopowder.....	146
Figure 4.82 :	Thermogravigrams of modified and unmodified SiO ₂ nanopowders.	146
Figure 4.83 :	Synthesis of calix[4]pyrrole functional silica nanoparticles.	147
Figure 4.84 :	FTIR spectrum of calix[4]pyrrole functional silica nanoparticle.	147
Figure A.1 :	¹³ C NMR spectrum of 3.1 recorded in CDCl ₃	163
Figure A.2 :	¹³ C NMR spectrum of 3.2 recorded in CDCl ₃	164
Figure A.3 :	¹³ C NMR spectrum of 3.3 recorded in CDCl ₃	164
Figure A.4 :	¹³ C NMR spectrum of 3.4 recorded in CDCl ₃	165
Figure A.5 :	¹³ C NMR spectrum of 3.5 recorded in CDCl ₃	165
Figure A.6 :	¹³ C NMR spectrum of 3.6 recorded in CDCl ₃	166
Figure A.7 :	¹³ C NMR spectrum of 3.7 recorded in CDCl ₃	166
Figure A.8 :	¹³ C NMR spectrum of 3.9 recorded in CDCl ₃	167
Figure A.9 :	¹³ C NMR spectrum of 3.10 recorded in CDCl ₃	167
Figure A.10 :	¹ H NMR spectrum of 3.11 recorded in CDCl ₃	168
Figure A.11 :	¹³ C NMR spectrum of 3.13 recorded in DMSO- <i>d</i> ₆	168
Figure A.12 :	¹³ C NMR spectrum of 3.15 recorded in CDCl ₃	169
Figure A.13 :	¹³ C NMR spectrum of 3.17 recorded in CDCl ₃	169
Figure A.14 :	¹³ C NMR spectrum of 3.18 recorded in CDCl ₃	170
Figure A.15 :	¹³ C NMR spectrum of 3.25 recorded in CD ₂ Cl ₂	170
Figure A.16 :	¹ H NMR spectrum of 3.26 recorded in CDCl ₃	171
Figure A.17 :	¹³ C NMR spectrum of 3.26 recorded in CDCl ₃	172
Figure A.18 :	¹ H NMR spectrum of 3.27 recorded in CDCl ₃	173
Figure A.19 :	¹³ C NMR spectrum of 3.27 recorded in CDCl ₃	174
Figure A.20 :	¹ H NMR spectrum of 3.28 recorded in CDCl ₃	175
Figure A.21 :	¹³ C NMR spectrum of 3.28 recorded in CDCl ₃	176
Figure A.22 :	¹³ C NMR spectrum of 3.29 recorded in CDCl ₃	177
Figure A.23 :	¹³ C NMR spectrum of 3.31 recorded in CDCl ₃	177
Figure A.24 :	¹³ C NMR spectrum of 3.32 recorded in CDCl ₃	178
Figure A.25 :	¹³ C NMR spectrum of 3.33 recorded in CDCl ₃	178
Figure A.26 :	¹⁹ F NMR spectrum of fluorobenzene in CD ₂ Cl ₂	179
Figure A.27 :	¹ H NMR spectra of copolymer 3.22 in CD ₂ Cl ₂ recorded after exposure to different aqueous KF concentrations.	179
Figure A.28 :	NH peak intensity and shifts of copolymer 3.22 in CD ₂ Cl ₂ as recorded by ¹ H NMR spectroscopy after exposure to different aqueous KCl concentrations (mM).	180
Figure A.29 :	¹ H NMR spectra of copolymer 3.22 in CD ₂ Cl ₂ recorded after exposure to different aqueous KCl concentrations.	180
Figure A.30 :	Unit cell packing diagram for 3.1 . The view is approximately down the <i>a</i> axis. Molecules 3.1a are shown in ball-and-stick format while molecules 3.1b are in wireframe display format. Dashed lines are indicative of H-bonding interactions.	181
Figure A.31 :	Unit cell packing diagram for 3.2 . The view is approximately down the <i>a</i> axis.	182
Figure A.32 :	Unit cell packing diagram for 3.17 . The view is approximately down the <i>a</i> axis.	182
Figure A.33 :	Unit cell packing diagram for 3.8 . The view is approximately down the <i>b</i> axis.	183
Figure A.34 :	ITC titration curves obtained from the titration of compound 2.20 (0.4 mM) with chloride anion (8 mM) in CH ₂ Cl ₂ at 25 °C. The curve shows the fit of the experimental data to 1:1 binding profile.	183

Figure A.35 : ITC titration curves obtained from the titration of compound 2.20 (0.40 mM) with acetate anion (7.91 mM) in CH ₂ Cl ₂ at 25 °C. The curve shows the fit of the experimental data to 1:1 binding profile.	184
Figure A.36 : ITC titration curves obtained from the titration of compound 2.14 (0.4 mM) with chloride anion (9 mM) in CH ₂ Cl ₂ at 25 °C. The curve shows the fit of the experimental data to 1:1 binding profile.	184
Figure A.37 : ITC titration curves obtained from the titration of compound 2.14 (0.40 mM) with acetate anion (9.84 mM) in CH ₂ Cl ₂ at 25 °C. The curve shows the fit of the experimental data to 1:1 binding profile.	185
Figure A.38 : ITC titration curves obtained from the titration of compound 3.1 (0.412 mM) with chloride anion (9 mM) in CH ₂ Cl ₂ at 25 °C. The curve shows the fit of the experimental data to 1:1 binding profile.	185
Figure A.39 : ITC titration curves obtained from the titration of compound 3.1 (0.403 mM) with acetate anion (9.840 mM) in CH ₂ Cl ₂ at 25 °C. The curve shows the fit of the experimental data to 1:1 binding profile.	186
Figure A.40 : ITC titration curves obtained from the titration of compound 3.2 (0.4 mM) with chloride anion (9 mM) in CH ₂ Cl ₂ at 25 °C. The curve shows the fit of the experimental data to 1:1 binding profile.	186
Figure A.41 : ITC titration curves obtained from the titration of compound 3.2 (0.4 mM) with acetate anion (9 mM) in CH ₂ Cl ₂ at 25 °C. The curve shows the fit of the experimental data to 1:1 binding profile.	187
Figure A.42 : ITC titration curves obtained from the titration of compound 3.7 (0.4 mM) with chloride anion (8 mM) in CH ₂ Cl ₂ at 25 °C. The curve shows the fit of the experimental data to 1:1 binding profile.	187
Figure A.43 : ITC titration curves obtained from the titration of compound 3.7 (0.5 mM) with acetate anion (7.5 mM) in CH ₂ Cl ₂ at 25 °C. The curve shows the fit of the experimental data to 1:1 binding profile.	188
Figure A.44 : ITC titration curves obtained from the titration of compound 3.8 (0.5 mM) with chloride anion (9 mM) in CH ₂ Cl ₂ at 25 °C. The curve shows the fit of the experimental data to 1:1 binding profile.	188
Figure A.45 : ITC titration curves obtained from the titration of compound 3.6 (0.5 mM) with chloride anion (8 mM) in CH ₂ Cl ₂ at 25 °C. The curve shows the fit of the experimental data to 1:1 binding profile.	189
Figure A.46 : ITC titration curves obtained from the titration of compound 3.6 (0.5 mM) with acetate anion (9 mM) in CH ₂ Cl ₂ at 25 °C. The curve shows the fit of the experimental data to 1:1 binding profile.	189
Figure A.47 : ITC titration curves obtained from the titration of compound 3.9 (0.4 mM) with chloride anion (8 mM) in CH ₂ Cl ₂ at 25 °C. The curve shows the fit of the experimental data to 1:1 binding profile.	190

Figure A.48 : ITC titration curves obtained from the titration of compound 3.10 (0.5 mM) with chloride anion (9 mM) in CH ₂ Cl ₂ at 25 °C. The curve shows the fit of the experimental data to 1:1 binding profile.	190
Figure A.49 : Thermogravigram of a PMMA homopolymer taken under an atmosphere of nitrogen at a scan rate = 10 °C/min.	191
Figure A.50 : Thermogravigram of a polymer 3.19 taken under an atmosphere of nitrogen at a scan rate = 10 °C/min.	191
Figure A.51 : Thermogravigram of a PMMA homopolymer (control), after being exposed to TBAF as described in the text, taken under an atmosphere of nitrogen at a scan rate = 10 °C/min.	192
Figure A.52 : Thermogravigram of a PMMA homopolymer (control), after being exposed to TBACl as described in the text, taken under an atmosphere of nitrogen at a scan rate = 10 °C/min.	192
Figure A.53 : Thermogravigram of copolymer 3.20 , after being exposed to TBACl as described in the text, taken under an atmosphere of nitrogen at a scan rate = 10 °C/min.	193
Figure A.54 : Thermogravigram of copolymer 3.20 , after being exposed to TBAF as described in the text, taken under an atmosphere of nitrogen at a scan rate = 10 °C/min.	193
Figure A.55 : Thermogravigram of polymer 3.20 taken under an atmosphere of nitrogen at a scan rate = 10 °C/min after exposing to KCl.	194
Figure A.56 : Thermogravigram of polymer 3.20 taken under an atmosphere of nitrogen at a scan rate = 10 °C/min after exposing to KF.	194
Figure A.57 : Thermogravigram of polymer 3.22 taken under an atmosphere of nitrogen at a scan rate = 10 °C/min.	195
Figure A.58 : Thermogravigram of polymer 3.22 taken under an atmosphere of nitrogen at a scan rate = 10 °C/min after exposing to KCl.	195
Figure A.59 : Thermogravigram of polymer 3.22 taken under an atmosphere of nitrogen at a scan rate = 10 °C/min after exposing to KF.	196
Figure A.60 : Thermogravigram of polymer 3.23 taken under an atmosphere of nitrogen at a scan rate = 10 °C/min.	196
Figure A.61 : Thermogravigram of polymer 3.23 taken under an atmosphere of nitrogen at a scan rate = 10 °C/min after exposing to KCl.	197
Figure A.62 : Thermogravigram of polymer 3.23 taken under an atmosphere of nitrogen at a scan rate = 10 °C/min after exposing to KF.	197
Figure A.63 : Thermogravigram of polymer 3.24 taken under an atmosphere of nitrogen at a scan rate = 10 °C/min.	198
Figure A.64 : FAB-MS spectrum of 3.16	198

SYNTHESIS OF FUNCTIONAL GROUP CONTAINING CALIX[4]PYRROLES

SUMMARY

Calix[4]pyrroles, originally named “tetrapyrrole-acetone” and known as *meso*-octaalkylporphyrinogens, are macrocycles consisting of four pyrrole rings connected to each other from α or *meso*-like positions *via* sp^3 hybridized carbon atoms. Calix[4]pyrroles cannot be readily oxidized to porphyrin-like structures as in porphyrinogens. This is the main difference between calixpyrroles and porphyrin precursors. Consequently, all of pyrrole units of calix[4]pyrroles are in their N-H-bearing, neutral forms without electron delocalization within the macrocyclic system as a whole.

In this dissertation, the study was focused on five main parts as summarized below.

(i) Synthesis of calix[4]pyrroles with long alkyl chains: This part of the dissertation was motivated by a desire to obtain calixpyrroles that would not partition significantly into water when studied under potential interfacial conditions. As a first step, it was sought to develop long chain *n*-alkyl ester modified, *meso*- and β -pyrrole functionalized calix[4]pyrroles bearing either hydrogen or bromine atoms in the β -pyrrolic positions that would prove soluble in nonpolar organic solvents. It was also tested whether the modifications in question, including β -pyrrole bromination, affected the inherent anion recognition properties of the parent calix[4]pyrrole core. Towards this end, the new ester-substituted systems have been prepared and their chloride and acetate anion binding properties have been analyzed by ITC in 1,2-dichloroethane. Single crystal X-ray structures for some calix[4]pyrrole derivatives were also reported.

(ii) Tetrabenzocalix[4]pyrrole: The synthesis of the bicyclo[2.2.2]-oct-2-ene fused calix[4]pyrrole with deep “walls” was performed starting from a masked pyrrole derivative. Conversion reaction of this precursor to the corresponding calix[4]pyrrole derivative that contains benzo units fused to the β -positions of the pyrrole rings was also investigated.

(iii) Polymers with pendant calix[4]pyrrole units: In this part, the synthesis and characterization of polymers and copolymers containing calixpyrrole and methyl methacrylate (MMA) units were detailed. In addition, it was demonstrated that organic solutions of the calixpyrrole-functionalized copolymers are capable of extracting tetrabutylammonium chloride (TBACl) and tetrabutylammonium fluoride (TBAF) from aqueous solutions significantly better than octamethylcalix[4]pyrrole and poly(methyl methacrylate) (PMMA). Additionally, the synthesis, characterization, and extraction properties of mixed MMA copolymers containing pendant calix[4]pyrrole subunits known to bind halide anions in a 1:1 ratio in organic media and benzo-15-crown-5 subunits capable of forming 2:1 sandwich complexes with potassium cations have been investigated. It was thus expected that strong, potentially mutually enhancing, interactions would enable these polymeric materials to extract selectively potassium halide salts, such as KCl and KF, from aqueous solutions.

(iv) Dendrimeric calix[4]pyrroles: In this part of the thesis, design synthesis and characterization of four different calixpyrrole based dendrimeric compounds were

studied. The target dendrimeric structures have been prepared starting from simple organic compounds. Although dendrimeric calixpyrrole systems could be accessed via various synthetic strategies, so called “click chemistry” would provide an easy and convenient synthetic approach. Therefore, synthesis of final dendrimeric compounds has been carried out using click chemistry.

(v): Calix[4]pyrrole on silica solid supports: Literature reports show that the attachment of a calixpyrrole receptor on to a silica based solid support was achieved *via* using commercially available or specially designed aminopropyl functional silica gels. In this junction, a calixpyrrole compound having siloxane functional group seems to be a convenient idea for the modification of silica solid supports. Therefore, in this part of the dissertation, synthesis of siloxane functionalized calix[4]pyrrole and its use in modification of inorganic polymers such as silica gel, fume silica, and nano silica have been studied.

FONKSİYONEL GRUP İÇEREN KALIKS[4]PIROLLERİN SENTEZİ

ÖZET

Önceleri oktaalkilporfirinojenler olarak bilinen kaliks[4]piroller dört pirol halkasının birbirine α veya *meso*-pozisyonlarından sp^3 hibritleşmiş karbon atomları vasıtası ile bağlı olduğu makrosiklik bileşiklerdir. Kaliks[4]piroller porfirinojenler gibi direkt olarak porfirin ve benzeri yapılara okside olamazlar. Bu özellik porfirin öncü bileşikleriyle kaliks[4]piroller arasındaki ana farklılıktır. Sonuç olarak, halkadaki tüm piroller N-H atomlarına sahip doğal formlarındadır ve halkanın tamamında herhangi bir elektron delokalizasyonu yoktur.

Bu çalışmada beş ana kalikspirol araştırma alanı üzerinde incelemeler yapılmıştır.

(i) Uzun alkil zincirleri içeren kaliks[4]pirollerin sentezi: Çalışmanın bu kısmına temel teşkil eden ana fikir kalikspirolerin birbirine karışmayan çözücü sistemlerinde çalışıldığında bu bileşiklerin polar olan su fazına geçmemesinin sağlanmasıdır. Bu nedenle *meso*- ya da β -pozisyonlarına uzun n-alkil zincirlerinin ester köprüleri ile takıldığı ve β -pirolik pozisyonlarının serbest ya da bromlanmış olduğu kaliks[4]pirol bileşikleri hazırlandı ve bunların apolar çözücülerde çözünebilir olduğu gösterildi. Ayrıca sentezlenen bileşiklerin anyon bağlama özellikleri ITC ile 1,2-dikloroetan içerisinde incelendi. Ayrıca sentezlenen bazı bileşiklerin X-ray kristal yapıları da aydınlatıldı.

(ii) Tetrabenzokaliks[4]pirol: Bu bölümde bisiklo[2.2.2]-oct-2-ene üniteleri içeren ve derin bir kaviteye sahip kaliks[4]pirol bileşiği bir maskelenmiş pirol türevinden çıkılarak sentezlenmiştir. Ayrıca bu kalikspirolün tetrabenzokaliks[4]pirole dönüşürülme reaksiyonu incelenmiştir.

(iii) Pendan kaliks[4]pirol üniteleri içeren polimerlerin sentezi: Araştırmanın bu kısmında metakrilat fonksiyonlandırılmış kaliks[4]pirol bileşiğinin sentezi ve bu bileşiğin homopolimeri ve MMA kopolimeri sentezlenmiştir. Ayrıca kaliks[4]pirol-MMA kopolimerinin organik çözücülerinin TBAF ve TBACl tuzlarını sulu çözümlerden oktametilikaliks[4]pirol ve PMMA'ya göre çok daha iyi ekstrakte edebildiği gösterilmiştir. Ayrıca kaliks[4]pirol, benz-15-crown-5 ve MMA monomerlerinin kopolimerleri hazırlanmış ve bu anyon ve katyon reseptörü içeren polimerlerin sulu çözümlerden KCl ve KF'ü anyon ve katyonu ile birlikte seçici olarak ekstrakte edebildiği gösterilmiştir.

(iv) Dendrimerik kaliks[4]piroller: Çalışmanın bu kısmında; dört farklı kalikspirol içeren dendrimerik bileşiğin sentez ve karakterizasyonu çalışılmıştır. Hedef dendrimerik bileşikler basit organik bileşiklerden yola çıkılarak sentezlenmiştir. Her ne kadar hedef dendrimerik sistemlere çeşitli sentetik stratejiler kullanılarak ulaşılması mümkünse de, bu bileşikler "click" kimyası olarak adlandırılan ve azidlerle alkinler arasında Huisgen 1,3-dipolar siklokatılma reaksiyonuna dayanan yöntem temel alınarak sentezlenmiştir.

(v) Katı desteklere kaliks[4]pirol bağlanması: Özellikle kalikspirol kimyasında; katı destek malzemeleri modifiye edilmek istendiğinde öncelikle katı yüzeyin aminopropil ile fonksiyonlandırılmış olması gerekmektedir. Bu noktada, siloksan fonksiyonlandırılmış kalikspirol bileşikleriyle herhangi bir katı yüzeyin

fonksiyonlandırılabilmesi için önemli bir fikir olarak öne çıkmaktadır. Bu nedenle, çalışmanın bu kısmında, siloksan fonksiyonlu kaliks[4]pirol bileşiğinin sentezlenmesi ve bu bileşik vasıtası ile çeşitli silika jel yüzeylerinin fonksiyonlandırılması incelenmiştir. Ayrıca yine bu çıkış bileşiği kullanılarak nano silika partiküllerinin sentezi gerçekleştirilmiştir.

1. INTRODUCTION

1.1 Anions

Anions are ubiquitous in our environment. Chloride anions are present in large quantities in the oceans (1.94%), salt lakes (upto 34%), and underground salt reservoirs. Bromide present in sea water (65 ppm). Dead Sea (Israel) and underground brines contain large quantities of bromide. Nitrate and sulfate are present in our environment in the form of their alkaline salts. They are also present in acid rains. Carbonates are present in everywhere including biomineralised materials in their different salt forms.

Applications of ionic species are wide spread including cation and anion exchange resins. These materials are used to remove unwanted ionic species from drinking or industrial water sources. Main principle of working mechanism of these resins is exchanging unwanted ionic species during a filtration process with desired harmless ones. Unfortunately, up to date, no convenient method has been reported for the removal of an anion along with its counter cation at the same time. Several applications of ionic species in everyday life can be exemplified here when the importance of anions is being considered in environment, biology, medicine and nuclear industry. Therefore, anion receptors and recognition of anions became one of the important subjects of various research fields including supramolecular chemistry.

The anion recognition represents an emerging area of supramolecular chemistry whose impact in such disparate areas as biomedicine [1-3] and environmental chemistry [4-6] is becoming increasingly appreciated. In addition, anion receptors can be used as ion-selective receptors [7], phase-transfer catalysis, anion-selective optical sensors [8, 9]. Moreover, chromatographic separation systems have been generated by attaching receptors to an appropriate stationary phase [10]. These and other practical considerations have led to spectacular growth within the anion recognition field. However, the weak nature of most anion–receptor interactions, particularly in the case of neutral anion receptor systems, reflecting the relatively low charge density of most anions [11], makes the design of selective and effective receptors one of ongoing challenge. Thus, while a number of research groups have

designed elegant anion receptors, many of which have proven to be quite effective, there remains a need for simple, easy-to-make anion binding systems. In this context, the so-called calix[4]pyrroles have emerged as molecules of particular interest [10]. This is because the core structure may be accessed in one synthetic step and a large number of modifications are readily conceivable.

1.2 Goal of the Thesis

The synthesis of novel functional groups containing calix[4]pyrroles is very important in terms of the further derivatization. Towards this end, goals of this dissertation can be categorized as below.

- Enhancing the anion binding property of calix[4]pyrroles and procuring the solubility in nonpolar solvents.
- Development of new calix[4]pyrrole sensors and expanding the range of application areas (e.g., tuning the anion binding ability and extraction of ions) by appending various functional groups.
- A new approach for the synthesis of calix[4]pyrrole-modified inorganic polymers by increasing the number of applicable supporting systems (e.g., silica gel, fume silica, SiO₂ nanoparticles).
- Using methacrylate containing calix[4]pyrrole as a monomer for polymeric materials providing ion extraction.
- Taking the advantage of “click chemistry” to enlighten the pathway towards calix[4]pyrrole based dendrimers.

In this study we wish to prepare new functional groups containing calix[4]pyrroles and fulfill the anion binding studies if necessary. Target molecules of this study can be classified as below:

- Synthesis of long alkyl chain containing calix[4]pyrroles.
- Synthesis of tetrabenzocalix[4]pyrrole *via* a masked pyrrole derivative.
- Preparation of calix[4]pyrrole containing MMA copolymers starting from methacrylate functionalized calix[4]pyrrole.
- A new approach for preparation of calix[4]pyrrole-modified silica gel and silica nanoparticles by using a siloxane functionalized calixpyrrole derivative.
- Synthesis of calix[4]pyrrole based dendrimers starting from alkyne and azide functional calix[4]pyrroles.

2. CALIX[4]PYRROLES

Calix[4]pyrroles (e.g., **2.1**), originally named “tetrapyrrole-acetone” and known as *meso*-octaalkylporphyrinogens, are macrocycles consisting of four pyrrole rings connected to each other from α or *meso*-like positions via sp^3 hybridized carbon atoms. Calix[4]pyrroles cannot be readily oxidized to porphyrin-like structures (e.g., **2.2**) as in porphyrinogens (Figure 2.1). This is the main difference between calixpyrroles and porphyrin precursors. Consequently, all of pyrrole units of calix[4]pyrroles are in their N-H-bearing, neutral forms without electron delocalization within the macrocyclic system as a whole. Calix[4]pyrroles cannot be directly studied using optical techniques (e.g., UV-vis and fluorescence emission spectroscopy) because of the absence of electron delocalization that results no visible absorption or fluorescence emission bands.

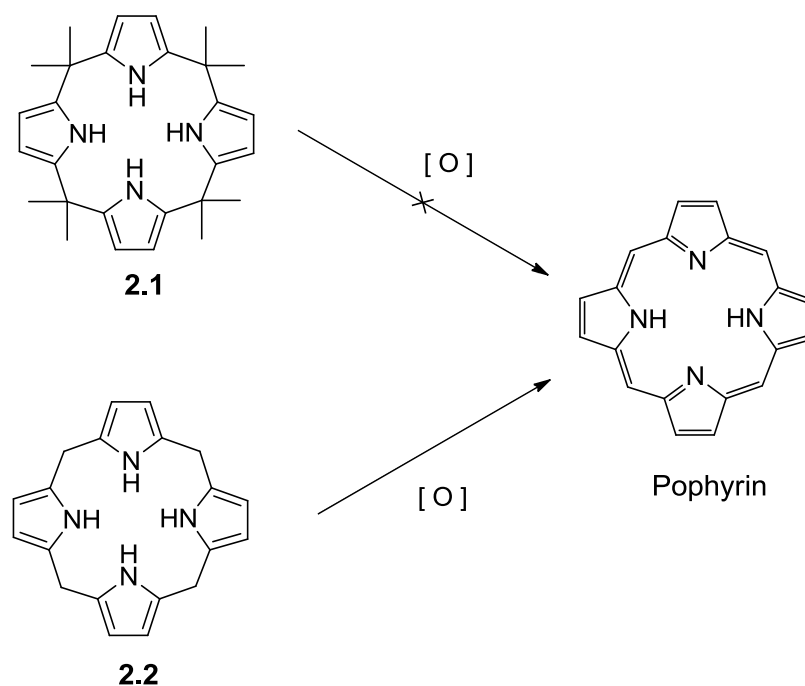


Figure 2.1 : Different oxidation behaviors of **2.1** and **2.2**.

NMR spectroscopic techniques provide meaningful characterization and study opportunity in this class of molecules. These techniques offer not only detailed structural elucidation, but also determination of host-guest interactions including anion binding. Different convenient estimation methods whose data supplied by

NMR spectroscopy provide to calculate anion binding affinities towards various anionic species (e.g., fluoride, chloride, phosphate etc.).

2.1 History of Calix[4]pyrroles

The first calixpyrrole compound synthesized by Baeyer in 1886 *via* condensation of pyrrole and acetone in the presence of hydrochloric acid. Thirty years later, Chelintzev and Toronov repeated the condensation of pyrrole and acetone and proposed a cyclic tetrameric structure for a calix[4]pyrrole which later proven to be correct [12]. These authors carried out several other reactions including an acid catalyzed condensation of pyrrole with methyl ethyl ketone, which afforded a single calix[4]pyrrole configurational isomer [13]. Additionally, methyl ethyl ketone and acetone were co-condensed with pyrrole forming a mixed meso-hexamethyldiethylcalix[4]pyrrole of unknown structure. Rothmund and Gage used methanesulfonic acid as a catalyst and obtained improved yields in 1950s [14]. In 1970s, Brown at al. reported a refined procedure that allowed them to obtain tetrspirocyclohexyl-calix[4]pyrrole **2.3** [15], a known compound reported earlier by Chelintzev, Toronov and Karmanov in 1916 [13] (Figure 2.2.).

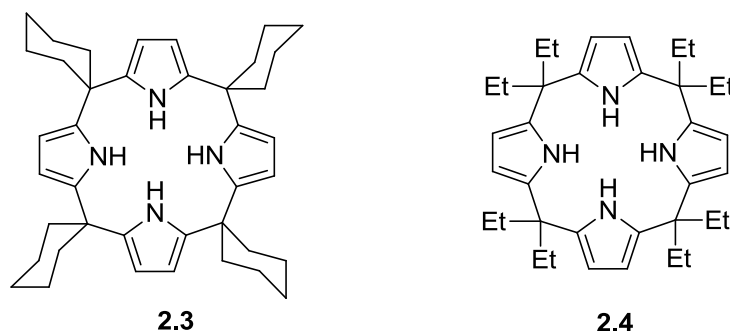


Figure 2.2 : Structures of meso-tetrspirocyclohexyl-calix[4]pyrrole and meso-octaethylcalix[4]pyrrole.

Calixpyrroles with functional groups (chloroalkyl or cyano) in the *meso*-positions were also reported by Lehn and co-workers.. Beside these important findings, calix[4]pyrroles were only studied irregularly over a century following their discovery most of which merely focused on the refined synthesis of these compounds and their meso-substituted derivatives. No significant studies have been observed during this period of time related to their applications. The situation has changed in 1990s by exploring the transition metal coordination chemistry of deprotonated calix[4]pyrroles, especially meso-octaethylcalix[4]pyrrole **2.4**, *via* an extensive study of Floriani and co-workers [16]. In their extensive study, Floriani has reported the various metal complexes of octamethylcalix[4]pyrrole.

In 1996, Sessler and co-workers discovered that this class of macrocycles can bind anions both in organic media and in solid state [17]. This finding gave the opportunity of exploring calix[4]pyrroles in novel application areas. Sessler and co-workers introduced the term “calix[4]pyrrole” to underscore the similarity of octaalkylporphyrinogens to calix[4]arenes in terms of the conformational behavior and not undergoing facile oxidation. Since that significant discovery, several novel calixpyrrole-based anion receptors have been prepared and studied by various research groups. These studies served to establish this branch of anion coordination chemistry. Several reviews and book chapters related to calixpyrrole chemistry have been reported, while further new reports about calixpyrrole based anion receptors are continuing to appear with an increasing regularity.

2.2 Anion Binding Properties of Calix[4]pyrroles

Using calix[4]pyrroles as an anion binding agent was first inspired from sapphyrin (Figure 2.3). Sapphyrin is a pentapyrrolic expanded porphyrin first synthesized by Woodward [18], is an excellent receptor for anions (particularly fluoride) when deprotonated. When a crystal structure of the sapphyrin-fluoride anion complex was obtained it was observed that NH protons of sapphyrin form hydrogen bonding with fluoride anion. This led Sessler and coworkers to seek another pyrrole based anion receptor with a question in mind whether neutral non-aromatic pyrrolic macrocycles would bind anions. Calix[4]pyrroles were addressed to answer this question because of their ease and cheap of synthesis in one synthetic step.

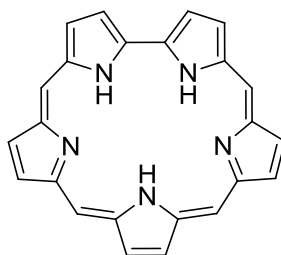


Figure 2.3 : Structure of sapphyrin.

Single crystal X-ray diffraction analysis of octamethylcalix[4]pyrrole **2.1** for both fluoride and chloride anions was carried out (Figure 2.4) [19]. These results revealed that calix[4]pyrrole changes its conformation when it was bound to an anion. While the compound **2.1** adopts a 1,3-alternate conformation wherein adjacent pyrrole rings oriented in opposite directions in the anion free state, it takes cone conformation in the presence of both fluoride and chloride anion. These crystal structures clearly show the cooperative hydrogen bonding interactions existing in the solid state between the four pyrrolic NH protons and the halide anions. While the

resulting structures are similar, in the case of the fluoride anion complex, the average of N...F distance is 2.767 Å, whereas the N...Cl distance is 3.303 Å in the corresponding chloride complex. Thus, fluoride anion appears to be more tightly bound in the solid state. In both cases, it is important to appreciate that the cone conformation, seen in the presence of anions, is very different from the 1,3-alternate form seen in their absence.

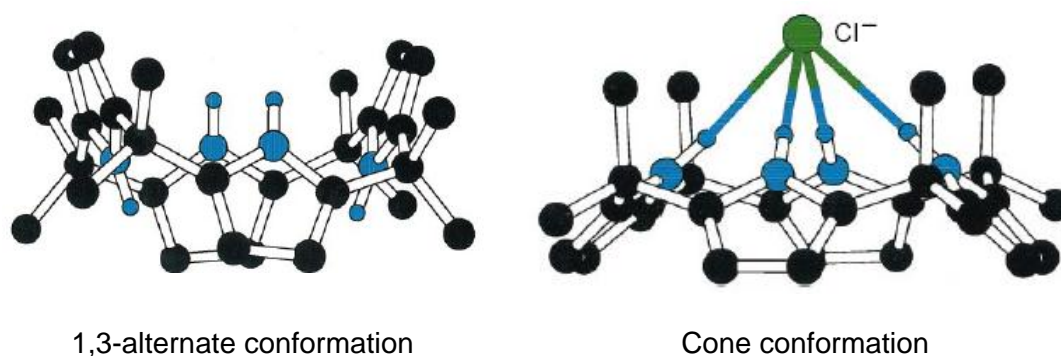


Figure 2.4 : X-ray crystal structures of calix[4]pyrrole **2.1** in the absence and presence of an anion.

The anion binding properties of calix[4]pyrrole **2.1** was carried out in deuterated methylene chloride (CD_2Cl_2) using $^1\text{H-NMR}$ titrations. In this method while keeping the concentration of host (in this case the host is octamethylcalix[4]pyrrole), the concentration of guest (in this case guests are fluoride and chloride salts of tetrabutylammonium) was increased gradually. Then changes in some specific peaks are observed.

Table 2.1 : Stability constants for **2.1** with different anionic substrates ($n\text{-Bu}_4\text{N}^+$ salts) at 25 °C.

	F^-	Cl^-	Br^-	I^-	H_2PO_4^-	HSO_4^-
CD_2Cl_2	17 170	350	10	<10	97	<10
CD_3CN	>10 000	>5 000			1 300	
$\text{DMSO-}d_6$	1 060	1 025				

A down field shift in the pyrrolic NH peak and an up field shift in the pyrrolic CH signal were observed in the case of **2.1**. Association constants were determined using the EQNMR computer software and revealed that calix[4]pyrrole **2.1** not only binds several anions in organic media but also displays a high selectivity against fluoride anion relative to other species studied (Table 2.1) [17, 20, 21].

Up to date, several efforts have been devoted to study anion binding properties of calix[4]pyrrole. These continuing efforts include a number of analyses carried out in various organic solvents using $^1\text{H-NMR}$ titration techniques under comparable

conditions such as different organic media. It can be concluded from Table 2.1 that calix[4]pyrrole **2.1** displays higher anion binding affinities in CD₂Cl₂ than CD₃CN and DMSO-*d*₆. The data in the table also leads to the conclusion that calix[4]pyrrole **2.1** shows lower anion binding affinity and loses the selectivity in the case of DMSO-*d*₆.

Other than ¹H-NMR titration technique to measure anion binding affinity of calix[4]pyrroles Schmidtchen applied isothermal titration calorimetry (ITC) to highlight further advantages and differences compared to ¹H-NMR titration in molecular recognition [22]. ITC measurement technique provides higher detection limits, increased dynamic range and greater reproducibility as compared to NMR spectroscopic methods. It also provides additional thermodynamic parameters (i.e. ΔH , $T\Delta S$, and ΔG) in one experiment which cannot be accessed by NMR spectroscopic techniques. Table 2.2 summarizes the results obtained by ITC measurement technique [22].

Table 2.2 : Energetics of binding of various anions to calix[4]pyrrole **2.1** in dry acetonitrile (<10 ppm H₂O) at 30 °C as determined by ITC.

	F ^{-a}	Cl ⁻	Br ⁻	H ₂ PO ₄ ⁻
ΔH [kcal mol ⁻¹]	-8.25	-8.81	-8.34	-11.60
ΔG [kcal mol ⁻¹]	-7.18	-6.90	-4.77	-5.79
$T\Delta S$ [kcal mol ⁻¹]	-1.05	-1.90	-3.56	-5.81
K_{ass} [M ⁻¹]	153 000	95 400	2 770	15 100

^a Fluoride anion was used in the form of [K-cryptand222]⁺ salt.

A brief inspection of table reveals that the association constants deduced from ITC experiments are higher than those inferred from the NMR titration studies.

2.3 Theoretical Studies about Calix[4]pyrroles

Theoretical studies about the conformational behaviors of calix[4]pyrroles predicted four different limiting structures. These conformational structures are: 1,3-alternate, 1,2-alternate, partial cone, and cone (Figure 2.5).

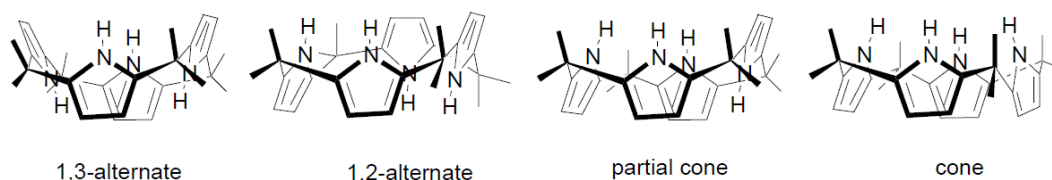


Figure 2.5 : Four limiting conformations of representative calix[4]pyrroles.

Monte Carlo simulations and energy minimizations (in the gas phase) of the compound **2.1** with anion complexes in a methylene chloride milieu were studied by Jorgensen [23]. 1,3-alternate conformation was the most stable state of **2.1** in the

absence of a halide anion, while the cone conformation was not stable under the conditions applied. On the other hand, cone conformation was the most stable state of **2.1** in the presence of halide anions among the various possible conformations (Figure 2.6). Solution phase simulations revealed that relative free energies of binding of chloride, bromide, and iodide with the compound **2.1** were in outstanding agreement with reported data. An exceptional result was observed in the case of the simulation of fluoride binding. In this case, the theoretical studies predicted higher free energy for fluoride anion binding. This difference was depicted to absence of trace water in theoretical calculations. Yet, commercial tetrabutylammonium fluoride contains trace amount of water and can never be used in a completely anhydrous form during experimental studies.

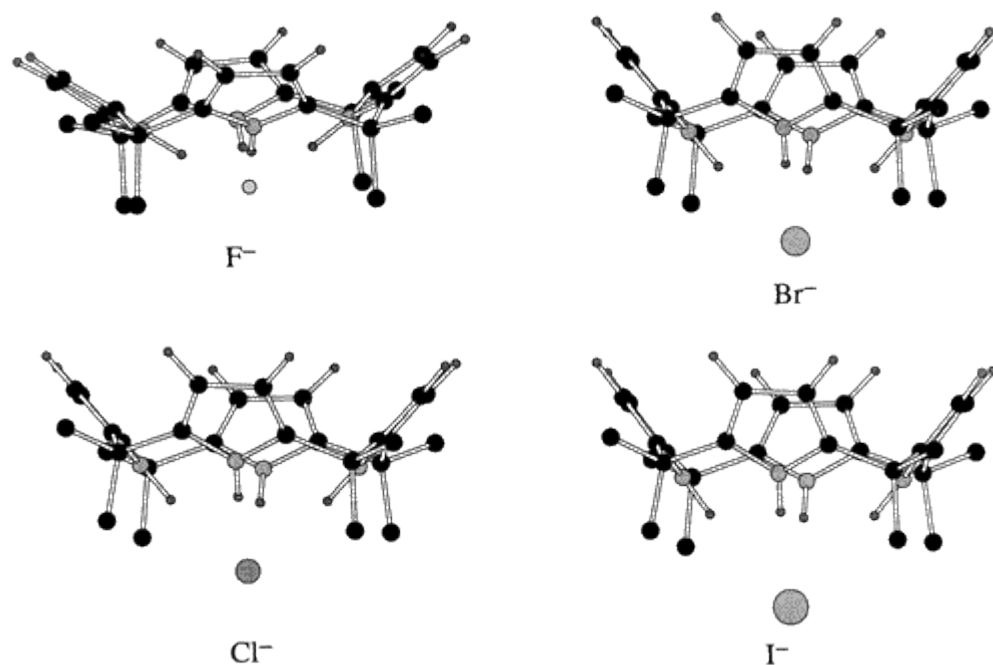


Figure 2.6 : Cone-like halide complexes of **2.1** energy-minimized in the gas phase.

Wu also studied the conformational preferences and fluoride and chloride anion binding properties of calix[4]pyrrole **2.1** by PM3 semiempirical method and density functional theory methods in the gas phase and in dichloromethane solution [24]. Several conclusions are summarized below.

- In agreement with experimental observations, the 1,3-alternate conformation is calculated as being most stable. The stability sequence is predicted to be 1,3-alternate > partial cone > 1,2-alternate > cone, either in the gas phase or in CH₂Cl₂ solution. The cone conformation, which is observed in the solid-state structure of the calix[4]pyrrole fluoride anion complex, is about 16.0 and 11.4 kcal/mol less stable in the gas phase and CH₂Cl₂ solution, respectively.

- Anion binding analysis reveals that the 1:1 calix[4]pyrrole fluoride binding mode with the cone conformation is more favorable than a possible 1:2 binding mode involving a 1,2-alternate conformation.
- A rough estimate of an average F·····H-N hydrogen bond strength in the cone structure resulted values of about 22 and 11 kcal/mol in the gas phase and in CH₂Cl₂ solution, respectively.

Analysis of the effect of meso substituents, specifically methyl and cyclohexyl groups, on the conformational and anion-binding properties revealed that the steric hindrance of these groups disfavors the cone conformer more than the 1,3-alternate conformer and that it is this difference that accounts for the experimental difference in anion affinity.

2.4 Synthetic Methods for the Preparation of Calixpyrrole Core Macrocycles

Three general methodologies can be used to synthesize calix[4]pyrroles. A one-pot [1+1+1+1] condensation, [2+2] condensation, and [3+1] condensation, where the digits refer to the number of pyrrole units in the reactants involved. One-pot synthesis is the most popular one for the preparation of simple calix[4]pyrroles.

2.4.1 One-pot condensation

As commonly used, a pyrrole and a ketone are condensed in a 1:1 ratio in the presence of an acid catalyst in the one-pot synthesis of calix[4]pyrroles. Hydrochloric acid, methanesulfonic acid, trifluoroacetic acid, and boron trifluoride diethyl etherate are the commonly used acid catalysts. Methanol, ethanol, acetonitrile, and dichloromethane are the favorite solvents for carrying out the reactions. Stoichiometric ratio of the different type of pyrroles and ketones determines whether the one-pot condensation is homo or mixed condensation.

2.4.1.1 Homo-condensation

The term homo-condensation is meant to define the reaction of a specific pyrrole with a specific ketone. Symmetry of the pyrrole or ketone components defines the type of the homo-condensation.

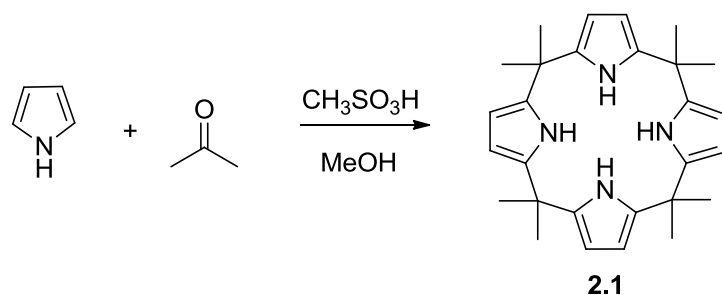


Figure 2.7 : Schematic representation of a symmetric homo-condensation.

If a symmetric pyrrole and a symmetric ketone were reacted to produce a calixpyrrole this type of condensation called symmetric homo-condensation. This type of homo-condensation generally produces only one easy-to-separate major product in good yield. A typical example of symmetric homo-condensation is the synthesis of **2.1** via the condensation of pyrrole with acetone in a 1:1 ratio in methanol in the presence of an acid catalyst (e.g., methanesulfonic acid) (Figure 2.7). Chromatographic separation or washing the crude product with methanol affords **2.1** in reasonable yields.

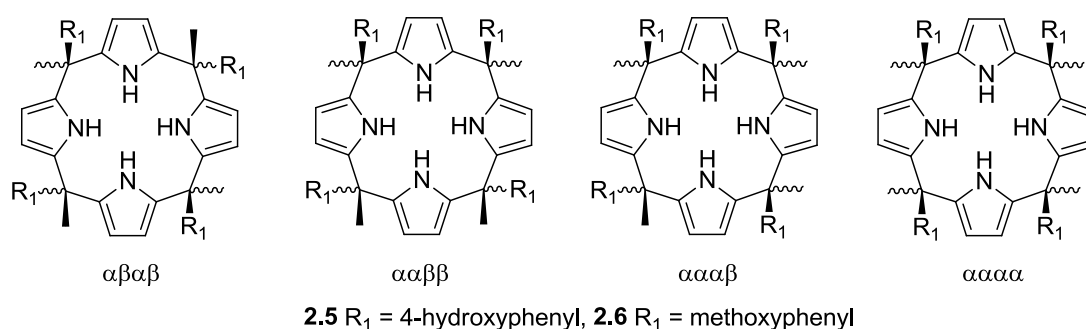


Figure 2.8 : Mixed homo-condensation products.

An asymmetric homo-condensation involves the reaction of a pyrrole with an asymmetric ketone. For instance, pyrrole condensed with *p*-hydroxyacetophenone in MeOH by using an acid catalyst [20]. The desired calix[4]pyrrole **2.5** was isolated, as a mixture of conformational isomers, via column chromatography in 62% yield. The relative yields of these latter isomers, denoted $\alpha\beta\alpha\beta$, $\alpha\alpha\beta\beta$, $\alpha\alpha\alpha\beta$, and $\alpha\alpha\alpha\alpha$ to indicate the relative position of the bulky substituted phenyl substituent (Figure 2.8), were on the order of <5%, 25%, 30%, and 45%, respectively.

The conformational difference of isomers is shown in Figure 2.9 [20]. In the specific case of the $\alpha\alpha\alpha\alpha$ isomer of **2.5**, a deep cavity structure was observed in the solid state, wherein the calixpyrrole core is in a so-called cone conformation. Structures of lower symmetry are seen in the case of the other isomers, with conformations other

than pure cone (e.g., 1,3-alternate, partial cone) being observed in certain instances (e.g., the $\alpha\alpha\alpha\beta$ isomer of **2.6**).

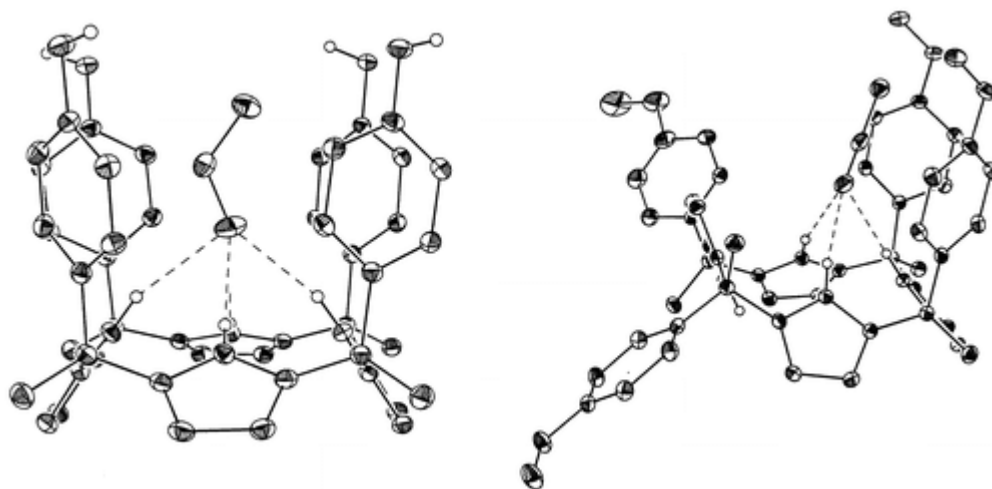


Figure 2.9 : View of the molecular structures of the ethanol adduct of the $\alpha\alpha\alpha\alpha$ isomer of **2.5** in the cone conformation (left) and the acetonitrile adduct of the $\alpha\alpha\alpha\beta$ isomer (methoxy) of **2.6** in the partial cone conformation (right).

2.4.1.2 Mixed condensation

In the case of a mixed condensation one type of pyrrole is reacted with more than one sort of ketone or one type of ketone is condensed with more than one kind of pyrrolic subunit. In general, one type of pyrrole is condensed with two different ketones to obtain asymmetric calix[4]pyrroles that can be used as special starting materials for further functionalization or find diverse application areas.

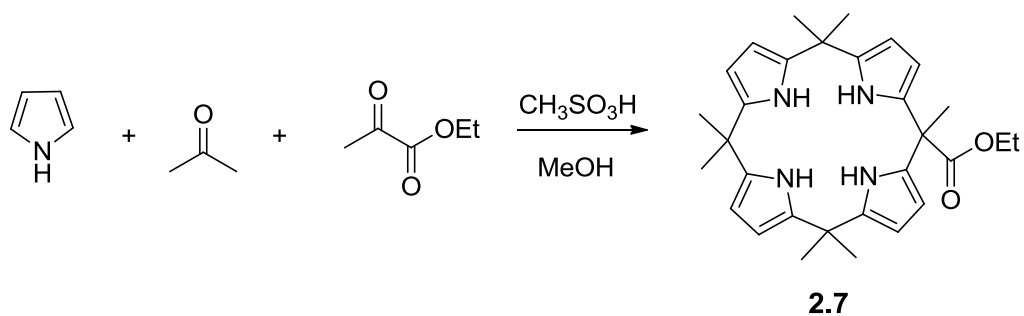


Figure 2.10 : Synthesis of calix[4]pyrrole monoester **2.7** via mixed condensation.

The disadvantage of mixed condensation involves the lowness of the yields. So, the ratio of reactants must be controlled carefully for optimizing the yield of products to be synthesized. For example, the calix[4]pyrrole monoester **2.7** was prepared by stirring pyrrole, acetone and ethyl pyruvate in a 4:3:1 ratio in methanol in the presence of methanesulfonic acid as the catalyst. Chromatographic purification (silica gel, DCM/hexanes : 80/20) yielded **2.7** in 16-20% yield (Figure 2.10) [25].

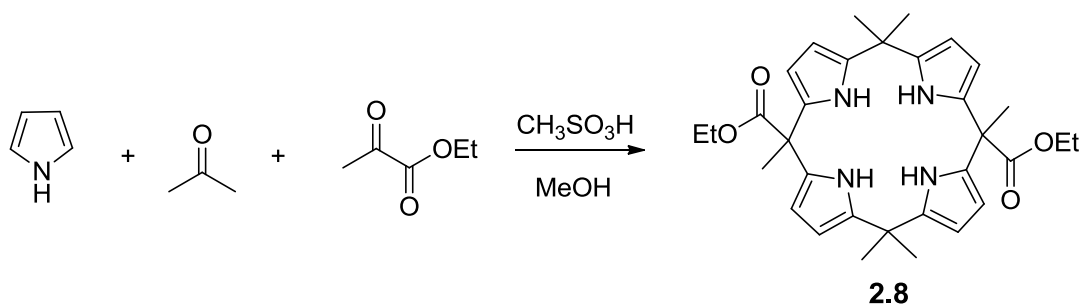


Figure 2.11 : Synthesis of diester functional calix[4]pyrrole **2.8** via mixed condensation.

Another example of mixed condensation was illustrated in the above example (Figure 2.11) by means of the same reactants used above example. However a 2:1:1 ratio was used to obtain diester functional calix[4]pyrrole **2.8** [25].

2.4.2 [2+2] Condensation

[2+2] condensation is used to state acid condensation of two identical dipyrromethane units or dipyrromethane derivatives in the presence of a ketone under acidic conditions.

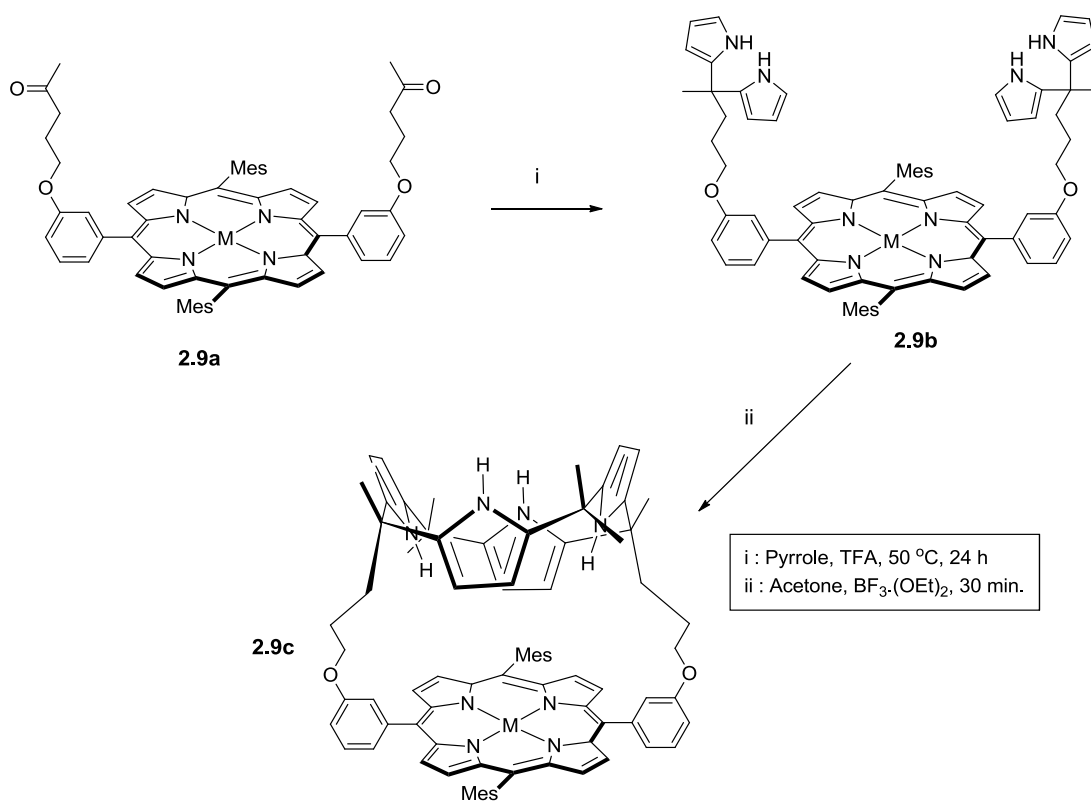


Figure 2.12 : [2+2] Condensation of dipyrromethane containing metalloporphyrin to obtain metalloporphyrin capped calix[4]pyrrole.

This approach represents an important means of constructing a range of calix[4]pyrrole macrocycles or strapped type macrocyclic compounds as illustrated in Figure 2.12 [26]. This type of capped calix[4]pyrroles could be used for anion recognition and ligand fixation.

The target compound **2.9c** is synthesized in two steps. The first step involves the preparation of dipyrromethane substituted metalloporphyrin *via* condensation of **2.9a** with acetone in the presence of trifluoroacetic acid as an acid catalyst. Second step of the synthesis was achieved by the condensation of bis(dipyrromethane) containing porphyrin **2.9b** with acetone in the presence of borontrifluoride diethyl etherate under high dilution conditions (~10 mM).

2.4.3 [3+1] Condensation

A tripyrrane or tripyrrane derivative is condensed with a pyrrole or pyrrole derivative in the presence of an acid catalyst in a typical [3 + 1] condensation. The restricting factors in [3+1] condensation are that the poor stability of tripyrranes in acidic medium and proceeding such reactions generally in low yields. In general, [3+1] condensation involves the synthesis of elaborated calix[4]pyrrole derivatives.

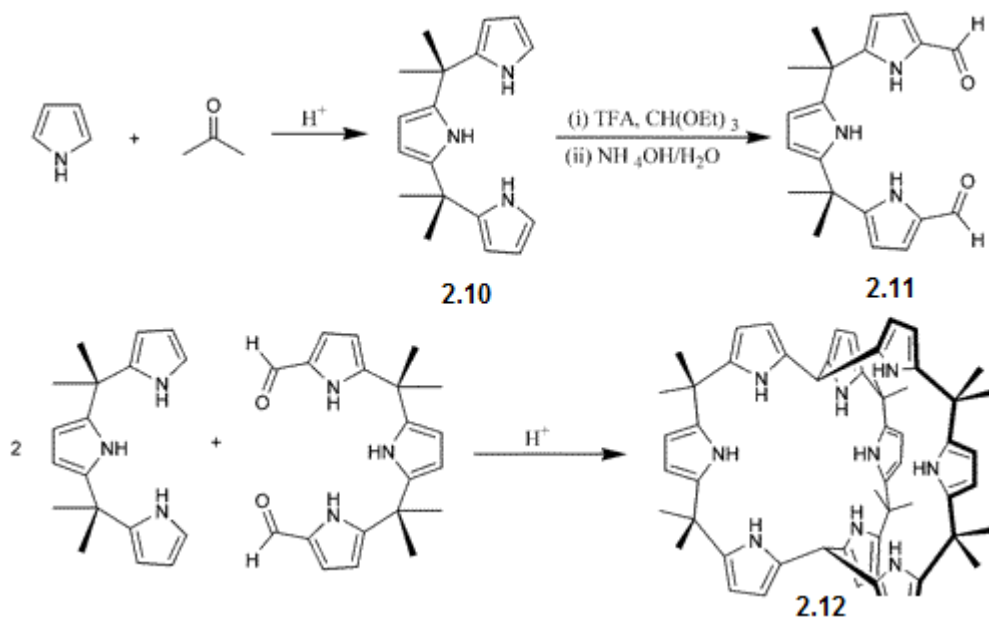


Figure 2.13 : Synthesis of a cryptand-like calix[4]pyrrole by [3+1] condensation.

Bucher reported first cryptand-like calixpyrrole [27] using [3+1] condensation (Figure 2.13). Tripyrranedialdehyde **2.11** was synthesized by formylation of tripyrrane **2.10** in a TFA, triethylorthoformate reaction matrix at $-10^\circ C$ and followed by the treatment of the crude product with aqueous NH_3 . Then, an acid-catalyzed condensation between this diformyl derivative **2.11** and 2 equivalent of **2.10** is used to produce the

three-dimensional bicyclic product **2.12**, in 15% yield. Anion binding properties of this compound were studied by NMR spectroscopic method. The NMR spectral studies revealed that **2.12** has been found to bind a wide range of anions in CD_2Cl_2 including fluoride, chloride, bromide, nitrate, dihydrogen phosphate, and thiocyanate. Although calix[4]pyrroles show 1:1 binding stoichiometry against anions, in the case of compound **2.12**; 1:1, 1:2, and 1:3 binding stoichiometry was observed upon addition of different kind of anions because of the existence of three identical binding cavities.

2.5 Modification of Calix[4]pyrrole Core Macrocycle

Calix[4]pyrrole macrocycle can be modified/functionalized at β -positions (C-rim) or *meso* positions even more at the pyrrolic nitrogen atoms (N-rim). Such modifications not only produce useful precursors for further functionalization to obtain special calixpyrroles useful for production of transporting agents and solid phase anion separation systems, but also affect the anion binding properties of calix[4]pyrroles.

2.5.1 Modification at C-rim

2.5.1.1 Lithiation of Octamethylcalix[4]pyrrole

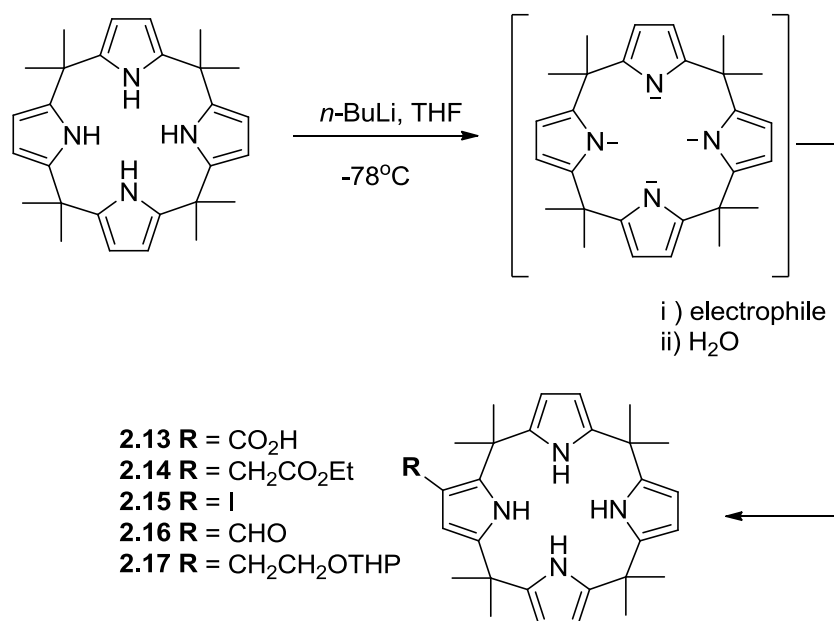


Figure 2.14 : C-rim modification of octamethylcalix[4]pyrrole.

Modification of pyrrole units of calix[4]pyrroles is attracting considerable attention to obtain β -modified calixpyrrole derivatives. In particular, treatment of octamethylcalix[4]pyrrole with *n*-butyllithium in THF at -78°C afforded a deprotonated calixpyrrole intermediate, which was then treated with various suitable

electrophiles followed by quenching the reaction in water, gave the β -mono-substituted calix[4]pyrroles and β -di-substituted derivatives [28]. This method served the synthesis of elaborated calixpyrrole derivatives, among which systems **2.16** have proved particularly useful as building blocks for further derivatization.

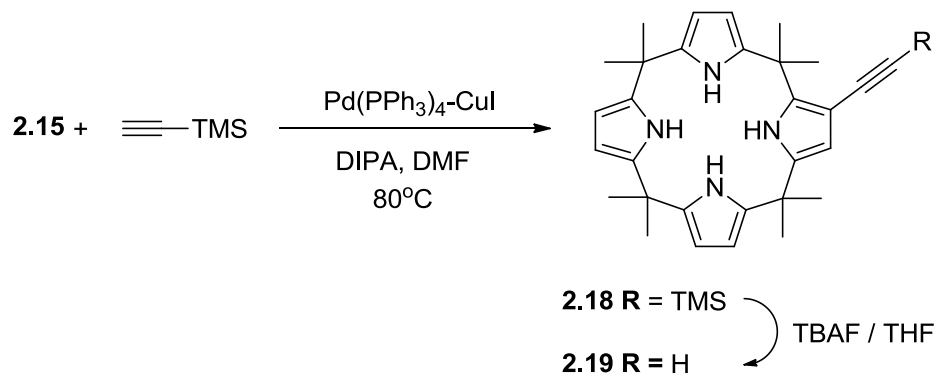


Figure 2.15 : Synthesis of alkyne functionalized calix[4]pyrrole.

For instance, the monoiodo derivative **2.15** was used to produce the β -mono-ethynylcalix[4]pyrrole **2.18**, a species that, in turn, has served as a versatile building block. The synthesis of **2.19** involved first reacting **2.15** with excess TMS acetylene in diisopropylamine-DMF at 80 °C in the presence of Pd(PPh₃)₄-CuI, to give **2.18** the TMS protected alkyne derivative in 73% yield. In a second step, this intermediate was subject to deprotection using tetrabutylammonium fluoride in THF at room temperature; this gave **2.19** in 89% yield [29].

2.5.1.2 Bromination of Calix[4]pyrrole

β -Octabromo-*meso*-octamethylcalix[4]pyrrole **2.20** was synthesized 90% yield by refluxing of *meso*-octamethylcalix[4]pyrrole with *N*-bromosuccinimide (NBS) in dry THF (Figure 2.16) [30]. Since regular one-pot condensation of 3,4-dibromopyrrole with acetone provides no product, this method represents an alternative and highly effective for the synthesis of octabromocalix[4]pyrrole. ¹H NMR titration revealed that the compound **2.20** has two order of magnitude higher anion binding affinity compare to octamethylcalix[4]pyrrole.

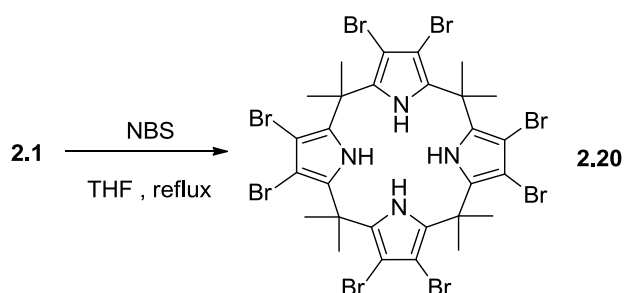


Figure 2.16 : Bromination of octamethylcalix[4]pyrrole.

2.5.2 Modification at *N*-rim

2.5.2.1 *N*-alkylation of *meso*-octaethylcalix[4]pyrrole

Production of useful ligands for metal ions in low oxidation state essentially requires modification of nitrogen atoms of calix[4]pyrroles. Takata and co-workers reported a procedure for modifying the calix[4]pyrrole *N*-rim [31]. Treatment of octaethylcalix[4]pyrrole **2.21** with sodium hydride and methyl iodide in the presence of 18-crown-6 as a phase transfer catalysis in THF gave a distribution of *N*-methylated calixpyrroles. Chromatographic separation over silica gel yielded *N*-mono-(**2.22**), neighboring-*N,N'*-di-(**2.23**), opposite-*N,N'*-di-(**2.24**), *N,N',N''*-tri-(**2.25**), and *N-N'-N''-N'''*-tetra-methylated (**2.26**) *meso*-octaethylcalix[4]pyrroles (Figure 2.17).

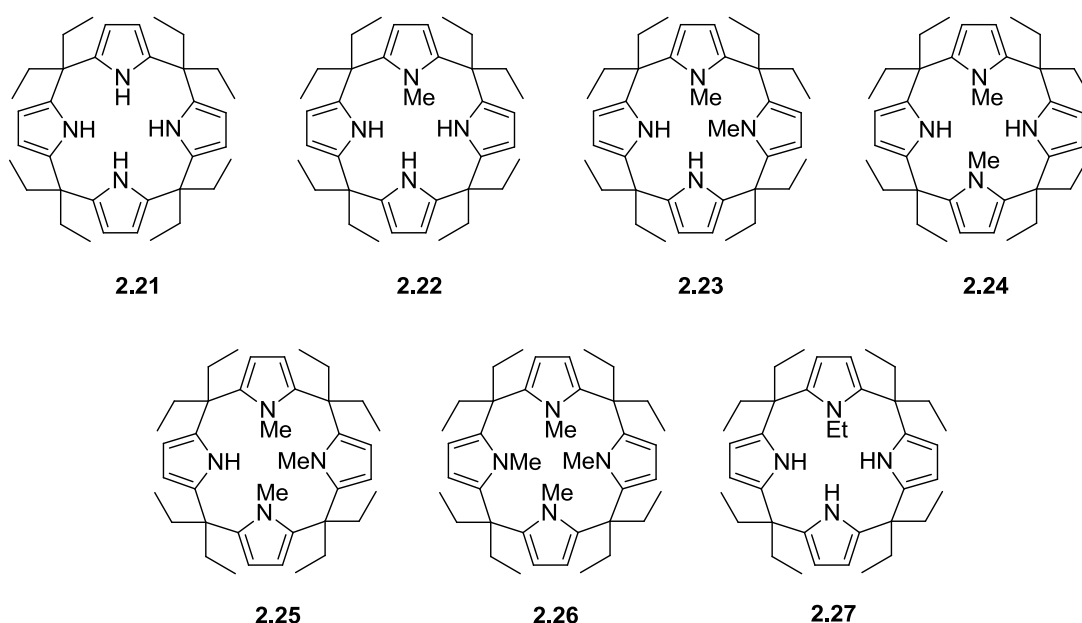


Figure 2.17 : *N*-rim modified *meso*-octaethylcalix[4]pyrroles.

The variation of product distribution was effected by the concentration of MeI used. When 1 equivalent of methyl iodide was used, the main product was the mono-*N*-methylated calixpyrrole **2.22**. On the other hand, when 2 equivalents were used the proportion of the bis-, tris- and tetrakis derivatives was obtained. *N*-ethylation of **2.21** with ethyl iodide was carried out under the similar conditions used to obtain **2.22-2.26**. However, only *N*-mono-ethylated calixpyrrole **2.27** was isolated.

2.5.2.2 Metallation of octamethylcalix[4]pyrrole

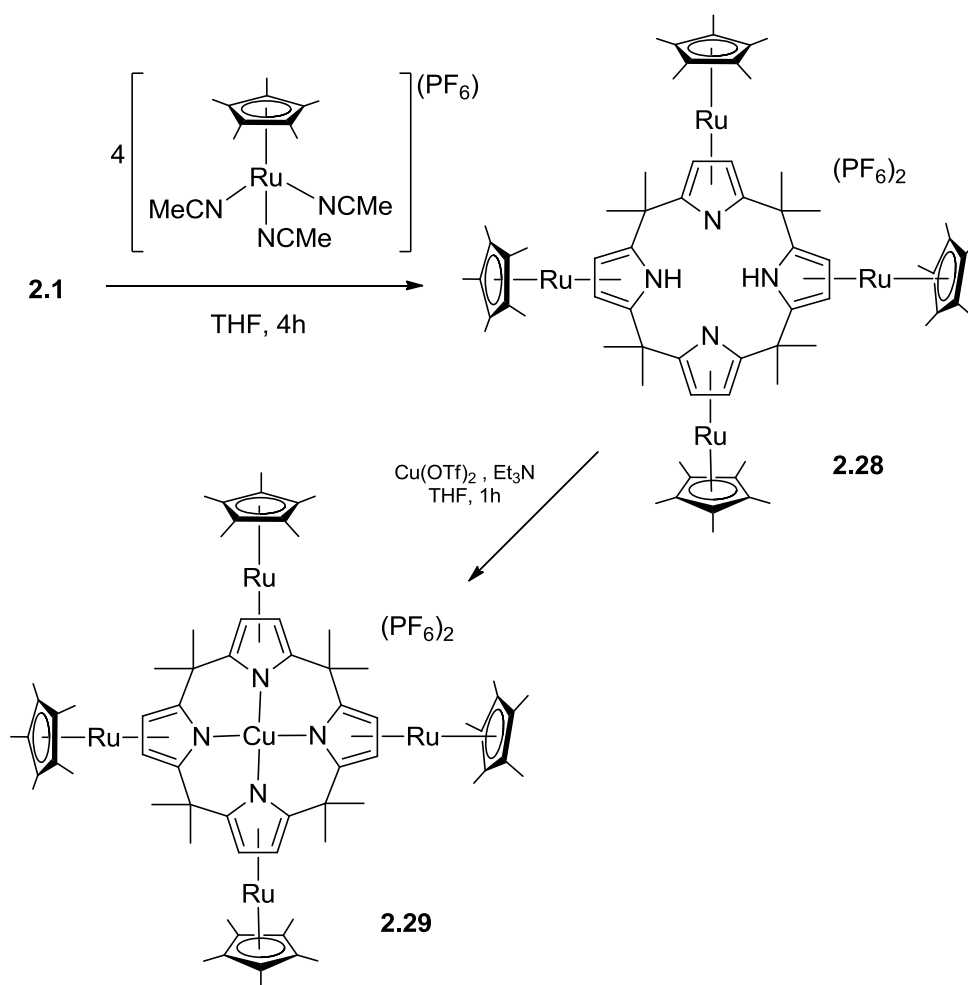


Figure 2.18 : Synthesis of tetrakisruthenocenecalix[4]pyrrole and its copper(II) complex.

Metalloenzymes that contain bi- or multimetallic reactive sites are important in chemical transformations such as oxygen reduction, nitrogen fixation, and redox reactions. Therefore, the synthesis of model chemical systems containing a large number of metal centers within a single ligand system is an incentive research area. Recently, Sessler and co-workers reported the design and synthesis of polymetallic complexes based on calixpyrrole **2.1** [32]. The ruthenium complex of **2.1** was prepared by treating octamethylcalix[4]pyrrole with $[\text{RuCp}(\text{CH}_3\text{CN})_3]\text{PF}_6$ in THF under reflux for four hours. It has been reported that the tetrakisruthenocene complex **2.28** was deprotonated during the reaction (Figure 2.18). Sessler and co-workers speculated that this ^1H NMR result confirms the degree of acidity of pyrrolic NH protons after the complex formation.

The reaction of **2.28** with $\text{Cu}(\text{OTf})_2$ in the presence of triethylamine afforded the pentametallic calix[4]pyrrole complex **2.29**. In a latter extend these new systems

Table 2.3 : Stability constants for **2.1** and **2.3** with anionic substrates in CD₂Cl₂ at 25 °C.

Anion ^a	Association Constant(M ⁻¹)	
	2.1	2.3
Fluoride	17 170	3 600
Chloride	350	117
Bromide	10	n/d ^b
Iodide	<10	n/d
Dihydrogen phosphate	97	<10
Hydrogen sulfate	<10	n/d

^a Anions were added as 0.1 M CD₂Cl₂ solutions of their tetrabutylammonium salts to 10 mM solutions of the receptors in CD₂Cl₂.

^b n/d : not determined.

These findings inspired scientists to investigate the effects of the changes in calix[4]pyrrole structure over anion binding property. Towards this end, On the other hand, in later experiments it was found that the *meso*-octaethyl- and *meso*-octa-*n*-propyl-substituted systems (compounds **2.21** and **2.30**) displayed anion binding affinities that were only slightly diminished as compared to the original *meso*-octamethyl system **2.1** [33].

In the light of above findings, the introduction of spiro-cycloalkyl substituents has been achieved to illuminate the question that if there is a modifying role of different substituents. On the other hand, this could affect the ease of the critical 1,3-alternate to cone interconversion. To answer these steric and conformational postulations, *meso*-tetraspirocyclopentyl- (**2.31**) and *meso*-tetraspirocyclobutyl-calix[4]pyrrole (**2.32**) systems synthesized starting from the acid catalyzed condensation of pyrrole with corresponding ketone moiety (Figure 2.20) [33].

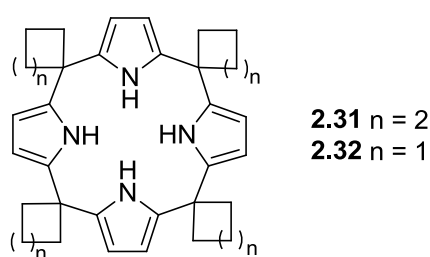


Figure 2.20 : Structures of *meso*-tetraspirocycloalkylcalix[4]pyrroles.

After isolation of the receptors **2.31** and **2.32** their anion binding abilities were examined using ¹H NMR titration in CD₂Cl₂ upon various anions. When Table 2.3 and Table 2.4 were inspected it can be concluded that generalized solution-phase anion binding properties decreased in the order Me₂>spiro-cyclohexyl>spiro-cyclopentyl>spiro-cyclobutyl (i.e. **2.1**>**2.3**>**2.31**>**2.32**).

Table 2.4 : Association constants for the formed between compounds **2.31** and **2.32** and fluoride, chloride, and dihydrogen phosphate anions.

Anion ^a	Association Constant (M ⁻¹)	
	2.31	2.32
Fluoride	3 000	2 300
Chloride	100	<100
Dihydrogen phosphate	n/d ^b	n/d

^a Anions were added as CD₂Cl₂ solutions of their tetrabutylammonium salts to solutions of the receptors at 25 °C.

^b n/d : not determined.

These results are consistent with the proposition that the decreased anion binding constant exhibited by **2.3**, **2.31**, and **2.32** relative to parent system 1 is caused by an increase in the energetic barrier needed to flip between 1,3-alternate and cone conformations.

Further studies were focused on the preparation of calix[4]pyrroles bearing substituted aryl groups in the meso positions to understand the effect of auxiliary meso substituents. Such rigid substituents would provide a rigid scaffold around the calixpyrrole macrocycle that would not only influence the ease of conformational changes but also provide a preorganization for complexation with the anions will be studied. For instance, acid catalyzed condensation of pyrrole with *p*- or *m*-substituted acetophenones were carried out [20] in a range of solvents [10]. *p*-Bromo and *p*-hydroxy acetophenones have been utilized and the resulting calix[4]pyrrole **2.5** was easily converted to corresponding methoxy derivative **2.6** by treatment with iodomethane (Figure 2.21).

As expected, condensation of pyrrole with acetophenone derivatives yielded a mixture of configurational isomers denoted as $\alpha\beta\alpha\beta$, $\alpha\alpha\beta\beta$, $\alpha\alpha\alpha\beta$, and $\alpha\alpha\alpha\alpha$ to indicate the relative positions of bulky aryl substituents or steroidal subunits (Figure 2.21). All of these isomers were isolated successfully using chromatographic methods. X-ray structural analysis of the two aryl systems **2.5** and **2.6** revealed receptor-substrate complexes having high walls and well-defined binding cavities (see Figure 2.9), at least in the case of the $\alpha\alpha\alpha\alpha$ isomers [20].

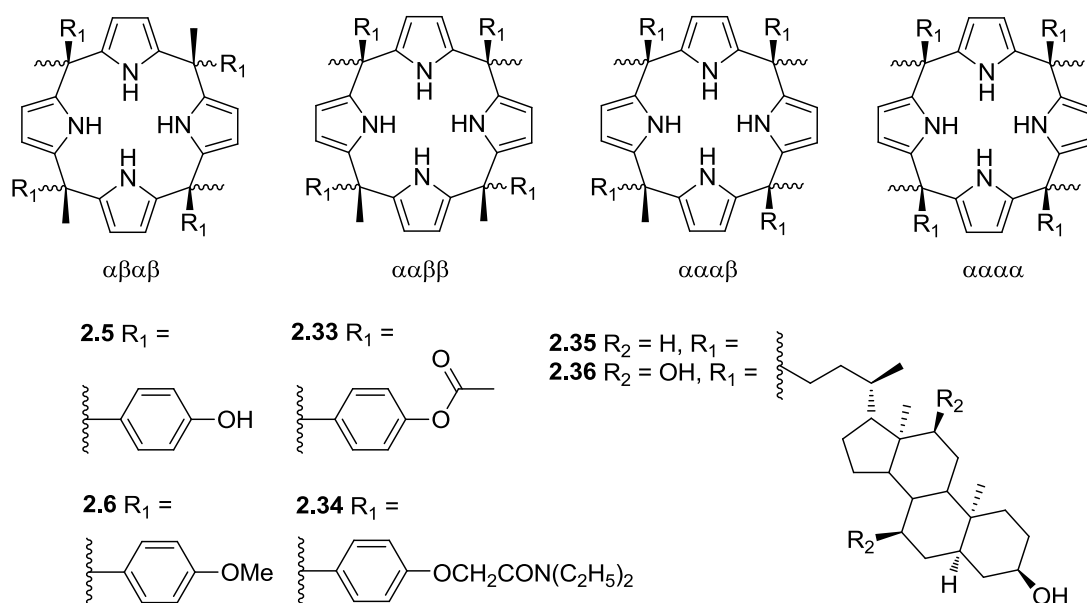


Figure 2.21 : Calix[4]pyrroles prepared from acetophenone derivatives and steroidal compounds.

The presence of well-defined binding cavity resulted in a greatly enhanced selectivity for fluoride anion, relative to chloride and dihydrogen phosphate anions. This enhancement reflects the fact that small fluoride anion can fit into the size-limited binding cavity. ^1H NMR spectroscopic anion binding studies supported this idea. For example the $\alpha\alpha\alpha\alpha$ and $\alpha\alpha\beta\beta$ isomers of the receptors **2.5** and **2.6** showed relatively significant enhanced association constants against fluoride anion compare to the other isomers. It can also be concluded from the data present in Table 2.5, the selectivity of the compounds **2.5** and **2.6** is notable compare to parent system **2.1**.

Table 2.5 : Association constants for the compounds **2.1**, **2.5**, and **2.6** with anionic substrates as determined from ^1H NMR spectroscopic titrations carried out in acetonitrile- d_3 (0.5% v/v D_2O) at 22 °C.

Anion	Compound						
	2.1	2.5			2.6		
		$\alpha\alpha\beta\beta$	$\alpha\alpha\alpha\beta$	$\alpha\alpha\alpha\alpha$	$\alpha\alpha\beta\beta$	$\alpha\alpha\alpha\beta$	$\alpha\alpha\alpha\alpha$
F^-	>10 000	>10 000	5 000	>10 000	460	1 100	>10 000
Cl^-	>5 000	1 400	260	320	<100	220	300
H_2PO_4^-	1 300	520	230	500	<100	<80	<100

In a more polar solvent than acetonitrile, $\text{DMSO}-d_6$, the isomers of the two extended cavity receptors **2.6** and **2.33** were found to bind only fluoride anion [21]. However, even for this anion, the binding affinities were relatively low. For instance, as determined from ^1H NMR spectroscopic titrations, the fluoride anion binding affinity of **2.33** in $\text{DMSO}-d_6$ is about 74 M^{-1} .

The steroidal calix[4]pyrrole systems **2.35** and **2.36** were reported by Král and Sessler in 2002 [34]. Steroid-based compounds were prepared in excellent yields from cholic acid derivatives using an efficient synthetic sequence. It was found that this calix[4]pyrroles also found to exist in the form of four different configurational isomers as in **2.5** and **2.6**. In this case, a FAB-MS screening process was used whether these systems effect the enantioselective recognition of tartaric acid and mandelic acid. It has been shown that the polyhydroxylated $\alpha\alpha\alpha\beta$ configurational isomer can exhibit enantioselective binding against L-tartaric acid and L-mandelic acid.

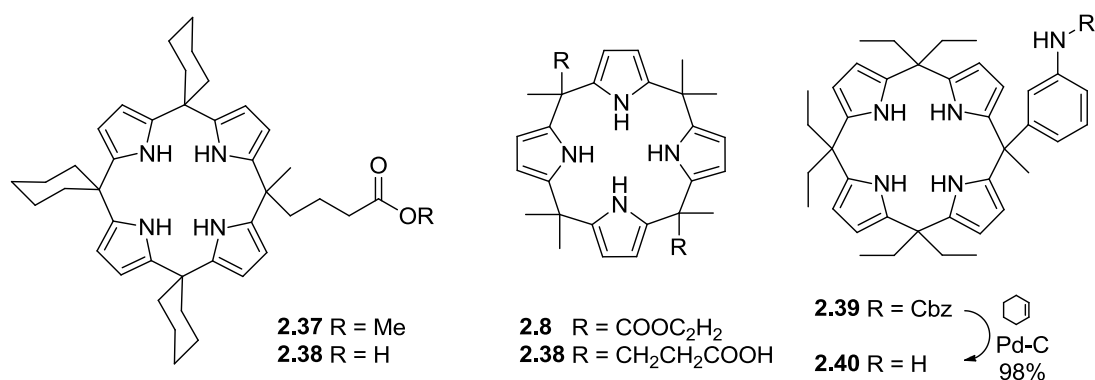


Figure 2.22 : Calix[4]pyrroles derivatized at *meso*-positions.

In another effort to obtain functionalized calix[4]pyrrole derivatives, introduction of butanoate group to a calix[4]pyrrole produced as anionic calixpyrrole with interesting self-assembly properties [35]. Aforementioned “meso-hook” calix[4]pyrrole monoester was prepared via a mixed-condensation of pyrrole with cyclohexanone and methyl-4-acetylbutyrate. Chromatographic purification afforded the monoester **2.37** in 12% yield from a mixture of calixpyrroles containing different number of ester functional groups. Consequent hydrolysis of **2.37** yielded the monoacid **2.38** (Figure 2.22). X-ray crystallographic analysis of **2.37** in the presence of Bu₄NF revealed an interesting result that the crystals did not contain any fluoride anions bound to NHs of calixpyrroles. Instead, this latter was found to be comprised entirely of the tetrabutylammonium calix[4]pyrrole carboxylate salt. The X-ray structure of the salt revealed that the carboxylate functionality of one calixpyrrole was found to be bound to the pyrrolic array of an adjacent calixpyrrole and *vice versa*. These interactions formed a dimeric cyclic structure as shown in Figure 2.23 [35].

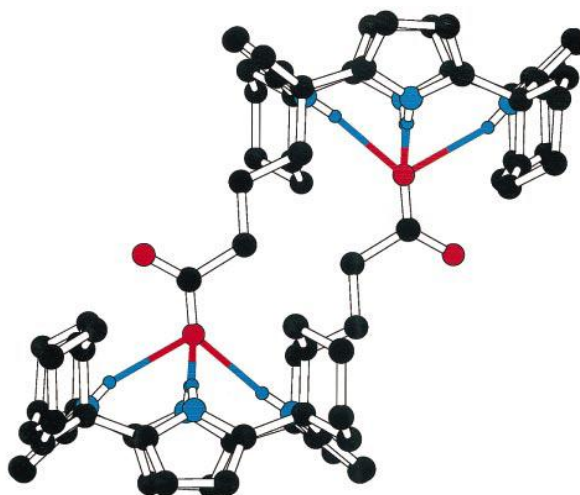


Figure 2.23 : X-Ray crystal structure of the calix[4]pyrrole carboxylate dimer.

Mixed condensation is a powerful method to synthesize asymmetric calix[4]pyrrole derivatives. In 2005, our group reported diester and diacid functional calixpyrroles by the condensation of pyrrole with both levulinic acid and ethyl pyruvate in the presence of HCl as an acid catalyst [25]. Isolation of the products achieved by column chromatography yielded calixpyrroles **2.8** and **2.38** in 48% and 55% respectively (Figure 2.22).

Efforts to obtain functionalized systems as fluorescent anions sensors lead several researchers to use mixed condensation as a useful tool. For this purpose various calix[4]pyrrole derivatives have been prepared with several functional groups. This class of functional or functionalized systems could be named as first generation sensors. Intense need for selective sensing of specific anionic species and sensors with high affinities towards anions prompted researchers to search for improved systems. Towards this end, so called “second generation” calix[4]pyrrole derivatives have been synthesized and used as fluorescent sensors. For instance, condensation of Cbz-protected 3-aminoacetophenone, 3-pentanone and pyrrole in the presence of $\text{BF}_3 \cdot \text{Et}_2\text{O}$ was found to afford the mono functionalized calixpyrrole **2.39** (Figure 2.22) [36].

Once **2.39** was in hand, efforts was then focused on the preparation of second generation anion sensors **2.41-2.43**. Rigid aromatic spacer units were used so as to fix the distance between the receptor and the fluorescence signaling moiety. This spacer unit contained either a sulfamide (**2.41** and **2.42**) or thiourea (**2.43**) group [36]. These spacer units could also provide additional hydrogen bond donor (NHs of sulfamide and thiourea) sites to enhance the overall anion binding affinities. Anion binding affinities of sensors **2.41-2.43** were calculated via fluorescence quenching experiments.

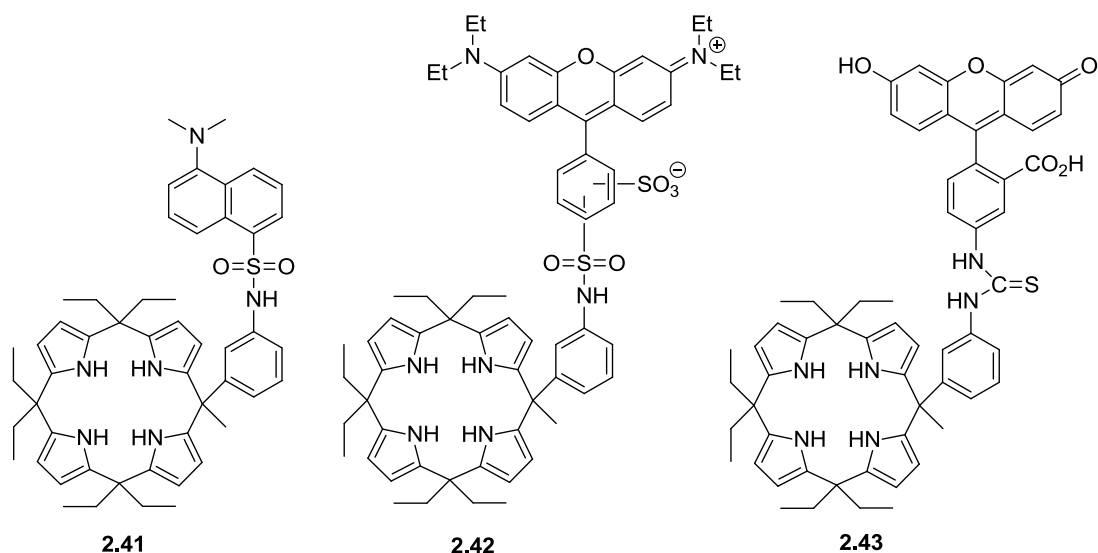


Figure 2.24 : Structures of second generation sensors **2.41-2.43**. These systems contain dansyl (**2.41**), lissamine-rhodamine B (**2.42**), and fluorescein (**2.43**) moieties as the fluorescent elements, respectively.

The results are listed in Table 2.6 revealed that while fluoride anion gave a rise to the largest response; sensors **2.41-2.43** are remarkably selective for phosphate and pyrophosphate anions relative to Cl^- .

Table 2.6 : Affinity constants for sensors **2.41-2.43** and anionic substrates as determined in acetonitrile (0.01% v/v water) for sensors **2.41** and **2.42** and acetonitrile–water (96:4, pH 7.0 \pm 0.1) for sensor **2.43**.

Anion ^a	Association Constant (M^{-1})		
	2.41	2.42	2.43
F^-	222 500	>1 000 000	>2 200 000
Cl^-	10 500	18 200	<10 000
H_2PO_4^-	168 300	446 000	682 000
$\text{HP}_2\text{O}_7^{3-}$	131 000	170 000	>2 000 000

This selectivity can be explained by the presence of multiple hydrogen bonding interactions involving these two nonspherical anions. Such effects, illustrated in Figure 2.25 [36], are likely to be particularly pronounced in the case of sensor **2.43** and pyrophosphate dianion where the coordination of the second anionic center within the pyrophosphate by the thiourea moiety is believed to be responsible for the dramatic increase in affinity.

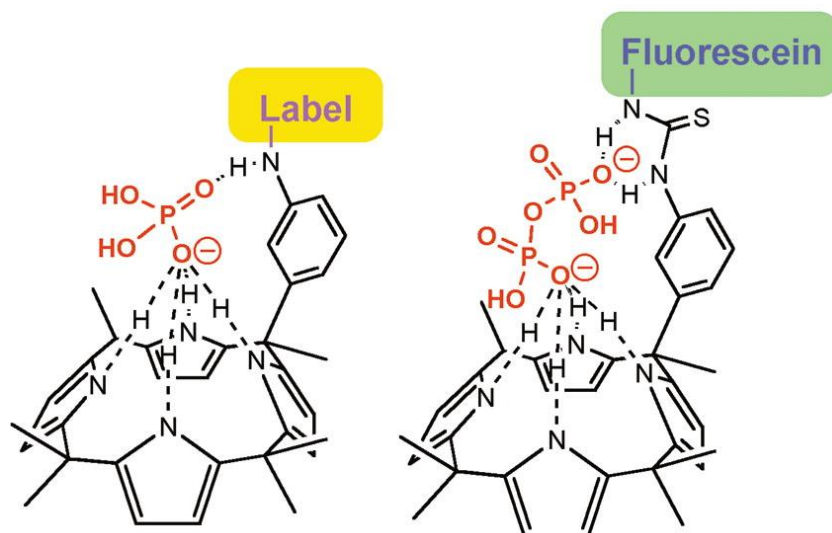


Figure 2.25 : Schematic representation of the multiple hydrogen bonding interactions that are believed to account for the high phosphate and pyrophosphate affinities observed for sensors **2.41**, **2.42**, and **2.43** respectively.

Mixed condensation is not the only way to obtain functional calixpyrrole derivatives. 2+2 condensation was found to be an efficient synthetic methodology to prepare difunctional calix[4]pyrrole products. Eichen and co-workers examined a two-step synthetic pathway for the preparation of dissymmetric meso-substituted calix[4]pyrroles [37].

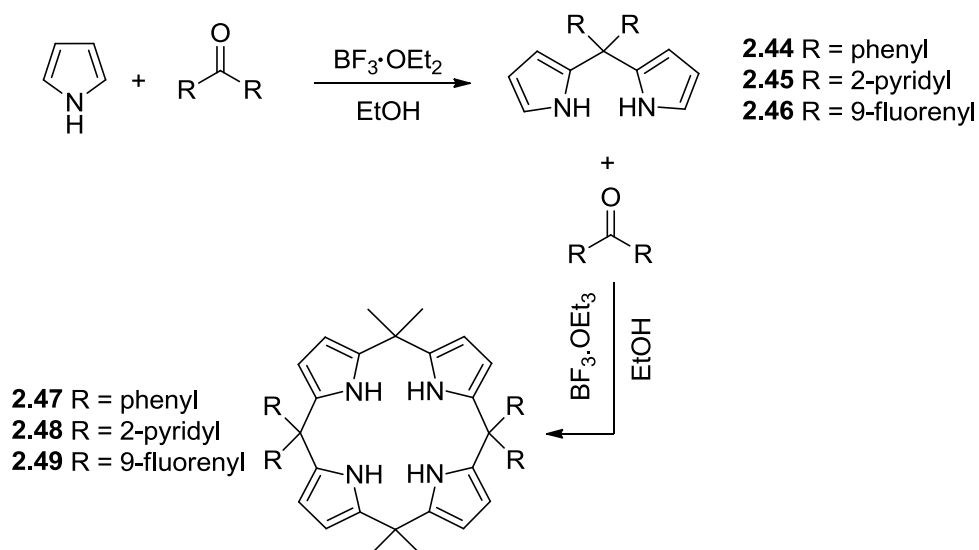


Figure 2.26 : Difunctional calix[4]pyrroles prepared via 2+2 condensation.

For instance, acid catalyzed condensation of pyrrole with aromatic ketones such as benzophenone, di-(2-pyridyl) ketone, and 9-fluorenone resulted in formation of the corresponding dipyrromethanes **2.44-2.46**. Once dipyrromethanes of aromatic ketones in hand, they were reacted readily with simple aliphatic ketones, such as

acetone, in the presence of catalytic amounts of trifluoroacetic acid to yield the corresponding difunctional calix[4]pyrroles **2.47-2.49** in 56%, 20%, 38% respectively (Figure 2.26).

2.6.2 Derivatization at C-rim

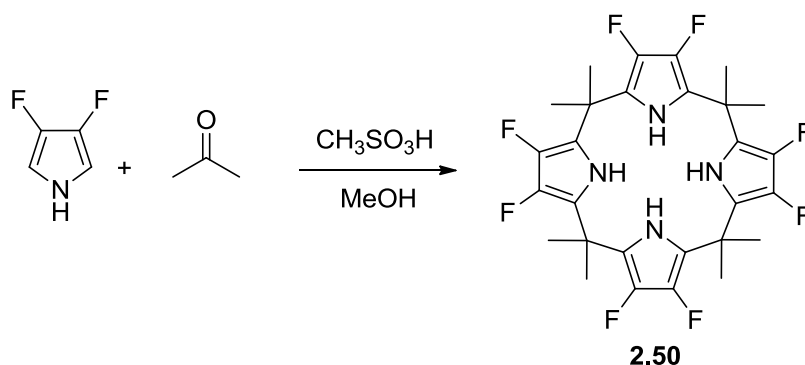


Figure 2.27 : Synthesis of octamethyloctafluorocalix[4]pyrrole.

The ubiquity of anions in biology has led considerable effort to be devoted to the preparation of receptors displaying high binding affinity and selectivity. In this field of supramolecular chemistry, much of the emphasis has been on neutral host molecules. This is because neutral receptors often show selective recognition than charged receptors as the result of more precisely oriented hydrogen bond donors. As the so called calixpyrroles is one of the easy to prepare anion receptor their powerful analogues could be established *via* increasing the acidity of pyrrolic NHs. Towards this end Sessler and coworkers reported a calix[4]pyrrole derivative having fluorine atoms on the β -positions of pyrrole rings [38, 39]. Specifically, 3,4-difluoropyrrole [40] was condensed with acetone in the presence of methanesulfonic acid in MeOH. The crude product **2.50** was isolated by flash column chromatography and obtained in 55-60% yield (Figure 2.27).

Table 2.7 : Association constants (K_a , M^{-1}) of **2.1** and **2.50** for chloride anion (tetrabutylammonium salt) in CH_3CN (2% v/v H_2O) as obtained from ITC analysis and NMR titrations carried out in the corresponding deuterated solvents at 22 °C.

Method	Association Constant (M^{-1})	
	2.1	2.50
NMR	7 600	50 000
ITC	5 400	31 000

Anion binding studies of the fluorinated calix[4]pyrrole was carried out using both 1H NMR and ITC titration experiments. Chloride anion binding studies revealed that receptor **2.50** binds chloride anion in around 7 times stronger than the parent octamethylcalix[4]pyrrole **2.1** (Table 2.7). Under identical conditions, ITC analysis

provide K_a values for **2.1** and **2.50** that matched reasonably well those from the NMR titrations. In general, ITC measurements provide relatively higher association constants compare to NMR titration techniques [22]. As can be noted, the data presented in Table 2.7 reveals lower binding constants than NMR titration results. In this study, the anion binding experiments for other anionic species (e.g. bromide, iodide, acetate, benzoate etc.) were also inspected For further detailed anion binding results and speculations about the data see reference [38].

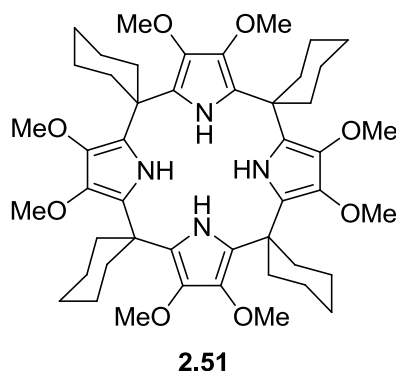


Figure 2.28 : Structure of methoxylated tetraspirocyclohexyl calix[4]pyrrole.

In another effort to obtain calix[4]pyrroles with enhanced anion binding ability and selectivity β -octamethoxy-meso-tetraspirocyclohexylcalix[4]pyrrole (Figure 2.28) has been prepared [30]. In this study, the target calixpyrrole **2.51** was synthesized via condensation of 3,4-dimethoxypyrrole [41] with cyclohexanone in glacial acetic acid. Removal of the acid under vacuum and subsequent purification of crude product by column chromatography afforded the compound **2.51** in 8% yield. Solution phase anion binding measurements of **2.51** was made using ^1H NMR spectroscopic titrations in CD_2Cl_2 . The results showed that calix[4]pyrrole **2.51** has lower binding affinities when it was compared with the parent system **2.1**. In detail, compound **2.51** binds fluoride and chloride anions with a lower affinity. From these results, it has been concluded that this may be due to the electron-donating ability of eight C-rim methoxy groups causing a decrease in the acidity of pyrrolic NH protons hence reducing anion binding ability of **2.51**.

2.7 Applications of Calix[4]pyrrole Derivatives

Importance of the anions in various interdisciplinary fields and other practical considerations has led to spectacular growth within the anion recognition field. However, the weak nature of most anion–receptor interactions, particularly in the case of neutral anion receptor systems, reflecting the relatively low charge density of most anions [11], makes the design of selective and effective receptors one of

ongoing challenge. Thus, while a number of research groups have designed elegant anion receptors, many of which have proven to be quite effective, there remains a need for simple, easy-to-make anion binding systems. In this context, the so-called calix[4]pyrroles have emerged as molecules of particular interest [10]. This is because the core structure may be accessed in one synthetic step and a large number of modifications are readily conceivable. Thus, several putative practical application areas have been developed.

2.7.1 Calix[4]pyrrole-based chromatographic separation systems

Selective recognition of guest molecules is closely related to the selective separation in chromatography. Host molecules can be added to a mobile phase as new additives, or covalently attached to a solid support to form a new stationary phase. The covalent attachment of molecular receptors to solid supports provides an opportunity to explore receptor-substrate interactions.

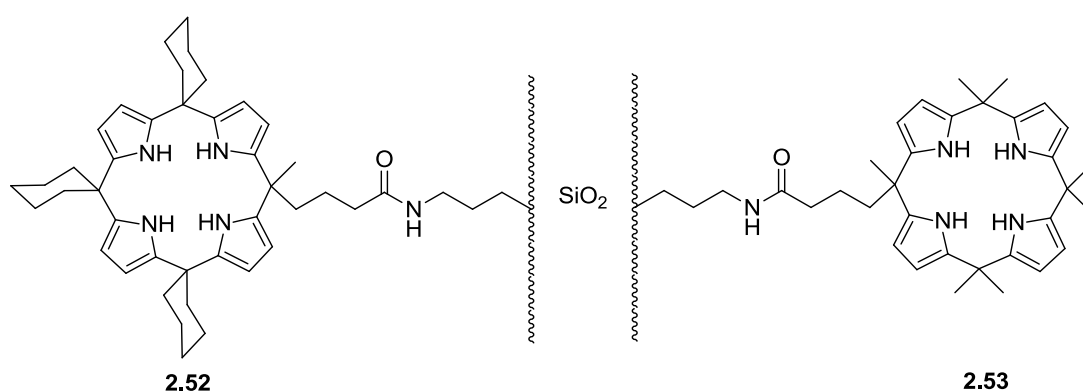


Figure 2.29 : Sessler's calix[4]pyrrole modified silica gels.

Up to date, several efforts have been devoted to develop cation separation systems. However, it has been less frequently applied in the field of anion recognition and separation. Some examples of anion receptor-based stationary phases are metallated porphyrin [42] and sapphyrin-modified silica gels [43, 44]. Calix[4]pyrrole-modified silica gels **2.52** and **2.53** have been reported by Sessler [45] and applied as new solid-phase HPLC support for investigating the binding characteristics of calix[4]pyrroles with anionic and neutral substrates (Figure 2.29). It also provided separation of nucleotides, oligonucleotides, N-protected amino acids and perfluorinated biphenyls.

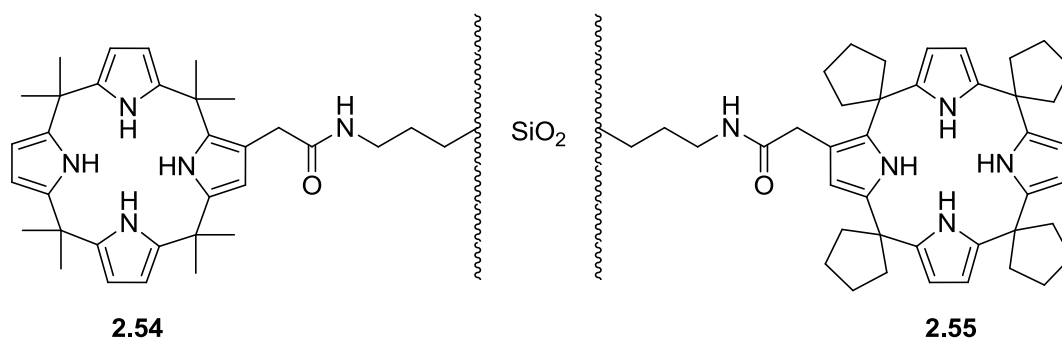


Figure 2.30 : Zhou's calix[4]pyrrole-modified silica gels.

Zhou designed β -hooked calix[4]pyrroles and attached these compounds on to silica gel solid support (Figure 2.30). These modified silica gels **2.54** and **2.55** supported on HPLC column and were studied to separate amino acids, phenols, benzenecarboxylic acids, and some medicines along with inorganic anions including F^- , Cl^- , Br^- , and I^- . As it can be seen in Figure 2.31 (Peaks; 1: DNP-serine; 2: DNP-glycine; 3: DNP-alanine; 4: DNP-valine; 5: DNP-leucine; 6: DNP-OH; 7: DNP-tyrosine; 8: DNP-phenylalanine; 9: DNP-glutamic acid) [46], calix[4]pyrrole-modified silica gel **2.55** is able separate dinitrophenyl (DNP) derivatives of amino acids.

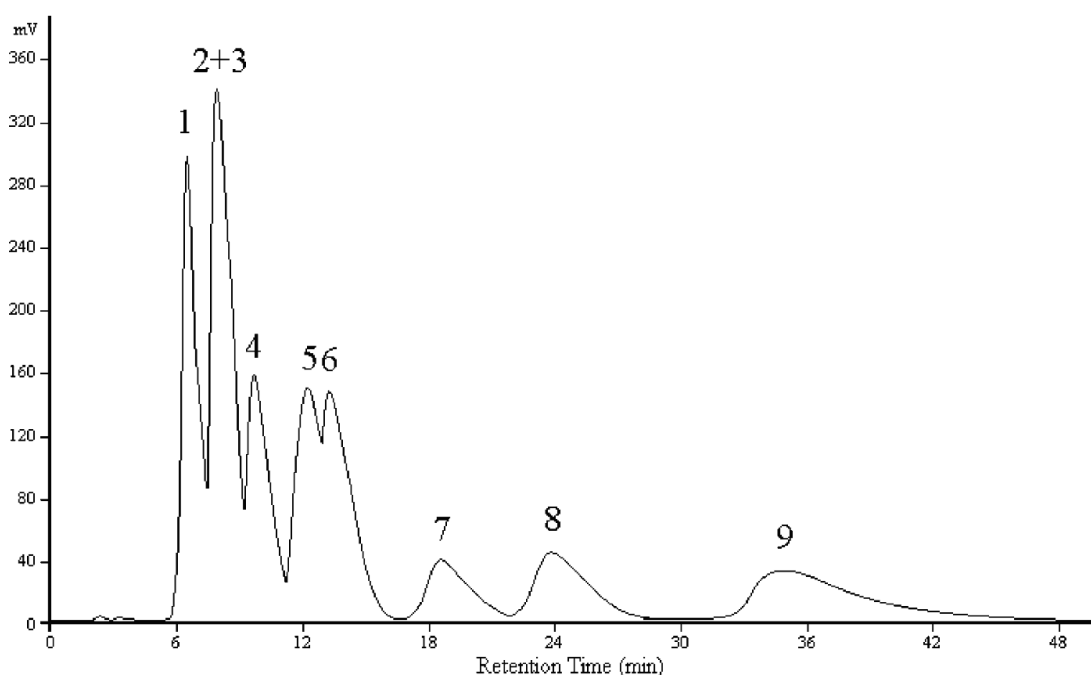


Figure 2.31 : HPLC separation of amino acids on gel **2.55** column.

2.7.2 Calix[4]pyrrole based optical sensors

The syntheses of novel host devices designed to sense and report the presence of a particular guest substrate attracting considerable attention. On the other hand, this signaling provides information about not only presence but also specific concentration of a particular guest. A response, detectable by visual or fluorescence-

based means, is produced by the perturbation of the electronic properties of reporter groups upon anion complexation. The main approach that has been used in the production of calix[4]pyrrole based optical sensors, is based on the covalent attachment of a colorimetric or fluorescent reporter unit to the calix[4]pyrrole skeleton. Throughout this end, a variety of known calix[4]pyrrole building blocks were successfully attached to various chromophores and fluorophores.

2.7.2.1 Anthracene linked calix[4]pyrroles

Fluorophore group containing system consisted of anthracene groups covalently attached to the core calix[4]pyrrole macrocycle via amide linkage. Mono-acid derivative of octamethylcalix[4]pyrrole was reacted with 1-aminoanthracene using dicyclohexylcarbodiimide (DCC) and hydroxybenzotriazole (HOBt) in DMF to afford a calix[4]pyrrole-anthracene conjugate **2.58**.

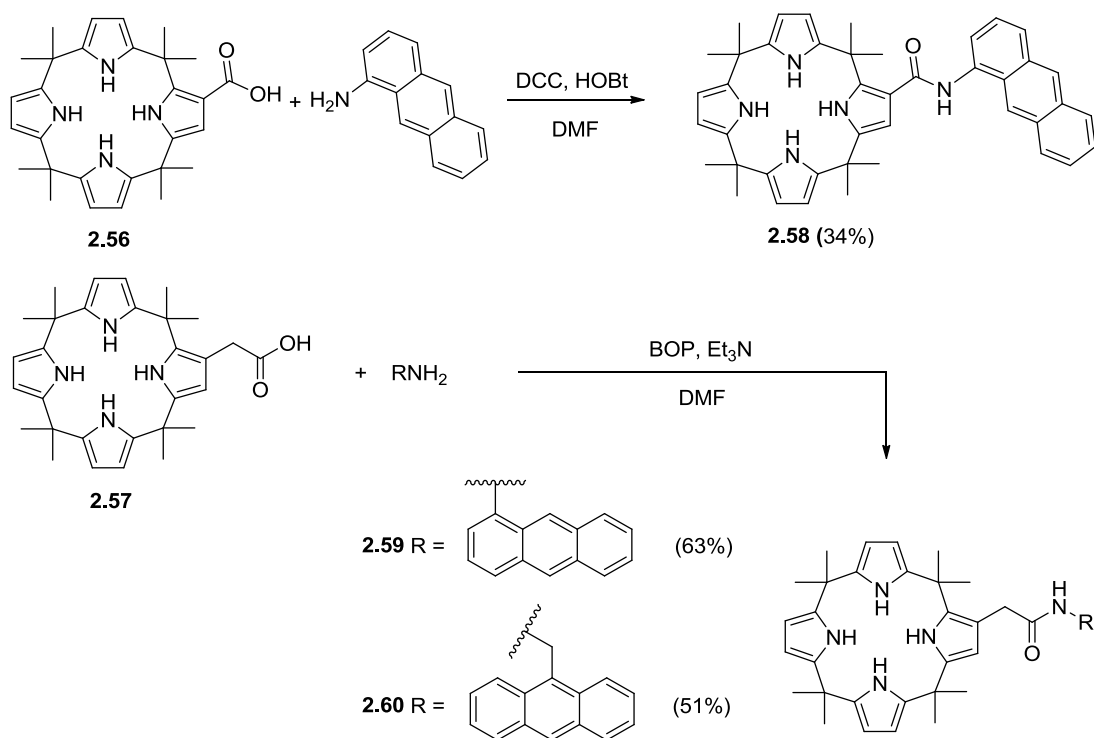


Figure 2.32 : Synthesis of anthracene linked calix[4]pyrroles.

Compounds **2.59** and **2.60** was prepared by coupling the calixpyrrole mono-acid **2.57** with 1-aminoanthracene in DMF in the presence of excess Et₃N [8]. Both calixpyrrole **2.58** and this system possesses a direct linkage between calix[4]pyrrole anion receptor sites and anthracene fluorophores that makes the whole systems fluorescent sensors.

When these systems exposed to titration with different anions (as their tetrabutylammonium salts) a fluorescence quenching was observed (Figure 2.33)

[47]. This is because that the complexation of the anion and the calix[4]pyrrole site of fluorescent receptor causes electron transfer to the anthracene fluorophore via amide linkage. Anion binding affinities calculated via fluorescence quenching revealed that anthracene linked calixpyrrole **2.58** seems to be the most sensitive sensor against anions among the three conjugates. For instance, when **2.58** titrated with tetrabutylammonium fluoride a dramatic quenching was observed depending on the equivalence of fluoride anion. The high sensitivity of the receptor **2.58** reflects the direct connection of anthracene group to the calix[4]pyrrole core via an amide bridge while other systems having a methylene linker between calixpyrrole and amide bridge.

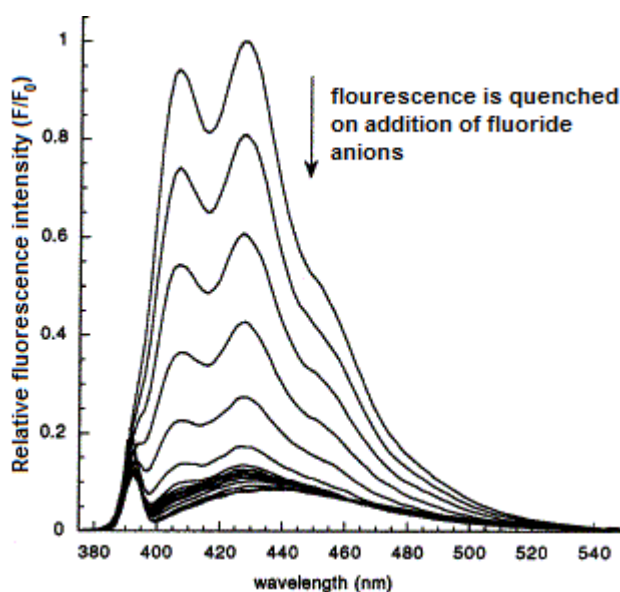


Figure 2.33 : Fluorescence spectra of calix[4]pyrrole **2.58** in CH_2Cl_2 showing the changes induced upon the addition of increasing quantities of tetrabutylammonium fluoride.

2.7.2.2 1,3-Indane-based calix[4]pyrroles

Calix[4]pyrrole anion sensors showing strong intramolecular charge transfer were synthesized via Knoevenagel condensation of 2-formyl-octamethylcalix[4]pyrrole **2.16** with 1,3-indanone derivatives by Anzenbacher et al [48]. 2-Formyl-octamethylcalix[4]pyrrole **2.16** was prepared with the Vilsmeier reagent (POCl_3 , DMF in CH_2Cl_2 at 0°C) in 44% yield (Figure 2.34).

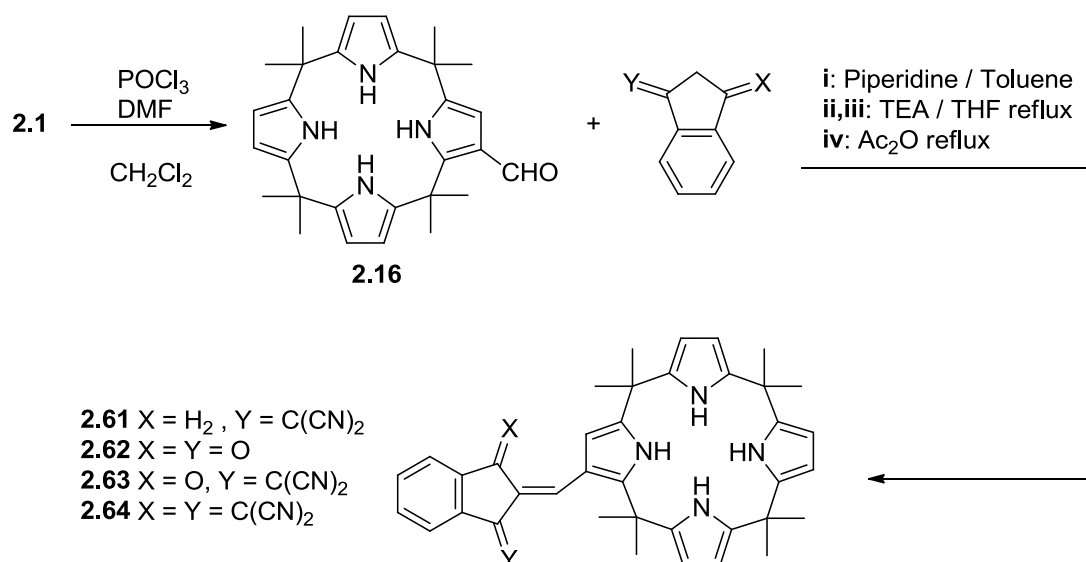


Figure 2.34 : Synthesis of 1,3-indane based calix[4]pyrroles

The push-pull nature of the chromophores (indanylidene units) provides here amplifying the signaling process. Hence, the hydrogen bonding between an anion and the electron-rich pyrrole results in intramolecular charge transfer from pyrrole (push) to the electron-poor 1-indanylidene moiety, thus enhancing the color transitions (Figure 2.35).

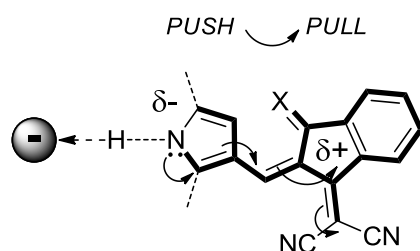


Figure 2.35 : Anion-hydrogen bonding results in partial charge transfer from electron-rich pyrrole to electron-poor indanylidene.

Quantitative absorption spectroscopic analysis of receptors **2.61-2.64** reveals that before and after the addition of anion salts showed a dramatic change in color in the case of fluoride, acetate, and dihydrogen phosphate. This result is in good agreement with the general calix[4]pyrrole behavior against anions bound strongly to calix[4]pyrrole. In contrast, weak or no color changes have been observed in the case of chloride, bromide, and nitrate anions which octamethylcalix[4]pyrrole has lower anion binding affinities. Figure 2.36 shows the different responses of the compound **2.61** against fluoride and bromide anions [48]. While **2.61** changes its color when treated with fluoride, there is no significant change when it was titrated with iodide.

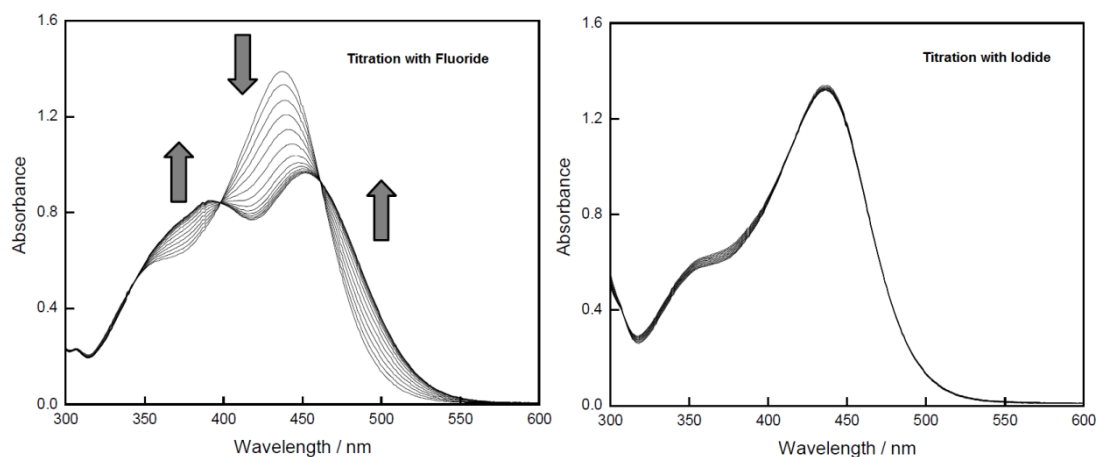


Figure 2.36 : Titration of receptor **2.61** with fluoride and iodide anions.

Another example of 1,3-indane based optical calix[4]pyrrole receptor reported by Sessler and co-workers. A strapped calix[4]pyrrole bearing 1,3-indanedione group at β -pyrrolic position has been synthesized and studied as a ratiometric cyanide-selective chemosensor and as an anion sensor [49]. The starting strapped calixpyrrole **2.65** was subjected to Vilsmeier-Haack formylation giving two different β -monoformylated regioisomers **2.66** and **2.67**. Knoevenagel condensation of **2.66** and **2.67** with 1,3-indanedione afforded the isomeric products **2.68** and **2.69** (Figure 2.37).

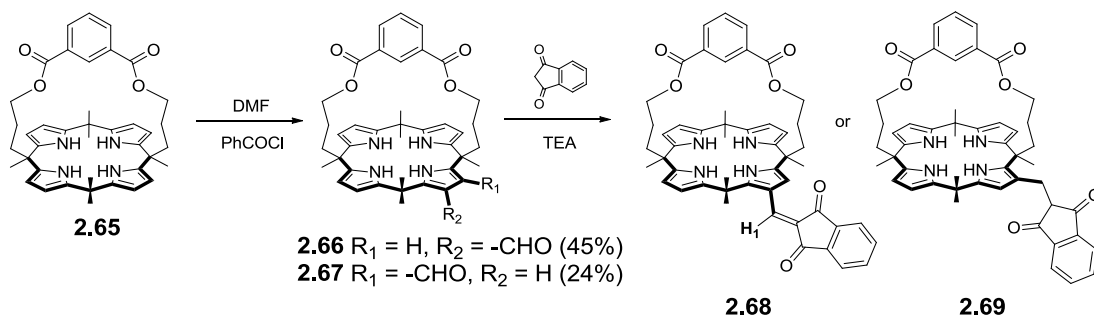


Figure 2.37 : Synthesis of receptors **2.68** and **2.69**.

Anion binding properties of receptor **2.68** was studied with both ^1H NMR spectroscopy and UV-vis spectrophotometer. While receptor **2.68** has a λ_{max} around 430 nm when titrated with tetrabutylammonium fluoride significant blue shift has been observed. Quantitative absorption spectral analysis of **2.68** revealed an association constant for F^- corresponding to 1.25×10^6 which as high as octamethylcalix[4]pyrrole. During the time dependent UV-vis spectral analysis of receptor **2.68** a color bleaching was observed upon addition of CN^- anion. Experimental efforts revealed that this color bleaching induced by cyanide addition to vinyl subunit.

2.7.2.3 Tetra-TTF calix[4]pyrrole

Attaching of redox-active units into the host molecules is one means of enhancing the guest recognition process via increased donor-acceptor interactions. This enhancement especially needed if the host-guest interaction is constructed through weak, non-covalent interactions and if host is a neutral species. Up to date there are few examples of neutral substrate binding calix[4]pyrroles [50, 51]. Nielsen et al. reported a tetra-TTF calix[4]pyrrole (**2.70**) acting as an effective receptor for neutral electron acceptors, such as 1,3,5-trinitrobenzene (**2.71**), tetrafluoro-*p*-benzoquinone, tetrachloro-*p*-benzoquinone, and *p*-benzo-quinone, in solution [9]. The synthesis of tetra-TTF calix[4]pyrrole is achieved by treating the monopyrrole-TTF [52] with an excess of TFA in a mixture of CH₂Cl₂ and acetone. This gave the tetra-TTF calix[4]pyrrole as a yellow solid in 18% (Figure 2.38).

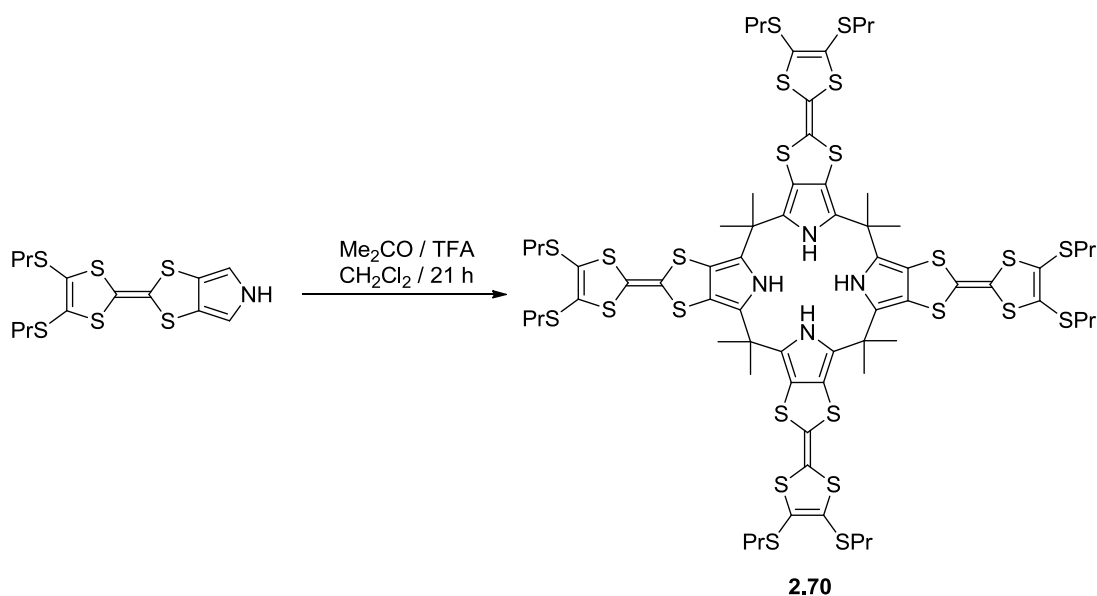


Figure 2.38 : Synthesis of tetra-TTF calix[4]pyrrole.

The interactions between host **2.70** and the electron-deficient guest 1,3,5-trinitrobenzene (**2.71**) was studied in CH₂Cl₂ solution using UV-vis spectroscopy. Addition of 2 equivalent of **41** to a CH₂Cl₂ solution of **2.70** resulted in a fast color change from yellow to green and the appearance (Figure 2.39) [9] of a charge transfer absorption band centered at $\lambda = 677$ nm in the UV-vis spectrum. This observation is thought to reflect the presence of charge transfer interactions between the donor and the acceptor units present in **2.70** and **2.71**, respectively.

Addition of chloride ions to the solution of the complex **2.70+2.71** resulted in a competition between the chloride ions and the electron-deficient guest for hydrogen-

bonding interactions with the NH protons of **2.70** and therefore a competition between the 1,3-alternate conformation and the cone conformation.

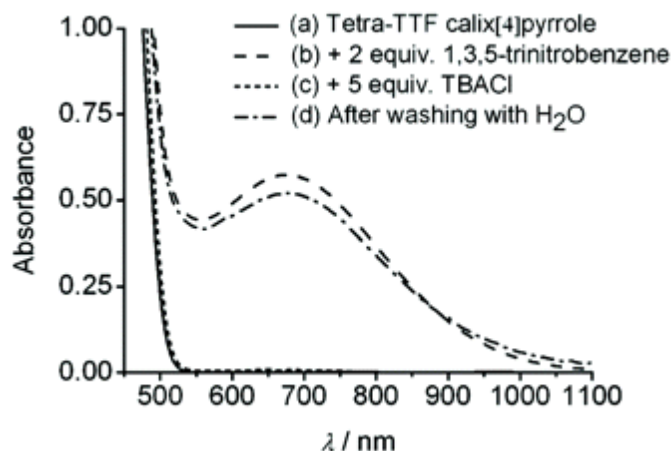


Figure 2.39 : Absorption spectra of tetra-TTF calixpyrrole under different conditions..

However, because of the high binding constant between **2.70** and chloride ions, the equilibrium was largely shifted in favor of the cone conformation. This, in turn, led to the release (Figure 2.40) [9] of the electron-deficient guest **2.71** since the cavities present in **2.70** in its 1,3-alternate conformation were no longer available for binding. Removing the TBACl salt from CH_2Cl_2 solution by washing with H_2O reestablished the charge transfer complex **2.70**+ **2.71**, and as a consequence, the green color of the CH_2Cl_2 solution was regenerated.

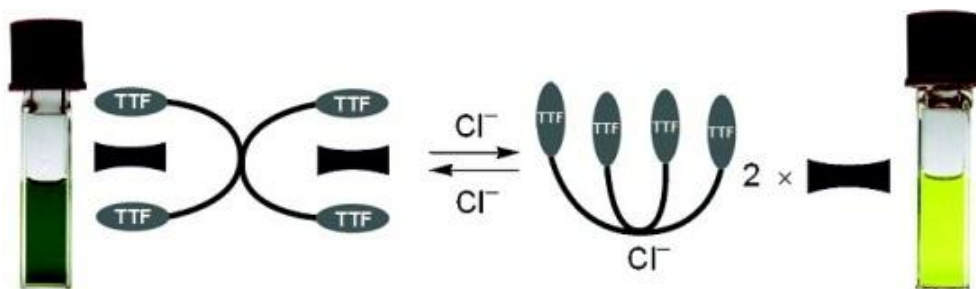


Figure 2.40 : Change in conformation associated with the addition/removal of chloride anion to a CH_2Cl_2 solution of the tetra-TTF calix[4]pyrrole **2.70** and the electron-deficient guest **2.71** (represented by the distorted rectangle).

2.7.2.4 Dipyrrolylquinoxaline strapped calix[4]pyrrole

A calixpyrrole having dipyrrolylquinoxaline moiety can be shown as the another example of calix[4]pyrrole based anion sensors. It is known that 2,3-dipyrrol-2'-yl-6-nitroquinoxaline **2.73** was demonstrated as a colorimetric anion sensor [53]. From this point, combining this class of molecules with calixpyrroles could serve novel colorimetric anion sensors that generally display affinity and selectivity toward

anions that are significantly enhanced relative to simple calix[4]pyrroles. The synthesis of receptor **2.75** starts with ketone **2.72**, a species that was prepared by the reaction of oxalyl chloride with 2 equivalent of 2-(3-oxobutyl)pyrrole. Once in hand, **2.72** was reacted with 1,2-diamino-4-nitrobenzene in the presence of acid to afford diketone **2.73** in 24% yield. Treatment of this latter intermediate with neat pyrrole in the presence of trifluoroacetic acid afforded the bis-dipyrromethane **2.74** in 74% yield. Acid-catalyzed condensation of **2.74** with acetone gave the desired strapped calix[4]pyrroles **2.75** in 7% yield (Figure 2.41) [54].

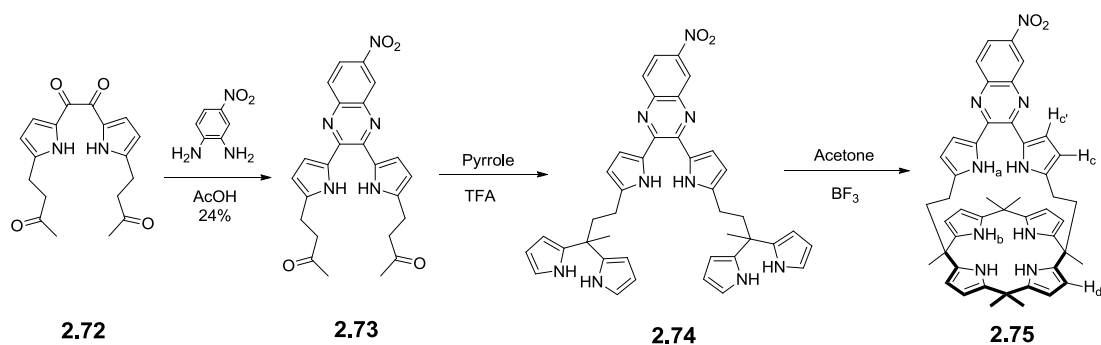


Figure 2.41 : Synthesis of dipyrrolylquinoxaline strapped calix[4]pyrrole.

Initial studies of the anion binding properties of receptor **2.75** were carried out in $\text{CD}_3\text{CN}/\text{DMSO}-d_6$ (9:1 v/v) using proton NMR spectroscopy (Figure 2.42). For instance, the signals corresponding to the pyrrole NH protons on the calix[4]pyrrole moiety, originally appearing at 7.47 ppm, were found to shift to 12.32 ppm and to undergo a splitting; such behavior is completely consistent with the presence of a centrally bound ^{19}F -containing fluoride anion. Likewise, the pyrrole NH signals on the strap, which were found to resonate originally at 9.92 ppm, were seen to shift to 10.34 ppm but to undergo relatively little, if any, splitting in the process. In addition, the β -pyrrole CH signals on the calix[4]pyrrole moiety were seen to shift from 5.99–5.96 to 5.57–5.54 ppm. Finally, the β -pyrrole CH signals of the strap underwent a shift from 6.54–6.49 and 5.80–5.74 to 6.85–6.80 and 5.92–5.90 ppm, respectively.

The strapped calixpyrrole **2.75** undergoes color change upon addition of various anions. Especially, it shows significant color change in the case of fluoride anion. Quantitative UV-vis absorption analysis of the compound **2.75** and fitting the associated changes to a 1:1 binding profile according to the standard methods revealed that the strapped calix[4]pyrrole **2.75** binds fluoride anion much more strongly than octamethylcalix[4]pyrrole and the other anions inspected. However,

the association constants for chloride and bromide anions smaller than those of the octamethylcalix[4]pyrrole.

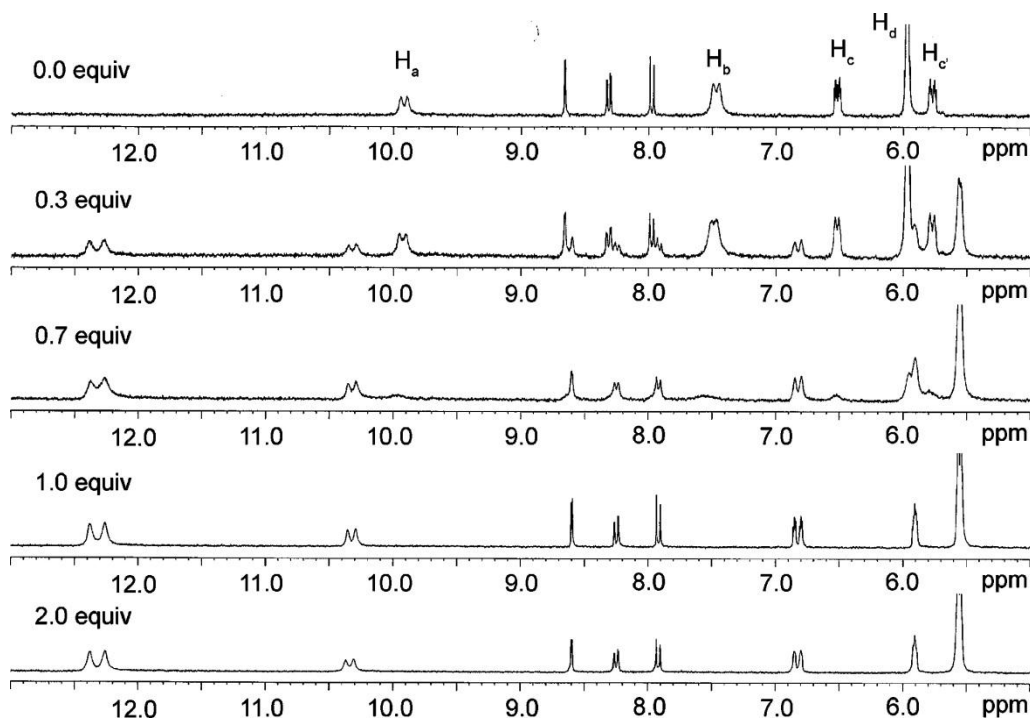


Figure 2.42 : ¹H NMR spectral changes of receptor **2.75** seen upon titration with F⁻ (as its tetrabutylammonium salt) in CD₃CN/DMSO-*d*₆ (9:1 v/v).

2.7.2.5 Chromogenic units attached *N*-confused calix[4]pyrroles

Recently, works on electrophilic aromatic substitution of calixpyrroles have led several research groups to investigate various electrophiles, including Vilsmeier–Haack formylation agent (electrophilic iminium cation), tetracyanoethane, and diazonium salts to obtain chromogenic calixpyrrole derivatives. Substitution at the β-position of calix[4]pyrroles is often difficult and separation of the product mixtures is very problematic. On the contrary, substitution at the α-position of the pyrrole ring is easier. Moreover, in a recent work it has been shown that octamethylcalix[4]pyrroles and its corresponding *N*-confused isomers could show unique features stemming from a different structure and different *pK_a* of hydrogen-bond donors [55]. Anzenbacher and co-workers reported the synthesis, structures, and anion-binding properties of chromogenic *N*-confused calix[4]pyrroles [56]. The structures of the isomers **2.76** and **2.77** are shown in Figure 2.43.

Azo-substituted **2.76** was prepared by electrophilic substitution using 4-nitrobenzenediazonium tetrafluoroborate in THF in the presence of triethylamine yielded **2.76** in 30%. Tricyanoethylene substituted **2.77** was also prepared by

electrophilic substitution of N-confused calix[4]pyrrole with tetracyanoethylene in 36% yield.

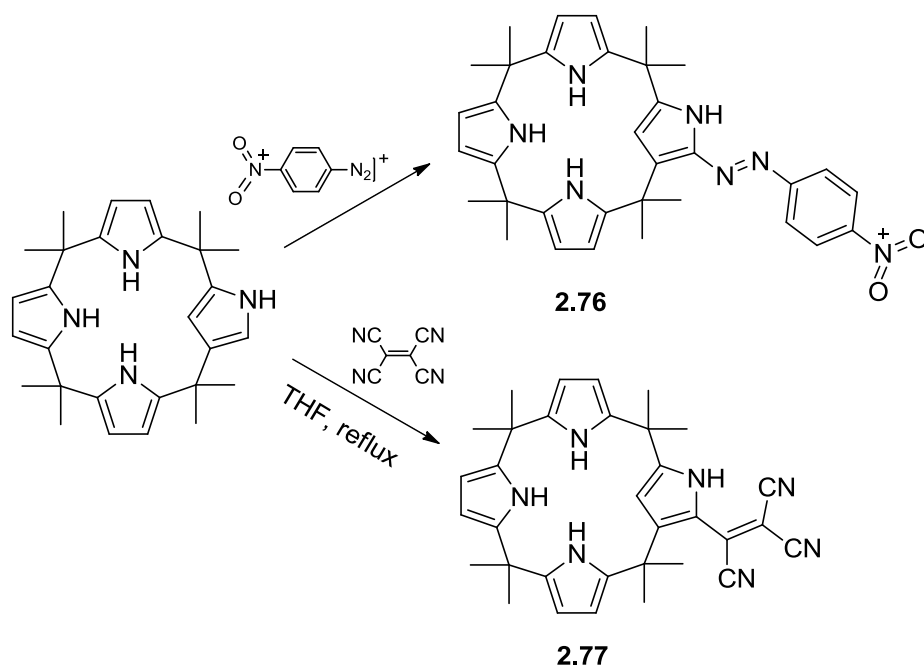


Figure 2.43 : Modification of N-confused calix[4]pyrroles.

Authors reported that ^1H NMR spectrum of the compound **2.77** showed only three broad pyrrole NH singlet signals instead of four broad pyrrole NH singlets. Absence of fourth NH signal indicated a substitution of the α -pyrrole position with the tricyanoethylene moiety. NMR spectra also suggested that the compound **2.77** shows an intramolecular cyclization with tricyanoethylene moiety with the confused pyrrole nitrogen. They observed a sharp singlet at 11.16 ppm corresponding to an imine proton. The intramolecular cyclization product containing bicyclic pyrrolizin-3-ylideneamine moiety was also supported by single crystal X-ray analysis (Figure 2.77).

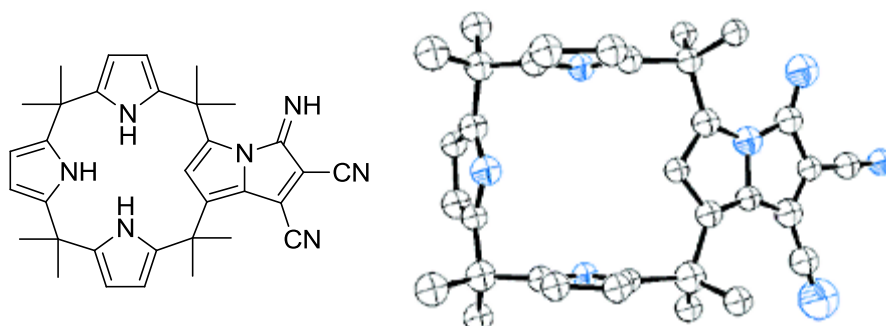


Figure 2.44 : Tautomer form of **2.77**.

Addition of anions to DMSO solutions of receptors **2.76** and **2.77** induced color changes which were supported by UV-vis spectrophotometer. For instance, upon

addition of 10 equivalents of fluoride and chloride anions, in the form of their tetrabutylammonium salts, to 5×10^{-5} M solutions of **2.77** resulted dramatic color changes. The same trend was also observed for the receptor **2.76** (Figure 2.45) [56].

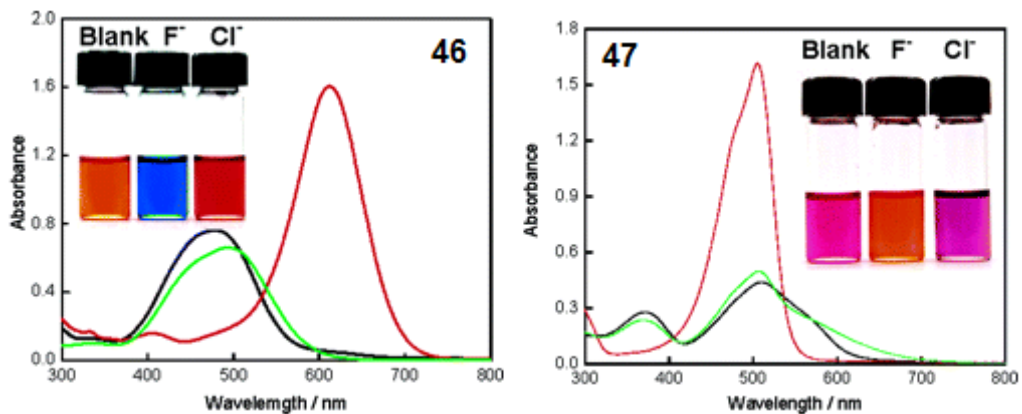


Figure 2.45 : Absorption spectra of **2.76** and **2.77** upon addition of fluoride and chloride anions. Insets: Solutions of **2.76** and **2.77** in the absence and presence of anionic species.

2.7.3 Calix[4]pyrrole based electrochemical sensors

The development of redox-active receptors containing a guest binding site connected to a redox-active reporter group is one of the important fields of supramolecular chemistry.

2.7.3.1 Ferrocene appended calix[4]pyrroles

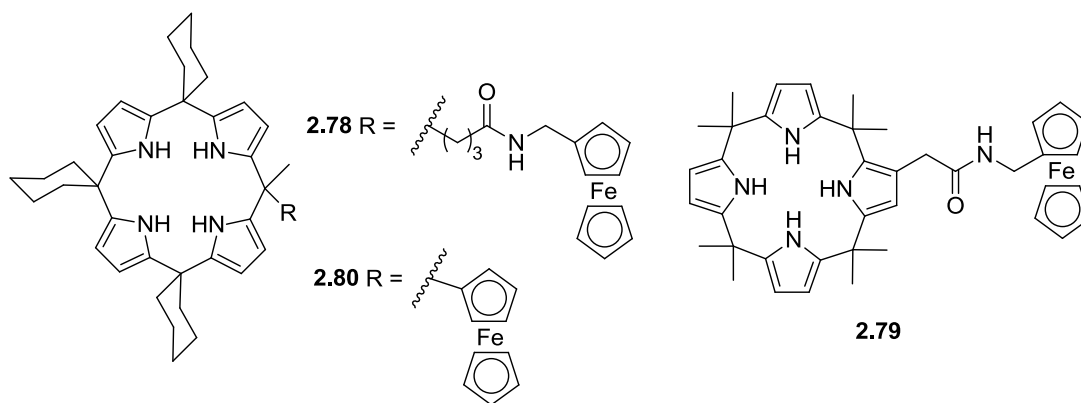


Figure 2.46 : Ferrocene appended calix[4]pyrrole derivatives.

As a part of calixpyrrole chemistry, appending anion receptor to a redox-active ferrocene group was achieved by Sessler et al [57]. It was thought that this would allow the solution phase anion binding properties of calixpyrroles to be studied using electrochemical techniques. By this purpose, aminomethyl-ferrocene was coupled to calix[4]pyrrole mono-acid derivatives using the BOP amid coupling reagent. Both

meso-bridged and C-rim bridged calix[4]pyrrole derivatives **2.78** and **2.79** was successfully prepared while an alternative system, **2.80**, was synthesized via a mixed condensation of pyrrole, cyclohexanone, and acetylferrocene [58]. These systems are shown in Figure 2.46.

Table 2.8 : Association constants and Fc/Fc⁺ redox potentials for compound **2.80** with various anionic guest species.

Anion ^a	K _a (M ⁻¹) ^b	E _{1/2} (Fc/Fc ⁺) (mV) versus Ag/AgCl ^c	ΔE(mV)
No anion	n/a	+444	n/a
F ⁻	3 375	+368	-76
Cl ⁻	3 190	+408	-36
Br ⁻	50	+432	-12
H ₂ PO ₄ ⁻	304	+350	-100
HSO ₄ ⁻	n/a	+436	<10

^a Used in the form of their (*n*-Bu₄N)⁺ salts.

^b Errors estimated <20%. Measured in acetonitrile-*d*₃/DMSO-*d*₆ 9:1 (v/v).

^c E_{1/2} values obtained from squarewave and cyclic voltammetric techniques.

Binding studies of the compound **2.80** were carried out using ¹H NMR titration techniques in DMSO-*d*₆/acetonitrile-*d*₃ (1:9 v/v), and the association constants being elucidated using the EQNMR computer program [59]. The results are shown in Table 2.8 and reveal that compound **2.80** coordinates fluoride, chloride and dihydrogen phosphate in the solvent mixture studied. It was reported that the NH proton resonances broadened during the titrations making them unsuitable for the calculation of the association constants. However, one ferrocene CH resonance shifted downfield allowing for the calculation of K_a and providing evidence for the formation of CH...anion hydrogen bonds in solution (Figure 2.47).

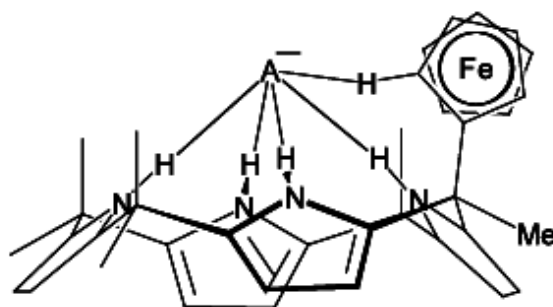


Figure 2.47 : Schematic representation of the ferrocene CH and calixpyrrole NH hydrogen-bonding interactions of the receptor **2.80**.

Electrochemical studies of the receptor **2.80** were carried out in acetonitrile/DMSO (9:1 v/v) and the results are shown in Table 2.9 [47]. Among the halide anions, binding of fluoride induces the largest cathodic shift in the ferrocene/ferrocenium

couple (76 mV), followed by chloride (36 mV) and bromide (12 mV). Dihydrogen phosphate causes to a shift cathodically by approximately 100 mV.

Table 2.9 : Association constants for compounds **2.78** and **2.79** in DCM and electrochemical parameters obtained from CV measurements.

Anion ^a	2.78			2.79		
	$K_a(\text{mol}^{-1} \text{dm}^3)^b$	$E_{1/2}(\text{mV})^c$	$\Delta E(\text{mV})^d$	$K_a(\text{mol}^{-1} \text{dm}^3)^b$	$E_{1/2}(\text{mV})^c$	$\Delta E(\text{mV})^d$
No anion	n/a	511	n/a	n/a	503	n/a
H_2PO_4^-	40 ^e	502	-9	40	534	31
F^-	n/d ^f	525	14	1496	566	63
Cl^-	202	718	207	444	481	-22

^a Used in the form of their (*n*-Bu₄N)⁺ salts.

^b Association constants for anion binding; recorded in dichloromethane-*d*₂ errors <20%; determined from $\Delta(\delta)$ (ppm) NH.

^c Determined in dichloromethane containing 0.1 mol dm⁻³ (*n*-Bu₄NPF₆) as the supporting electrolyte. Solutions of 41/42 were 5×10⁻⁴ mol dm⁻³ and potentials were determined with reference to Ag/AgCl.

^d Shifts determined by square wave voltammetry.

^e This value was determined using the chemical shift of the β-CH of the pyrrole since the pyrrole-NH signal became too broad to be followed accurately during the titration.

^f NMR signals became very broad in this case so that an accurate determination of this value was impossible.

Association constants of **2.78** and **2.79** were also elucidated using ¹H NMR spectroscopic titration methods. Results showed that the expected affinity series inferred to $\text{F}^- > \text{Cl}^- > \text{H}_2\text{PO}_4^-$. Both ¹H NMR titration and electrochemical experiment results for the receptors **2.78** and **2.79** are presented in Table 2.9.

2.7.3.2 Calix[4]pyrrole modified electrodes

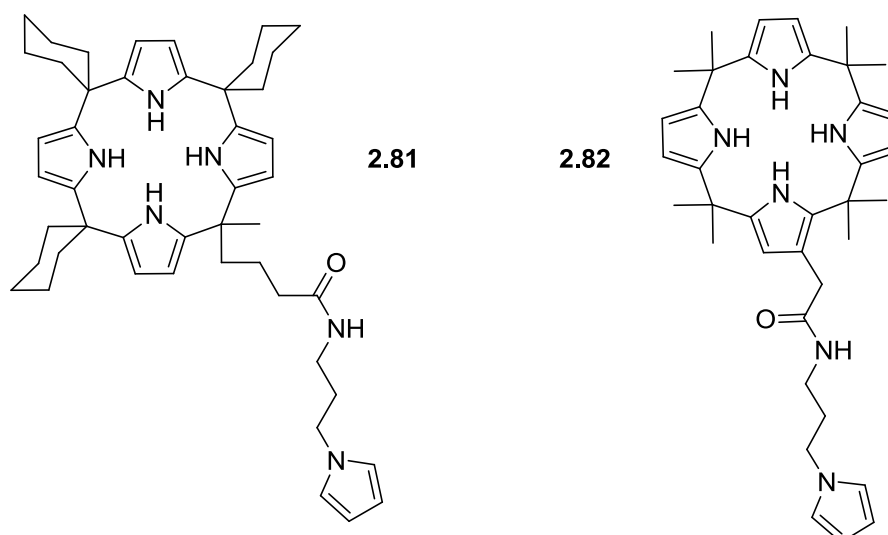


Figure 2.48 : Calix[4]pyrrole appended α -free pyrrole derivatives.

An incentive method to the production of calixpyrrole modified electrode is by the production of an electropolymerized matrix formed via a receptor bound

electropolymerizable moiety. It is well known that pyrrole rings that do not carry substituents in the 2- and 5-positions are polymerizable electrochemically via either potential cycling or chronoamperometry. Inspiring from this, chemically modified electrodes were prepared from calix[4]pyrrole monomers containing α -free pyrrole units. α -Free pyrrolic compounds **2.81** and **2.82** (Figure 2.48) were synthesized using the similar methods those affiliated to prepare **2.78** and **2.79**. Precisely, they were prepared via coupling the relevant calix[4]pyrrole mono-acid compounds with 3-aminopropylpyrrole using the BOP amide coupling reagent [60].

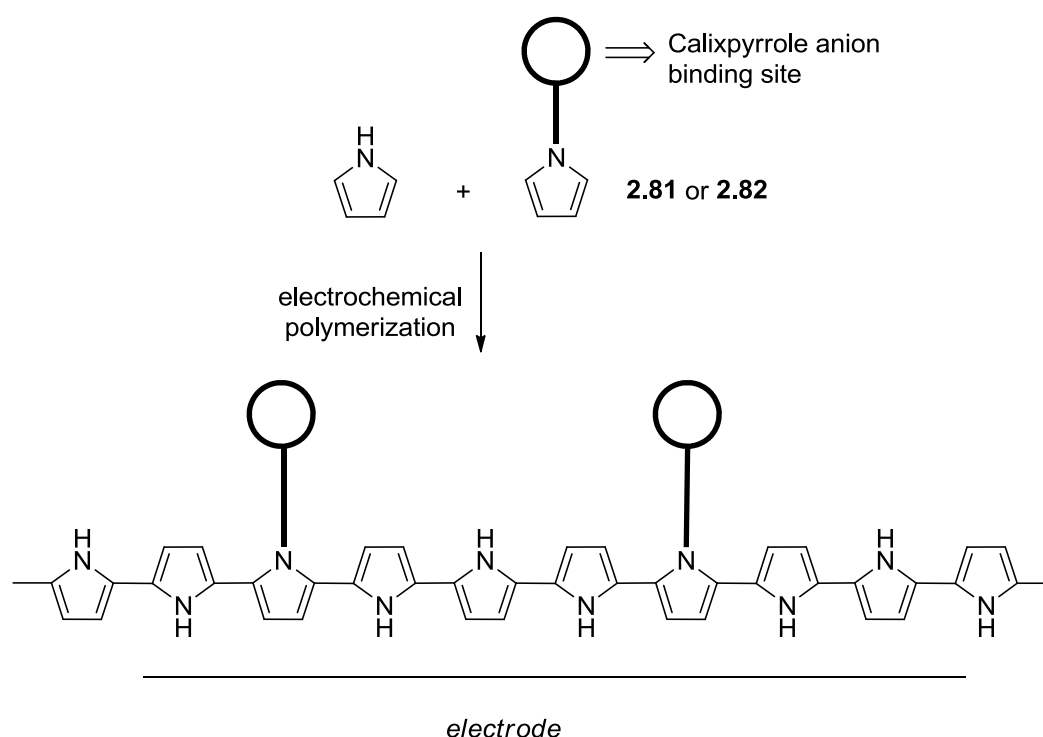


Figure 2.49 : Electrochemical copolymerization of pyrrole and calix[4]pyrrole appended α -free pyrroles.

After preparation of the calix[4]pyrrole appended α -free pyrrole derivatives **2.81** and **2.82**, efforts were devoted to prepare their conducting polymers *via* electrochemical polymerization techniques. First attempt was made by using cyclic voltammetric methods. Unfortunately this process did not produce a conducting polymer, as judged from the fact that current waves prior to monomer oxidation did not seem to increase with the number of cycles. In contrast, during the forward and backward potential scans the current was seen to decrease with each consecutive cycle. Controlled potential electrolysis was also utilized to obtain desired polymer films but this method was also failed. Authors speculated that this is due to the unfavorable steric interactions associated with N-substituents precluding film growth. After experiencing an unsuccessful attempt, polymerization of the calixpyrrole monomers

was carried out in the presence of pyrrole which thought to act as a spacer unit for reducing the potential steric interactions (Figure 2.34). The CV results of **2.81 + pyrrole** and **2.82 + pyrrole** revealed that during potential cycling an increasing current was observed indicating the in situ generation of conducting polymers. To confirm that co-polymerization of pyrrole and calixpyrroles had indeed occurred, CVs of the presumed co-polymers were compared to those obtained from a solution containing an equivalent concentration of pyrrole. It was found that both a higher initial oxidation current and a faster current increase with the number of cycles were observed in the case of the mixed polymer systems, results that are consistent with the participation of the calix[4]pyrrole subunits in the polymerization process.

2.8 Measurement Methods of Anion Binding Constants

In the field of anion receptor chemistry, a variety of techniques have been employed to measure the association constants of hosts (receptors) interacting with guests (anions). Before introducing various measurement methods, it is necessary to consider a basic question: “What is an association constant?” In terms of the host-guest terminology, association constants generally expressed as stability, binding, and equilibrium constants. Based on the following chemical equilibrium,



It is generally considered that when the rates of the forward and reverse reactions are equal (i.e., equilibrium is attained), the concentration of the host, guest, and host-guest complex will remain constant with time. Under these conditions, the equilibrium expression can be written and the corresponding association constant (K_a) can be calculated. For the simple equilibrium given above, the general expression of K_a is:

$$K_a = \frac{[HG]}{[H][G]} = \frac{k_1}{k_2} = \frac{1}{K_d} \quad (2.2)$$

,where [H] is the concentration of the free host, [G] is the concentration of free guest, [HG] is concentration of the pure host-guest complex, k_1 the rate constant for the forward reaction, k_2 is the rate constant for the back reaction, and K_d is the dissociation constant. To measure quantitative K_a values, so-called titrations are often performed. These are carried out by using one or more of a variety of spectroscopic or calorimetric tools, including ^1H NMR spectroscopy (or spectroscopy

involving another NMR detectable nuclei), UV-vis absorption spectroscopy, fluorescence emission spectroscopy, or isothermal titration calorimetry (ITC). Each of these techniques looks at a different part of the binding process and/or overall equilibrium. For instance, titrations involving ^1H NMR spectroscopy that involved monitoring the *NH* proton shifts in, e.g., amide- or pyrrole-type receptors, provide insights into the direct interaction of the anion with the hydrogen bond donor subunits of the receptor. By contrast, UV-vis and fluorescence spectroscopy reflect changes in the optical properties of the light absorbing/emitting portions of the receptor (including any appended chromophore), whereas ITC provides information about the change in the energy of the system as a whole. These techniques often operate over different sensitivity ranges, typically 10^{-3} M for NMR spectroscopy, 10^{-4} for ITC, and 10^{-5} or lower for UV-vis and fluorescence spectroscopy.

Measurements are often made in a range of different solvents and the polarity of the solvent often has a direct effect on the binding affinities, with, in general, the affinities being considerably higher in less competitive aprotic organic solvents. In such latter solvents, studies involving tetrabutylammonium anion salts are common. This is due to the high solubility of these salts in organic solvents. However, these salts are difficult to keep dry, being in some cases extremely hygroscopic. In addition to concerns involving salt purity, assumptions are made about ion pairing in solution that may not be valid. For example, tetrabutylammonium is generally regarded as an 'innocent' counter cation with little tendency to form ion pairs in solution. This assumption is incorrect and, in fact, it has been suggested that 1 mM solutions of tetrabutylammonium chloride in dichloromethane are less than 20% dissociated at 22°C [61]. Therefore, going from one solvent to another can change not only the strength of the interaction between the anion and receptor, but also the degree of ion pairing in solution between the anion and its counter cation. What this means is that when comparing data sets of binding constants across a range of receptors, it is essential that the binding studies be conducted under identical conditions (e.g., temperature, solvent, concentration, and even measurement method).

In this part of the thesis a brief discussion of a few analytical techniques commonly used in the area of calix[4]pyrrole-based anion recognition, namely NMR, UV-Vis, and fluorescence spectroscopies, as well as ITC measurements is provided, along with some of the underlying assumptions inherent to their practical application.

2.8.1 Sample preparation

To achieve accurate association constants, it is very important to choose an appropriate concentration range for the sample being subject to analysis. In the case of standard ^1H NMR spectroscopic titrations, wherein the change in the chemical shift of one or more proton signals are monitored as a function of anion (actually anion counter cation salt) concentration (vide infra), Wilcox proposed that the most reliable titration curves can be obtained when the concentration range of the sample is chosen to be in a numeric range of 1 to 10 times the dissociation constant K_d ; units of M. In other word, $K_a \times [\text{S}] = 1$ to 10, where K_a is the association constant and $[\text{S}]$ is the molar concentration of the sample [62]. However, a concentration range given by $K_a \times [\text{S}] = 10$ to 50 has been suggested as being the best for ITC-based studies. To allow for a correct comparison of results obtained from these two methods, it is clear that choosing a proper (i.e., overlapping) sample concentration from the outset of the study will be helpful.

2.8.2 NMR spectroscopy

NMR spectroscopic titrations constitute one of the techniques most widely used to determine the association constants (K_a) for host-guest interactions. The advantage of NMR compared to other spectroscopic techniques (i.e., UV-vis and fluorescence) is that more extensive structural information is potentially forthcoming with regard to, e.g., the nature of the host-guest interaction. On the other hand, its low detection limit blocks reliable measurement of strong host-guest interaction cases (i.e., $K_a > 10^5 \text{ M}^{-1}$). Often, the concentration for NMR titration (i.e., $\sim 10^{-3} \text{ M}$) is too high to make the proper host or guest solution.

Various equations have been developed to facilitate the fitting process that have paralleled (or at least taken advantage of) advances in computer technology. For instance Wilcox and Cowart reported a curve fitting equation (2.3) in 1986 [62]. This equation was designed for calculation of K_d (cj. $1/K_a$) values for the interaction between a synthetic host and a guest.

$$\delta_{obs} = \delta_H + \frac{\delta_{HG} - \delta_H}{2[H]_t} \left[\frac{1}{K_a} + [H]_t + [G]_t - \sqrt{\left(\frac{1}{K_a} + [H]_t + [G]_t \right)^2 - 4[H]_t[G]_t} \right] \quad (2.3)$$

Here, $[H]_t$ is the total concentration of host, which in the experimental set-up for which this equation is designed is also the compound whose resonances (one or more) are being monitored by NMR spectroscopy; $[G]_t$ is the total concentration of the guest, and δ is chemical shift. This equation can be only applied to systems where a 1:1 host-guest stoichiometry pertains and the establishment of equilibrium is fast on the NMR time scale. Usually, both $[H]_t$ and $[G]_t$ are varied linearly at the same time. However, this equation may also be applied if only one of term (i.e., just $[H]_t$ or just $[G]_t$) is varied and the other kept constant.

Another equation (2.4) for the calculation of 1:2 host-guest stoichiometry was reported by Connors providing a different approach for line fitting [63].

$$\delta_{obs} = \frac{(\delta_{HG} - \delta_H)K_{a1}[G]_t + (\delta_{HG_2} - \delta_H)K_{a1}K_{a2}[G]_t^2}{1 + K_{a1}[G]_t + K_{a1}K_{a2}[G]_t^2} + \delta_H \quad (2.4)$$

2.8.3 Optical methods

As one of the most popular methods, optical techniques have broad detection limits over 10^7 M^{-1} and is easy and quick process to measure association constants. However, it is recommended performing many background experiments as much as possible. There are many facts having the ability of changing color of host or guest solution (i.e., pH, aggregation of host or guest, and so on). Particularly, some of anions are basic and most of neutral anion receptors have acidic protons. Even, it is small acid-base interaction; their effect toward optical changes during the titration cannot be ignored. Additionally, either host or guest molecule must have chromophore units; otherwise no spectral change will be detected.

2.8.3.1 UV-vis spectroscopy

Spectroscopy in the ultraviolet and visible regions of the spectrum involves observing transitions associated with the excitation of electrons. An electron is excited if the frequency of the incident electromagnetic radiation matches the difference in energy between two electronic states. This energy difference depends on the electronic structure and environment of the molecule being investigated.

Bouguer, Lambert, and Beer discovered a relationship between the concentration of sample, the path length of the sample, and the absorbance A [64]. This relationship is expressed by the Lambert-Beer-Bouguer law:

$$A = \epsilon bc \quad (2.5)$$

, where A is the absorbance, ε is absorption coefficient, and c is the concentration of studied specie.

Connors introduced two simple equations (2.6 and 2.7) for equilibriums involved to 1:1 and 1:2 host-guest binding motifs.

For a 1:1 host-guest interactions,

$$\frac{\Delta A}{l} = \frac{[H]_t K_a \Delta \varepsilon [G]_t}{1 + K_a [G]_t} \quad (2.6)$$

, where $\Delta A = A - A_0$, $\Delta \varepsilon = \varepsilon_{HG} - \varepsilon_H - \varepsilon_G$, $[H]_t$ is the total concentration of host, $[G]_t$ is the total concentration of guest, and l is path length of solution studied in.

For a 1:2 host-guest case,

$$\frac{\Delta A}{l} = \frac{[H]_t (K_{a1} \Delta \varepsilon_1 [G]_t + K_{a1} K_{a2} \Delta \varepsilon_2 [G]_t^2)}{1 + K_{a1} [G]_t + K_{a1} K_{a2} [G]_t^2} \quad (2.7)$$

, where $\Delta A = A - A_0$, $\Delta \varepsilon_1 = \varepsilon_{HG} - \varepsilon_H - \varepsilon_G$, and $\Delta \varepsilon_2 = \varepsilon_{HG2} - \varepsilon_H - \varepsilon_G$.

2.8.3.2 Fluorescence spectroscopy

In comparison to methods based on absorption spectrometry (i.e. UV-vis), the use of corresponding fluorescence techniques offers an enhancement in sensitivity by a factor of roughly 100-1000. Ideally, the Lambert-Beer-Bouguer law is fully applicable to an understanding of fluorescence titrations. This is because the fluorescence intensity (F) is directly related to the concentration of sample (c) of fluorescent molecules in solution, at least at low concentrations ($F = 2.3 \times I_0 \times \phi \times \varepsilon \times l \times c$, where I_0 is the intensity of the excitation source, ε is the molar absorption at the excitation wavelength, l is the path length of solution, and ϕ is the fluorescence quantum yield).

Like UV-vis titration methods, the use of fluorescence quenching to determine K_a values has been extensively studied. Among the typical equations used for the treatment of typical fluorescence quenching-based titration data is the one introduced by Connors (2.8) [63].

$$F = \frac{1 + \left(\frac{k_{HG}}{k_H}\right) K_a [G]_t F_0}{1 + K_a [G]_t} \quad (2.8)$$

, where the “constant” k represents a complicated mix of several factor and F_0 is the initial fluorescence intensity.

2.8.4 Isothermal titration calorimetry

Calorimetry is one of the oldest experimental techniques in chemical science; the most familiar example is the ice calorimeter, already in use by the end of 18th century and developed further into a precision instrument about 100 years later by Bunsen. For the past several decades, basically three different types of microcalorimeters, bath, flow, and titration calorimeters, have been developed and used. The term “isothermal titration calorimetry” is commonly used for calorimeters designed for titrations carried out under essentially isothermal conditions. The meaning of “isothermal” is normally an indication that the temperature of the calorimeter is precisely constant with aid of electrical compensation and other methods. The ITC either measures directly the binding thermodynamics (i.e., ΔH , $T\Delta S$, ΔG , and K_a) of host-guest interactions or permits their ready calculation by detecting the heat absorbed (endothermic process) or released (exothermic process) at constant temperature. In fact, it is only ΔH that is obtained directly, with ΔG , and K_a coming as the result of modeling the experimental data to a binding profile, a process that permits the calculation of $T\Delta S$. Thus, the choice of curve fit methods and model(s) for the proposed equilibrium events underlying the experimental observations is absolutely critical. If this is not done correctly, ITC can produce numbers that have little physical meaning.

Comparing to the other methods, the detection limit of ITC is located between NMR and optical method. However, ITC can detect system globally and provide thermodynamic parameters with association constants. Therefore, trivial interaction or factor can give a rise huge interruption for measuring host-guest interactions. In other words, the titrations need to be performed under well-fined conditions.

Basic schematic illustration of the ITC instrument (A) inset to Figure 2.50 [65], showing the two cells (sample and reference) surrounded by the thermostatic jacket, the injection syringe that also works as stirring device, and the computer-controlled thermostatic and feedback systems (using Peltier and resistor devices as sensor and actuator subsystems). (B) Example of a typical ITC experiment. The top panel shows the sequence of peaks, each one corresponding to each injection of the solution in the syringe. The monitored signal is the additional thermal power needed to be supplied or removed at any time to keep a constant temperature in the sample cell and as close as possible to the reference cell temperature. This example

corresponds to an endothermic binding. The bottom panel shows the integrated heat plot. The areas under each peak, calculated and normalized per mole of ligand injected in each injection, are plotted against the molar ratio (quotient of the total concentrations of ligand and macromolecule in the sample cell). From this plot, and applying the appropriate model, the thermodynamic parameters of the binding can be obtained: binding affinity, binding enthalpy, and stoichiometry.

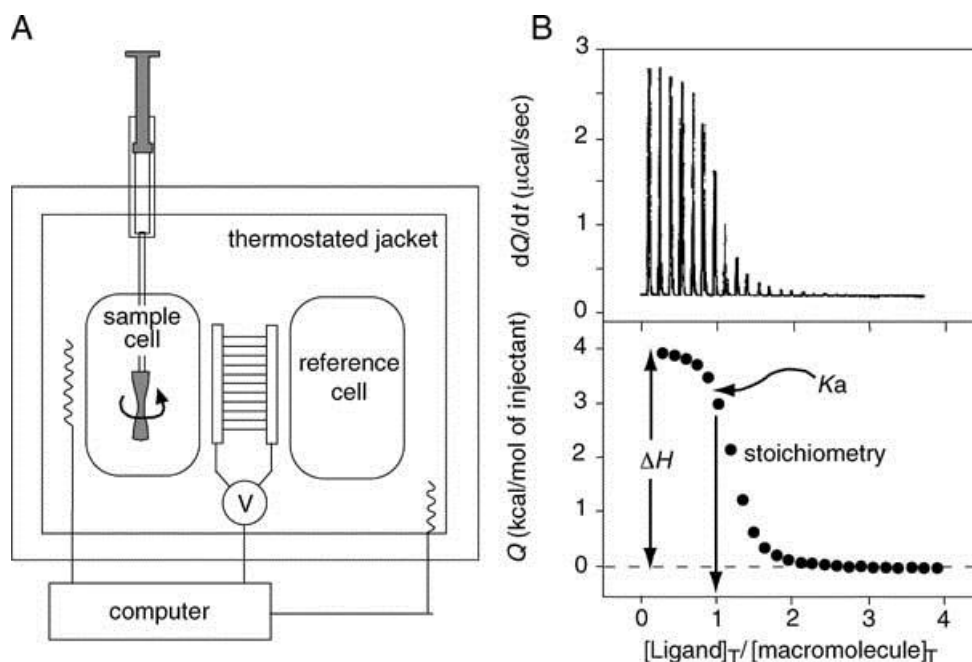


Figure 2.50 : Basic schematic illustration of the ITC instrument.

Although several approaches have been reported for curve fitting to the data obtained from an ITC experiments, in this dissertation, following equations provided by MicroCal VP-ITC manual have been used to evaluate both the various ITC-based K_a values and associated thermodynamic parameters. According to this, total heat content Q was calculated by;

$$Q = \frac{[H]_t \Delta H V_0}{2} \times \left[1 + \frac{[G]_t}{[H]_t} + \frac{1}{K_a [H]_t} - \sqrt{\left(1 + \frac{[G]_t}{[H]_t} + \frac{1}{K_a [H]_t} \right)^2 - \frac{4[G]_t}{[H]_t}} \right] \quad (2.9)$$

, where Q is the total heat content, V_0 is the active cell volume. Heat content of every single injection calculated by;

$$\Delta Q(i) = Q(i) + \frac{\Delta V_i}{V_0} \left[\frac{Q(i) + Q(i-1)}{2} \right] - Q(i-1) \quad (2.10)$$

, where ΔV_i is the injection volume and ΔQ_i is the heat content from the i^{th} injection.

Four steps are required to complete the analysis once experimental data is in hand. The first involves in putting initial guesses for the values of K_a , and ΔH into equation **2.9**; the second, is the calculation of $\Delta Q(i)$ for each injection and comparison of these values with the observed heats (equation **2.10**); the third step involves in putting improved values of K_a and ΔH to equation **2.9** and the fourth step involves repeating these first three steps iteratively until no further significant change in the value of the parameters is observed. This process including multiple binding cases is now automated and may be done by computer; in the case of the present work, it was performed by Origin® software provided by the manufacturer.

2.8.5 Job Plots

Job's plot also known as continuous variation plot is a well-known and useful tool for the determination of stoichiometries for any kind of complexes. This method finds application in various analytical techniques including ^1H NMR, UV-vis, and fluorescence spectroscopy. In each case, the Job plot is based on the spectral changes obtained for either host or guest.

Let assume a generic reaction,



In this method, the total molar concentration of the two binding partners (e.g. a calix[4]pyrrole and an anion) are held constant, but their mole fractions are varied. An observable that is proportional to complex formation (such as absorption signal or resonance change in NMR) is plotted against the mole fractions of these two components. The maximum at a mole fraction of 0.3, 0.5, and 0.6 indicates formation of a 1:2, 1:1, and 2:1 host:guest complex (Figure 10.1).. This method is named after P. Job, who first introduced this methodology in 1928 [66].

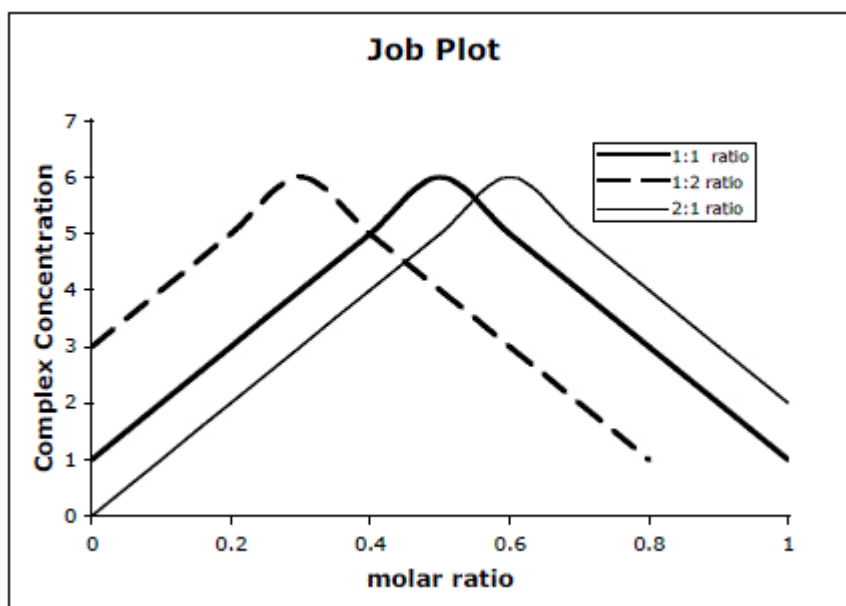


Figure 2.51 : Example of a Job plot.

3. EXPERIMENTAL SECTION

3.1 General

Melting points were measured on a Mel-Temp II instrument and are uncorrected. Proton and ^{13}C -NMR spectra used in the characterization of products were recorded on Varian Unity 300, 400 MHz and Bruker 250 MHz spectrometers. Low-resolution FAB and CI mass spectra were obtained on a Finningan MAT TSQ 70 mass spectrometer. High resolution FAB and CI mass spectra were obtained on a VG ZAB2-E mass spectrometer. GPC analyses were performed using a Waters HPLC system consisting of HR-1, HR-3, and HR-5E Styragel® columns arranged in series, a 1515 pump, and a 2414 RI detector; reported molecular weights are relative to polystyrene standards in DMF (0.01 M LiBr) at 40 °C (column temperature). Thermogravimetric analyses were performed using a Mettler Toledo TGA/SDTA851e equipped with a TSO801RO sample automated loader. A Varian SpectrAA-40 Atomic Absorption Spectrometer was used in flame emission mode with an acetylene/air (18:2) mixture to quantify the extracted potassium salts; the samples for these measurements were diluted with ethyl acetate prior to recording the emission intensities at 766.5 nm. UV-vis analyses were performed with a Chebios Optimum-One UV-vis spectrophotometer.

3.2 Materials

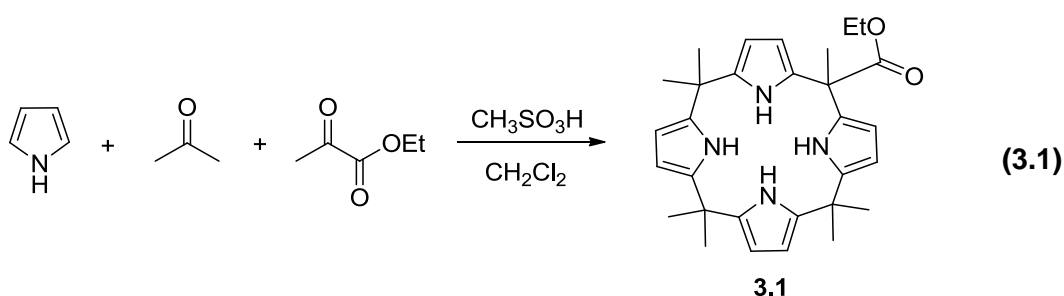
Tetrabutylammonium chloride (TBACl) and tetrabutylammonium acetate (TBAOAc) were dried under vacuum at 40°C for 24 h before use. All solvents were dried before use according to standard literature procedures. Unless specifically indicated, all other chemicals and reagents used in this study were purchased from commercial sources and used as received.

3.3 ITC Titration Studies

Microcalorimetric titrations were performed using an isothermal titration calorimeter (ITC) purchased from Microcal Inc., MA. Experimental temperature is 25 °C. The ORIGIN software provided by Microcal Inc. was used to calculate the binding constants (K_a) and the enthalpy change (ΔH). The solvent, CH_2Cl_2 , was HPLC grade (Fisher) but was not further dried or purified before use.

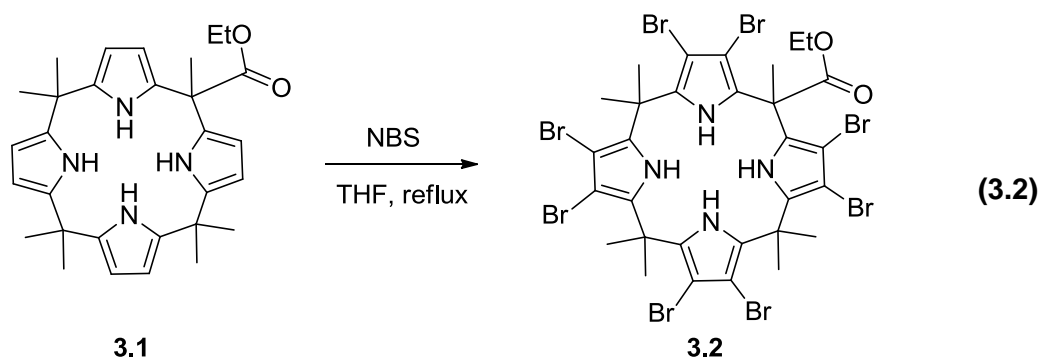
3.4 Synthesis of Calix[4]pyrroles with Long Alkyl Chains

3.4.1 Monoester functional calix[4]pyrrole



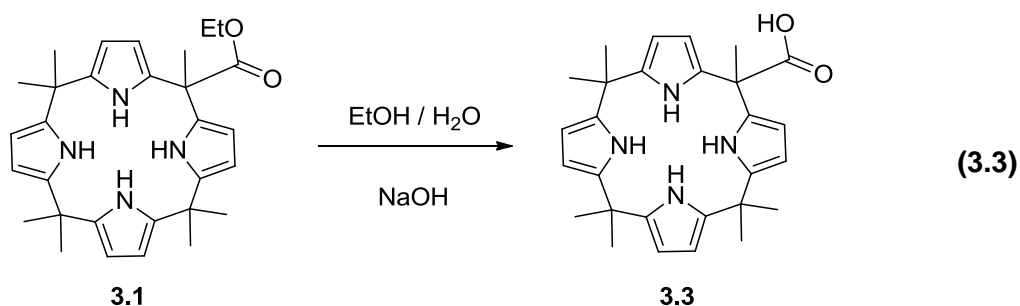
Pyrrole (3 mL, 42 mmol) and ethyl pyruvate (1.15 mL, 10 mmol) were dissolved in methanol (50 mL) at 0°C and bubbled with Ar for 10 minutes. Acetone (2.34 mL, 30 mmol) was then added to the mixture. Following this addition, methanesulfonic acid (1.95 mL) was added drop-wise over the course of 10 minutes while shielding the reaction vessel from light. The mixture was then stirred first at 0°C for 3 hours and subsequently at room temperature overnight. The white precipitate that formed during this time was collected by filtration. Chromatographic purification (silica gel, dichloromethane/hexanes: 80/20) yielded calixpyrrole **3.1** as a yellow solid (0.7 g, 14%). M.p. decomposes over 200°C; ¹H NMR (300 MHz, CDCl₃, 25°C): δ = 1.28 (t, *J* = 7.2 Hz, 3H; ester CH₃), 1.49–1.51 (m, 18H; meso CH₃), 1.72 (s, 3H; meso CH₃), 4.21 (q, *J* = 7.2 Hz, 2H; ester CH₂), 5.89–5.93 (m, 8H, pyrrole-CH), 7.169 (br.s, 2H, pyrrole NH), 7.49 ppm (br. s, 2H, pyrrole NH); ¹³C NMR (75 MHz, CDCl₃, 25°C): δ = 14.11, 25.07, 28.26, 29.00, 29.36, 29.68, 35.20, 35.27, 47.31, 61.58, 102.80, 103.03, 103.12, 104.98, 131.76, 138.20, 138.63, 139.18, 167.12 ppm; LRMS (FAB MS): *m/z* [M⁺]: 486; HRMS (FAB MS): *m/z* calcd for C₃₀H₃₈N₄O₂ [M⁺]: 486.2995; found: 486.2997. This compound was further characterized by single crystal X-ray diffraction analysis.

3.4.2 Monoester octabromocalix[4]pyrrole



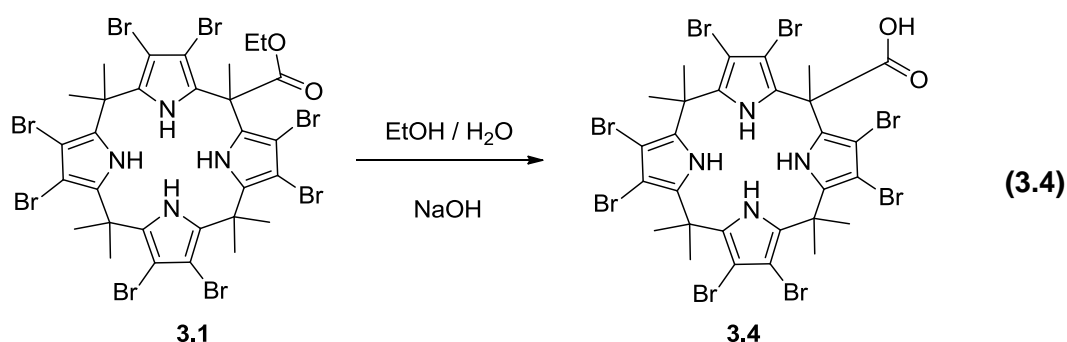
Calixpyrrole **3.1** (0.46 g, 0.95 mmol) and NBS (1.35 g, 7.6 mmol) were dissolved in dry THF (50 mL) under an Ar atmosphere with the reaction vessel shielded from light. The mixture was heated at reflux for 5 h and allowed to cool to room temperature. The solvent was removed under vacuum and the resulting solid purified by flash column chromatography (silica gel, dichloromethane/hexanes: 1/1) to afford **3.2** in the form of a white solid (0.96 g, 90%). M.p. decomposes over 160 °C; ¹H NMR (400 MHz, CDCl₃, 25 °C): δ = 1.35 (t, *J* = 7.2 Hz, 3H; ester CH₃), 1.69–2.139 (21H; meso CH₃), 4.31 ppm (q, *J* = 7.2 Hz, 2H; ester CH₂), NH protons were not observed at room temperature; ¹³C NMR (100 MHz, CDCl₃, 25 °C): δ = 25.25, 37.87, 46.41, 49.02, 51.09, 63.02, 64.72, 130.29, 161.07, 192.3 ppm; LRMS (FAB MS): *m/z* [M] 1117; HRMS (FAB MS): *m/z* calcd for C₃₀H₃₀ Br₈N₄O₂ [M⁺]: 1117.5754; found: 1117.5762. This compound was further characterized by single crystal X-ray diffraction analysis.

3.4.3 Monocarboxylic acid functionalized calix[4]pyrrole



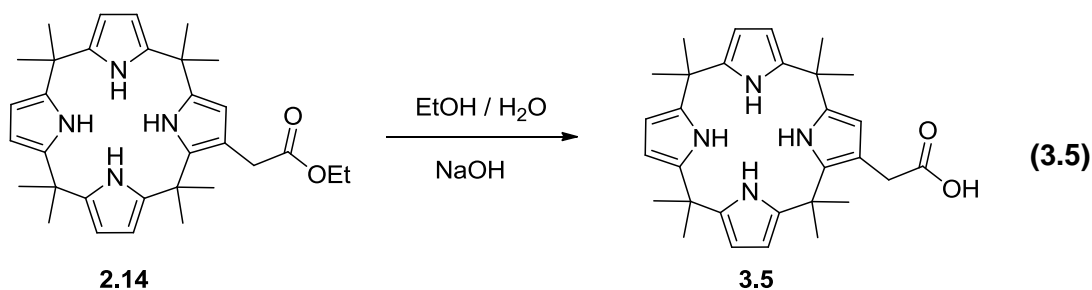
Calixpyrrole **3.1** (1.11 g, 2.28 mmol) was dissolved in 80mL EtOH and heated to reflux under an Ar atmosphere. Once reflux was established, NaOH (0.3 g, 7.7 mmol in 50mL H₂O) was added drop-wise. Heating at reflux was then continued for 5 h, after which the mixture was allowed to cool to room temperature. The bulk of the volatiles were then removed under vacuum. The remaining, largely aqueous solution was acidified with HCl (0.2 M) until a white precipitate was obtained. This precipitate, corresponding to product **3.3** (0.95 g, 91%), was collected by filtration and dried under reduced pressure. M.p. decomposes over 190 °C; ¹H NMR (300MHz, CDCl₃, 25 °C): δ = 1.52–1.54 (m, 18H; meso CH₃), 1.76 (s, 3H; meso CH₃), 5.92–6.01 (m, 8H; pyrrole CH), 7.11 (br. s, 2H, pyrrole NH), 7.42ppm (br. s, 2H; pyrrole NH); ¹³C NMR (75 MHz, CDCl₃, 25 °C): δ = 25.00, 28.31, 29.05, 29.37, 29.51, 35.15, 35.26, 47.23, 102.79, 103.19, 103.33, 105.52, 130.77, 137.96, 138.58, 139.47, 178.61 ppm; LRMS (FAB MS): *m/z* [M⁺] 458; HRMS (FAB MS): *m/z* calcd for C₂₈H₃₄N₄O₂ [M⁺]: 458.2682; found: 458.2690.

3.4.4 Octabromomonocarboxylic acid functionalized calix[4]pyrrole



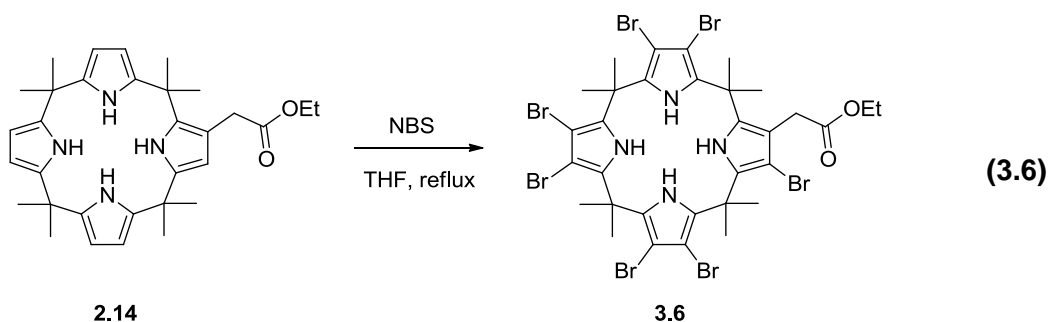
This compound was prepared from **3.2** (0.86 g, 0.77 mmol) using the same procedure used to produce **3.3**. The product was a white solid (0.71 g, 85%). M.p. decomposes over 170°C; ^1H NMR (300MHz, CDCl_3 , 25 °C): δ = 0.86–2.16ppm (21H; meso CH_3), NH protons were not observed at room temperature; ^{13}C NMR (75MHz, CDCl_3 , 25 °C): δ = 14.36, 24.58, 29.47, 35.60, 47.55, 61.83, 63.397, 103.54, 103.62, 105.31, 132.18, 139.27, 172.94ppm; LRMS (FAB MS): m/z [M^+] 1090; HRMS (FAB MS): m/z calcd for $\text{C}_{28}\text{H}_{26}\text{N}_4\text{O}_2$ [M^+]: 1089.5441; found: 1089.5450.

3.4.5 Hydrolysis of C-rim modified calix[4]pyrrole



This compound was prepared from **2.14** (0.23 g, 0.45mmol) using the same procedure used to produce **3.3** [45]. The product was a white solid (0.2 g, 93%). M.p. decomposes over 180 °C; ^1H NMR (300 MHz, CDCl_3 , 25 °C): δ = 1.48–1.59 (24H; meso CH_3), 3.71 (s, 2H; CH_2), 5.75–5.92 (br. m, 7H; pyrrole CH), 6.96 (s, 2H; pyrrole NH), 7.16 (s, 1H; pyrrole NH), 7.78ppm (s, 1H; pyrrole NH); ^{13}C NMR (75MHz, CDCl_3 , 25 °C): δ = 28.81, 29.03, 29.13, 33.35, 34.95, 35.10, 35.20, 36.78, 101.78, 102.24, 102.58, 102.77, 106.72, 108.67, 133.48, 136.96, 138.02, 138.12, 138.56, 138.88, 139.43, 178.96 ppm; LRMS (CI): m/z [M^+] 487; HRMS (FAB MS): m/z calcd for $\text{C}_{30}\text{H}_{38}\text{N}_4\text{O}_2$ [M^+]: 486.6483; found: 486.6492.

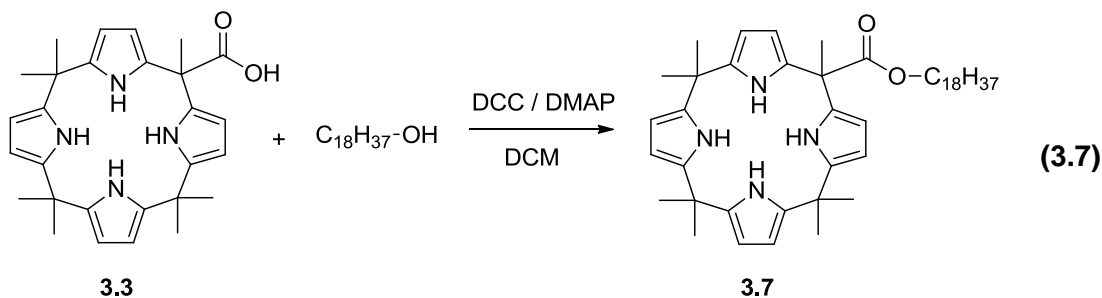
3.4.6 Bromination of C-rim modified calix[4]pyrrole



This compound was prepared from **2.14** (0.5 g, 0.97mmol) using the same procedure used to produce **3.2**. The product was a white solid (0.92 g, 89%). M.p. decomposes over 180 °C; ^1H NMR (400 MHz, CDCl_3 , 25 °C): δ = 0.88 (t, J = 7.2 Hz, 3H; ester CH_3), 1.24–1.82 (m, 24H; meso CH_3), 3.35 (s, 2H; CH_2), 4.09 (q, J = 7.2 Hz, 3H; ester CH_2), 6.64 (s, 1H; pyrrole NH), 6.79 (s, 1H; pyrrole NH), 7.95 (s, 1H; pyrrole NH), 8.48 ppm (s, 1H; pyrrole NH); ^{13}C NMR (75MHz, CDCl_3 , 25 °C): δ = 14.12, 26.06, 37.48, 37.75, 37.93, 38.28, 49.68, 94.16, 96.08, 99.94, 100.52, 110.41, 130.41, 190.38 ppm; LRMS (CI): m/z [M^+] 1067; HRMS (FAB MS): m/z calcd for $\text{C}_{32}\text{H}_{35}\text{Br}_7\text{N}_4\text{O}_2$ [M^+]: 1065.6982; found: 1065.6990.

3.4.7 Attaching long alkyl chains

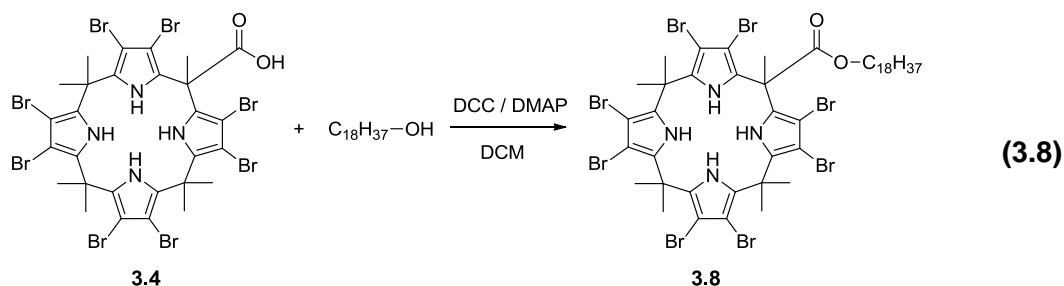
3.4.7.1 Octadecyl meso-Calix[4]pyrrole carboxylate



Acid **3.3** (100 mg, 0.22mmol), 1-octadecanol (65 mg, 0.24mmol), and 4-dimethylaminopyridine (DMAP) (2.7mg, 0.022mmol) were dissolved in 4mL dichloromethane under an Ar atmosphere. At this point, dicyclohexylcarbodiimide (DCC) (45.4mg, 0.22 mmol) mixed in 1mL dichloromethane was added to the mixture. The reaction mixture stirred for 24 h and the insoluble matter was filtrated off. The resulting filtrate was collected and was washed with first 0.5N HCl (10mL), followed by saturated NaHCO_3 (10mL), and then finally water (10mL). The organic layer was then dried over Na_2SO_4 and the solvent was removed under vacuum. Column chromatography (silica gel, dichloromethane/hexanes: 80/20) afforded **3.7**

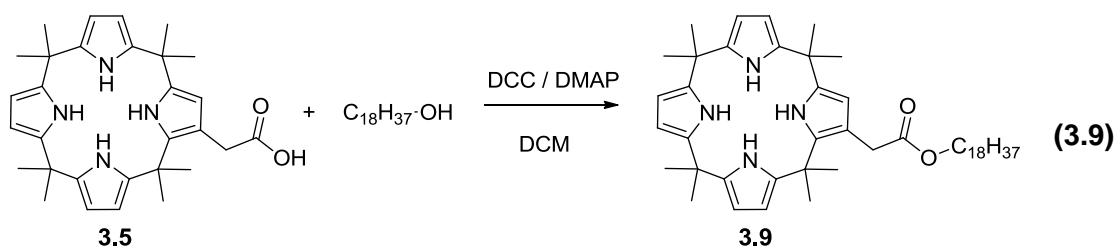
in the form of a yellowish solid (79.8mg, 51%). M.p. 65°C; ^1H NMR (400MHz, CDCl_3 , 25 °C): δ = 0.88 (t, J = 6.9Hz, 3H; long alkyl tail CH_3), 1.6 (br. s, 28H; long alkyl tail CH_2), 1.51–1.53 (br. m, 18H; meso CH_3), 1.61–1.65 (br. m, 2H; long alkyl tail CH_2), 1.75 (s, 3H; meso CH_3), 2.17 (m, 2H; long alkyl tail CH_2), 4.14 (t, J = 6.9Hz, 2H; long tail CH_2), 5.90–5.94 (m, 8H; pyrrole CH), 7.07 (br. s, 2H; pyrrole NH), 7.42 ppm (br. s, 2H; pyrrole NH); ^{13}C NMR (75MHz, CDCl_3 , 25 °C): δ = 14.11, 22.68, 25.01, 25.87, 28.28, 28.50, 28.97, 29.19, 29.30, 29.48, 29.57, 29.69, 31.90, 35.15, 35.23, 47.30, 54.14, 65.77, 102.82, 103.04, 103.13, 104.98, 131.75, 138.11, 138.49, 139.06, 172.84 ppm; LRMS (CI): m/z [M^+] 711; HRMS (FAB MS): m/z calcd for $\text{C}_{46}\text{H}_{70}\text{N}_4\text{O}_2$ [M^+]: 711.5499; found: 711.4483.

3.4.7.2 Octadecyloctabromocalix[4]pyrrolylcarboxylate



This compound was prepared from **3.4** (180mg, 0.16 mmol) using a procedure analogous to that used to prepare **3.7**. The product was a white solid (0.16 g, 72%). M.p. 75°C; ^1H NMR (300MHz, CDCl_3 , 25 °C): δ = 0.88–5.46 (m, 58H; long alkyl tail CH_3 , CH_2 and meso CH_3), 6.74 (br. s, 2H; pyrrole NH), 8.04 (br. s, 1H; pyrrole NH), 11.81 ppm (br. s, 1H; pyrrole NH); ^{13}C NMR (75 MHz, CDCl_3 , 25 °C): δ = 14.34, 23.16, 25.43, 27.18, 28.35, 28.82, 29.32, 29.41, 29.54, 29.65, 29.78, 32.49, 36.14, 37.46, 49.40, 57.73, 67.12, 103.63, 104.11, 104.19, 105.67, 135.46, 141.13, 143.82, 144.19, 174.54 ppm; LRMS (FAB): m/z [M^+] 1342; HRMS (FAB MS): m/z calcd for $\text{C}_{46}\text{H}_{62}\text{Br}_8\text{N}_4\text{O}_2$ [M^+]: 1342.24208; found: 1342.24251.

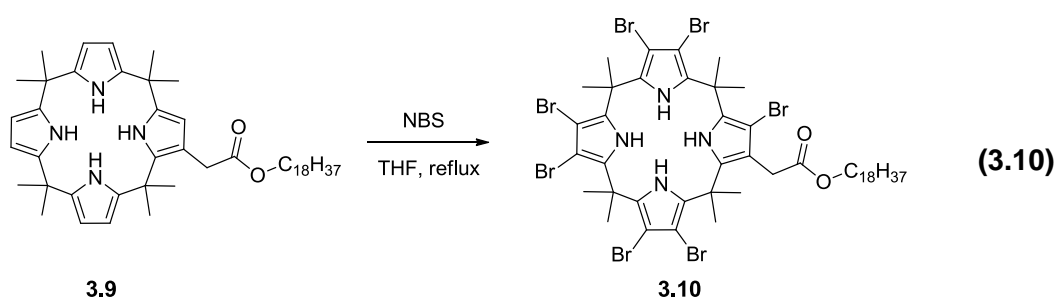
3.4.7.3 Octadecyl2- β -calix[4]pyrrolyl acetate



This compound was prepared from **3.5** (100 mg, 0.2 mmol) using a procedure analogous to that used to prepare **3.7**. The product was a white solid (110.8 mg,

75%). M.p. 70°C; ^1H NMR (400 MHz, CDCl_3 , 25 °C): δ = 0.91 (t, J = 6.8 Hz, 3H; long alkyl tail CH_3), 1.29 (br. s, 28H; long alkyl tail CH_2), 1.49–1.58 (br. m, 24H; meso CH_3), 1.66–1.69 (br m, 4H; long alkyl tail CH_2), 3.64 (s, 2H; CH_2), 4.15 (t, J = 6.8 Hz, 2H; long alkyl tail CH_2), 5.71–5.94 (m, 7H; pyrrole CH), 7.96 (d, 2H; pyrrole NH), 7.09 (br. s, 1H; pyrrole NH), 8.49 ppm (br. s, 1H; pyrrole NH); ^{13}C NMR (100 MHz, CDCl_3 , 25 °C): δ = 14.10, 22.67, 25.93, 28.55, 28.61, 28.87, 29.24, 29.34, 29.53, 29.57, 29.63, 29.68, 31.90, 34.86, 35.11, 35.18, 36.72, 38.34, 65.15, 101.02, 101.94, 102.29, 102.42, 102.72, 103.09, 106.61, 109.42, 133.52, 136.73, 137.35, 137.88, 138.36, 138.96, 139.47, 139.88 ppm; LRMS (CI): m/z [M^-] 739; HRMS (FAB MS): m/z calcd for $\text{C}_{46}\text{H}_{70}\text{N}_4\text{O}_2$ [M^-] 739.5890; found: 739.5858.

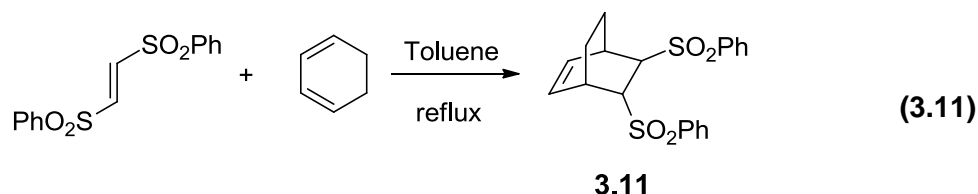
3.4.7.4 Octadecyl 2- β -heptabromocalix[4]pyrrolyl acetate



This compound was prepared from **3.9** (68 mg, 0.09 mmol) using a procedure analogous to that used to produce **3.6**. The product **3.10** was a white solid (106.9 mg, 90%). M.p. 92°C; ^1H NMR (300 MHz, CDCl_3 , 25 °C): δ = 0.88 (t, J = 6.9 Hz, 3H; long alkyl tail CH_3), 1.26 (br. s, 28H; long alkyl tail CH_2), 1.59 (br. m, 4H; long alkyl tail CH_2), 1.71–1.83 (br. m, 24H; meso- CH_3), 3.35 (s, 2H; CH_2), 4.00 (br. t, J = 6.9 Hz, 2H; long alkyl tail CH_2), 6.64 (s, 1H; pyrrole NH), 6.79 (s, 1H; pyrrole NH), 7.95 (s, 1H; pyrrole NH), 8.48 ppm (s, 1H; pyrrole NH); ^{13}C NMR (75 MHz, CDCl_3 , 25 °C): δ = 14.12, 22.68, 25.88, 27.28, 28.52, 29.64, 29.69, 31.41, 31.91, 37.48, 37.73, 37.93, 38.28, 65.18, 95.39, 95.87, 96.07, 96.43, 99.82, 99.93, 100.51, 129.91, 129.97, 130.37, 131.10, 131.34, 131.85, 171.84 ppm; LRMS (FAB MS): m/z [M^+] 1290; HRMS (FAB MS): m/z calcd for $\text{C}_{48}\text{H}_{67}\text{Br}_7\text{N}_4\text{O}_2$ [M^+] 1290.9564; found: 1290.9576.

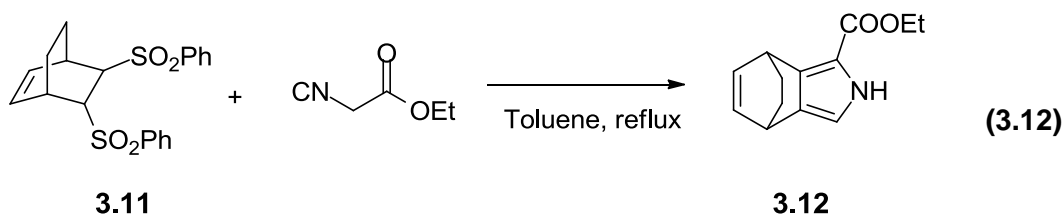
3.5 Tetrabenzocalix[4]pyrrole

3.5.1 Synthesis of 2,3-bis(phenylsulfonyl)bicyclo[2.2.2] oct-2-ene



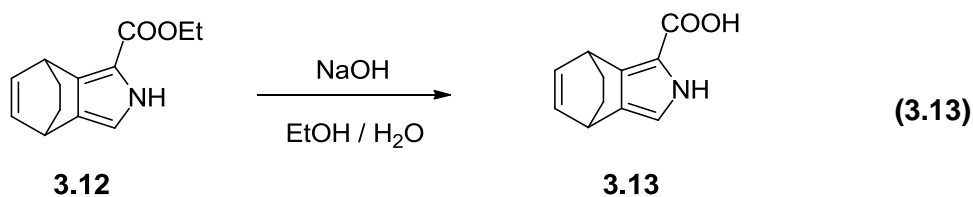
A mixture of (E)-1,2-bis(phenylsulfonyl)ethene (1.78 g, 5.8 mmol) and 1,3-hexadiene (0.9 g, 11.3 mmol) were dissolved in dry toluene and heated at reflux for 20 h. After the reaction was deemed complete (TLC), the solvent was removed using a rotary evaporator. The crude white solid was filtered and washed with ether three times; this afforded **3.11** as a white solid. ^1H and ^{13}C NMR spectral data for this product proved consistent with literature reports [67].

3.5.2 Ethyl 4,7-dihydro-4,7-ethano-2H-isoindole-1-carboxylate



Compound **3.12** was prepared in analogy to a reported procedure [68-70]. To a stirred solution of **3.11** (2 g, 5.15 mmol) and ethyl isocyanoacetate (0.7 g, 6.18 mmol) in dry THF (70 mL) was added KO^tBu (1.39 g, 12.36 mmol) at 0°C. The resulting reaction mixture was stirred at room temperature for 24 h upon which it was poured into water containing dilute hydrochloric acid. After extraction with ethyl acetate, work-up and column chromatography over silica gel (methylenechloride–hexane, eluent) gave **3.12** (1 g, 90%) as colorless needles. ^1H and ^{13}C NMR spectral data for this product were consistent with the reported literature data [68].

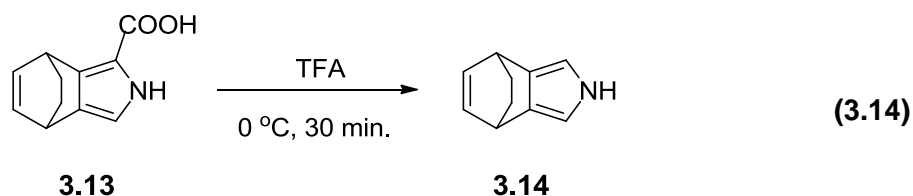
3.5.3 Ethyl 4,7-dihydro-4,7-ethano-2H-isoindole-1-carboxylic acid



Compound **3.12** (0.2 g, 0.92 mmol) was dissolved in 30 mL EtOH and heated to reflux. Once reflux was established, NaOH (3.68 g, 147.2 mmol in 30 mL H₂O) was

added drop-wise. Heating at reflux was then continued for 5 h, after which point the mixture was allowed to cool to room temperature. The bulk of the volatiles were then removed under vacuum. The remaining, largely aqueous solution was acidified with HCl (0.2 M) until a white precipitate was obtained. This precipitate, corresponding to product **3.13** (0.17 g, 97%), was collected by filtration and dried under reduced pressure. ^1H NMR (400 MHz, DMSO- d_6): δ = 11.99 (br s, 1 H, NH), 10.72 (s, 1 H, COOH), 6.55 (d, $J=2.8$ Hz, 1 H, pyrrole CH), 6.42 (m, 2 H, CH), 4.24 (m, 1 H, CH), 3.81 (m, 1 H, CH), 1.46 (m, 2 H, CH $_2$), 1.32 ppm (m, 2 H, CH $_2$); ^{13}C NMR (100 MHz, DMSO- d_6): δ = 26.4, 26.9, 113.8, 129.9, 135.7, 162.3 ppm; LRMS: 190 [MH^+]; HRMS: calcd for C $_{11}$ H $_{11}$ NO $_2$ [MH^+] 190.0868, found 190.0866.

3.5.4 Synthesis of 4,7-dihydro-4,7-diethano-2*H*-isoindole

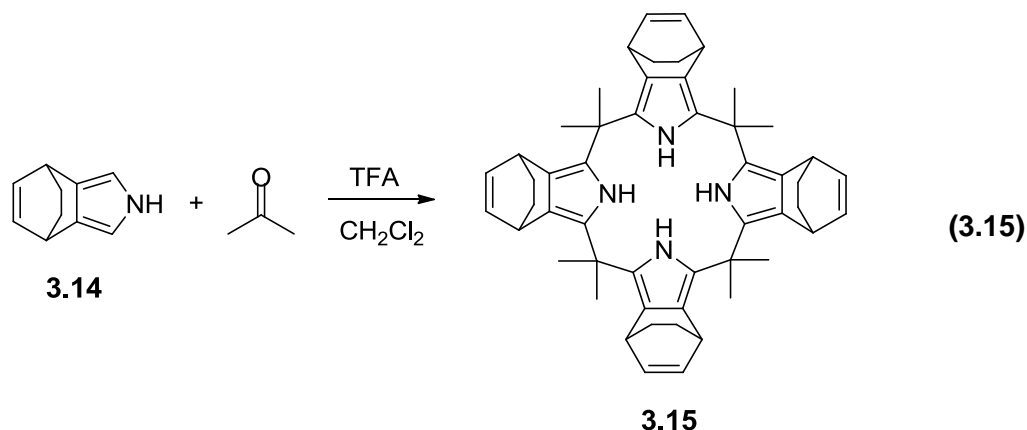


Compound **3.13** (0.12 g, 0.62 mmol) was dissolved in freshly distilled and degassed TFA (30 mL) at 0 °C under an Ar atmosphere and stirred for 30 min while protecting from light. TFA was removed under vacuum and the remaining residue was dissolved in CH $_2$ Cl $_2$ (30 mL) and then washed with saturated NaHCO $_3$ (2 x 30 mL). The solution was then dried over Na $_2$ SO $_4$ and filtered. Evaporation of the CH $_2$ Cl $_2$ -based filtrate afforded **3.14** as a white solid (85 mg, 95%). ^1H NMR (400 MHz, CDCl $_3$): δ = 7.51 (br s, 1 H, NH), 6.51 (dd, J = 6.5 Hz, 2 H, CH), 6.46 (d, J = 6.5 Hz, 2 H, pyrrole CH), 3.86 (m, 2 H, CH), 1.56 ppm (m, 4 H, CH $_2$); ^{13}C NMR (100 MHz, CDCl $_3$): δ = 27.55, 33.12, 107.95, 129.25, 135.72 ppm; LRMS: 145 [M^+]; HRMS: calcd for C $_{10}$ H $_{11}$ N [M^+] 145.0891, found 145.0886.

3.5.5 Synthesis of tetra-bicyclo[2.2.2]-oct-2-ene fused calix[4]pyrrole

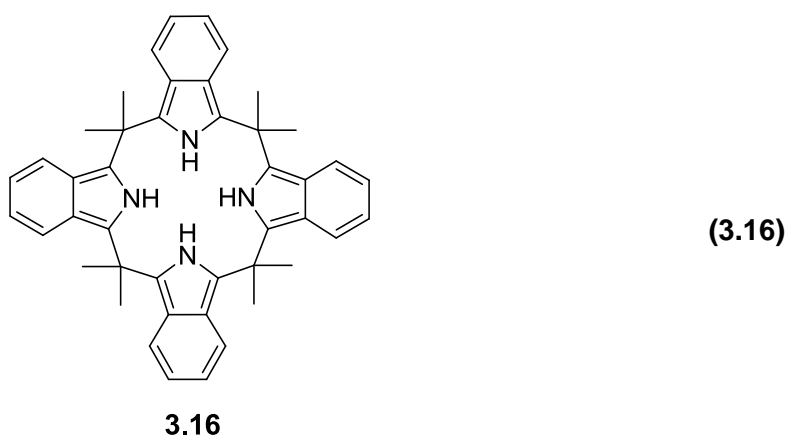
Compound **3.14** (70 mg, 0.48 mmol) was dissolved in dry CH $_2$ Cl $_2$ (50 mL) at 0 °C and bubbled with Ar for 10 minutes. Acetone (35.8 μL , 0.48 mmol) was then added to the solution. Following this addition, TFA (25 μL) was added drop-wise over the course of 10 minutes while shielding the reaction vessel from light. The mixture was then stirred first at 0 °C for 3 hours and subsequently at room temperature overnight. At this point, the reaction mixture was washed with sat. NaHCO $_3$ dried over Na $_2$ SO $_4$. After removing the drying agent by filtration, and removing the

volatiles, flash chromatography (silica gel, dichloromethane/hexanes:1/1) yielded calixpyrrole **3.15** as a white solid (45 mg, 50%).



^1H NMR (400 MHz, CDCl_3): δ = 1.25-1.56 (br m, 40 H, CH_3 and CH_2), 3.92 (br m, 8H, CH), 5.94-6.04 (br m, 4H, NH), 6.44 ppm (br m, 8H, CH); ^{13}C NMR (100 MHz, CDCl_3): δ = 27.4, 29.2, 33.8, 37.1, 124.2, 126.0, 136.2 ppm; LRMS: 742 [MH^+]; HRMS: calcd for $\text{C}_{52}\text{H}_{60}\text{N}_4$ [MH^+] 742.4974., found 742.4979.

3.5.6 Tetrabenzocalix[4]pyrrole

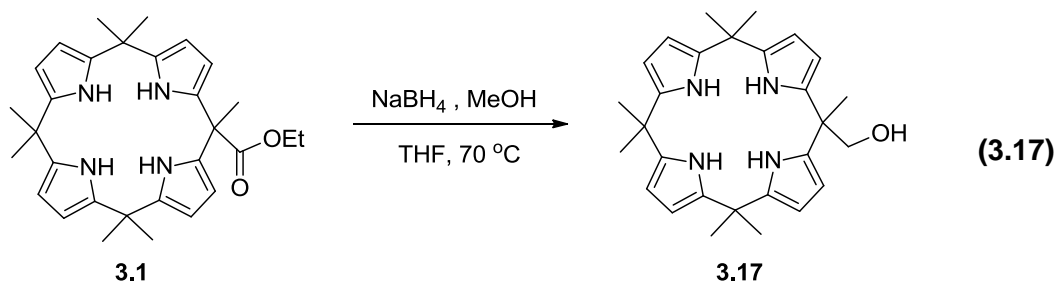


With compound **3.15** in hand, an effort was made to obtain the corresponding tetrabenzocalix[4]pyrrole **3.16**. With goal in mind, compound **3.15** was subject to retro Diels-Alder reaction conditions. Specifically, compound **3.15** was heated to 200°C under vacuum at 10 mmHg for 10 min, with the resulting crude product being subject to column chromatography. Unfortunately a quantitative conversion of **3.15** into **3.16** could not be achieved in this work even though similar retro Diels-Alder reaction conditions have proved effective in creating porphyrin derivatives analogous to **3.16** [68]. Moreover, separation of product **3.16** from the starting material **3.15** using column chromatography was not successful. Therefore, ^1H NMR

spectroscopic and mass spectrometric analyses of the reaction mixture were employed to track the course of the putative conversion.

3.6 Synthesis of Polymers with Pendant Calix[4]pyrroles

3.6.1 Mono-hydroxy functionalized calix[4]pyrrole

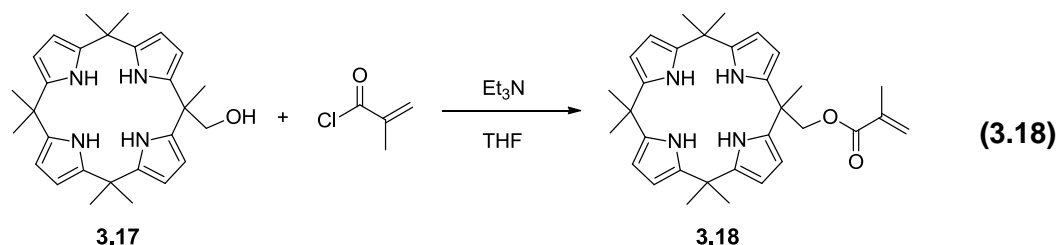


In a 25 mL round bottom flask, the respective calix[4]pyrrole ethyl ester **3.1** (500 mg, 1.027 mmol) was first dissolved in 10 mL THF and placed under an atmosphere of Ar. After adding NaBH_4 (233 mg, 6.165 mmol) in a single portion, the resulting mixture was heated to reflux for 15 min. To the hot mixture, 10 mL of dry MeOH was added dropwise over the course of 15 min. After 24 h of additional heating at reflux, the reaction was cooled to ambient temperature and quenched with 20 mL of an aqueous solution saturated with ammonium chloride. The organic components were then extracted with CH_2Cl_2 (3 x 20 mL) and dried over Na_2SO_4 . The crude product was then purified by column chromatography (silica gel; eluent: 80:20 CH_2Cl_2 :hexanes gradually changing to 10:90 MeOH: CH_2Cl_2) which, after removal of residual solvent, afforded 343 mg of **3.17** as a yellow solid (75% yield). $R_f = 0.15$ (80:20 CH_2Cl_2 :hexanes); ^1H NMR (500 MHz, CDCl_3): $\delta = 1.42$ (s, 3H, *meso*- CH_3), 1.51-1.55 (m, 18H, *meso*- CH_3), 1.94 (t, 1H, $J = 5$ Hz, OH), 3.85 (d, 2H, $J = 5$ Hz, *meso*- CH_2), 5.90-5.96 (m, 8H, pyrrole CH), 7.11 (br s, 2H, NH), 7.57 ppm (br s, 2H, NH); ^{13}C NMR (100 MHz, CDCl_3): $\delta = 24.76, 28.33, 29.45, 41.19, 69.83, 102.65, 102.91, 103.06, 103.37, 134.36, 138.21, 138.46, 138.82$ ppm; HRMS (CI) calcd for $\text{C}_{28}\text{H}_{37}\text{N}_4\text{O}$ $[\text{M}+\text{H}^+]$: 445.2967, found: 445.2966. This compound was further characterized by single crystal X-ray diffraction analysis.

3.6.2 Methacrylate functionalized calix[4]pyrrole

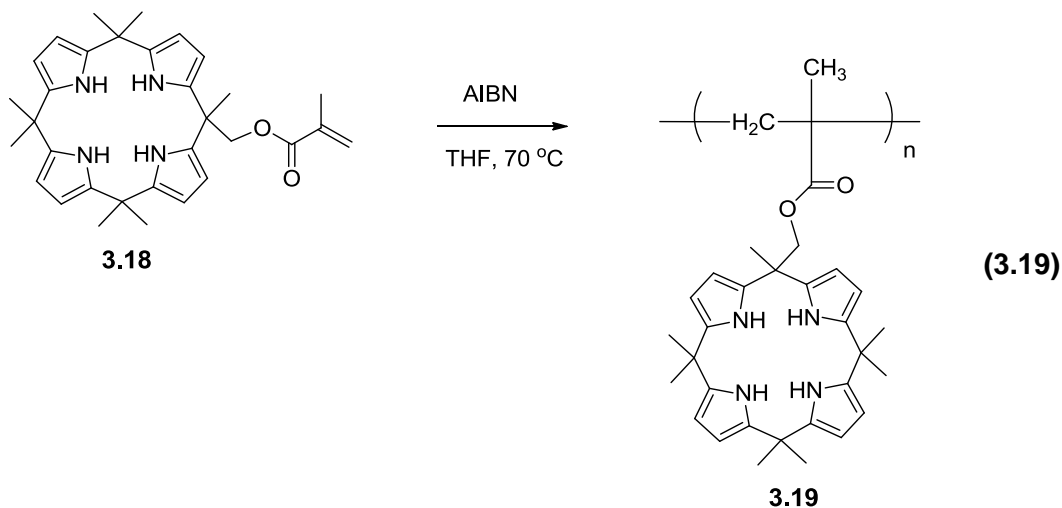
A 25 mL round bottom flask was charged with 250 mg (0.56 mmol) of alcohol **3.17**, triethylamine (97.5 μL , 0.7 mmol) and 10 mL of dry, degassed THF. After cooling the flask to 0 $^\circ\text{C}$ using an ice bath, methacryloyl chloride (60 μL , 0.62 mmol) was added dropwise *via* syringe. The reaction was then allowed to warm to ambient temperature over the course of 24 h. After 50 mL of water was added, the mixture

was extracted with CH₂Cl₂ (3 x 20 mL). The organic layer was then dried over Na₂SO₄ and filtered. The crude product was then purified by column chromatography (silica gel; eluent: CH₂Cl₂) which, after removal of residual solvent, afforded 236 mg of **3.18** as a white powder (82% yield).



$R_f = 0.80$ (CH₂Cl₂); ¹H NMR (500 MHz, CD₂Cl₂): $\delta = 1.45\text{-}1.52$ (m, 18H, *meso*-CH₃ protons), 1.87 (dd, 3H, CH₃), 4.34 (s, 2H, CH₂), 5.55 (m, 1H, CH), 5.84-5.92 (m, 8H, pyrrole CH), 5.97 (m, 1H, CH), 7.03 (br s, 2H, NH), 7.11 ppm (br s, 2H, NH); ¹³C NMR (100 MHz, CDCl₃): $\delta = 18.40, 28.92, 29.27, 33.34, 39.43, 70.59, 102.74, 102.88, 103.08, 104.18, 133.18, 138.31, 138.51, 138.86, 191.65$ ppm; HRMS (CI) calcd for C₃₂H₄₁N₄O₂ [M+H⁺]: 513.3230, found: 513.3232. This compound was further characterized by single crystal X-ray diffraction analysis.

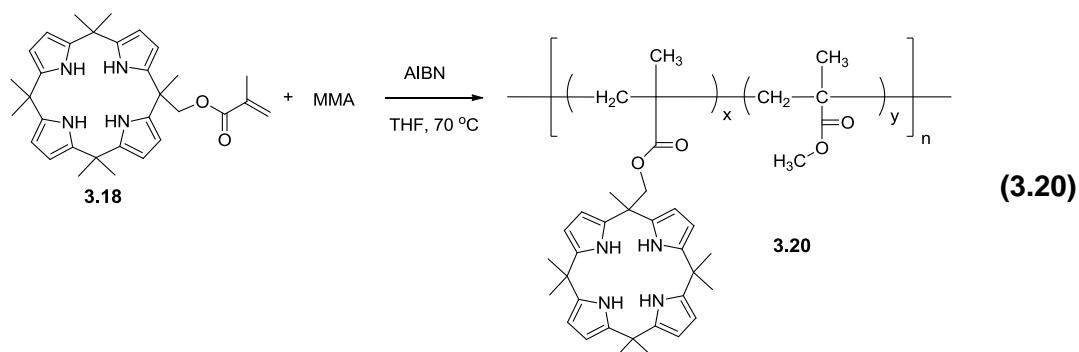
3.6.3 Homopolymer of methacryloyl functionalized calix[4]pyrrole



Homopolymer **3.19** was prepared by dissolving monomer **3.18** in THF (0.3 M) followed by treatment with 1 mol% of azoisobutyronitrile (AIBN). After stirring at 70 °C for 17 h under a nitrogen atmosphere, the resulting viscous solution was added dropwise into an excess of methanol that rapidly stirred. This caused precipitation of polymer **3.19**, which was subsequently isolated *via* filtration in 66% yield as a yellow solid. Using gel permeation chromatography, the polymer was found to have a number-average molecular weight (M_n) of 23,600 Da (relative to PMMA standards)

and a polydispersity index (PDI) of 2.3. ^1H NMR (500 MHz, CD_2Cl_2): δ = 0.34-0.95 (br s, 2H, polymer backbone CH_2), 1.25-1.85 (br m, 24H, *meso*- CH_3 and polymer backbone CH_3), 4.15 (br s, 2H, *meso*- CH_2), 5.89 (br s, 8H, pyrrole CH), 7.12 ppm (br s, 4H, NH).

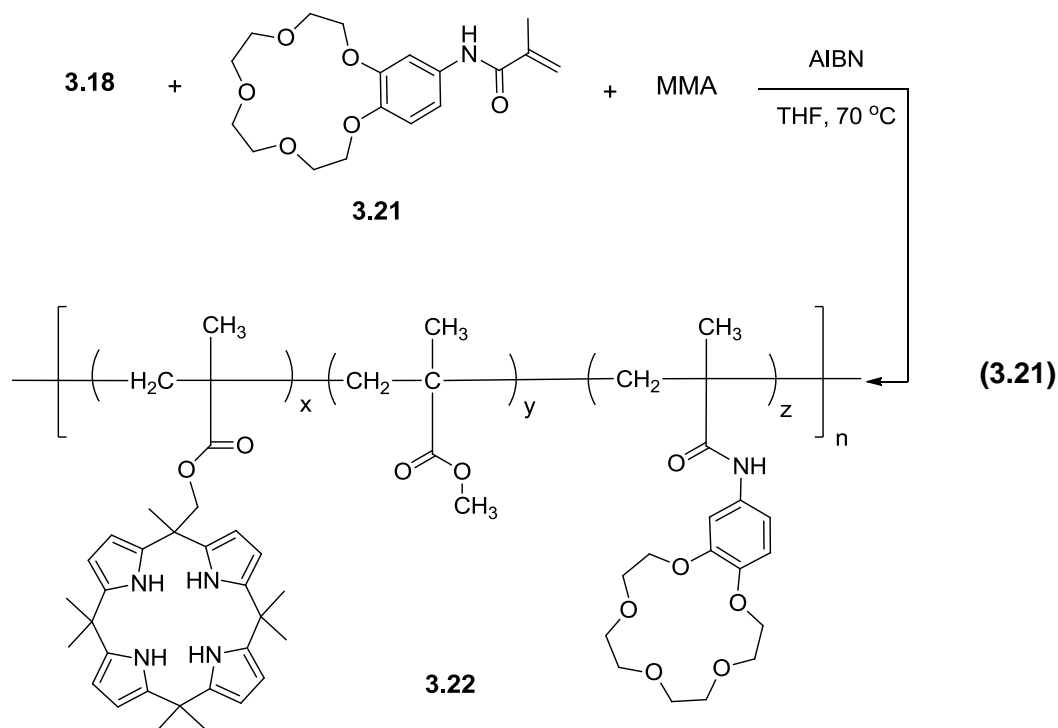
3.6.4 Copolymerization of monomer **3.18** and MMA



Using the conventional free radical polymerization conditions described above, a 77% yield of copolymer **3.20** was obtained as a white solid from a 1:10 mixture of **3.18** and MMA. Using GPC, **3.20** was found to possess a M_n of 85,500 Da and a PDI of 2.1 (relative to PMMA standards). ^1H NMR (500 MHz, CD_2Cl_2): δ = 0.82 (br s, 30H, polymer backbone CH_2), 0.99 (br s, 13.21H, polymer backbone CH_2), 1.52-1.55 (br m, 29.13H, calixpyrrole *meso*- CH_3), 1.80-1.88 (br m, 25.76H, MMA CH_3), 3.58 (br s, 43.57H, MMA CH_3), 4.11 (br s, 2H, calixpyrrole *meso*- CH_2), 5.89-5.95 (br m, 8H, pyrrole CH), 7.11 ppm (br s, 4H, NH).

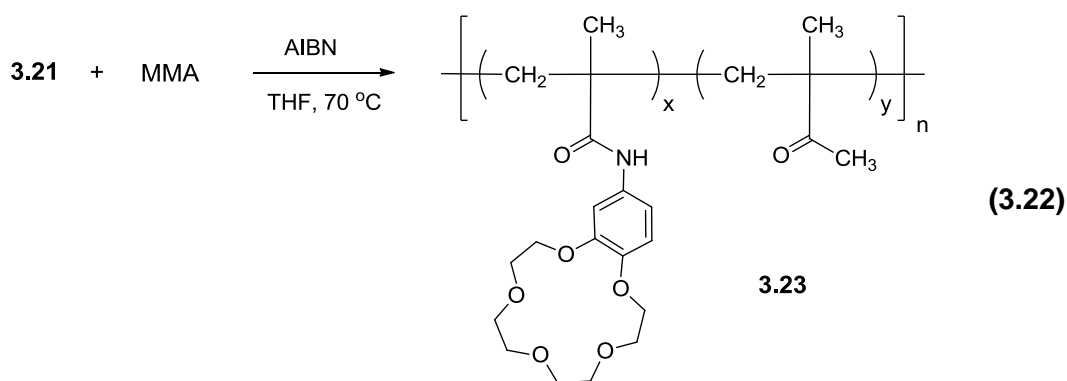
3.6.5 Polymerization of monomer **3.18**, monomer **3.21** and MMA

Copolymer **3.22** was prepared by dissolving monomer **3.18**, monomer **3.21** and MMA in 1:1:10 ratio in THF (total conc.: approx. 0.3 M) followed by treatment with 1 mol% of azoisobutyronitrile (AIBN). After stirring at 70 °C for 17 h under an atmosphere of nitrogen, the resulting viscous solution was added dropwise to excess methanol. This caused precipitation of copolymer **3.22**, which was subsequently isolated *via* filtration in 79% yield as a white solid. ^1H NMR (500 MHz, CD_2Cl_2) δ : 0.82 and 0.89 (br singlets, 59.56H, PMMA CH_3), 1.51 (br s, 21H, calixpyrrole *meso*- CH_3), 1.82 (br m, 48.25H, PMMA CH_2), 3.57 (br s, 68H, PMMA OCH_3), 3.68 (br m, 7.5H, crown ether CH_2), 3.84 (br s, 3.75H, crown ether CH_2), 4.08 (br s, 6H, crown ether CH_2 and calixpyrrole *meso*- CH_2), 5.89 (b, 8H, pyrrole CH), 6.83-7.26 ppm (6H, NH and crown ether aromatic protons). GPC: M_n : 50.2 kDa, PDI: 2.1.



3.6.6 Copolymerization of 3.21 and MMA

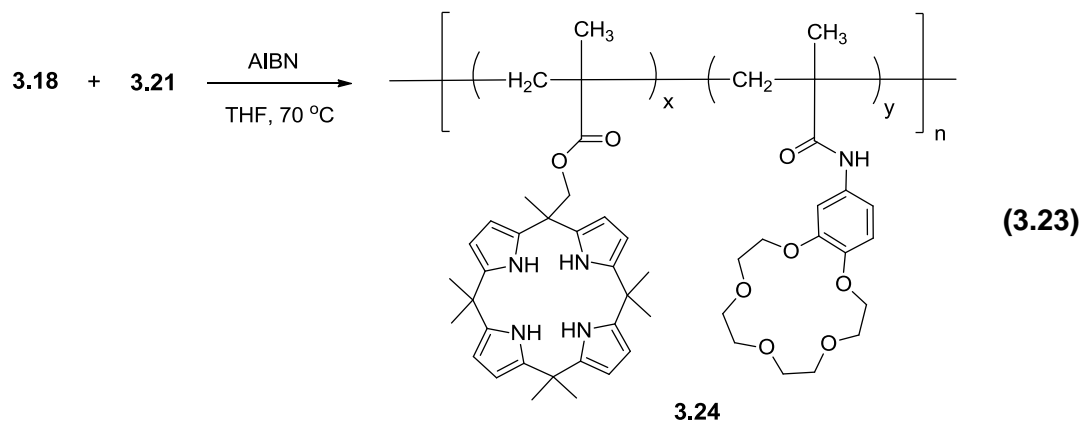
Using conditions analogous to those used to prepare **3.20**, a 76% yield of copolymer **3.23** was obtained as a yellow solid from a 1:10 mixture of **3.21** and MMA. $^1\text{H NMR}$ (500 MHz, CD_2Cl_2): $\delta = 0.81$ (br s, 16.86H, polymer backbone CH_3), 0.81 (br s, 10.30H, polymer backbone CH_3), 1.80 (br m, 19.12H, polymer backbone CH_2), 3.58 and 3.68 (s and s, 32.96H polymer backbone CH_3 and crown ether CH_2), 3.84 (br s, 2H, crown ether CH_2), 4.07 (br s, 2H, crown ether CH_2), 6.81-7.26 ppm (3H, crown ether aromatic protons). GPC: M_n : 33.2 kDa, PDI: 2.1.



3.6.7 Copolymerization of 3.18 and 3.21

Using conditions analogous to those used to prepare **3.20**, an 81% yield of copolymer **3.24** was obtained as a white solid from a 1:1 mixture of **3.18** and **3.21**. $^1\text{H NMR}$ (500 MHz, CD_2Cl_2): $\delta = 1.49$ (br, 36.1H, polymer backbone CH_2 and CH_3)

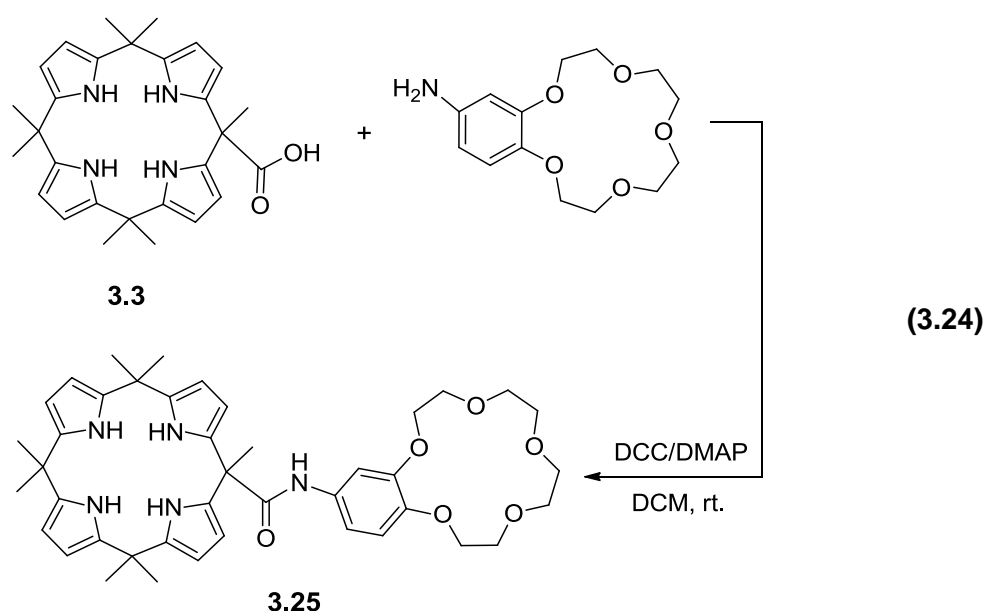
and calixpyrrole *meso*-CH₃), 3.67-4.07 (br singlets, 18.06H, crown ether CH₂), 5.87 (br s, 8H, pyrrole β -protons), 6.82-7.32 ppm (pyrrolic NH and crown ether aromatic protons). GPC: M_n: 38.5 kDa, PDI: 2.3.



3.6.8 Synthesis of control pseudo dimers

3.6.8.1 Pseudo dimer I

Carboxylic acid functionalized calixpyrrole **3.3** (0.22 mmol, 100 mg), 4'-aminobenzo-15-crown-5 (68 mg, 0.24 mmol), dicyclohexylcarbodiimide (DCC) (0.22 mmol, 46 mg) and 4-dimethylaminopyridine (DMAP) (0.022 mmol, 2.7 mg) were dissolved in dry dichloromethane (4 mL) under an atmosphere of argon. After stirring the reaction mixture for 24 h, insoluble material was filtered off.

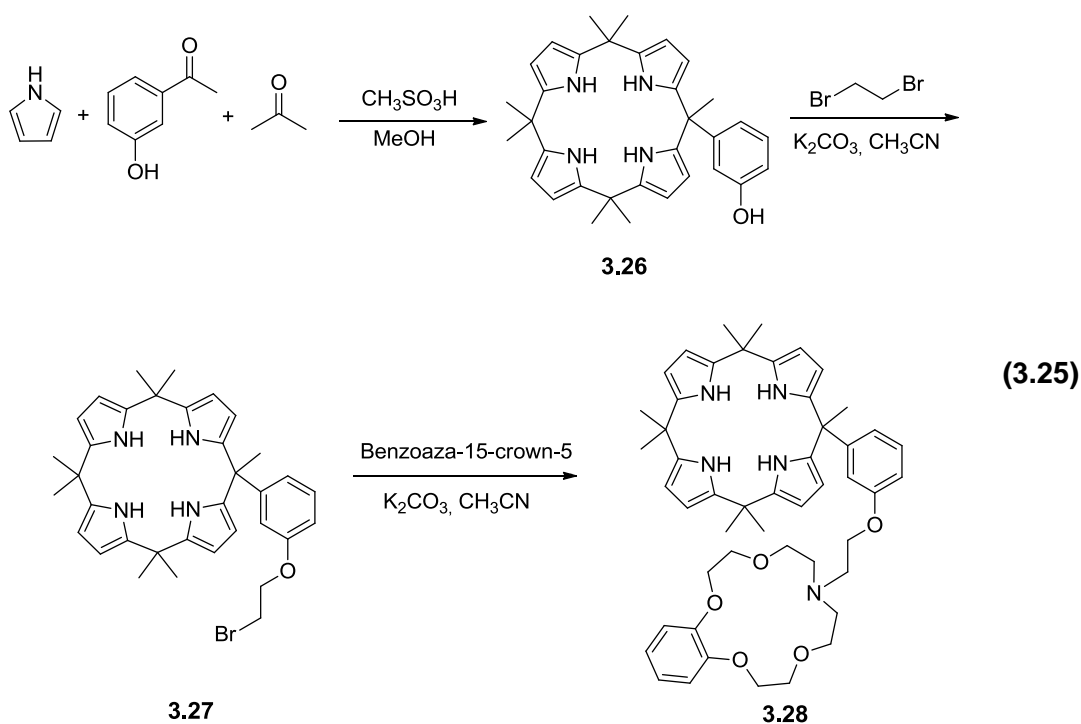


The resulting filtrate was collected and was washed with first with 0.1 N HCl (10 mL), followed by an aqueous solution saturated with NaHCO₃ (10 mL), and then finally water (10 mL). The organic layer was then dried over Na₂SO₄ and the solvent

was removed under vacuum. Column chromatography (silica gel, first dichloromethane/hexanes: 80/20, then 1% MeOH in CH₂Cl₂) afforded **3.25** in the form of a dark yellow solid (110.69 mg, 68%). ¹H NMR (250 MHz, CD₂Cl₂): δ = 1.47 (br m, 18H, *meso*-CH₃), 1.77 (br s, 3H, *meso*-CH₃), 3.63 (br m, 8H, CH₂), 3.78 (br m, 4H, CH₂), 4.01 (br m, 4H, CH₂), 5.86 (br s, 8H, pyrrole CH), 6.69 (m, 1H), 7.12 (br m, 1H), 7.13-7.32 ppm (6H, calixpyrrole NHs, benzene ring CH, amide NH). ¹³C NMR (60 MHz, CDCl₃): δ = 24.70, 26.35, 29.26, 30.79, 32.28, 34.07, 50.28, 57.24, 68.01, 70.91, 103.63, 106.40, 131.64, 132.09, 138.82, 154.41 ppm. HRMS (CI) calcd for C₄₂H₅₃N₅O₆ [M+H⁺]: 723.3996, found: 723.3983.

3.6.8.2 3'-Hydroxyphenyl substituted calix[4]pyrrole

To a mixture of pyrrole (10.2 mL, 146.9 mmol), 3'-hydroxyacetophenone (5.00 g, 36.7 mmol), acetone (8.10 mL, 110.2 mmol), and methanol (250 mL) was added slowly methanesulfonic acid (2.38 mL, 36.7 mmol) at 0 °C.



After stirring for 2 h at room temperature, the reaction mixture was evaporated *in vacuo* to give brownish sticky oil. Dichloromethane (300 mL), water (300 mL), and triethylamine (20 mL) were added to the crude product and the organic phase was separated and washed three times with water (300 mL). The organic layer was dried over anhydrous MgSO₄ and evaporated *in vacuo* to give yellowish sticky oil. Column chromatography over silica gel (eluent: dichloromethane) gave 4.8 g (26% yield) of **3.26** as a white solid. ¹H NMR (400 MHz, CDCl₃): δ = 7.25 (broad s, 2H, NH), 7.14

(broad s, 2H, NH), 7.13-7.09 (t, 1H, ArH, $J = 8.01$ & 8.41 Hz), 6.67-6.65 (d, 1H, ArH, $J = 8.41$ Hz), 6.62-6.60 (d, 1H, ArH, $J = 8.01$ Hz), 6.47 (s, 1H, ArH), 5.94-5.91 (m, 6H, pyrrole-H), 5.72-5.70 (t, 2H, pyrrole-H, $J = 3.02$ & 2.40 Hz), 4.85 (broad s, 1H, ArOH), 1.87 (s, 3H, ArC(pyrrole)₂CH₃), 1.60 (s, 6H, pyrrole-C(CH₃)₂), 1.52 (s, 9H, pyrrole-C(CH₃)₂), 1.27 ppm (s, 3H, pyrrole-C(CH₃)₂). ¹³C NMR (100 MHz, CDCl₃): $\delta = 155.3, 149.8, 138.9, 138.8, 138.6, 136.6, 129.1, 120.2, 115.0, 113.6, 106.1, 103.4, 103.1, 103.0, 44.9, 35.5, 35.4, 30.3, 30.0, 29.9, 28.8, 28.7, 28.4$ ppm; HRMS (ESI) m/z 507.3125 M⁺ calcd for C₃₃H₃₈N₄O⁺, found 507.31184.

3.6.8.3 3-(2-Bromoethoxy)phenyl substituted calix[4]pyrrole

Under an atmosphere of argon, compound **3.26** (2.50 g, 4.93 mmol), 1,2-dibromoethane (27.1 g, 148.0 mmol) and K₂CO₃ (2.05 g, 14.8 mmol) in acetonitrile (125 mL) were heated to reflux. After being heated at reflux for 4 d, the acetonitrile was removed *in vacuo*. The resulting brownish solid was extracted with dichloromethane (50 mL) and then water (50 mL) for a three consecutive cycles. The organic layer was then separated and dried over anhydrous MgSO₄. Evaporation of the solvent *in vacuo* gave a yellowish solid, which was recrystallized from methanol to give 2.20 g (73% yield) of **3.27** as a white solid. ¹H NMR (400 MHz, CDCl₃): $\delta = 7.22$ (broad s, 2H, NH), 7.18-7.14 (t, 1H, ArH, $J = 8.01$ & 8.01 Hz), 7.01 (broad s, 2H, NH), 6.77-6.74 (dd, 1H, ArH, $J = 7.61$ Hz), 6.68-6.66 (d, 1H, ArH, $J = 8.80$ Hz), 6.52 (s, 1H, ArH), 5.92-5.91 (t, 2H, pyrrole-H, $J = 2.80$ & 3.20 Hz), 5.90-5.89 (d, 4H, pyrrole-H, $J = 2.40$ Hz), 5.68-5.67 (t, 2H, pyrrole-H, $J = 3.20$ & 2.80 Hz), 4.19-4.16 (t, 2H, ArOCH₂CH₂, $J = 6.40$ & 6.40 Hz), 3.59-3.56 (t, 2H, OCH₂CH₂Br, $J = 6.40$ & 6.80 Hz), 1.87 (s, 3H, ArC(pyrrole)₂CH₃), 1.56 (s, 6H, pyrrole-C(CH₃)₂), 1.52-1.51 ppm (m, 12H, pyrrole-C(CH₃)₂). ¹³C NMR (100 MHz, CDCl₃): $\delta = 157.9, 149.8, 139.0, 138.8, 138.6, 136.6, 128.9, 120.9, 114.3, 113.0, 106.1, 103.4, 103.0, 67.9, 51.0, 44.9, 35.5, 35.4, 30.3, 30.0, 29.4, 28.8, 28.6, 28.4$ ppm. HRMS (ESI) m/z 613.2542 M⁺ calcd for C₃₅H₄₅BrN₄O⁺, found 613.25365.

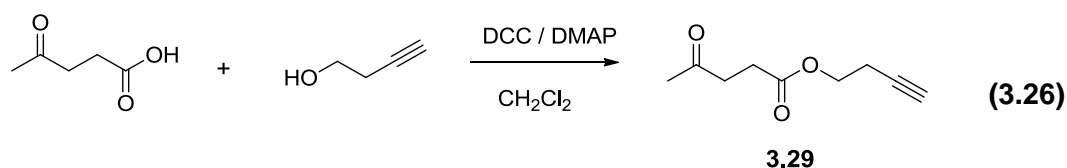
3.6.8.4 Pseudo dimer II

A mixture of compound **3.27** (0.25 g, 0.41 mmol), benzoaza-15-crown-5 (0.11 g, 0.41 mmol) and K₂CO₃ (0.17 g, 1.22 mmol) in acetonitrile (30 mL) was heated at reflux for 3 d under an atmosphere of argon. After the reaction solvent was removed *in vacuo*, the resulting sticky oil was extracted with dichloromethane (50 mL) and then washed three times with water (50 mL). The organic layer was then separated and dried over anhydrous MgSO₄. Evaporation of the solvent gave a yellowish sticky oil, which was purified by column chromatography over silica gel (eluent: 3%

triethylamine solution of ethyl acetate) to afford 0.12 g (36% yield) of **3.28** as a white solid. ^1H NMR (400 MHz, CD_2Cl_2): δ = 7.27 (broad s, 2H, NH), 7.14 (broad t, 1H, ArH; 2H, NH), 6.75-6.73 (dd, 1H, ArH, J = 7.20 Hz), 6.59-6.57 (d, 1H, ArH, J = 7.61 Hz), 6.48 (s, 1H, ArH), 5.92 (broad s, 2H, pyrrole-H), 5.88 (broad s, 4H, pyrrole-H), 5.69 (broad s, 2H, pyrrole-H), 4.01 (broad t, 4H, $\text{ArOCH}_2\text{CH}_2\text{O}$), 3.93 (broad t, 2H, $\text{ArOCH}_2\text{CH}_2\text{N}$), 3.83 (broad t, 4H, $\text{ArOCH}_2\text{CH}_2\text{O}$), 3.71 (broad t, 4H, $\text{OCH}_2\text{CH}_2\text{N}$), 2.92 (broad t, 2H, $\text{ArOCH}_2\text{CH}_2\text{N}$), 2.84 (broad t, 4H, $\text{OCH}_2\text{CH}_2\text{N}$), 1.87 (s, 3H, $\text{ArC}(\text{pyrrole})_2\text{CH}_3$), 1.58-1.52 (three singlets, 15H, pyrrole- $\text{C}(\text{CH}_3)_2$), 1.28 (s, 3H, pyrrole- $\text{C}(\text{CH}_3)_2$). ^{13}C NMR (100 MHz, CD_2Cl_2): δ = 149.4, 139.1, 138.8, 138.6, 136.7, 128.7, 121.5, 120.1, 114.0, 112.5, 105.9, 102.9, 71.0, 69.6, 55.6, 44.9, 35.2, 30.0, 28.2, 27.6, 27.4 ppm. HRMS (ESI) m/z 800.4759 [M^+] calcd for $\text{C}_{49}\text{H}_{62}\text{N}_5\text{O}_5^+$, found 800.47455. This compound was further characterized by single crystal X-ray diffraction analysis.

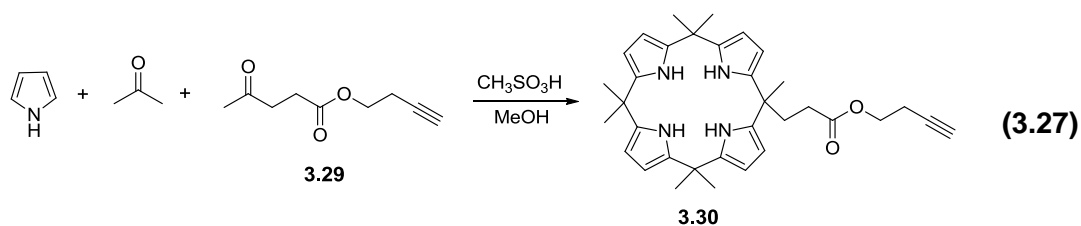
3.7 Synthesis of Dendrimeric Calix[4]pyrroles

3.7.1 But-3-yn-1-yl 4-oxopentanoate



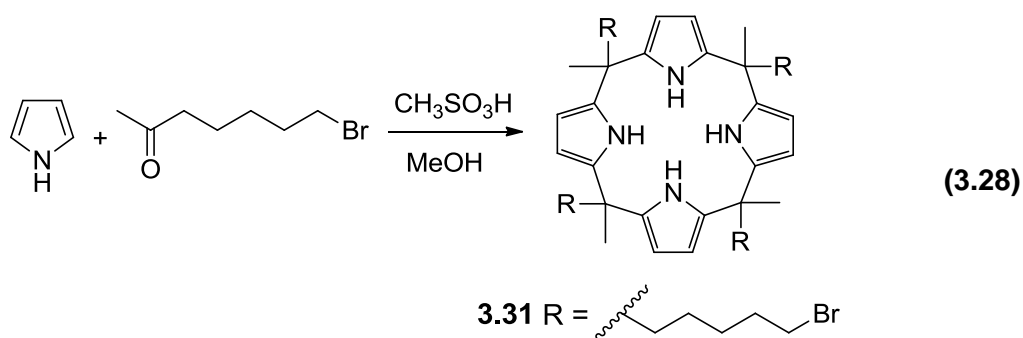
Levulinic acid (3 g, 25.8 mmol), 3-butyn-1-ol (1.75 mL, 23.48 mmol), and DMAP (32 mg, 0.26 mmol) were dissolved in 30 mL dichloromethane. At this point, DCC (5.32 g, 25.8 mmol) was added to the mixture. The reaction mixture stirred for 24 h at room temperature and the insoluble matter was filtrated off. The resulting filtrate was collected and was washed with first 0.5N HCl (30 mL), followed by saturated NaHCO_3 (30 mL), and then finally water (30 mL). The organic layer was then dried over Na_2SO_4 and the solvent was removed under vacuum. Flash column chromatography (silica gel, dichloromethane) afforded **3.29** in the form of a yellowish liquid (3.8 g, 96%). FTIR: 3281, 2964, 2916, 1715, 1408, 1356, 1154, 1068, 1031, 1001 cm^{-1} ; ^1H NMR (250 MHz, CDCl_3): δ = 1.99 (t, J =2.4 Hz, 1H, CH), 2.18 (s, 3H, CH_3), 2.51 (td, J =2.4, 6.8 Hz, 2H, CH_2), 2.59 (t, J =6.6 Hz, 2H, CH_2), 2.75 (t, J =6.3 Hz, 2H, CH_2), 4.17 ppm (t, J =6.8 Hz, 8H, CH_2); ^{13}C NMR (75 MHz, CDCl_3): δ = 18.89, 27.85, 29.74, 37.85, 62.23, 69.85, 79.95, 172.37, 206.32 ppm; HRMS (EI-GCMS): m/z [MH^+]: 168.98492.

3.7.2 Alkyn functionalized calixpyrrole



Pyrrole (3 mL, 43.2 mmol) and **3.29** (1.82 g, 10.8 mmol) were dissolved in methanol (50 mL) at 0°C and bubbled with Ar for 10 minutes. Acetone (2.38 mL, 32.4 mmol) was then added to the mixture. Following this addition, methanesulfonic acid (1.97 mL) was added drop-wise over the course of 10 minutes while shielding the reaction vessel from light. The mixture was then stirred first at 0°C for 3 hours and subsequently at room temperature overnight. The yellow precipitate that formed during this time was collected by filtration. Chromatographic purification (silica gel, dichloromethane/hexanes: 80/20) yielded calixpyrrole **3.30** as a yellow solid (1 g, 17%). M.p. decomposes over 200°C; FTIR: 3421, 3363, 3231, 2968, 1730, 1576, 1414, 1303, 1273, 1177, 1040, 759, 705 cm⁻¹; ¹H NMR (250 MHz, CDCl₃): δ = 1.41 (br. s, 3H, meso CH₃), 1.98 (t, J=2.5 Hz, 1H, CH), 2.17 (br. m, 4H, CH₂), 2.46 (td, J=6.7, 2.5 Hz, 2H; CH₂), 4.10 (t, J=6.7 Hz, 2H, CH₂), 5.88 (br. s, 8H; pyrrole CH), 7.03 ppm (br. s, 4H; pyrrole NH); LRMS (ESI): m/z [M⁻]: 537.29.

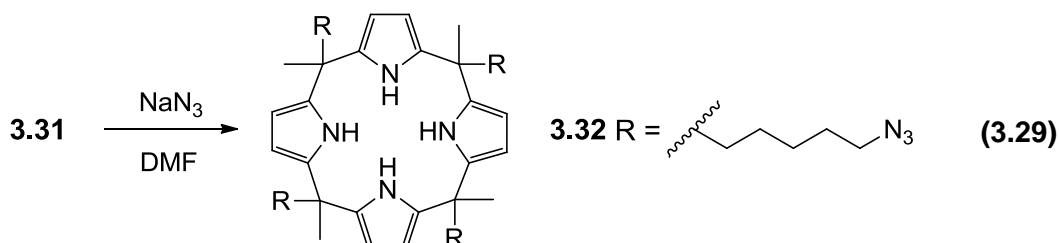
3.7.3 Tetra-1-bromopentyl-tetramethylcalix[4]pyrrole



Pyrrole (1.74 g, 25.9 mmol) and 7-bromoheptane-2-one [71] (5 g, 25.9 mmol) was dissolved in dry methanol (100 mL) at 0°C and bubbled with Ar for 10 minutes. Following this bubbling methanesulfonic acid (1.18 mL, 18.1 mmol) was added drop-wise over the course of 10 minutes while shielding the reaction vessel from light. The mixture was then stirred first at 0°C for 3 hours and subsequently at room temperature overnight. The white precipitate was collected by filtration and washed with methanol. This yielded the calixpyrrole **3.31** as a white solid (4.9 g, 78.1%). FTIR: 3420, 2932, 2857, 1574, 1501, 1414, 1247, 1193, 1037, 756, 711 cm⁻¹; ¹H

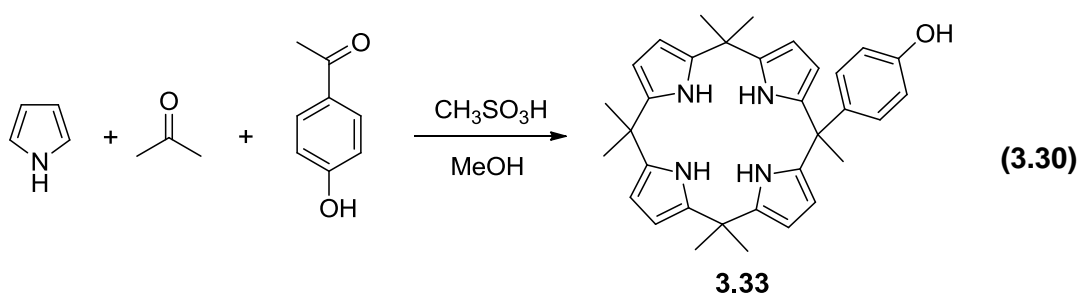
NMR (250 MHz, CDCl₃): δ = 1.08 (br m, 8H, CH₂), 1.41 (br, 20H, meso-CH₃, CH₂), 1.80 (br m, 16H, CH₂), 3.35 (br t, *J*=6.75 Hz, 8H, CH₂), 5.88 (8H, pyrrole-CH), 6.96 ppm (4H, NH); ¹³C NMR (75 MHz, CDCl₃): δ=23.63, 26.64, 28.72, 32.71, 33.65, 38.79, 40.51, 103.84, 137.30 ppm; LRMS (ESI): *m/z* [M⁻]: 967.05.

3.7.4 Tetraazidocalix[4]pyrrole



3.31 (200 mg, 0.2 mmol) and sodium azide (134.2 mg, 2 mmol) was dissolved in dry DMF (25 mL) at room temperature and stirred for 2 days. After the completion of the reaction DMF was removed under vacuum at 60°C. Resulting crude material was dissolved in dichloromethane and washed with water 3 times. The organic layer was dried over Na₂SO₄ and the solvent was removed under vacuum. This yielded the calixpyrrole **3.32** as a light yellow solid (166 mg, 98.4%). FTIR: 3415, 3358, 2968, 2858, 2086, 1680, 1572, 1453, 1415, 1396, 1244, 1038, 756, 711 cm⁻¹; ¹H NMR (250 MHz, CDCl₃): δ= 1.09 (br, 8H, CH₂), 1.27 (br, 8H, meso-CH₃, CH₂), 1.40 (12H, meso-CH₃), 1.53 (16H, CH₂), 1.79 (8H, CH₂), 3.20 (t, *J*=6.68 Hz, 8H, CH₂), 5.87 (8H, pyrrole-CH), 7.00 ppm (4H, NH); ¹³C NMR (75 MHz, CDCl₃): δ=137.30, 103.83, 51.40, 40.56, 38.78, 28.90, 27.25, 26.39, 23.97 ppm.

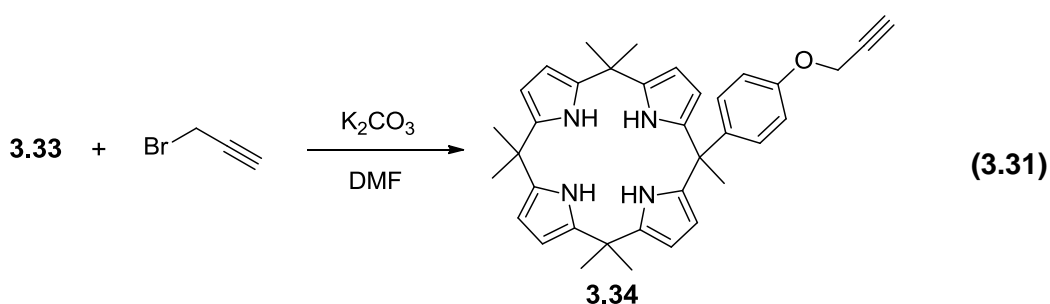
3.7.5 4'-Hydroxyphenyl functional calix[4]pyrrole



Pyrrole (6 mL, 86.7 mmol) and 4-hydroxyacetophenone (2.95 g, 21.7 mmol) were dissolved in methanol (250 mL) at 0°C and bubbled with Ar for 10 minutes. Acetone (4.78 mL, 65.1 mmol) was then added to the mixture. Following this addition, methanesulfonic acid (4.22 mL) was added drop-wise over the course of 10 minutes while shielding the reaction vessel from light. The mixture was then stirred first at 0 °C for 3 hours and subsequently at room temperature overnight. The white

precipitate that formed during this time was collected by filtration. Chromatographic purification (silica gel, DCM/hexanes: 80/20, DCM/MeOH: 99/1) yielded calixpyrrole **3.33** as a white solid (1,83 g, 16.6%). ^1H NMR (400 MHz, CDCl_3): δ = 7.18 (s, 2H, NH), 7.07 (s, 2H, NH), 6.86 (d, $J=6.85$ Hz, ArH), 6.66 (d, $J=6.85$ Hz, ArH), 5.89 (s, 6H, pyrrole CH), 5.65 (s, 2H, pyrrole CH), 4.74 (s, 1H, OH), 1.83 (s, 3H, CH_3), 1.54-1.49 (s, 18H, CH_3); ^{13}C NMR (101 MHz, CDCl_3) δ = 154.17, 138.95, 138.84, 138.72, 137.18, 128.79, 114.75, 105.92, 103.31, 103.03, 44.25, 35.45, 29.92, 28.85; LRMS (ESI MS): m/z [MH^+]: 507; HRMS (ESI MS): m/z calcd for $\text{C}_{33}\text{H}_{38}\text{N}_4\text{O}$ [M^+]: 506.3046; found: 506.2641.

3.7.6 Propargyl ether of 4'-hydroxyphenyl functional calix[4]pyrrole



A mixture of compound **3.33** (0.669 g, 1.32 mmol), propargyl bromide (0,294 g, 1,98 mmol), and potassium carbonate (0,365 g, 2.64 mmol) in DMF (50 mL) was allowed to react at 50°C for 24h. After the completion of the reaction DMF was removed under vacuum and the resulting crude solid was dissolved in DCM. The DCM solution was washed with water and dried over Na_2SO_4 . Chromatographic purification (silica gel: methylene chloride) yielded the compound **3.34** in form of a white solid (0,650 g, 90%). ^1H NMR (250 MHz, CDCl_3): δ = 1.50-1.54 (br m, 18H; meso CH_3), 1.84 (s, 3H; meso CH_3), 2.50 (t, 1H; $\text{C}\equiv\text{CH}$), 4.65 (d, 2H; CH_2), 5.65 (s, 2H, pyrrole-CH), 5.89 (s, 6H, pyrrole-CH), 6.81 (d, $J=8,5$ Hz, 2H, ArH), 6.91 (d, $J=8,5$ Hz, 2H, ArH), 7.07 (b s, 2H, NH), 7.19 ppm (b s, 2H, NH); LRMS (ESI): m/z [M^+]: 543.58.

3.7.7 Dendrimeric structures

3.7.7.1 Dendrimer I

In a flask, **3.32** (50 mg, 61 μmol), **3.30** (145.05 mg, 269.25 μmol) dissolved in 50 mL of THF. Freshly prepared aqueous solution of sodium ascorbate (106.7 mg, 0.54 mmol) was added followed by aqueous solution of copper(II) sulfate pentahydrate (64.8 mg, 0.27 mmol). The ratio of azide and alkyne groups was 1/4. The mixture

stirred for 2 days of ambient temperature. THF was removed under vacuum and the remaining crude mixture was dissolved in DCM and washed with water three times. The organic layer was then dried over Na₂SO₄ and the excess of solvent was removed under vacuum. Precipitation in to hexane afforded the **3.35** as white solid (95%). FTIR: 3423, 2965, 1730, 1575, 1417, 1224, 1165, 1039, 764 cm⁻¹; ¹H NMR(250 MHz, CDCl₃): δ = 7.39-7.03 (br m, 24H, NH and CH), 5.87 (br s, 40H, pyrrole CH), 4.24 (br m, 16h, N-CH₂ and O-CH₂), 2.96 (br t, 8H, CH₂), 2.15-1.40 ppm (br m, 144H, CH and CH₂).

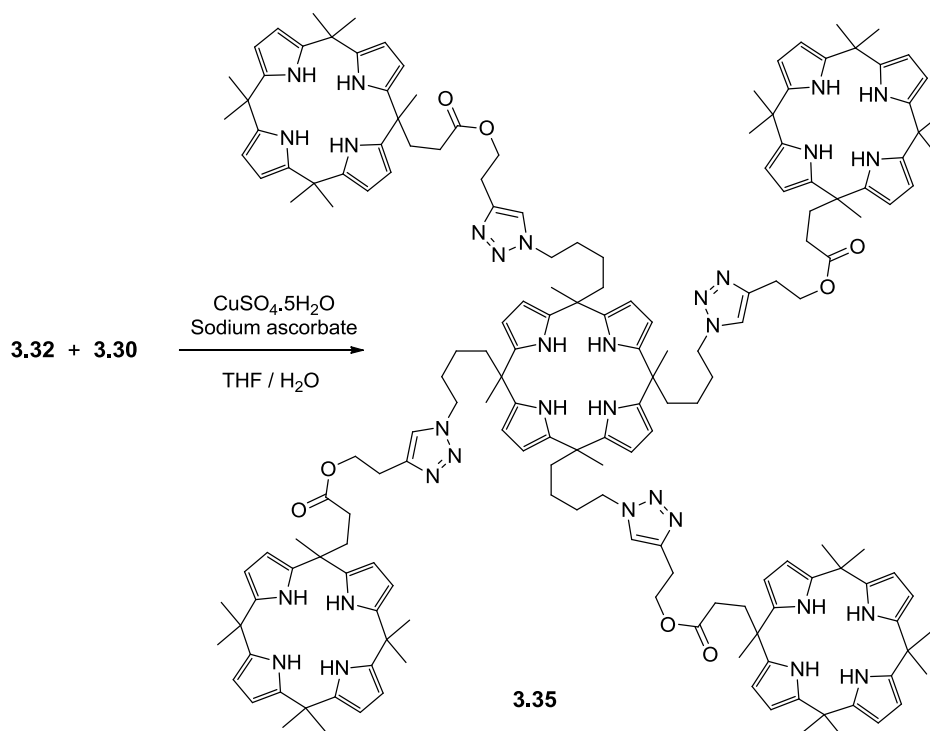


Figure 3.1 : Synthesis of calix[4]pyrrole based dendrimer I.

3.7.7.2 Dendrimer II

This compound was prepared via triazole ring formation reaction of **3.32** (50 mg, 61.19 μmol) and **3.34** (146.7 mg, 269.25 μmol) using the same procedure used to produce **3.35**. The product **3.36** was a white solid (169 mg, 92%). FTIR: 3428, 2967, 2931, 1693, 1575, 1506, 1460, 1416, 1223, 1038, 766 cm⁻¹; ¹H NMR (250 MHz, CDCl₃): δ = 7.64- 7.54 (b m, 4H, CH), 7.24 (br s, 12H, NH), 7.11 (br s, 8H, NH), 6.89 (br t, 8H, ArH), 6.83 (br t, 8H, ArH), 5.88 (br s, 32H, pyrrole CH), 5.63 (br s, 8H, pyrrole CH), 5.13 (br s, 8H, CH₂), 4.26 (br t, 8H, CH₂), 1.83-1.23 ppm (br m, 128H, CH₃ and CH₂).

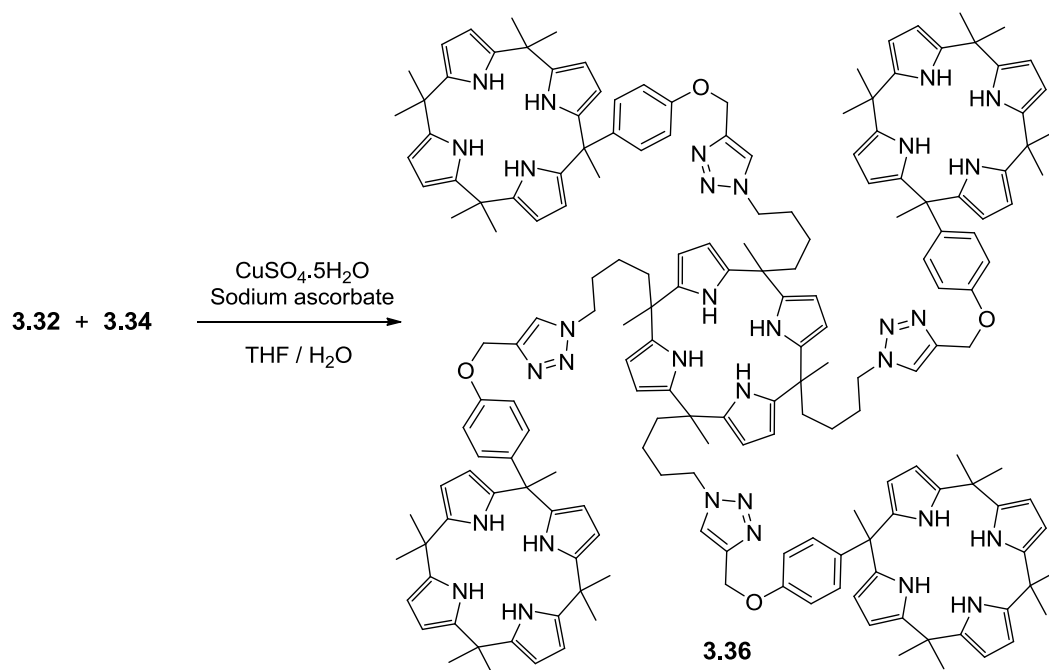


Figure 3.2 : Synthesis of calixpyrrole based dendrimer II.

3.7.7.3 Dendrimer III

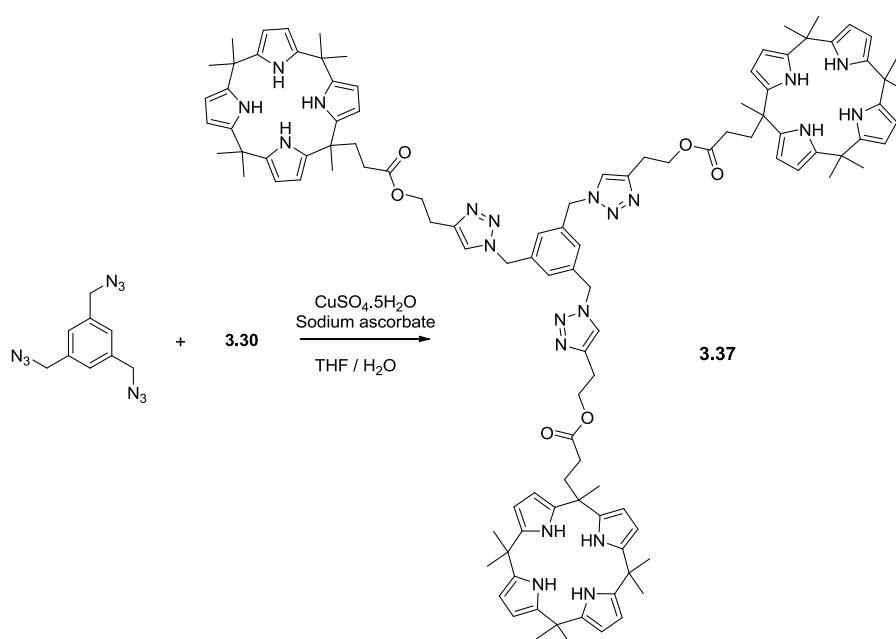


Figure 3.3 : Synthesis of dendrimer III.

This compound was prepared via triazole ring formation reaction of **3.30** (219.27 mg, 407 μmol) and 1,3,5-tris(azidomethyl)benzene [72] (30 mg, 123.34 μmol) using the same procedure used to produce **3.35**. The product **3.37** was a white solid (215 mg, 94%). FTIR: 3424, 2967, 1729, 1577, 1419, 1226, 1166, 1040, 767 cm^{-1} ; ^1H NMR (250 MHz, CDCl_3): δ = 7.25 (b s, 6H, CH + ArH), 7.15 (br s, 12H, NH), 5.87 (br

s, 24H, pyrrole CH), 5.41 (br m, 6H, CH₂), 4.25 (br t, 6H, CH₂), 2.97 (br t, 6H, CH₂), 2.13-1.73 (br m, 12H, CH₂), 1.48-1.39 ppm (br, 63H, CH₃).

3.7.7.4 Dendrimer IV

This compound was prepared via triazole ring formation reaction of **3.34** (221.72 mg, 407 μ mol) and 1,3,5-tris(azidomethyl)benzene (30 mg, 123.34 μ mol) which was prepared from 1,3,5-tris(bromomethyl)benzene [73], using the same procedure used to produce **3.35**. The dendrimeric product **3.38** was a white solid (215 mg, 93%). FTIR: 3419, 2968, 1605, 1578, 1416, 1223, 1039, 768 cm⁻¹; ¹H NMR (250 MHz, CDCl₃): δ = 7.56 (br s, 3H, CH), 7.25 (br s, 9H, NH + ArH), 7.13 (br s, 6H, NH), 6.92 (d, J = 6.8Hz, 6H, ArH), 6.83 (d, J = 6.8Hz, 6H, ArH), 5.88 (d, 18H, pyrrole CH), 5.62 (s, 6H, pyrrole CH), 5.46 (s, 6H, N-CH₂), 5.15 (s, 6H, O-CH₂), 1.83 (s, 9H, CH₃), 1.54-1.49 (br m, 54H, CH₃); LRMS (ESI): m/z [M]: 1857.89.

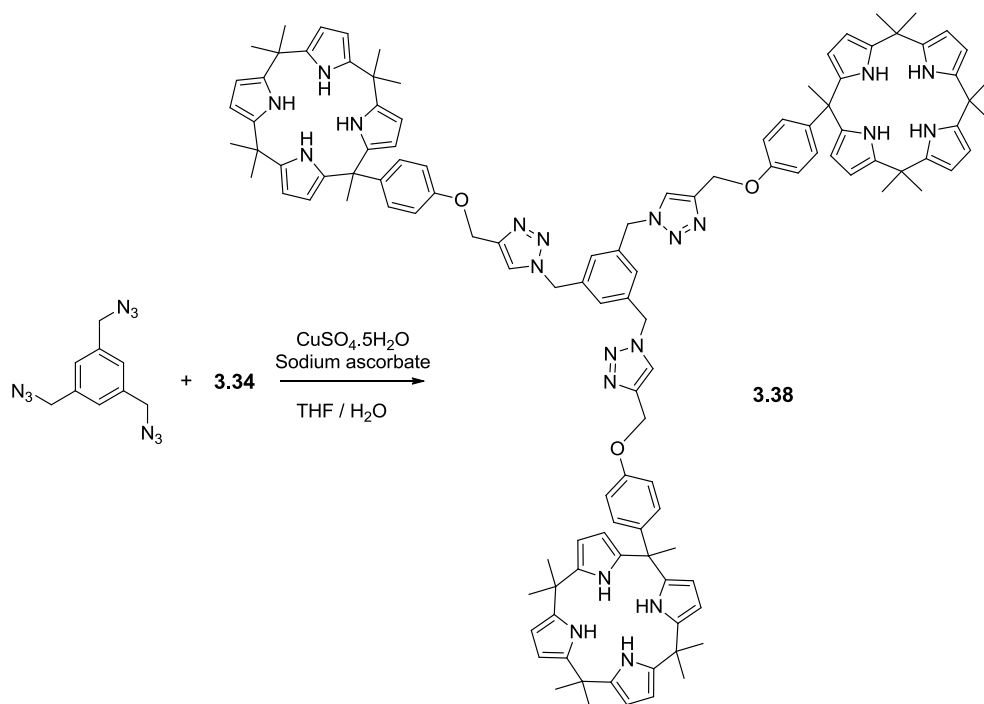
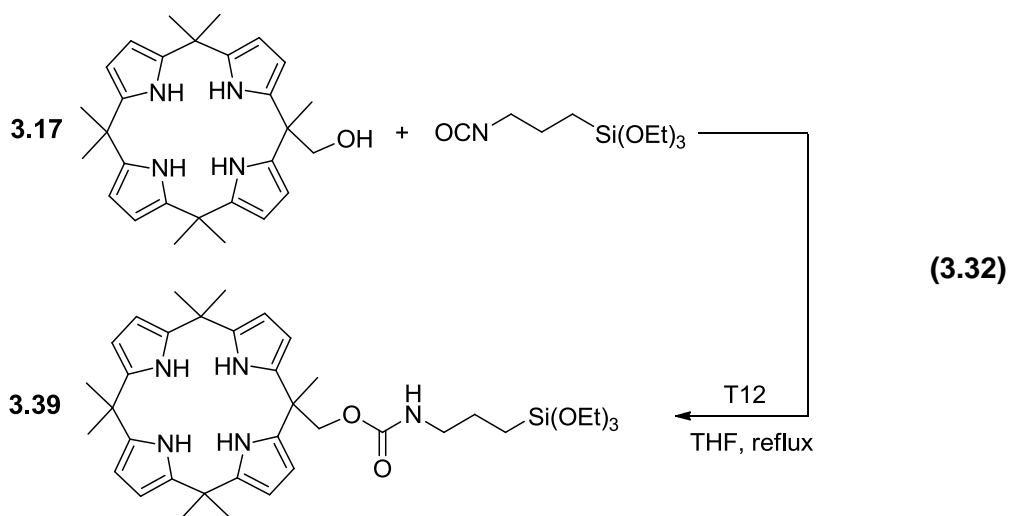


Figure 3.4 : Synthesis of dendrimer IV.

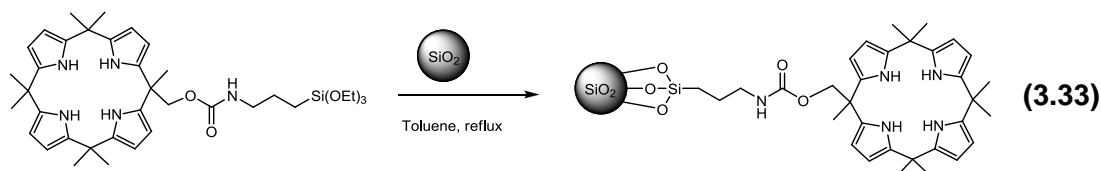
3.8 Supporting of Calix[4]pyrrole on Silica

3.8.1 Siloxane functionalized calix[4]pyrrole



The compound **3.17** (250 mg, 0.56 mmol) and 3-isocyanatotriethoxysilane (153 mg, 0.62 mmol) was dissolved in dry THF under an Ar atmosphere. 2-3 drops of dibutyltindilaurate (T12) was added to the reaction mixture. Resulting solution was heated up to reflux temperature and continued for 24 h. Reaction mixture was cooled down to room temperature and the excess of THF was removed under vacuum. Precipitation of residue in to hexanes was yielded the product **3.39** (95%) as a white solid. ^1H NMR (500 MHz, CDCl_3): δ = 0.59 (t, 2H, J = 8.35 Hz, CH_2), 1.21 (t, 9H, J = 7 Hz, CH_3), 1.47-1.49 (m, 21H, *meso*- CH_3), 1.55 (br m, 2H, CH_2), 3.13 (q, 2H, J = 6.6 Hz, CH_2), 3.81 (q, 6H, J = 7 Hz, CH_2), 4.29 (s, 2H, CH_2), 4.79 (t, 1H, J = 5.5 Hz, NH), 5.88-5.90 (m, 8H, pyrrole-CH), 7.04 (2H, NH), 7.17 ppm (2H, NH); ^{13}C NMR (100 MHz, CDCl_3): δ = 156.00, 138.56, 138.48, 138.39, 134.03, 103.99, 103.07, 102.89, 102.74, 70.48, 43.49, 39.55, 35.22, 35.19, 29.30, 29.09, 29.00, 28.61, 24.69, 23.33, 18.28, 7.62 ppm. This compound was further characterized by single crystal X-ray diffraction analysis.

3.8.2 Modification reactions

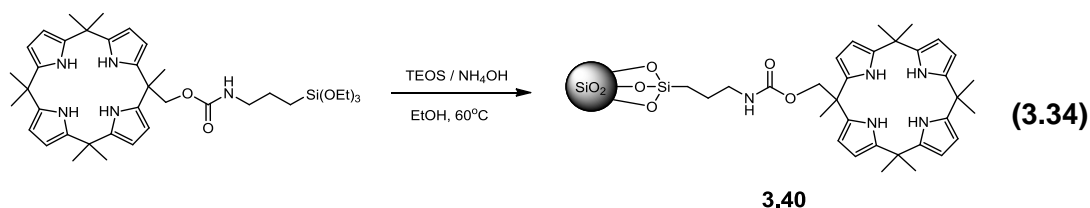


Modification of silica gels was performed using following procedure [74]. Silica gels (1-5 g) were first dried in an oven at 120°C for 2 days, was suspended in dry toluene (100 mL). **3.39** (350 mg, 0.5 mmol) was added over suspension at rt. Then, the

resulting mixture was stirred for 24 h and cooled down to rt. Resulting solid was filtered off and washed with toluene, DCM, EtOH, MeOH and DCM respectively and dried under vacuum at rt.

Using this procedure Silica gel (5.8 g, porosity = 60 Å; particle size = 40-63 μm; surface area = 500-600 m²/g; bulk density = 0.4 g/mL), Fume silica, and SiO₂ nanopowder (10-20 nm particle size) were modified with siloxane functionalized calix[4]pyrrole **3.39**. Functionalization percentages determined by TGA analysis are 5%, 16%, and 25% for silica gel 60, fume silica, and SiO₂ nanopowder respectively.

3.8.3 Synthesis of silica nanoparticles



3.39 (200 mg) and TEOS (3 mL) were added to EtOH (100 mL) solution of NH₄OH (25%, 7.5 mL) which was first heated up to 60 °C. Resulting reaction mixture was stirred at 250 rpm for 24 h. White precipitate was filtered off and washed with toluene, DCM, EtOH, MeOH and DCM respectively and dried under vacuum at rt. This afforded a calix[4]pyrrole modified silica nanoparticles **3.40**. Scanning Electron Microscopic (SEM) analysis of the obtained material revealed that the SiO₂ nanoparticles have a 55 nm mean particles size.

4. RESULTS AND DISCUSSION

Anions are omnipresent in the natural world although often neglected in terms of their importance. For instance, phosphate and nitrates from agricultural industry, pertechnetate a radioactive product of nuclear fuel cycling, cause major pollution hazards. Carbonates are key anions of biomineralized materials; nitrate and sulfate are present in acid rains, and chloride anion present in large quantities in the oceans. Anions also have critical roles in biological systems. They are critical for storage and manipulation of genetic information in DNA and RNA. For example, the DNA helicase RepA sulfate complex structure was solved by X-ray crystallography and the results showed the hydrogen-bonding interactions between the sulfate anion and RepA protein scaffold [75]. Anions are also involved in production of electrical signals in living organisms, regulating osmotic pressure, and activating signal transduction pathways. Therefore, a simple irregularity of anion flux across cell membranes is the key constituent of many diseases, including cystic fibrosis [76], Dent's disease [77], osteopetrosis [78], Pendred's syndrome [79], and Bartter's syndrome [80]. Several examples can be given here in terms of the importance of anions in biological systems and nature. But above examples are capable to show how anions play critical roles in our life. Therefore, complexation and recognition of anions represent a key field of supramolecular chemistry.

Of course, there are challenges of anion complexation. Number of reasons can be given for these challenges. First of all, anions are larger than the equivalent isoelectronic cations and hence have a lower charge to radius ratio [11]. Electrostatic binding interactions of anions are less effective than the corresponding isoelectronic cations because of more diffuse nature of anions. The data presented in Table 4.1 underscore the more diffuse nature of anionic species.

Table 4.1 : Radii differences of typical isoelectronic cations and anions.

Group I cations		Group 7 anions		Δr
Na ⁺	1.16 Å	F ⁻	1.19 Å	0.03 Å
K ⁺	1.52 Å	Cl ⁻	1.67 Å	0.15 Å
Rb ⁺	1.66 Å	Br ⁻	1.82 Å	0.16 Å
Cs ⁺	1.81 Å	I ⁻	2.06 Å	0.25 Å

There may be some need to design specific anion receptors functioning within the limited pH window. Anions may be protonated at low pH and lose their negative charge. This could be a particular problem when working with protonated receptors (e.g., ammonium containing receptors) as the protonation window of both receptor and anion must be considered. Another aspect of challenges about anion complexation is that the designing complementary receptors that are selective for particular anionic guests. This is because anionic species have a wide range of geometries. Figure 4.1 shows some examples of anions and their geometries.

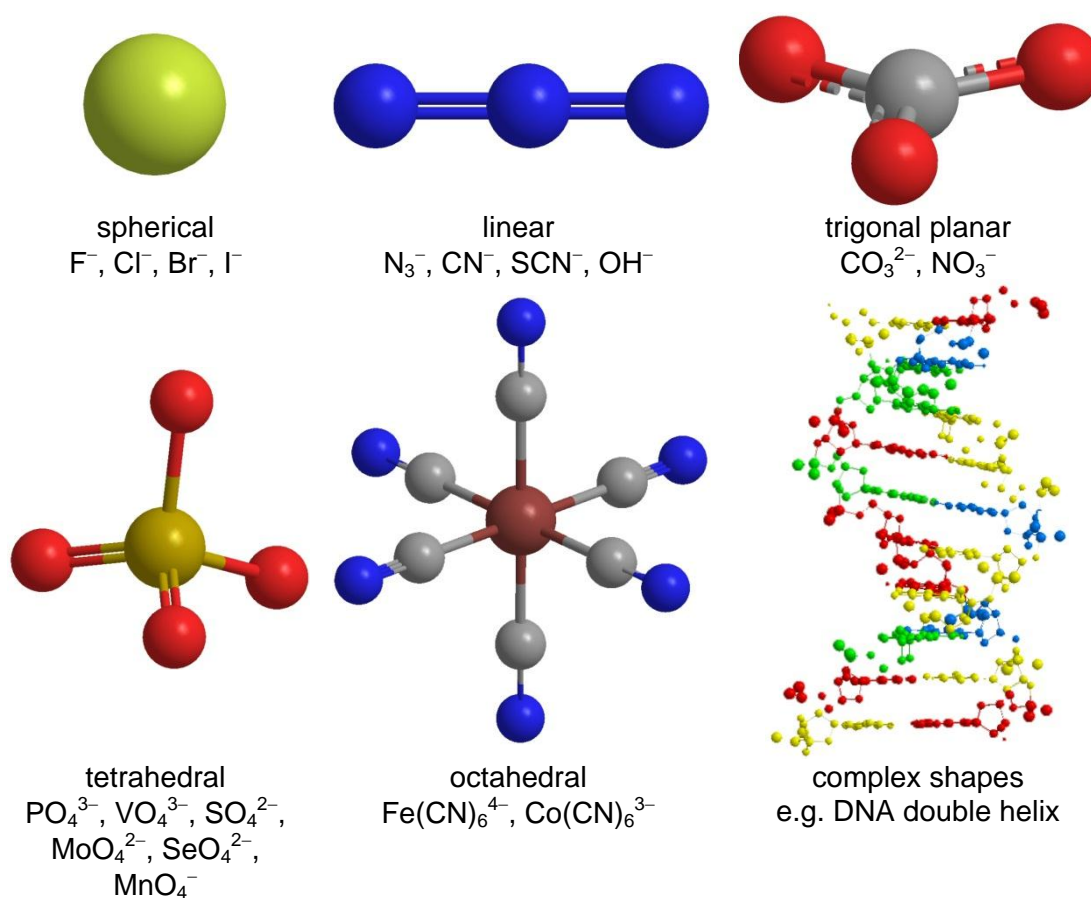


Figure 4.1 : Shapes of some anionic species.

Molecular recognition is one of the upraising areas of receptor design chemistry for a long time. Particularly, anion recognition is a new and growing area in terms of the biomedical and environmental importance. Ubiquity of anions in biological systems, playing important roles in the areas of medicine and potential application areas in nuclear fuel industry make this research area fast growing. In addition, anion receptors can be used as ion-selective receptors, phase-transfer catalysis, anion-selective optical sensors and chromatographic separation systems when it is attached on an appropriate stationary phase.

However, low anion-receptor interactions because of low ion charge density of anions and necessity of well-designed receptor architecture; make this research field hard to work. A number of research groups have designed simple and highly sophisticated anion receptor systems. Such receptors bind anions selectively, but they often have complicated structures and require multistep synthetic approaches. In this junction, calix[4]pyrrole compounds has emerged attentions and became readily accessible binding agents for anions, transition metal ions and neutral species.

In this study, synthesis of a variety of functional groups containing calix[4]pyrroles was aimed. For this purpose easy-to-prepare starting materials were chosen. The classification of research field can be summarized as below.

- Synthesis of long alkyl chain containing calix[4]pyrrole derivatives.
- Preparation of tetrabenzocalix[4]pyrrole starting from a masked pyrrole derivative.
- Synthesis of MMA polymers with calix[4]pyrrole pendant groups and their use in ion and ion pair extraction.
- Novel functionalized calix[4]pyrrole derivatives for the synthesis of dendrimeric calixpyrroles.
- And finally, covalently attaching of calixpyrroles to silica solid supports *via* a siloxane functionalized calix[4]pyrrole derivative.

Investigation of anion binding properties of final products was carried out as well as intermediate products if necessary. Structure elucidation of products was examined using applicable spectroscopic techniques.

4.1 Calix[4]pyrroles with Long Alkyl Chains

In this part of the thesis the subject is involved to detailed synthesis and structural characterization of a new set of highly organic solubilized calixpyrroles, along with a summary of their chloride and acetate anion binding properties as determined by ITC measurements carried out in 1,2-dichloroethane.

The present part was motivated by a desire to obtain calixpyrroles that would not partition significantly into water when studied under potential interfacial conditions. Specifically, it grew out of an appreciation that certain calix[4]pyrroles could be used to reverse the so-called Hofmeister bias [81-83] and were thus potentially useful as anion extractants.

Anion extraction is an application that could be of use both in the nuclear processing industry [81-83] and in terms of obtaining systems that could be used in such recognized environmental applications as minimizing surface water eutrophication resulting from agricultural runoff [84].

Highly organic soluble calixpyrrole derivatives are also potentially useful as through-membrane chloride anion carriers, an application that might have implications in the treatment of cystic fibrosis [85, 86]. As a first step towards these long term goals, we sought to develop long chain n-alkyl ester modified, *meso*- and β -pyrrole functionalized calix[4]pyrroles bearing either hydrogen or bromine atoms in the β -pyrrolic positions that would prove soluble in nonpolar organic solvents.

We also felt it necessary to test whether the modifications in question, including β -pyrrole bromination, affected the inherent anion recognition properties of the parent calix[4]pyrrole core. Towards this end, we have prepared the new ester-substituted systems **8**, **9**, **12**, and **13** (cf. Schemes 2 and 3) and analyzed their chloride and acetate anion binding properties, as well as for the first time those of the control system **2**, by ITC in 1,2-dichloroethane. We also report single crystal X-ray structures for the control ester systems **4** and **5**.

4.1.1 Synthesis and crystal structures

Although a large number of approaches leading to highly organic solvent soluble calix[4]pyrroles can be conceived, one of the more attractive strategies involves the use of long n-alkyl esters as the key solubilizing substituent. Such systems can be obtained from calix[4]pyrroles bearing carboxylic acids and/or smaller ester substituents in either the *meso*- and β -positions. Over the last decade, we have developed several syntheses of monofunctional calix[4]pyrrole carboxylic acids and esters and have recently extended these efforts to prepare polyfunctional calix[4]pyrroles containing carboxylic acid and ester functional groups [25]. The synthesis of β -pyrrole brominated calixpyrroles have been reported, including **2.20**, generated from the corresponding hydrido systems, but as yet have not extended this chemistry into the corresponding ester or carboxylic acid functionalized series. Given this, our synthetic goal was not only to produce long n-alkyl chain esters of carboxy-functionalized calix pyrroles, but also to develop methods for obtaining the corresponding β -pyrrole brominated systems, either by effecting bromination at an early stage and carrying the product through the remaining synthetic steps or by brominating after the final esterification. In point of fact, both of these latter strategies were pursued.

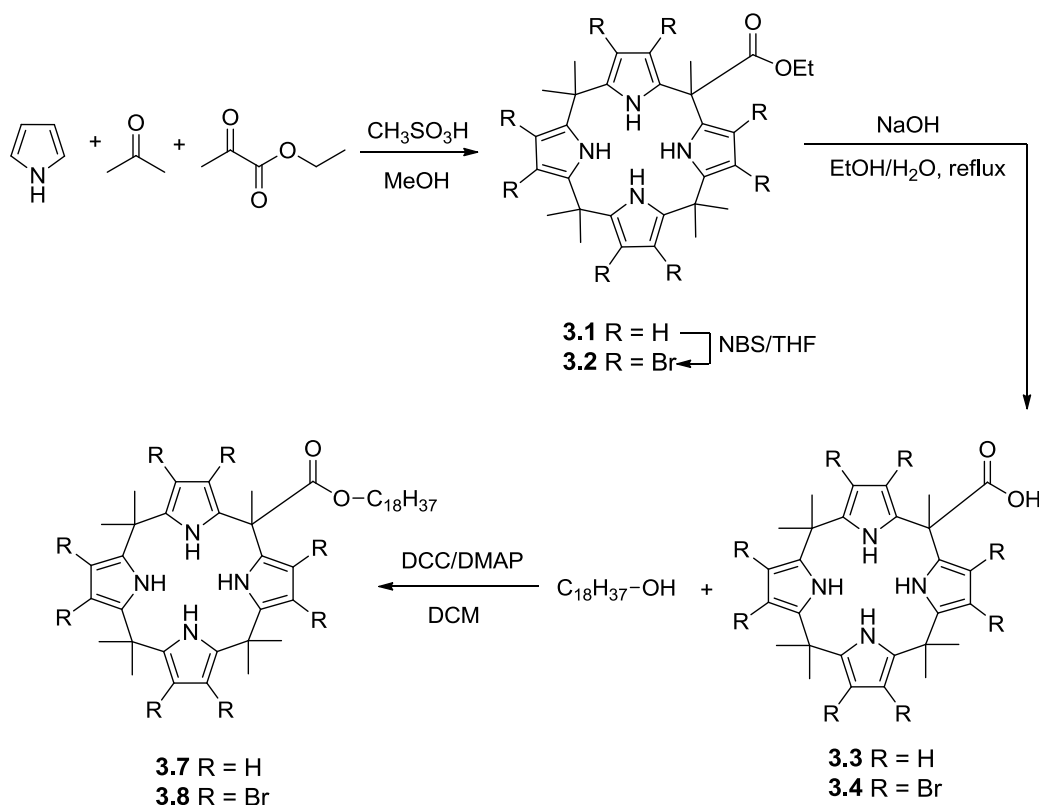


Figure 4.2 : Synthesis of n-alkyl ester calix[4]pyrroles over *meso* positions.

In this part, we also wish to present long alkyl chain substituted calix[4]pyrroles starting from basic and readily available calix[4]pyrrole compounds (e.g., **2.1**, **2.14** and **3.1**). Synthesis and binding results of **2.1**, **2.14** and **2.20** have been reported in previous publications. We have selected the esterification of the carboxylic acid containing calix[4]pyrroles (**3.3**, **3.4** and **3.5**) for the synthesis of long alkyl chain substituted compounds which are soluble in nonpolar solvents (e.g., hexane and pentane). We also wish to report the results of anion binding studies carried out by ITC.

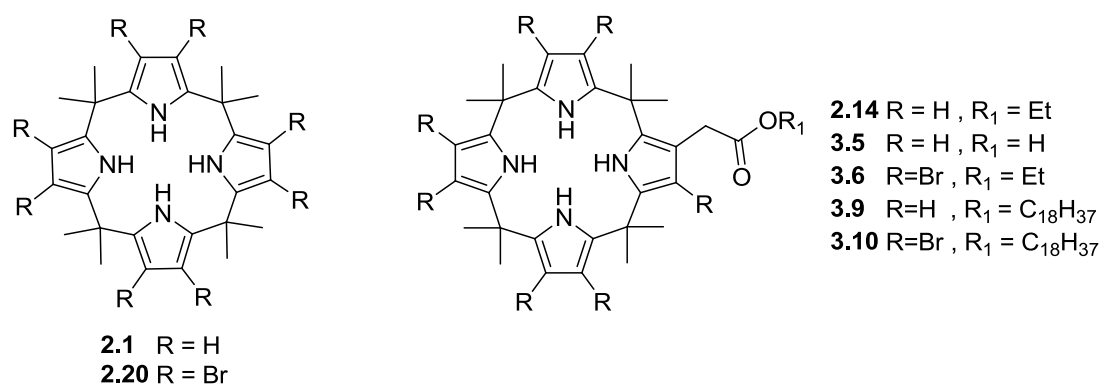


Figure 4.3 : Synthesis of n-alkyl ester calix[4]pyrroles over β positions.

Figures 4.2 and 4.3 provide a summary of the new preparative chemistry presented in this report. It reveals that the key organic solubilization step involves the esterification of compounds **3.3**, **3.4** and **3.5**. These systems, in turn, were prepared from the simpler ester systems **2.14**, **3.1**, and **3.2**. The synthesis of the key starting material **2.14** has been reported earlier [28], whereas the mono ester substituted calix[4]pyrrole **3.1** was prepared from the mixed condensation reaction of acetone and requisite ketoester using the same strategy used previously to generate polyfunctional calix[4]pyrroles [25]. In detail acid catalyzed condensation of pyrrole, acetone and ethyl pyruvate afforded a mixture of products including octamethylcalix[4]pyrrole **2.1**, the monoester **3.1**, and diester functional calix[4]pyrrole. Chromatographic purification using silica gel (DCM/hexanes : 80/20) as stationary phase yielded the monoester starting compound **3.1** in 14%. Structural elucidation of this yellowish solid compound was carried out using ^1H NMR spectroscopy (Figure 4.4).

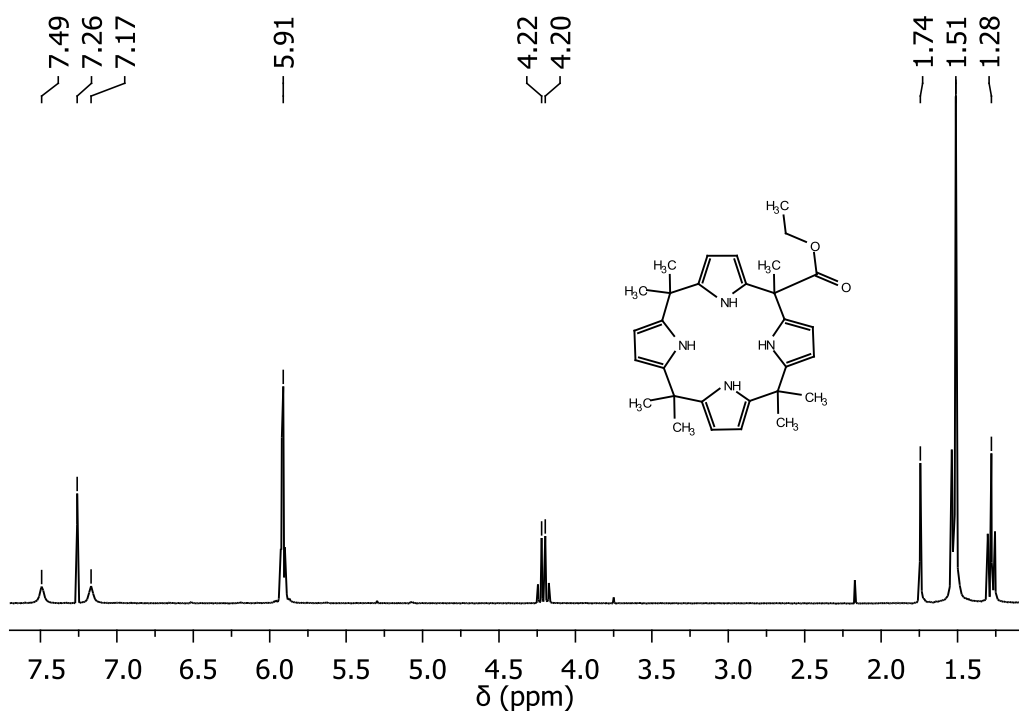


Figure 4.4 : ^1H NMR (CDCl_3) spectrum of the compound **3.1**.

NH protons of the compound **3.1** were observed at 7.49 and 7.17 ppm. Pyrrole CH protons were observed at 5.91 ppm. Ester CH_2 and CH_3 gave quartet and triplet peaks at 4.21 and 1.28 ppm respectively. Meso CH_3 protons of mono ester **3.1** were observed at 1.74 and 1.51 ppm respectively. ^{13}C NMR and mass analysis of the compound **3.1** were also consistent with the expected cyclic structure.

Compound **3.1** was also characterized by X-ray diffraction analysis. Single crystals of **3.1** were grown by slow evaporation of a solution of **3.1** in dichloromethane and diethyl ether. X-ray structural analysis of this compound revealed that the molecule has two crystallographically unique molecules, designated **3.1a** and **3.1b**, per asymmetric unit (Figure 4.5). Both unique molecules adopt 1,3-alternate conformations as is true in general for the anion-free forms of simple calix[4]pyrroles [17]. The ester group of structure **3.1a** is found to be tilted out of the plane defined by C15-C5-C21 with a torsion angle of 125.55° while in molecule **3.1b** the corresponding angle is 136.38° (as defined by C15'-C5'-C21').

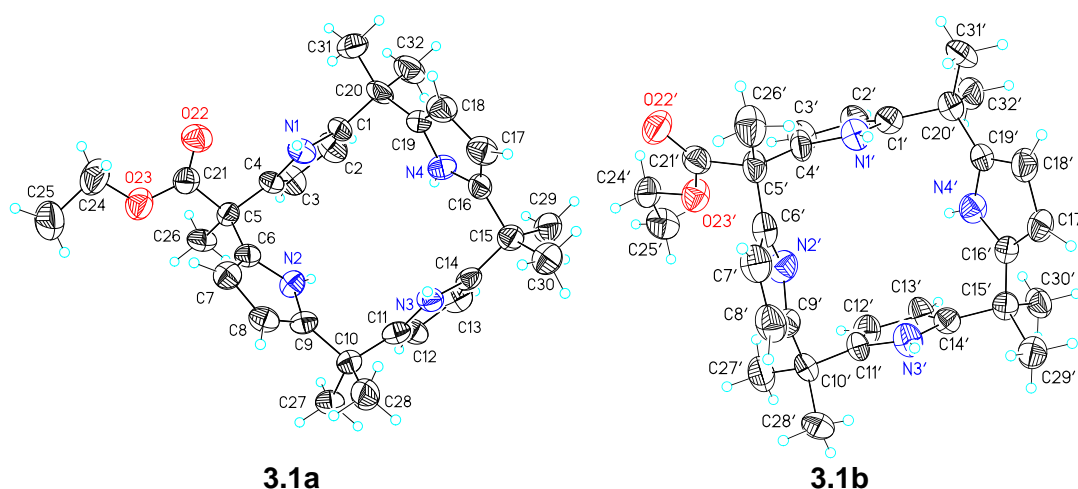


Figure 4.5 : View of the mono ester calix[4]pyrrole **3.1** in **3.1a** and **3.1b** showing the atom labeling scheme. Displacement ellipsoids are scaled to the 50% probability level.

In the case of both structures, the individual calix[4]pyrrole units interact with one another via H-bonding (Figure A.30). The geometry of these interactions are: N3···H3N···O22'; N···O 3.344(6)Å, H···O 2.46Å, N–H···O 168°; N1'–H1'N···O22, N···O 3.068(6) Å, H···O 2.17Å, and N–H···O 176°. These interactions create a one by one continuous crystal series of two unique crystals.

Solution ¹H NMR spectroscopic studies of **3.1** were carried out to see if these interactions are maintained in CDCl₃ solution. Both dilution and low temperature measurements were made. However, no appreciable shifts in the NH proton (or other) signals were observed in any of these experiments. It is thus concluded that the intermolecular interactions observed under the conditions of the X-ray diffraction analysis are a particular feature of the solid state.

Bromination of **3.1** with NBS proved just as effective as in the case of **2.1**[30](yielding **2.20** as the product) and allowed for the isolation of the hepta bromine-functionalized calix[4]-pyrrole **3.2** in 90% yield. To a dry THF solution of **3.1**

was added NBS and the resulting mixture was refluxed for 5 h. Flash column chromatographic purification (silica gel, DCM/hexanes: 1/1) of the crude product allowed to isolate **3.2** in 90% yield. ^1H NMR spectrum of **3.2** in CD_2Cl_2 revealed ester CH_3 protons at 1.33 ppm, *meso*- CH_3 protons between 1.53 and 2.14 ppm, ester CH_2 protons at 4.30 ppm, and no significant NH protons (Figure 4.6).

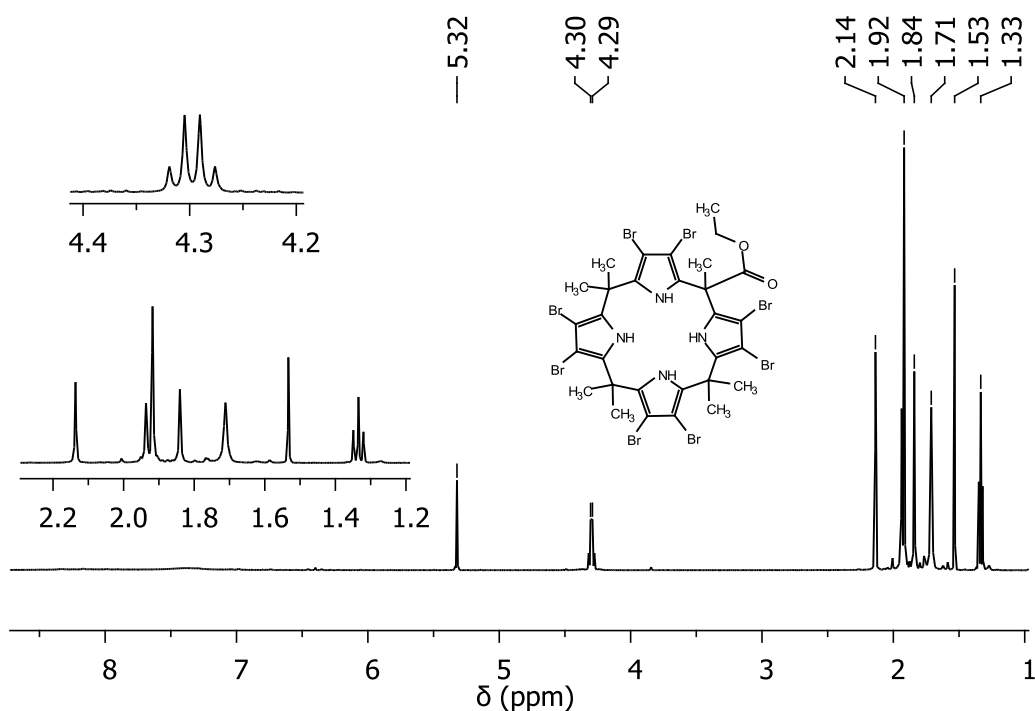


Figure 4.6 : ^1H NMR spectrum of **3.2** recorded in CD_2Cl_2 .

In general, it is possible to observe the NH proton signals of calix[4]pyrroles using ^1H -NMR spectroscopy, at least when common deuterated aprotic solvents, such as CDCl_3 , CD_2Cl_2 and $\text{DMSO}-d_6$, are used. However, in the case of compound **3.2**, the NH proton signals are not seen at room temperature when the spectrum is recorded in any of these solvents. Accordingly, efforts were made to record the ^1H -NMR spectrum under a range of temperatures. The appearance of NH proton signals at $-40\text{ }^\circ\text{C}$ in CD_2Cl_2 that are not observable over the temperature range $27\text{ }^\circ\text{C}$ to $-20\text{ }^\circ\text{C}$ (Figure 4.7), leads us to suggest that the electron withdrawing Br subunits make the NH protons more acidic, and hence more labile, than is true in the case of the corresponding non-brominated calix[4]pyrrole **3.1**. This increased acidity was expected to be reflected in the anion binding properties of this system, as well as those of other brominated derivatives. Included among the latter is **2.20**, a prototypical compound that has been the subject of previous ^1H NMR, but not ITC, based binding studies [87].

In contrast to what proved true for the pyrrolic *NH* protons, the ester *CH*₂ protons (4.30 ppm) were easily observable in the case of **3.2**. These are seen to be split into two multiplet peaks with a *J* = 7 Hz at low temperature. This splitting starts with a single peak at room temperature that undergoes broadening at 0 °C and is fully apparent at -40 °C.

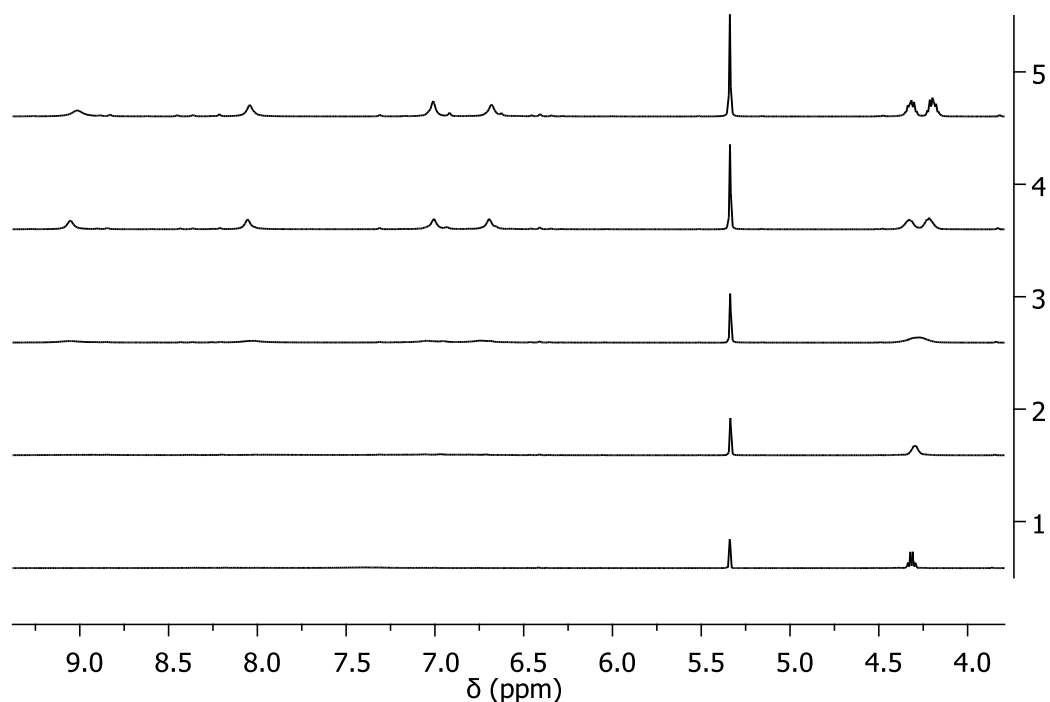


Figure 4.7 : ¹H NMR spectrum of **3.2** in CD₂Cl₂ recorded at various temperatures. Temperatures: 1 = 27 °C, 2 = 0 °C, 3 = -20 °C, 4 = -40 °C, 5 = -60 °C.

Such temperature dependence is consistent with a steric effect at low temperature that is sufficient to limit rotation of the pyrrole rings adjacent to the ester unit. As can be seen from the X-ray crystal structure of **3.2** (Figure 4.8), one of the pyrrole rings adjacent to the ester unit lies almost perpendicular to the core of the compound while the other one sits almost parallel. Hence, each ester *CH*₂ protons can exist in a different chemical environment, a phenomenon reflected in the splitting seen at low temperature. This proposed steric hindrance also affects the *meso-CH*₃ protons and results in different chemical shifts being seen for these signals at lower temperatures (Figure 4.7).

Diffraction grade crystals of **3.2** were obtained by slow evaporation of a dichloromethane/diethyl ether solution. X-ray analysis of **3.2** revealed that compound **3.2**, in spite of the bulky bromine units on the β-positions of pyrrole rings, adopts a 1,3-alternate conformation. However, two of the opposing pyrrole units (containing N2 and N4, respectively) are found to be tilted more in toward the central

ring cavity when compared to the corresponding pyrrole units of **3.1** (Figure 4.8). Presumably, this reflects substituent-induced steric effects. In the event, in contrast to what proved true for **3.1**, there is no evidence for appreciable hydrogen bonding based intermolecular interactions in the case of **3.2**, as can be inferred from an inspection of the unit cell packing diagram of **3.2** shown in Figure A.31.

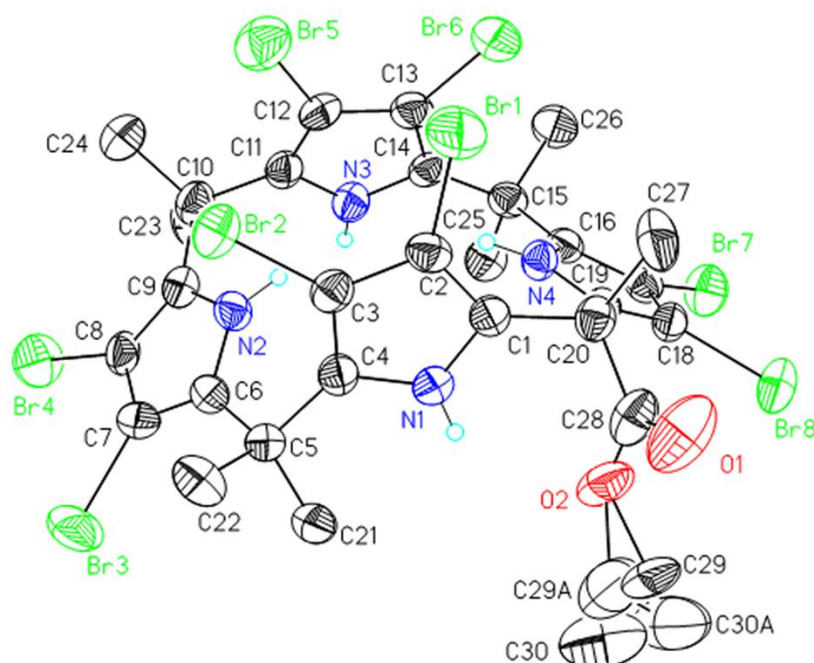


Figure 4.8 : View of **3.2** showing the atom labeling scheme. Displacement ellipsoids are scaled to the 50% probability level. The methyl hydrogen atoms have been removed for clarity. The ethyl group was disordered as shown.

After a successful afford to bromination of starting mono ester **3.1**, the next step was involved to preparation of carboxylic acid functionalized systems (**3.3** and **3.4**) which would have play as key intermediates to establish long alkyl chain substituted calixpyrrole derivatives. For this purpose, the compound **3.1** was exposed to hydrolysis under basic conditions (Figure 4.2). Specifically, **3.1** was refluxed in a mixture of EtOH/water containing NaOH. The solution was then acidified with concentrated HCl solution. This induced the precipitation of carboxylic acid functionalized calix[4]pyrrole **3.3** which was then easily isolated via filtration. ^1H NMR spectrum of the compound **3.3** was raised pyrrolic *NH* peaks 7.71 and 7.45 ppm, pyrrole *CH* peaks around 5.90 ppm, carboxylic acid proton at 2.85 ppm, and the *meso*- CH_3 protons between 1.73 and 1.50 ppm (Figure 4.9). Both ^{13}C NMR and mass analysis results of the product were consistent with the expected structure.

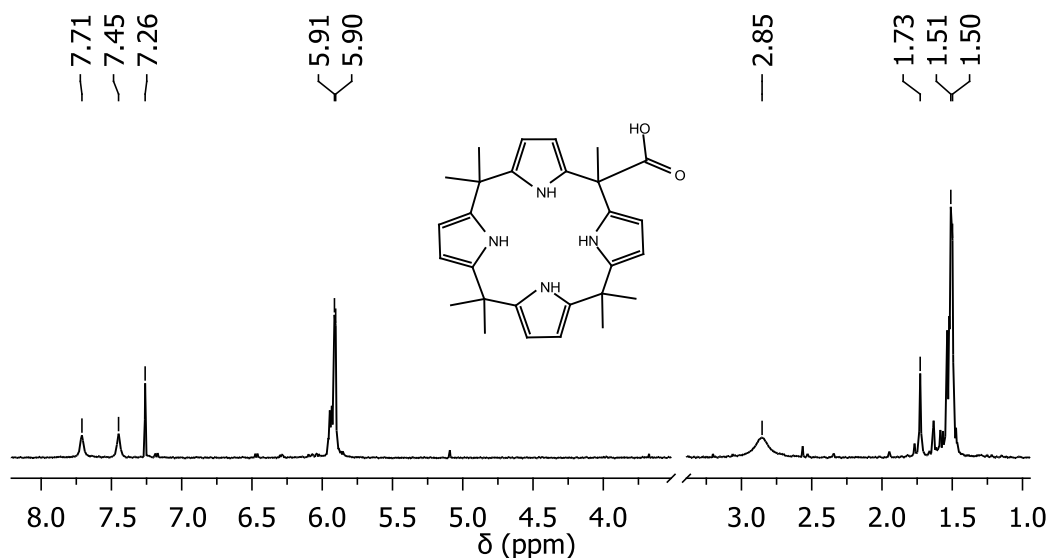


Figure 4.9 : ¹H NMR spectrum of **3.3** recorded in CDCl₃.

Using the same conditions above, the octabromocalix[4]pyrrole mono ester **3.2** was successfully hydrolyzed to its corresponding carboxylic acid derivative **3.4**. The compound **3.4** was not also reveal NH protons at ¹H NMR spectrum because of more acidic nature of NH protons as observed in the case of **3.2**. Carboxylic acid OH was observed at 3.88 ppm as a broad peak, meso CH₃ protons was also raised between 0.88 and 2.16 ppm (Figure 4.10).

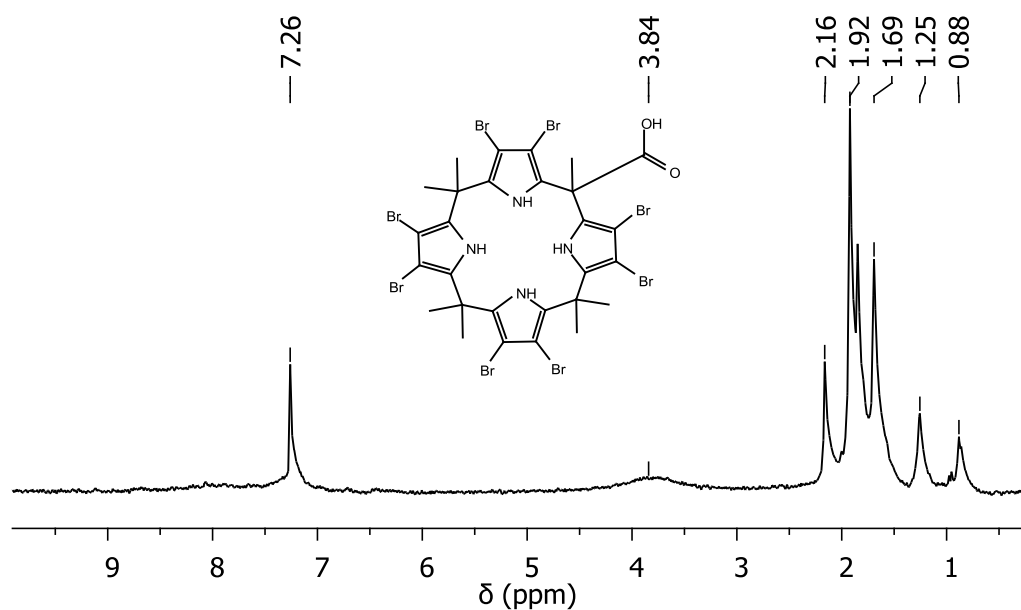


Figure 4.10 : ¹H NMR spectrum of **3.4** recorded in CDCl₃.

Using the same bromination agent (NBS) and reaction conditions applied to obtain **3.2**, compound **3.6** was synthesized in 89% yield starting from **2.14** which was reported earlier [28]. ¹H NMR analysis of isolated pure compound was carried out in

CDCl₃; revealed that because of the highly asymmetric nature of **3.6**, all of the NH protons maintained resonances in different regions of the spectrum (8.48, 7.95, 6.79, and 6.64 ppm). Ester CH₂ protons were observed at 4.09 ppm as a broad triplet, β-CH₂ protons at 3.35 ppm as a sharp singlet, meso-CH₃ protons between 1.82 and 1.26 ppm, and the ester CH₂ protons at 0.88 ppm in a triplet form as expected (Figure 4.11). The disappearance of pyrrole CH protons (5.88-5.69 ppm) of **2.14** upon bromination can be judged from Figure 4.11.

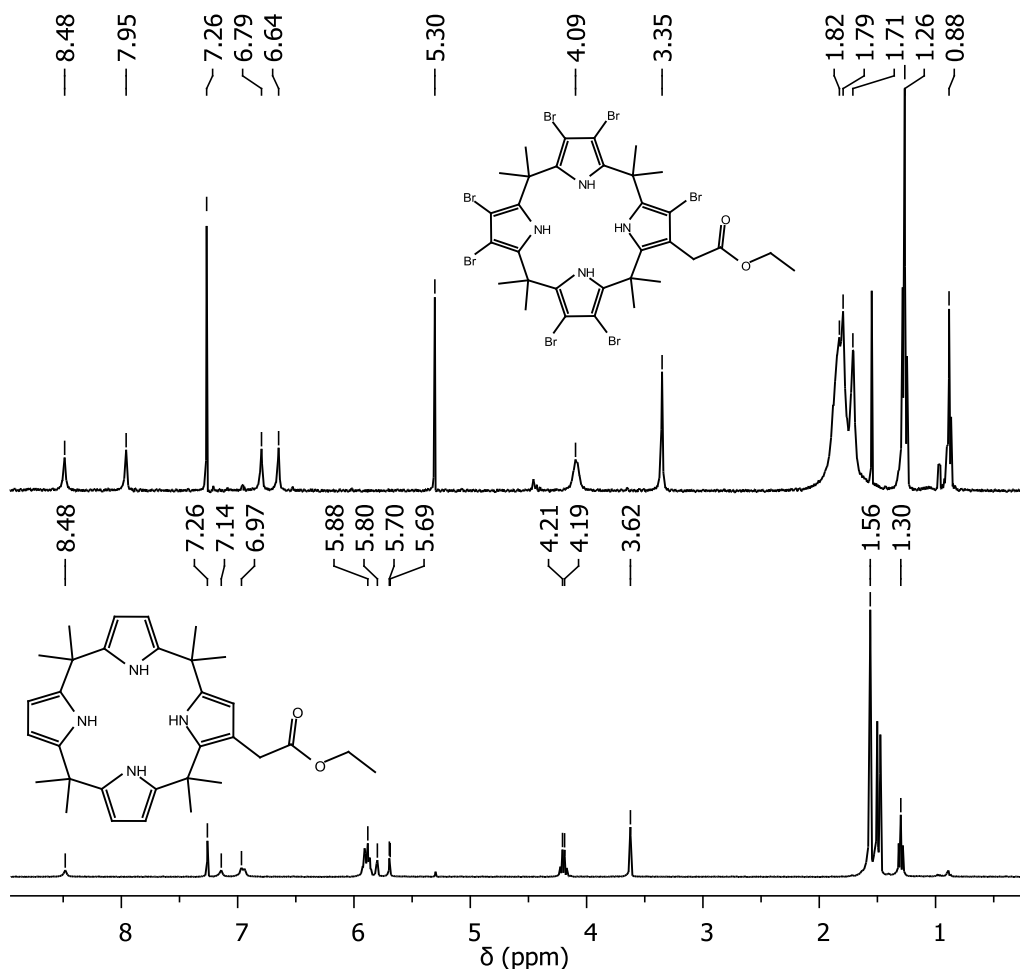


Figure 4.11 : ¹H NMR spectra of the C-rim modified heptabromocalix[4]pyrrole **3.6** (up) and **2.14** (down).

The next effort was dedicated to obtain carboxylic acid derivative (Figure 4.15) of the compound **3.6** as a starting material to reach long alkyl ester of this compound. Unfortunately, compound **3.6** was found to decompose under the conditions of ester hydrolysis circumstances applied to **3.1** and **3.2**. But this unsuccessful attempt did not cut off the achievement of obtaining corresponding long alkyl ester derivative of **3.6** as will be detailed in the next pages.

The actual attachment of the long n-alkyl ester chains to the carboxylic acid substituted calix[4]pyrroles (**3.3**, **3.4** and **3.5**) was carried out using DCC/DMAP in dichloromethane. This provided **3.7**, **3.8**, and **3.9** in good yield. However, as noted above, we were able to prepare compound **3.10** via direct bromination of **3.9**. Thus, both the initial, and “post synthetic modification” bromination strategies had to be employed to obtain the final ester functionalized perbrominated products **3.8** and **3.10**.

For instance, attachment of n-octadecyl unit to the compound **3.3** was achieved via esterification of carboxylic acid functional **3.3** and 1-octadecanol in the presence of DCC/DMAP at room temperature in CH₂Cl₂. These smooth conditions afforded a reaction mixture containing the product **3.7**. Isolation of the product via column chromatography yielded **3.7** in 51%. In this case pyrrole NH proton signals was observed at 7.42 and 7.07 ppm, pyrrole CH protons at 5.92 ppm as a narrow multiplet, and the O-CH₂ protons at 4.14 ppm as a triplet and the remaining protons between 1.75 and 0.86 ppm (Figure 4.12).

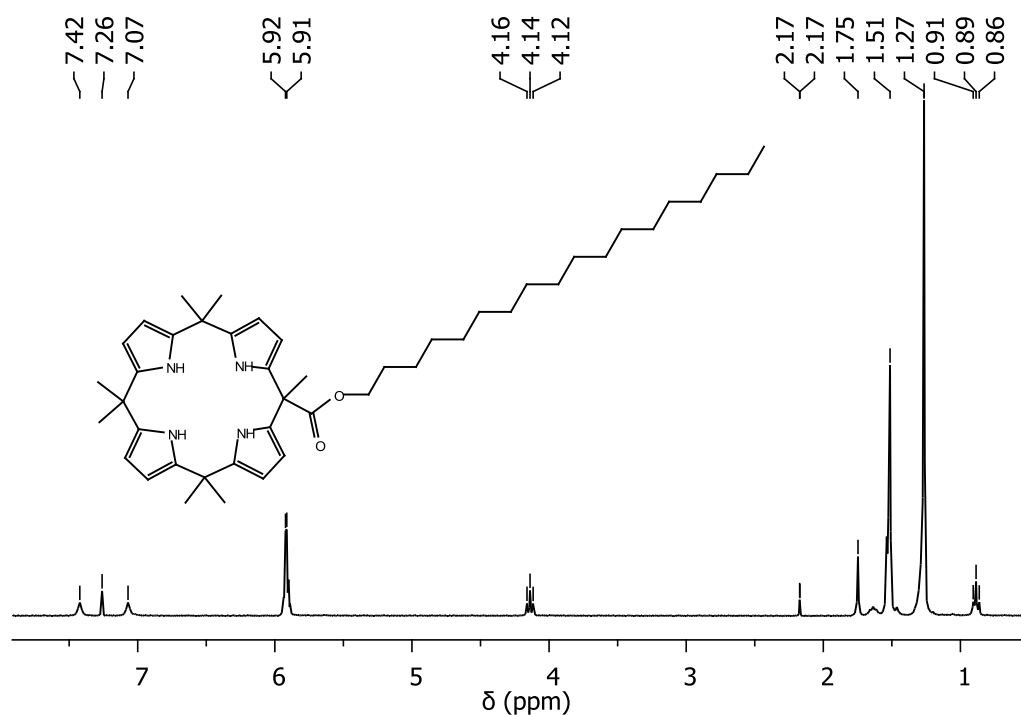


Figure 4.12 : ¹H NMR spectrum of **3.7**.

After the synthesis of n-alkyl ester substituted calix[4]pyrrole, the next effort was focused on the preparation of its octabromo derivative **3.8**. The aim of preparation of this compound is increasing the anion binding ability via electron withdrawing bromo substituents. For this purpose octabromocalix[4]pyrrole mono carboxylic acid **3.4** was reacted with 1-octadecanol using the same conditions used to prepare **3.7**. This

gave a white solid in 72% yield. ^1H NMR spectroscopic analysis of the product **3.8** revealed similar results except pyrrole CH proton signals (Figure 4.13). Interestingly, one of the pyrrole NH protons was revealed a down field shift at 11.82 ppm.

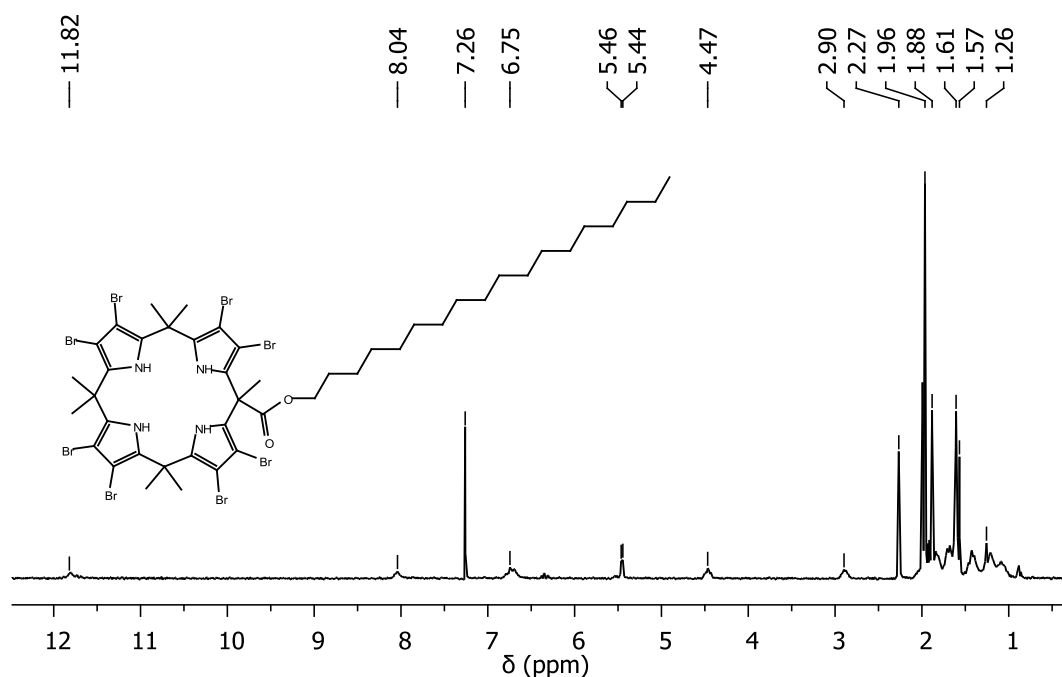


Figure 4.13 : ^1H NMR spectrum of **3.8** recorded in CDCl_3 .

Once the synthesis and structural elucidation of the *meso*-*n*-alkyl substituted calix[4]pyrroles **3.7** and **3.8** were succeeded, the next idea was the enrichment of *n*-alkyl ester substituted calixpyrrole derivatives. The first and convenient candidate would be preparation of β -substituted calixpyrrole derivatives. This would allow us to compare anion binding properties of *meso*- and β -substituted compounds.

In this junction, β -long alkyl chain substituted calix[4]pyrrole derivative **3.9** was synthesized starting from its corresponding carboxylic acid derivative **3.5** [45] via standard esterification conditions applied to obtain **3.7** and **3.8**. ^1H NMR spectroscopic analysis of the final product revealed that pyrrole NH proton signals located at 8.49, 7.10, 6.97, and 6.95 ppm. Pyrrole CH protons were spread between 5.90 and 5.71 ppm because of asymmetric nature of calixpyrrole. Ester CH_2 and β - CH_2 proton signals were observed at 4.15 (triplet) and 3.64 ppm, respectively. Remaining *meso*- CH_3 and long alkyl chain proton signals was observed between 1.69 and 1.29 ppm. The end CH_2 proton signal of octadecyl substituent was arisen at 0.91 ppm in expected triplet form (Figure 4.14).

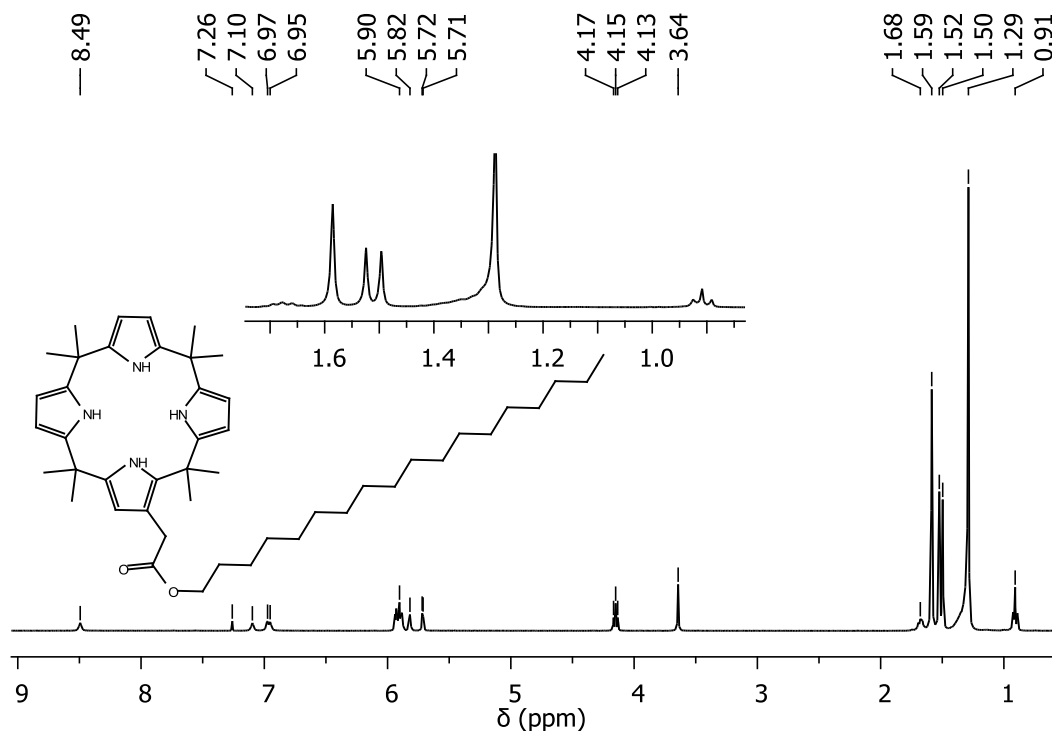


Figure 4.14 : ^1H NMR spectrum of **3.9** recorded in CDCl_3 .

The next step was involved to preparation of perbrominated derivative of **3.9** for enhanced anion binding ability. For this purpose, we thought to prepare carboxylic acid derivative of **3.6** (Figure 4.15) using the similar reaction conditions of ester hydrolysis applied to obtain **3.3** or **3.4**. Unfortunately, as noted above, starting material **3.6** was proved to decompose under ester hydrolysis conditions.

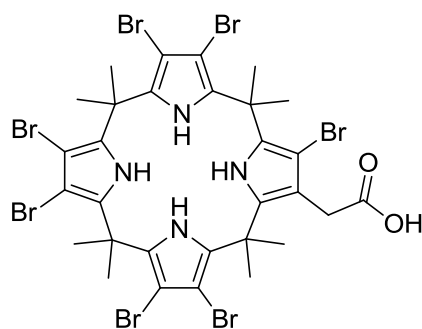


Figure 4.15 : Structure of 2-heptabromo- β -calix[4]pyrrolyl acetic acid.

While hydrolysis of **3.6** could not be achieved, direct bromination of **3.9** using NBS as a bromination agent under the conditions applied to obtain **3.2** and **3.6** afforded Octadecyl 2- β -heptabromocalix[4]pyrrolyl acetate **3.10** as a white solid in 90% yield. ^1H NMR spectroscopic analysis of **3.10** revealed the pyrrole NH proton signals at 8.48, 7.95, 6.79, and 6.64 ppm. Ester CH_2 and $\beta\text{-CH}_2$ proton signals was observed at 4.00 (broad triplet) and 3.35 ppm, respectively. *Meso-CH*₃ and remaining long alkyl chain CH_2 proton signals was arisen between 1.83 and 1.25 ppm. The end

CH_2 proton signal of octadecyl substituent was observed at 0.88 ppm as a triplet (Figure 4.16).

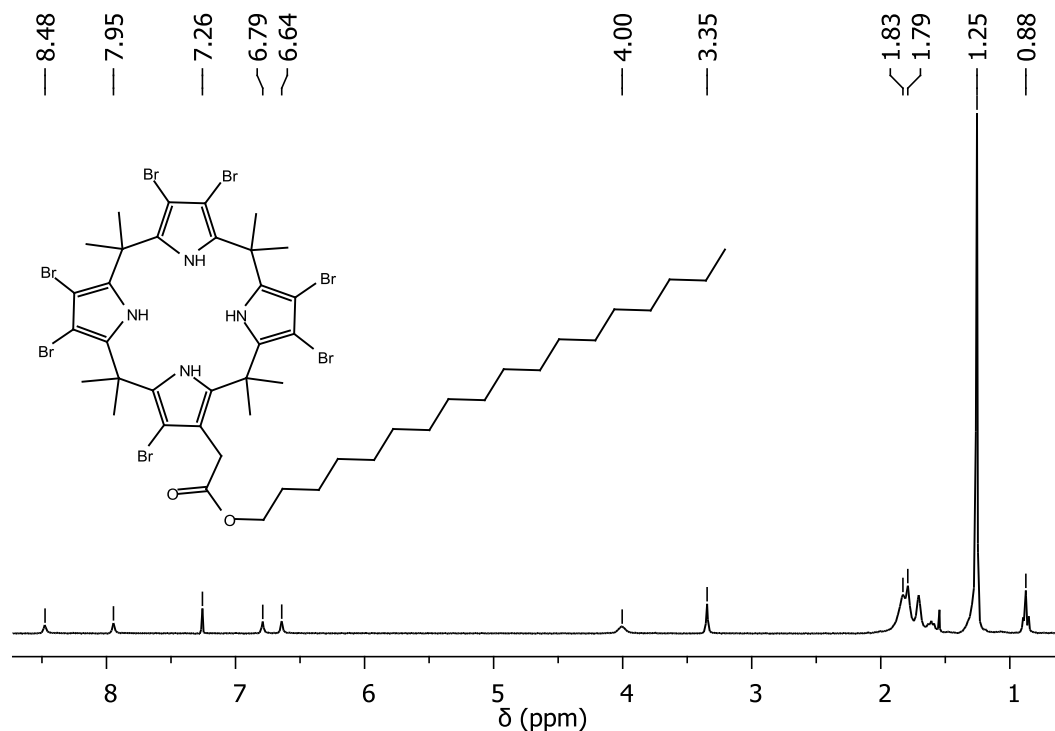


Figure 4.16 : 1H NMR spectrum of **3.10** recorded in $CDCl_3$.

Table 4.2 summarizes some structural elucidation data for the compounds prepared in this chapter.

Table 4.2 : Structural specifications of the compounds prepared for long alkyl chain substituted calix[4]pyrroles.

Compound	1H NMR (δ , ppm)			Mass (m/z)	
	NH	Pyrrole CH	meso- CH_3	Calcd.	Found
3.1	7.49, 7.17	5.91	1.74, 1.51	486.2995	486.2997
3.2	9.01- 6.68 ^a	–	2.14 - 1.53	1117.5754	1117.5762
3.3	7.71, 7.45	5.90	1.73 - 1.50	458.2682	458.2690
3.4	–	–	2.16 - 0.88	1089.5441	1089.5450.
3.6	8.48 - 6.64	–	1.82 - 1.26	1065.6982	1065.6990
3.7	7.42, 7.07	5.92	1.75, 1.52	711.5499	711.4483
3.8	11.82 - 6.75	–	2.27 - 1.88	1342.24208	1342.24251
3.9	8.49 - 6.65	5.90 - 5.71	1.59 - 1.50	739.5890	739.5858
3.10	8.48 - 6.64	–	1.79 - 1.25	1290.9564	1290.9576

^a Observed at -40 °C.

4.1.2 Anion binding studies

Although the long chain esters of this study proved fully soluble in such apolar solvents as pentanes and hexanes, anion binding measurements were carried out in 1,2-dichloroethane. This relatively apolar solvent was chosen, since 1) the

substituted calix[4]pyrroles of interest (i.e., **3.7**, **3.8**, **3.9**, and **3.10**) are not soluble in more polar solvents commonly used for such analyses, e.g., CH₃CN and DMSO, and 2) 1,2-dichloroethane was used in a recently published solvent dependence analysis of the chloride anion binding properties of **2.1** [88]. Thus, ready reference to these benchmark data could be made and, with this goal in mind, the chloride and acetate anion binding properties of **3.7**, **3.8**, **3.9**, and **3.10** were analyzed in 1,2-dichloroethane at room temperature using ITC (In general, 0.4 mM host solution was titrated with 8 mM guest solution (Figure 4.17, for other ITC titration curves see Figure A.34-A.48). Table 4.3 shows the binding constants for the novel calix[4]pyrroles of this study interacting with Cl⁻ and CH₃CO₂⁻ (studied as the corresponding TBA salts). Also included in Table 4.3 are previously reported chloride anion affinities of **2.1** [88, 89], as well those for compound **2.20** determined using ITC for the first time. The results in Table 4.3 reveal that the unfunctionalized and β-pyrrole perbrominated calix[4]pyrroles **2.1** and **2.20** bind chloride anion with similar affinity, with the brominated species proving to be somewhat less effective as a chloride anion receptor. This result is somewhat surprising. Based on previous studies involving fluorinated calix[4]pyrroles [38], it was expected that the presence of the electron withdrawing substituents on the β-positions of the pyrrole rings would lead to an enhanced chloride anion affinity.

Table 4.3 : Chloride and acetate anion-binding affinities measured in 1,2-dichloroethane (as the tetrabutylammonium salts) using ITC. Estimated errors are less than 10%.

Compound	Association Constant (M ⁻¹)	
	Cl ⁻	CH ₃ CO ₂ ⁻
2.1	2.8 × 10 ^{4a}	4.4 × 10 ⁴
2.20	1.8 × 10 ⁴	3.5 × 10 ³
2.14	2.4 × 10 ³	1.5 × 10 ³
3.1	9.4 × 10 ³	5.1 × 10 ³
3.2	2.9 × 10 ³	1.9 × 10 ³
3.7	5.8 × 10 ³	6.8 × 10 ³
3.8	1.8 × 10 ³	n/d ^b
3.6	2.8 × 10 ³	1.5 × 10 ³
3.9	2.0 × 10 ³	n/d
3.10	1.8 × 10 ³	n/d

^a Taken from reference [88]. ^b n/d : not determined.

However, the fact that this is not observed leads us to suggest that conformational effects play a critical role. Compound **2.20** possesses considerably bulkier substituents (i.e., bromine atoms) in the β-pyrrolic positions than does **1**; as a result, it is unable to adjust its conformation in favor of the cone conformation (dominant in

the anion bound form) as readily as **2.1**. To the extent such an analysis is correct; it would lead to a reduction in the chloride anion affinity based on an analysis of electronic factors alone. Consistent with this conclusion is the finding that the acetate anion affinity of **2.20** is also lower than that of **2.1**. This same trend is seen in the case of the brominated ester derivatives, with the chloride and acetate anion affinities of the ethyl ester system **3.1** being substantially higher than those of the corresponding brominated derivative **3.2**. Likewise, the chloride anion affinity of the long n-alkyl ester **3.7** proved ca. 3 times larger than that of the analogous brominated product **3.8**. Interestingly, however, the chloride anion affinities of **3.9** and **3.10**, both of which were among the lowest observed for the present study set, proved nearly identical.

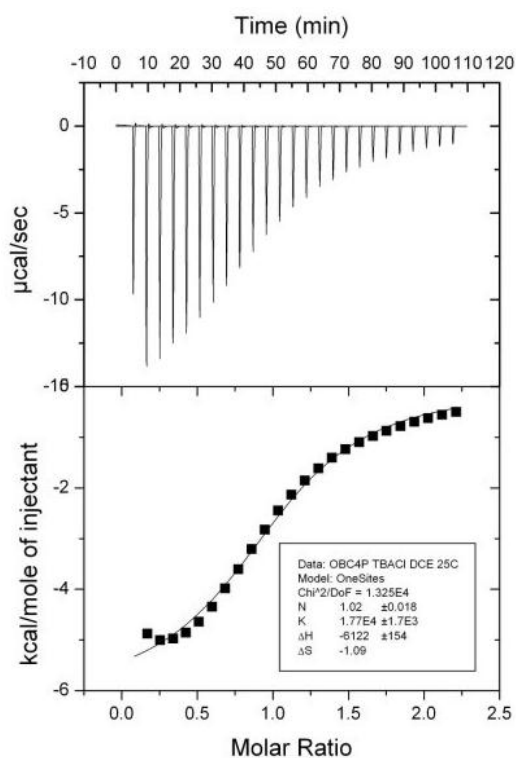


Figure 4.17 : ITC titration curve obtained from the titration of compound **2.20**.

The other major conclusion supported by the data in Table 4.3 is that functionalization of the calix[4]pyrrole core with an acetyl ester group serves to reduce the anion binding affinity by a factor of 2–10 depending on the system involved (e.g., *meso* vs. β -pyrrole substituted) but that the effect of the long chain n-alkyl ester per se is small. For instance, the chloride anion affinity of the ethyl ester **3.1** is roughly 2 times lower than that of **2.1**, whereas that of the long chain analogue **3.7** is lower by only a factor of ca. 3 (again compared to **2.1**). The relative effect of long chain ester functionalization is even less dramatic in the case of the β -pyrrole substituted esters. For instance, the chloride anion affinity of **2.14** and **3.9**, albeit

substantially reduced compared to that of **2.1**, are basically the same within error. Similar across the board trends are revealed in the case of acetate anion binding, although affinity constants for compounds **3.8**, **3.9**, and **3.10** could not be determined because of competing, but as yet unidentified, interactions observed in the ITC traces.

4.1.3 Conclusion

In conclusion, new mono carboxylic acid and ester functionalized calix[4]pyrroles bearing both short and long n-alkyl chains on the ester positions have been synthesized. ¹HNMR studies revealed that the brominated derivative **3.2** gives rise to nonobservable NH peaks at room temperature (CD₂Cl₂), but that these signals can be readily detected at lower temperatures (i.e., below -20°C). These results are consistent with the brominated calix[4]pyrroles of this study being endowed with more acidic NH protons. However, this presumed greater acidity is not reflected in higher chloride or acetate binding affinities relative to the hydrogen atom substituted forms, at least as judged from ITC measurements carried out at room temperature in 1,2-dichloroethane. These same anion binding studies revealed that all the new compounds, including the long n-alkyl esters, display relatively good anion binding affinities, albeit ones that are somewhat reduced compared to those of the parent calix[4]pyrrole (**2.1**). This combination of decent anion affinity and high solubility in nonpolar solvents, such as hexanes, makes the ester systems **3.7**, **3.8**, **3.9**, and **3.10** potentially attractive for use in further applications including anion extraction and transport.

4.2 Tetrabenzocalix[4]pyrrole

Calix[4]pyrroles are also emerging as useful elements in the construction of ion-pair receptors. At least in principle, such systems may allow for a higher level of control over ion recognition than simpler monotopic receptors. This enhanced recognition capability is expected to correlate with improved sensitivity, something that could be particularly useful in the area of extraction-based separations. Recently, we have made some progress in the latter area, demonstrating, for instance, that PMMA polymers containing pendant calix[4]pyrrole groups can extract tetrabutylammonium salts of fluoride and chloride from aqueous solutions [90]. Subsequently, crown ether moieties were incorporated into the basic calix[4]pyrrole-containing PMMA structure to create organic soluble polymeric systems capable of extracting KF and KCl from neutral aqueous media [91]. This result highlights the potential benefits that could accrue from being able to extract concurrently both an anion and a

corresponding counter cation. However, to date, this has proved difficult to do with simple (i.e., non-polymerized) neutral receptors. On the other hand, Sessler and coworkers recently demonstrated that octamethylcalix[4]pyrrole (**2.1**) would extract cesium halide salts as ion-pairs [83]. Here, small halide anions were used to organize the octamethylcalix[4]pyrrole framework into a cone conformation, thereby creating an electron-rich cup that favored Cs⁺ cation complexation. Extending the size of this “cup” beyond the simple “rim” provided by the β-pyrrolic protons of unfunctionalized calix[4]pyrrole **2.1** might allow this approach to work for harder, more highly hydrated cations such as K⁺ and Na⁺. This, in turn, is providing an incentive to prepare new modified calix[4]pyrrole derivatives. Inspiring from the results mentioned above the synthesis of the bicyclo[2.2.2]-oct-2-ene fused calix[4]pyrrole **3.15** with deep “walls”, as well as the results of efforts to convert this precursor to the corresponding calix[4]pyrrole derivative **3.16** that contains benzo units fused to the β-positions of the pyrrole rings.

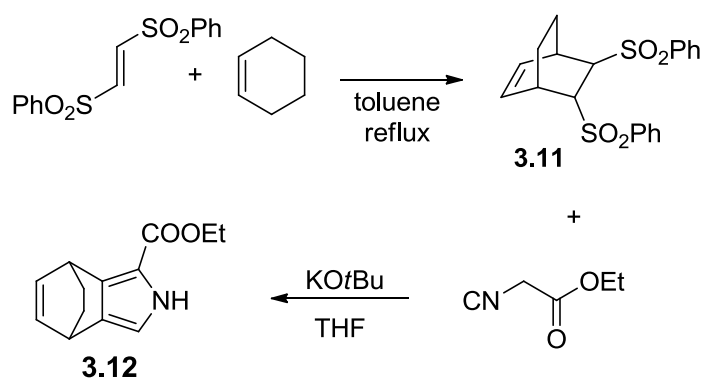


Figure 4.18 : Synthesis of **3.11** and **3.12**.

An attractive method to synthesis of calix[4]pyrrole targets **3.15** and **3.16** involves the use of 4,7-dihydro-4,7-ethano-2H-isoindole **3.14** as an isoindole equivalent [68]. This intermediate can be built up from (E)-1,2-bis(phenylsulfonyl)ethylenes detailed in Figure 4.18 and described briefly below; it was expected to allow access to the bicyclo[2.2.2]-oct-2-ene functionalized calix[4]pyrrole **3.15**, from which the benzo fused system **3.16** could presumably be accessed.

The synthesis of compound **3.12** is summarized in Figure 4.18. Briefly, (E)-1,2-bis(phenylsulfonyl)ethene was heated with 1,3-cyclohexadiene at reflux in toluene for 24 h. After removal of the solvent, the resulting crude product was purified by washing with ether; this yielded the Diels-Alder adduct **3.11** in 96% yield. ¹H NMR spectral data (Figure 4.19) of **3.11** was complementary with the reported literature specifications [92]. For full spectrum of **3.11** see Figure A.10.

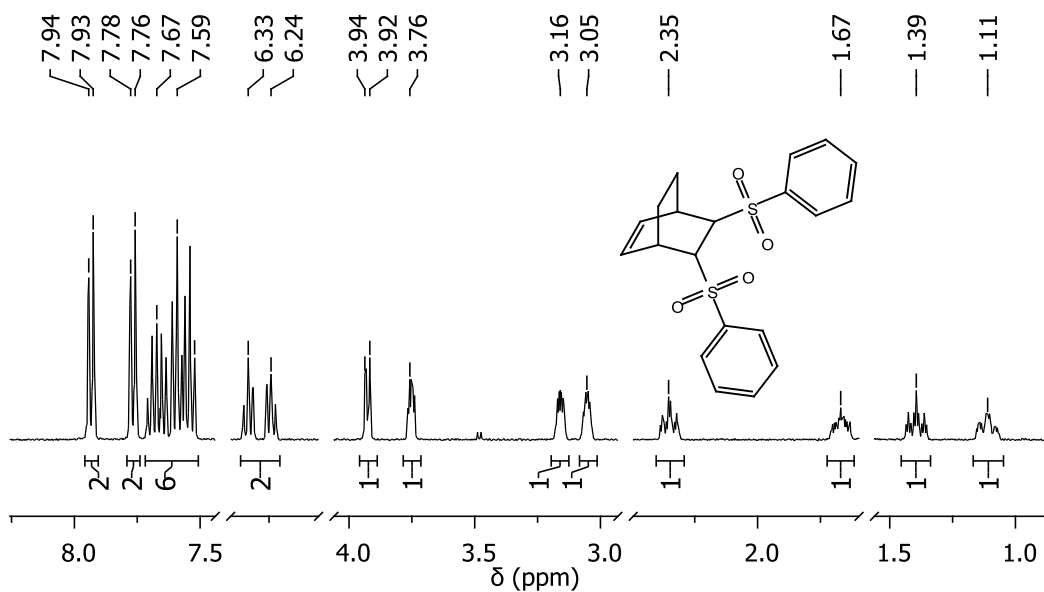


Figure 4.19 : ^1H NMR spectrum of **3.11** recorded in CDCl₃. Empty baselines were removed for clarity.

Once compound **3.11** was obtained, it was treated with ethyl isocyanoacetate and KO^tBu in dry THF at 0 °C. The reaction vessel was then kept at room temperature overnight. After workup, compound **3.12** was isolated by column chromatography over silica gel; it was obtained in 90% yield.

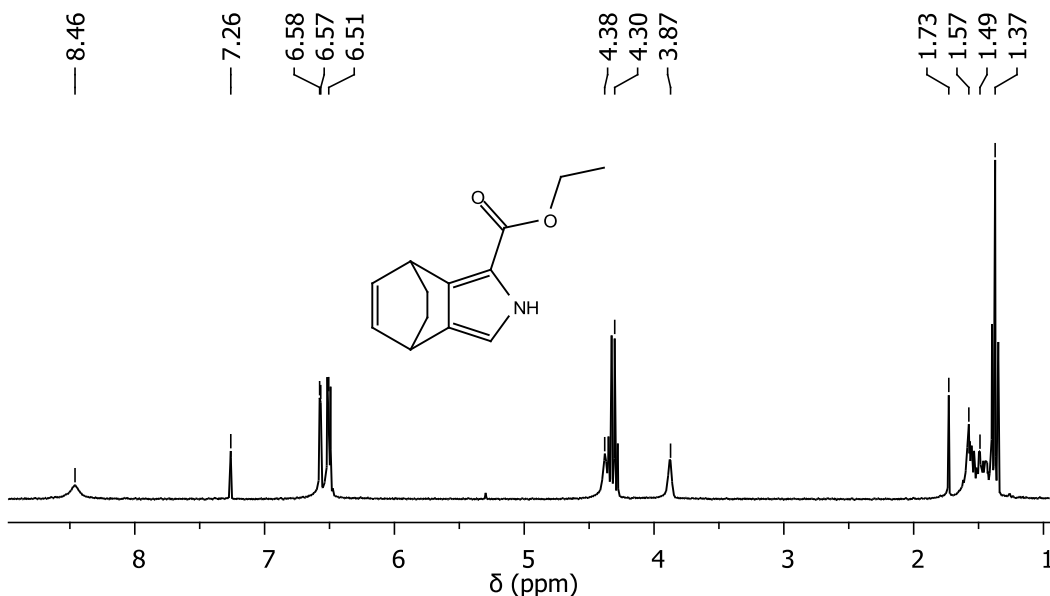


Figure 4.20 : ^1H NMR spectrum of **3.12** recorded in CDCl₃.

^1H NMR spectrum of **3.12** (Figure 4.20) revealed NH peak at 8.45 ppm, pyrrole ring α -proton at 6.56 ppm as a doublet, olefin protons between 6.47-6.50 ppm as multiplet, bicyclic-ring bridge protons at 3.86 and 4.36 ppm as multiplet peaks, ester CH₂ protons at 4.29 ppm as quartet, bicyclic-ring ethano protons between 1.40-1.60

ppm as multiplet peaks and ester CH_3 protons at 1.35 ppm as triplets. This proton NMR data is in good agreement with the literature data [68].

Direct decarboxylation of **3.12**, as illustrated in Figure 4.22, *via* treatment with KOH in ethylene glycol at 160 °C for 3.5 h proved problematic, giving product **3.14** in only low yield[68]. Therefore, we decided to synthesize compound **3.13** through a step-wise route that involved first saponification of ester **3.12** to give **3.13** then decarboxylation in cold TFA. Briefly, **3.12** was hydrolyzed with NaOH in an Ethanol/H₂O mixture at reflux temperature. The white product **3.13** was precipitated by dropwise addition of 0.1 N HCl solution after removal of excess of ethyl alcohol under vacuum. ¹H NMR spectroscopic analysis of **3.13** revealed broad pyrrole NH proton signal at 10.72 ppm, pyrrole α -CH proton at 6.55 ppm, olefinic CH protons at 6.44 ppm, bridge head CH protons at 4.25 and 3.82 ppm, COOH proton at 11.97, bridge CH₂ protons at 1.46 and 1.31 ppm (Figure 4.21). ¹³C NMR spectroscopic and mass spectrometry analyses of the compound **3.13** are consistent with the expected structure.

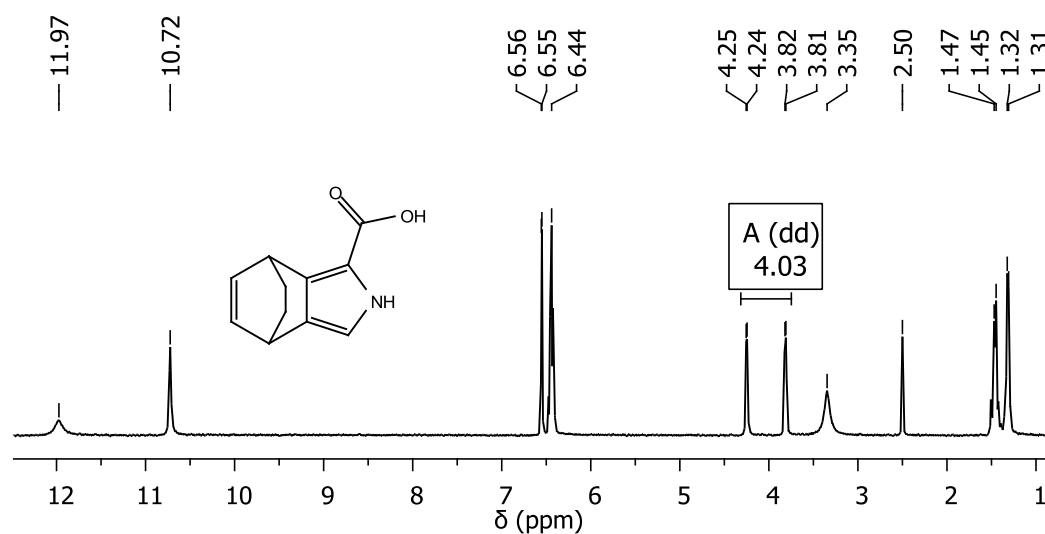


Figure 4.21 : ¹H NMR spectrum of **3.13** recorded in *d*₆-DMSO.

Once the carboxylic acid derivative **3.13**, corresponding to the starting ester, was obtained, it was decarboxylated by treating with TFA at 0 °C for 30 min under an Ar atmosphere. Using this strategy, 4,7-dihydro-4,7-ethano-2*H*-isoindole **3.14** was obtained in 92% overall yield.

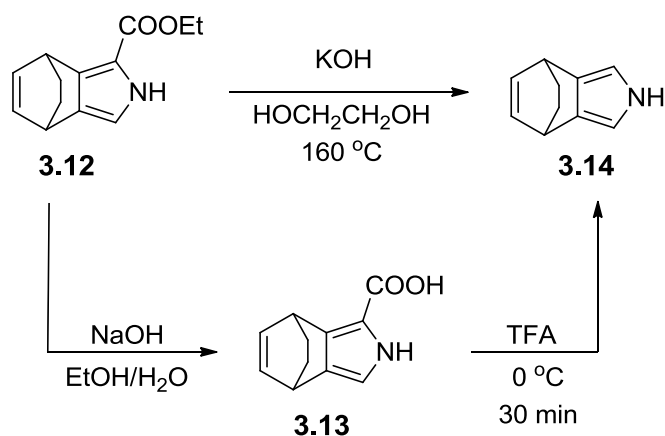


Figure 4.22 : Saponification pathways of **3.12**.

^1H NMR spectroscopic analysis of the masked pyrrole derivative is given in Figure 4.23. **3.14** raised NH proton signal at 7.51 ppm, olefinic CH protons signals at 6.53 ppm, pyrrole CH protons at 6.47 ppm, bridge head CH protons at 3.86 ppm, and bridge CH₂ protons at 1.55 ppm.

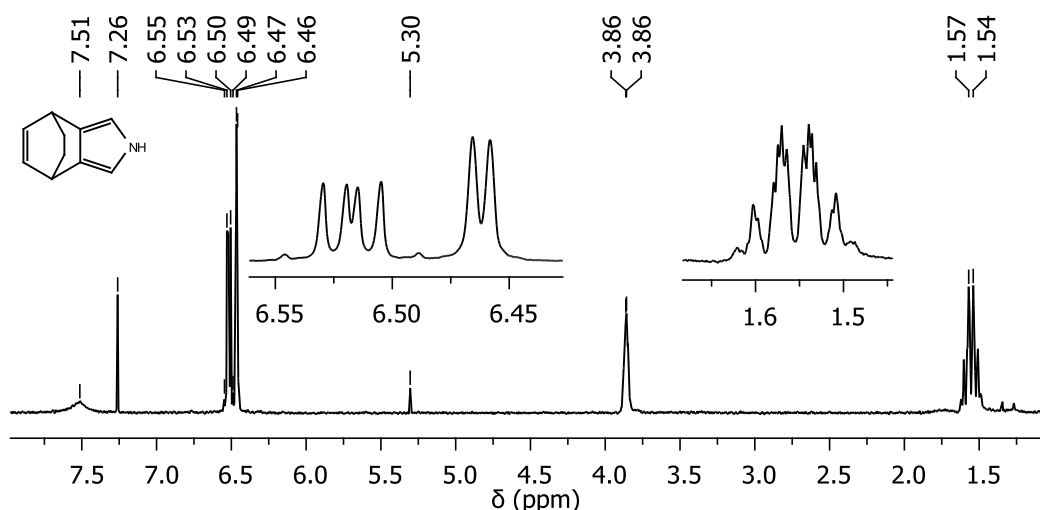


Figure 4.23 : ^1H NMR spectrum of **3.14** recorded in CDCl_3 .

Efforts were then made to prepare the corresponding calix[4]pyrrole derivative **3.15** by condensing **3.14** with acetone in the presence of an acid catalyst, as shown in Figure 4.24. Towards this end, the general calix[4]pyrrole forming condition, involving the use of an acid catalyst (e.g., $\text{CH}_3\text{SO}_3\text{H}$) in MeOH. However, the desired calix[4]pyrrole compound **3.15** was not obtained in isolable quantities.

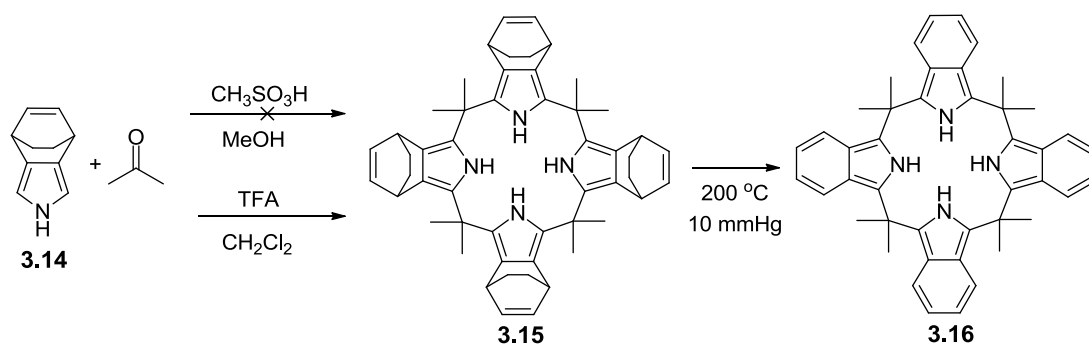


Figure 4.24 : Synthesis of the compound **3.15** and tetrabenzocalix[4]pyrrole (**3.16**).

Therefore, the condensation reaction was carried out in CH_2Cl_2 using TFA as the acid catalyst. In this case, workup and column chromatography gave compound **3.15** in 50% yield as a white solid. The resonances corresponding to the aliphatic CH protons were found to lie between $\delta = 1.25$ and 1.58 ppm, in the ^1H NMR spectrum. This result, considered in concert with the disappearance of the pyrrole α -proton signals, led to the conclusion that product **3.15** contains an intact calix[4]pyrrole structure (Figure 4.25). Furthermore, FAB mass analysis of compound **3.15** revealed only one signal at 742 amu, a value corresponding to the molecular mass of the compound **3.15** plus one proton (Figure A.64).

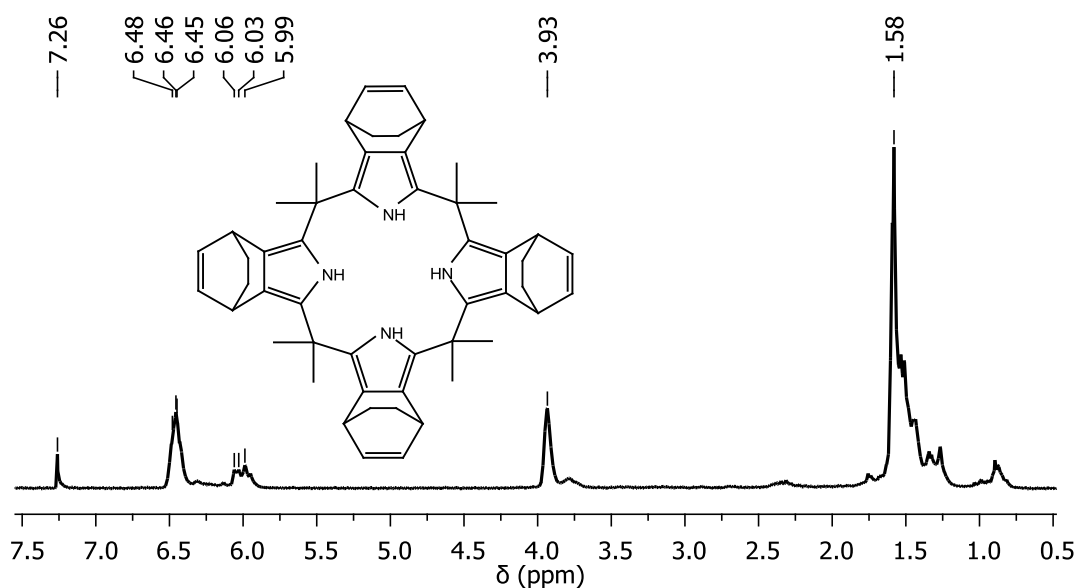


Figure 4.25 : ^1H NMR spectra of **3.15** recorded in CDCl_3 .

With compound **3.15** in hand, an effort was made to obtain the corresponding tetrabenzocalix[4]pyrrole **3.16**. With goal in mind, compound **3.15** was subject to retro Diels-Alder reaction conditions (Figure 4.24). Specifically, compound **3.15** was heated to 200 $^\circ\text{C}$ under vacuum at 10 mmHg for 10 min, with the resulting crude product being subject to column chromatography. Unfortunately a quantitative

conversion of **3.15** into **3.16** could not be achieved in this work even though similar retro Diels-Alder reaction conditions have proved effective in creating porphyrin derivatives analogous to **3.16** [68]. Moreover, separation of product **3.16** from the starting material **3.15** using column chromatography was not successful. Therefore, ^1H NMR spectroscopic and mass spectrometric analyses of the reaction mixture were employed to track the course of the putative conversion.

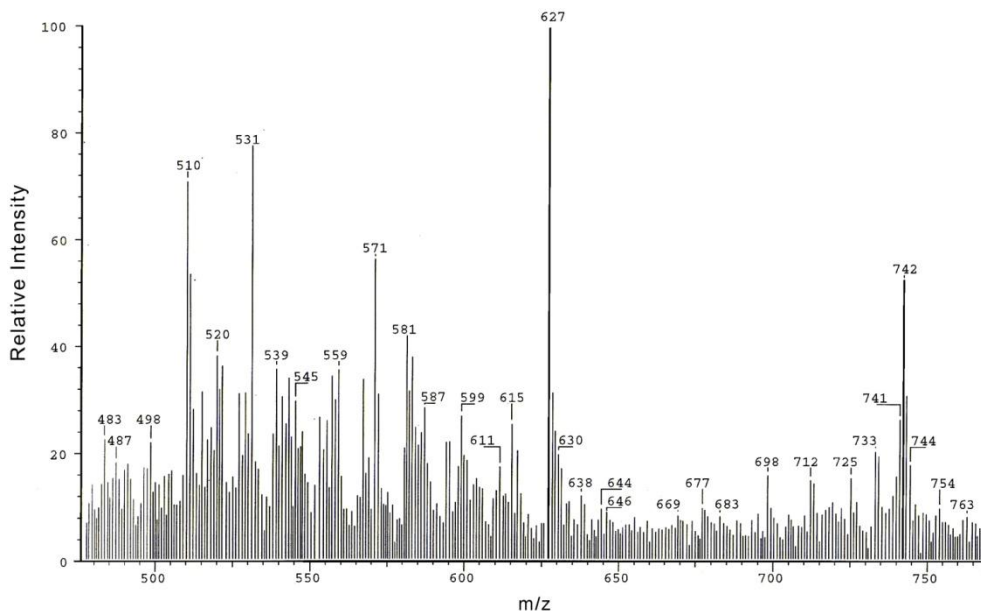


Figure 4.26 : FAB Mass spectrum of **3.16**.

The ^1H NMR spectra recorded after heating **3.15** for an extended period revealed the appearance of peaks at $\delta = 6.89$ and 7.71 ppm, signals that were ascribed to the aromatic CH protons expected for **3.16**. Likewise, as shown in Figure 3.16, a mass spectrometric analysis of the reaction mixture revealed a signal at 627 amu corresponding to the expected tetrabenzocalix[4]pyrrole product **3.16** ($[M]^+$), as well as signal corresponding to the molecular mass signal of the compound **3.15**. Taken in concert, these two findings provide support for the notion that at least partial conversion to **3.16** takes place upon heating **3.15** under vacuum.

In conclusion, the synthesis of the tetra-bicyclo[2.2.2]-oct-2-ene fused calix[4]pyrrole **3.15** and its partial conversion to the corresponding tetrabenzocalix[4]pyrrole **3.16** were studied. Possible efforts would be improving this latter conversion and studying system **3.15** as a possible ion-pair receptor and deep-walled “molecular container”.

4.3 Polymers with Pendant Calix[4]pyrrole Units

The nature of the binding interactions involved, primarily hydrogen bonds, would lead to the expectation, generally supported by experiment, that in highly

competitive media this and other neutral, pyrrole-derived receptors [21, 22] would display anion affinities that are substantially reduced. However, recent studies wherein pyrrolic systems are either embedded in various types of functional materials, e.g., ion selective electrodes [93, 94] and colorimetric sensors [95], or covalently attached to solid supports to produce anion-selective HPLC packings [45], have served to show that ostensibly weak anion binding agents, including calix[4]pyrrole and its derivatives, can be highly effective anion receptors under mixed organic-aqueous interfacial conditions. This has led us to consider that soluble polymeric materials containing calix[4]pyrrole subunits linked directly to the macromolecular backbone (as opposed to covalently attached to a preformed polymer support) might prove particularly useful for the purpose of anion-binding materials. These materials could have a role in addressing a variety of current challenges, including corrosion prevention (e.g., chloride, carbonate, and sulfate control under conditions of combustion [96]), waste remediation (e.g., sulfate extraction from tank waste [97, 98]), toxin control (e.g., mitigating the effects of overexposure to cyanide [99] or fluoride [100]), and health care (i.e., enhanced phosphate removal under conditions of hemodialysis [101]), to name but a few.

4.3.1 Tetrabutylammonium fluoride and chloride extraction studies

In this chapter, the synthesis and characterization of polymers and copolymers containing calixpyrrole (**3.18**) and MMA will be detailed. In addition, it will be demonstrated that organic solutions of the calixpyrrole-functionalized copolymer are capable of extracting TBACl and TBAF from aqueous solutions significantly better than calixpyrrole **2.1** and PMMA. To the best of our knowledge, this is the first example of an anion receptor appended to a PMMA backbone and the first study wherein an anion receptor-based polymeric system of any type has been used to effect anion extraction under interfacial aqueous-organic conditions (Examples of polymeric anion receptor systems are limited, see ref. [102-106]).

4.3.1.1 Synthesis of methacryloyl functionalized calix[4]pyrrole

Attachment of methacryloyl functionality was achieved using simple esterification reaction of hydroxymethyl calix[4]pyrrole **3.17** and methacryloyl chloride. The starting hydroxymethyl calix[4]pyrrole **3.17** was prepared via reduction of respective ethyl ester (**3.1**) using NaBH₄/MeOH in THF at reflux temperature. Quenching the reaction with NH₄Cl and extraction of organic residue with CH₂Cl₂ followed by chromatographic separation afforded **3.17** in 75% yield (Figure 4.27).

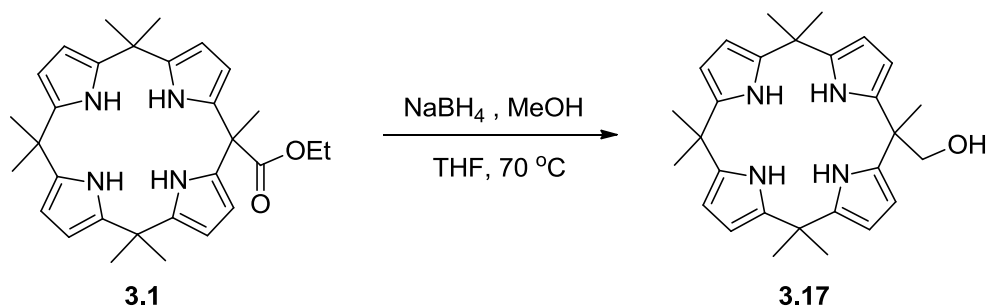


Figure 4.27 : Synthesis of hydroxymethyl calix[4]pyrrole **3.17**.

NMR spectroscopic analysis of the compound **3.17** was carried out in CDCl_3 and revealed pyrrole NH proton signals at 7.57 and 7.11 ppm, multiplet pyrrole CH proton signals was arisen between 5.96 and 5.91 ppm, CH_2 proton signals at 3.86 ppm as a doublet, OH proton signal at 1.94 ppm as a triplet and *meso*- CH_3 protons proton signals between 1.54 and 1.42 ppm.

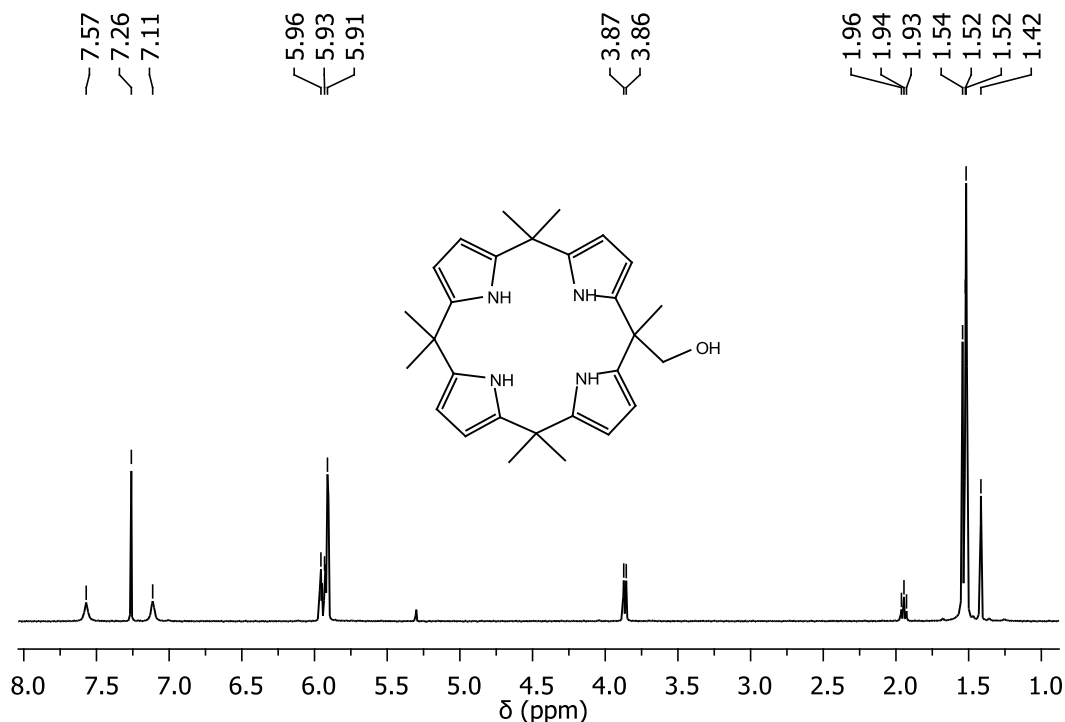


Figure 4.28 : ^1H NMR spectrum of **3.17** recorded in CDCl_3 .

Single crystals of **3.17** grew as pale yellow lathes by colorless laths by vapor diffusion of hexanes into a dichloromethane solution of the calixpyrrole. The data crystal was a long lathe that had approximate dimensions; 0.34 x 0.13 x 0.04 mm. The data were collected on a Nonius Kappa CCD diffractometer using a graphite monochromator with $\text{MoK}\alpha$ radiation ($\lambda = 0.71073\text{\AA}$). A total of 341 frames of data were collected using ω -scans with a scan range of 1.2° and a counting time of 198

seconds per frame. The data were collected at 153 K using an Oxford Cryostream low temperature device (Figure 4.29).

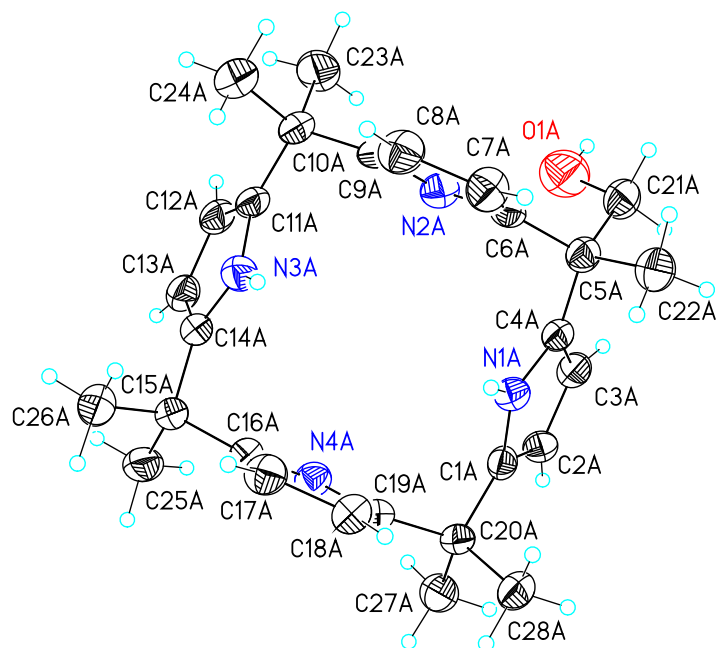


Figure 4.29 : View of molecule **3.17** in the atom labeling scheme. Displacement ellipsoids are scaled to the 50% probability level (CCDC 668095).

The functionalized calix[4]pyrrole monomer **3.18** was prepared in 82% yield from the hydroxymethyl calixpyrrole derivative **3.17** through treatment with methacryloyl chloride under basic conditions. Briefly, alcohol **3.17** and methacryloyl chloride was stirred in cold THF in the presence of Et₃N. Quenching of the reaction with water, extraction of organic residue with CH₂Cl₂ and purification with flash column chromatography were yielded monomer **3.18** (Figure 4.30).

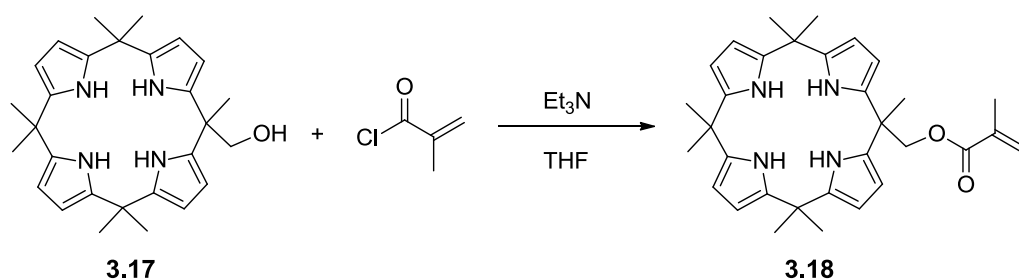


Figure 4.30 : Synthesis of methacryloyl substituted calix[4]pyrrole.

After the synthesis of the compound **3.18**, its structural elucidation was carried out first using ¹H NMR spectroscopy (Figure 4.30). **3.18** revealed the NH proton signals at 7.14 and 7.05 ppm, methacryloyl CH proton signals at 6.01 and 5.55 ppm, pyrrole CH protons between 5.93 and 5.89 ppm, meso-CH₂ protons at 4.38 ppm, methacryloyl CH₃ at 1.90 ppm, and remaining calixpyrrole meso-CH₃ protons between 1.54 and 1.48 ppm.

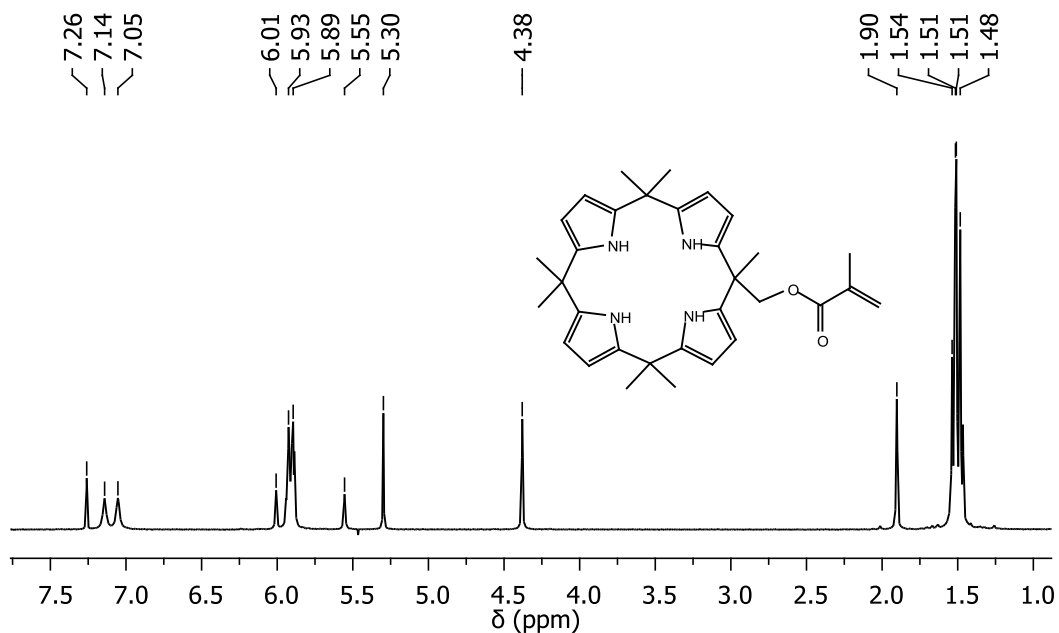


Figure 4.31 : ^1H NMR spectrum of **3.18** recorded in CDCl_3 .

Further characterization support about the structure of **3.18** came from single crystal X-ray diffraction analysis (Figure 4.32). Single crystals of **3.18** were grown as colorless prisms by slow evaporation from dichloromethane. The data crystal was cut from a larger crystal and had approximate dimensions; 0.30 x 0.26 x 0.14 mm. The data were collected on a Nonius Kappa CCD diffractometer using a graphite monochromator with $\text{MoK}\alpha$ radiation ($\lambda = 0.71073\text{\AA}$).

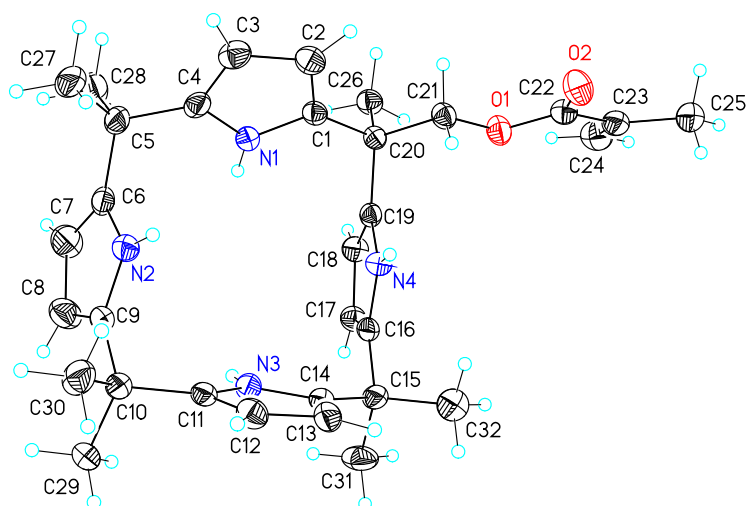


Figure 4.32 : View of **3.18** showing the atom labeling scheme. Displacement ellipsoids are scaled to the 50% probability level.

Monomer **3.18** contains a methacrylate functionality and proved amenable to polymerization using conventional free radical methods [107].

4.3.1.2 Synthesis of homopolymer and MMA copolymer

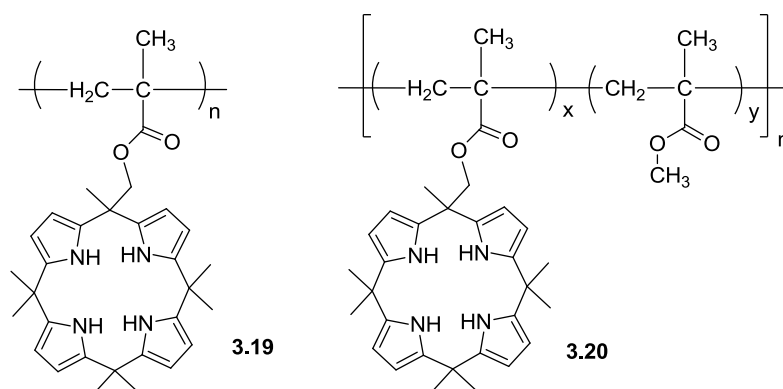


Figure 4.33 : Structures of the homopolymer and MMA copolymer of **3.18**.

In initial studies, homopolymer **3.19** was prepared by dissolving monomer **3.18** in THF (0.3 M) followed by treatment with 1 mol% of AIBN. After stirring at 70 °C for 17 h under an atmosphere of nitrogen, the resulting viscous solution was added dropwise into excess methanol with rapid stirring. This caused precipitation of polymer **3.19**, which was later isolated via filtration in 66% yield. Using gel permeation chromatography (GPC), the polymer was found to have a number-average molecular weight (M_n) of 23.600 Da (relative to PMMA standards) and a polydispersity index (PDI) of 2.3. ^1H NMR spectroscopic analysis of the homopolymer **3.19** revealed NH proton signal 7.12 ppm, pyrrole CH protons at 5.89 ppm, *meso*- CH_2 protons at 4.15 ppm, *meso*- CH_3 and polymer backbone CH_3 protons between 1.25 and 1.85 ppm, and polymer backbone CH_2 proton signals between 0.34 and 0.95 ppm (Figure 4.34).

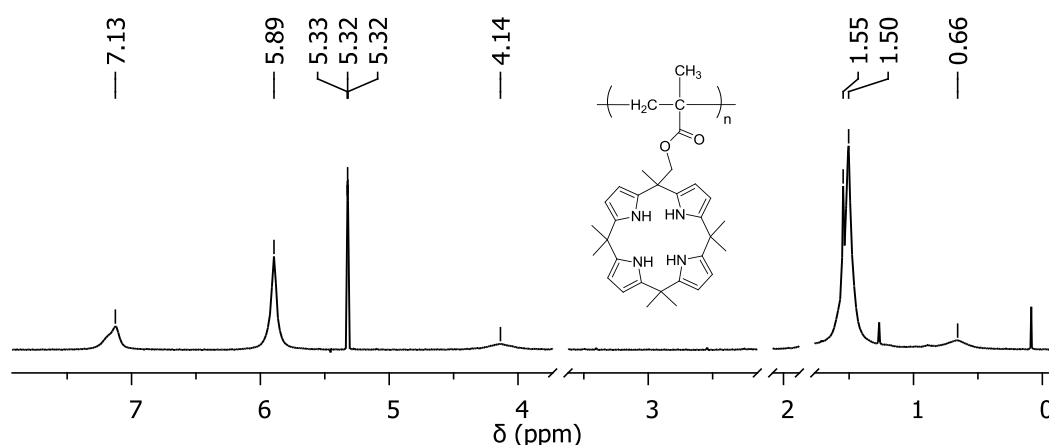


Figure 4.34 : ^1H NMR spectrum of homopolymer **3.19** recorded in CD_2Cl_2 . Solvent peaks were removed for clarity.

To improve the physical properties of the calix[4]pyrrole functionalized PMMAs (including their potential ability to serve as anion extractants), a copolymer of

methacrylate functionalized calixpyrrole **3.18** and MMA was prepared. Using the conventional free radical polymerization conditions described above, a 77% yield of copolymer **3.20** was obtained from a 1:10 mixture of **3.18** and MMA. Using GPC, copolymer **3.20** was found to possess a M_n of 85500 Da and a PDI of 2.1. The relatively high molecular weight, compared to **3.19**, led us to conclude that the incipient and/or growing polymer chains may be negatively influenced by the large steric bulk of the calix[4]pyrrole in monomer **3.18**. Regardless, polymer **3.20** proved to be highly soluble in most common organic solvents, including dichloromethane. ^1H NMR spectroscopic analysis (CD_2Cl_2) revealed that there were ca. 14 methacrylate units per calixpyrrole unit within **3.20**.

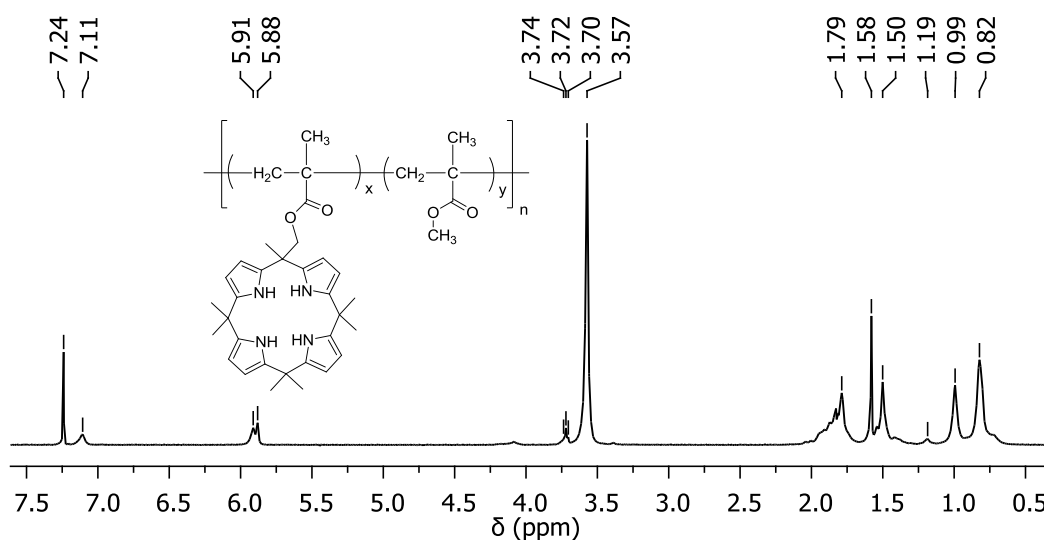


Figure 4.35 : ^1H NMR spectrum of calixpyrrole-MMA copolymer **3.20** recorded in CDCl_3 .

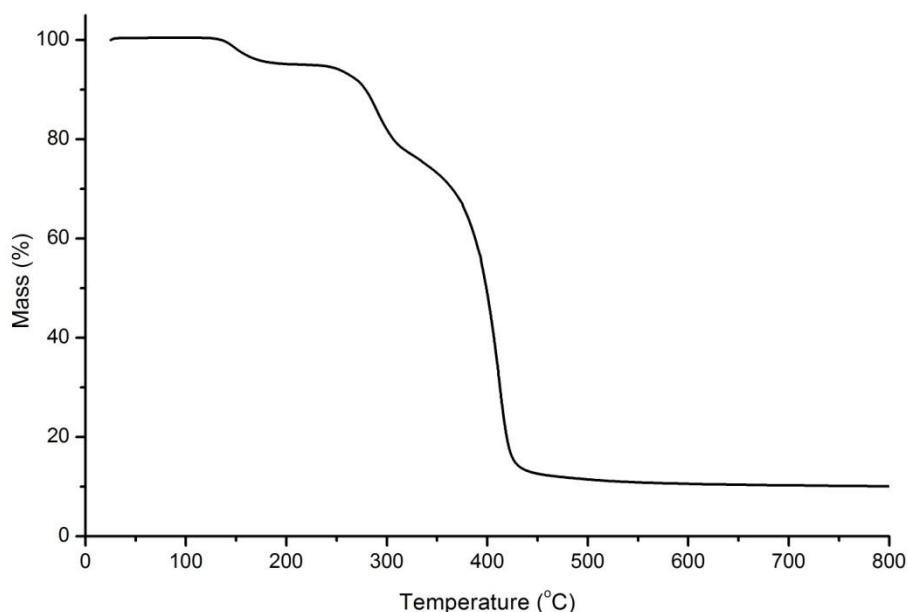
Figure 4.35 shows ^1H NMR spectroscopic analysis of copolymer **3.20**. Following results were concluded from the NMR analysis. Polymer backbone CH_2 proton signals was observed at 0.82 and 0.99 ppm, calixpyrrole *meso*- CH_3 protons between 1.50-1.58 ppm, MMA CH_3 protons between 1.80-1.88 and 3.57 ppm, calixpyrrole *meso*- CH_2 protons at 4.11 ppm, pyrrole CH proton signals between 5.89-5.95 ppm, and finally pyrrole NH protons at 7.11 ppm.

Although the ratio of **3.18**:MMA observed (1:14) in copolymer **3.20** was slightly higher than the monomer feed ratio (1:10), ^1H NMR analysis of **3.20** leads us to suggest that the microstructure of this material is largely random and not a block copolymer of MMA and polymerized **3.18**. Specifically, two signals attributed to the methyl ester of MMA were found at $\delta = 3.3$ and 3.4 ppm (C_6D_6) in relative integrals of 2:1. Table 4.3 summarizes the specifications of homopolymer **3.19** and copolymer **3.20**.

Table 4.4 : Specifications of polymers **3.19** and **3.20**.

Specification	3.19	3.20
Monomer ratio (3.18 :MMA)	1:0	1:10
Product Ratio (3.18 :MMA)	1:0	1:14
M_n	23 600 Da	85 500 Da
PDI	2.3	2.1
NH proton signal	7.13 ppm	7.11 ppm
Pyrrole CH proton signal	5.89 ppm	5.89 ppm
meso-CH ₂ signal	4.15 ppm	4.11 ppm
MMA O-CH ₃ signals	–	3.57 ppm

For comparison, a sample of PMMA ($M_n = 40700$; PDI = 1.5) was prepared using a procedure analogous to that used to obtain **3.19** and **3.20**. Thermal analysis of **3.20** revealed a decomposition temperature (T_d) at 272 °C (Figure 4.36), which is intermediate of respective T_d s found for **3.19** (270 °C) and the PMMA homopolymer (276 °C) used for comparison (All thermal analyses were performed under an atmosphere of nitrogen at a scan rate = 10 °C/min, for thermogravimetric graphics of all compounds see Figure A.49-A.63). Collectively, these results provide support for the proposal that the physical properties of copolymers prepared from MMA and **3.18** may be tuned through judicious monomer selection.

**Figure 4.36** : Thermogravigram of polymer **3.20** taken under an atmosphere of nitrogen at a scan rate = 10 °C/min.

4.3.1.3 Extraction Studies

Once polymer **3.20** was fully characterized, efforts shifted toward exploring its ability to bind anions under interfacial conditions. Extraction studies were carried out in NMR tubes using CD₂Cl₂ solutions of polymers and control compounds. D₂O solutions of TBA salts were added to polymer solutions and tubes were shaken

vigorously. Afterwards, the organic and aqueous phases allowed to separate and centrifuged at 5000 rpm to maintain full phase separation. After obtaining a separated clear solution ^1H NMR spectra of CD_2Cl_2 phase were recorded to see changes in organic phase.

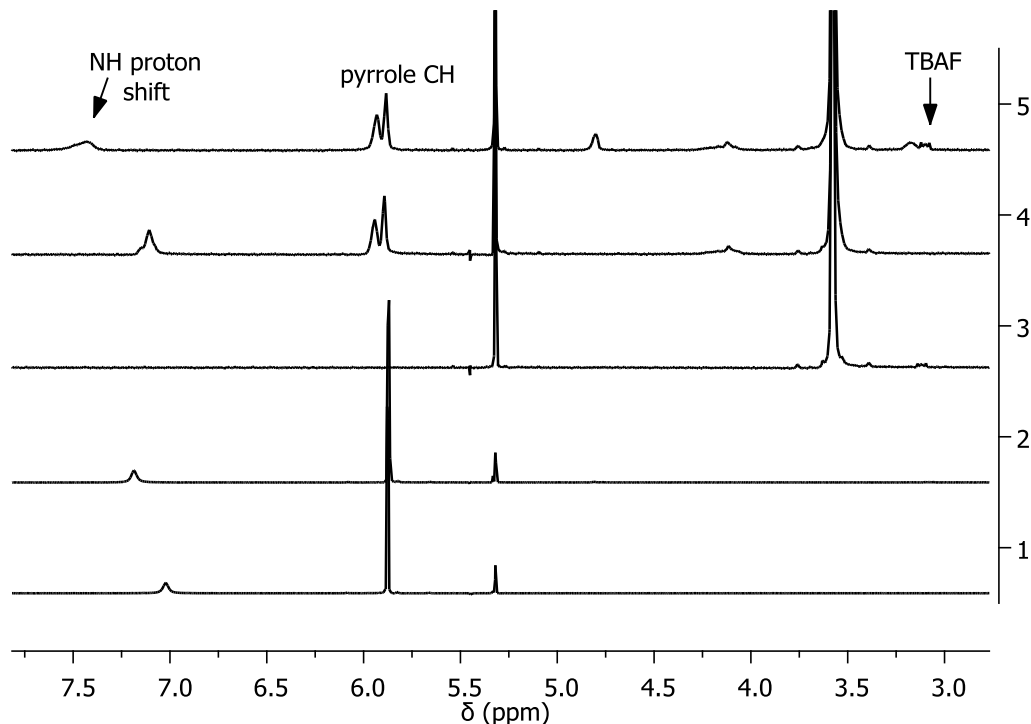


Figure 4.37 : ^1H NMR spectra of CD_2Cl_2 solutions of (1) octamethylcalix[4]pyrrole (**2.1**), (2) **2.1** + TBAF (29 mM) and, (3) PMMA (125 mM, based on the repeat unit) + TBAF, (4) polymer **3.20** (effective concentration of the calix[4]pyrrole repeat unit = 6.5 mM), (5) polymer **3.20** + TBAF.

As shown in Figure 4.37, addition of a D_2O solution of tetrabutylammonium fluoride (TBAF, 90 mM) to a CD_2Cl_2 solution of polymer **3.20** (effective concentration of the calix[4]pyrrole repeat unit = 6.5 mM) resulted in a substantial downfield shift in the pyrrole NH protons (as typically seen upon anion binding).¹ In addition, peaks ascribable to the methylene units in the TBA^+ counter cation (at $\delta = 3.2$ ppm) were seen, lending support to the notion that both the anion (F^-) and the cation were present in the organic phase. In contrast, no shifts in the NH resonances and no TBA^- ascribable peaks were observed when a 29 mM solution of octamethylcalix[4]pyrrole (**2.1**) in CD_2Cl_2 was exposed to aqueous solutions of TBAF. Likewise, no evidence of uptake of TBA^+ into the organic phase (absence of any discernible peak at $\delta = 3.2$ ppm) was seen when analogous experiments were repeated with the MMA homopolymer.

The ability of polymer **3.20** to extract several other TBA⁺ salts was also tested. While no extraction was seen in the case of aqueous solutions of tetrabutylammonium dihydrogen phosphate, upon addition of TBACl downfield shifts in the NH proton signals were seen to be greater than those observed with TBAF for analogous anion concentrations (Figure 4.38). The numbers at the right side of the Figure 4.38 corresponds to CD₂Cl₂ solutions of (1) octamethylcalix[4]pyrrole (**2.1**) (29 mM), (2) **2.1** (29 mM) after i) adding 0.5 mL of a D₂O solution of TBACl (108 mM), ii) shaking the tube vigorously, and iii) allowing the phases to separate, (3) PMMA (125 mM based on the repeat unit) after being subjected to the same treatment noted in (1), (4) polymer **3.20** (effective concentration of the calix[4]pyrrole repeat unit = 6.5 mM), and (5) after being subjected to the same treatment noted in (1). Such findings, which are consistent with an enhanced ability to extract chloride relative to fluoride or dihydrogen phosphate, run counter to the relative anion affinities seen in dichloromethane [17]. However, they are in accord with what one would expect based on the so-called Hofmeister bias [108], namely that a more hydrophobic anion, such as chloride ($\Delta G_h = -340 \text{ kJ mol}^{-1}$), is extracted more easily than a highly hydrophilic species, such as dihydrogen phosphate ($\Delta G_h = -465 \text{ kJ mol}^{-1}$), or fluoride ($\Delta G_h = -465 \text{ kJ mol}^{-1}$) [109].

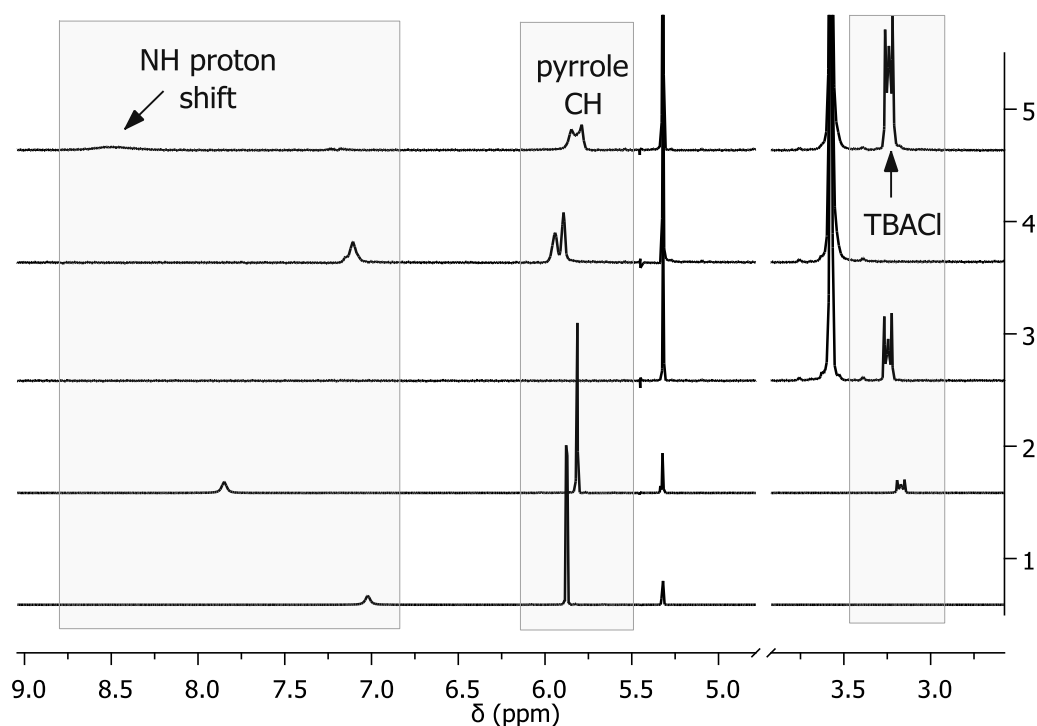


Figure 4.38 : ¹H NMR spectra of CD₂Cl₂ solutions of **3.20** and other control systems.

Consistent with this rationale is the finding that both the control MMA homopolymer and calixpyrrole **2.1** were able to extract TBACl under the aforementioned interfacial conditions, albeit with efficiencies of less than 35% relative to polymer **3.20** (as calculated from NMR integrations of the MMA methyl ester, β -pyrrolic, and TBA⁺ signals, as appropriate). On the other hand, the fact that efficient extraction of TBAF, was only seen in the case of polymer **6** (and not the PMMA control or free **2.1**) underscores the fact that the calixpyrrole receptor appended to the PMMA backbone is playing a critical role in overcoming the Hofmeister bias that would militate away from the out-of-water extraction of this highly hydrophilic species.

Further support that copolymer **3.20** could bind fluoride and chloride anions came from thermal analyses. Specifically, after independently exposing TBAF or TBACl to **3.20** as described above, these samples as well as PMMA controls were subjected to thermogravimetric analysis which was performed under an atmosphere of nitrogen at a scan rate = 10 °C/min. For the sample of **3.20** exposed to TBAF, a 10% mass loss was observed upon heating to 230 °C, a temperature just below the T_d of the copolymer (262 °C). This compares well with the theoretical mass loss of 11.5% assuming the TBAF became completely volatilized over the aforementioned temperature range and was present in a 1:1 stoichiometry relative to each calix[4]pyrrole unit in the polymer chain. In contrast, the sample of **3.20** exposed to TBACl exhibited a 19% mass loss (theoretical: 12.1%) upon heating to 230 °C. Considering the relative extraction abilities of **3.20** towards TBACl and TBAF (see above), the observed mass loss was considered reasonable. For comparison, the PMMA controls lost $\leq 2\%$ of their masses prior to polymer decomposition (277 °C), which leads us to conclude that only minimal amounts TBAF or TBACl were present in these samples after extraction.

In conclusion, the first bona fide polymeric systems containing a calixpyrrole anion receptor directly appended to a polymer backbone were prepared. One main advantage of these materials is that, at least in principle, other MMA derivatives (e.g., a hydrophilic derivative such as hydroxyethyl methacrylate) could be used to control the solubility, water swellability, thermal- and chemical stability, of the resulting PMMA-type polymers. This versatility leads us to believe that polymers such as **3.20** could be readily optimized for use in a range of ion binding and extraction applications.

4.3.2 KCl and KF extraction studies

The selective separation of alkaline salts from aqueous media is of fundamental importance in chemistry. It is, for instance, critical to the production of commodity materials (e.g., bromine, potassium, etc.) from high salt sources, such as the Dead Sea and the Great Salt Lake [110-112] and, on a very different scale, to the regulation of taste [113, 114] and the maintenance of osmotic balance in cells [115, 116]. Materials that could allow for such separations are thus of potential interest in a wide range of applications [21, 94, 96]. Polymeric systems are particularly attractive in this regard because they are generally easy to isolate from solutions or mixtures.

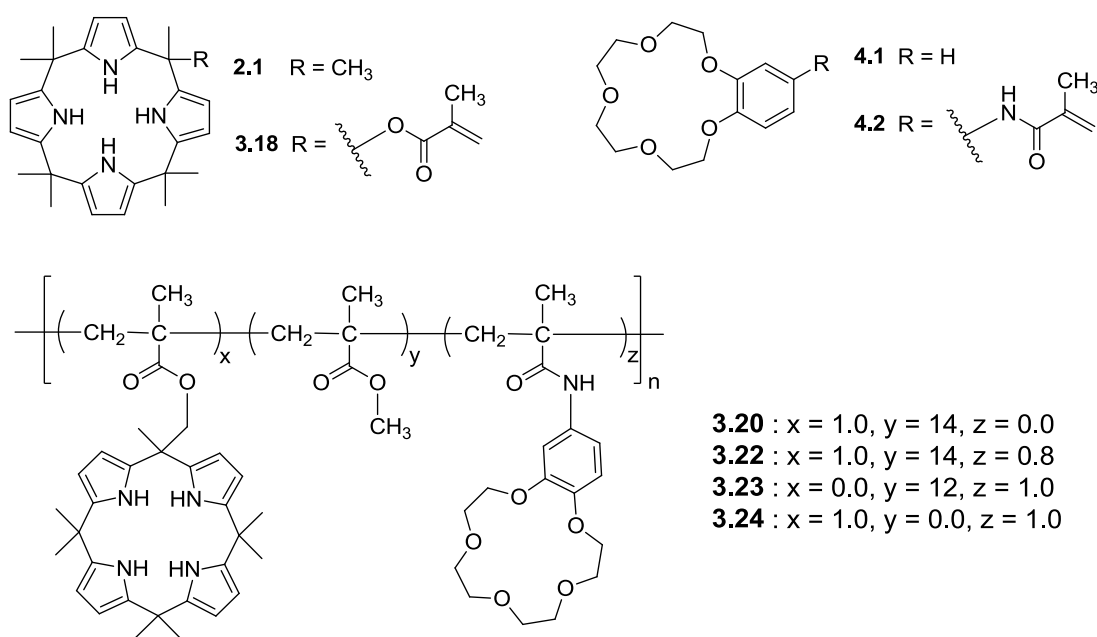


Figure 4.39 : Structures of calixpyrrole, crown ether monomers and their polymers.

In previous chapter, it has been showed that copolymers of a polymerizable derivative of octamethylcalix[4]pyrrole **2.1** (i.e., **3.18**) and methyl methacrylate (MMA), are effective at extracting tetrabutylammonium chloride or fluoride from aqueous media [90]. Unfortunately, these polymeric materials displayed relatively low affinities for the corresponding salts containing less organic soluble cations (e.g., Na, K, etc.). We envisioned that by appending recognition groups capable of binding such ions to modified calixpyrrole-containing polymers, their affinities toward common salts would be improved. For example, crown ethers (e.g., **4.1**) are well-known for their ability to complex alkali cations, particularly potassium [117]. This has led to their use in phase transfer catalysis [118-120], and as extractants for picrate anion salts under organic-aqueous interfacial conditions [121]. In fact,

polymeric systems containing crown ethers have been used to extract the potassium salts of relatively hydrophobic anions [121]. However, neither these latter systems nor any of which we are aware possess the capability of extracting "hard" potassium salts, such as KF or KCl, from aqueous media.

Herein, the synthesis, characterization, and extraction properties of mixed MMA copolymers containing pendant calix[4]pyrrole subunits known to bind halide anions in a 1:1 ratio in organic media [17] and benzo-15-crown-5 subunits capable of forming 2:1 sandwich complexes with potassium cations [117] have been showed. It was thus expected that strong, potentially mutually enhancing, interactions would enable these polymeric materials to extract potassium halide salts, such as KCl and KF, from aqueous solutions.

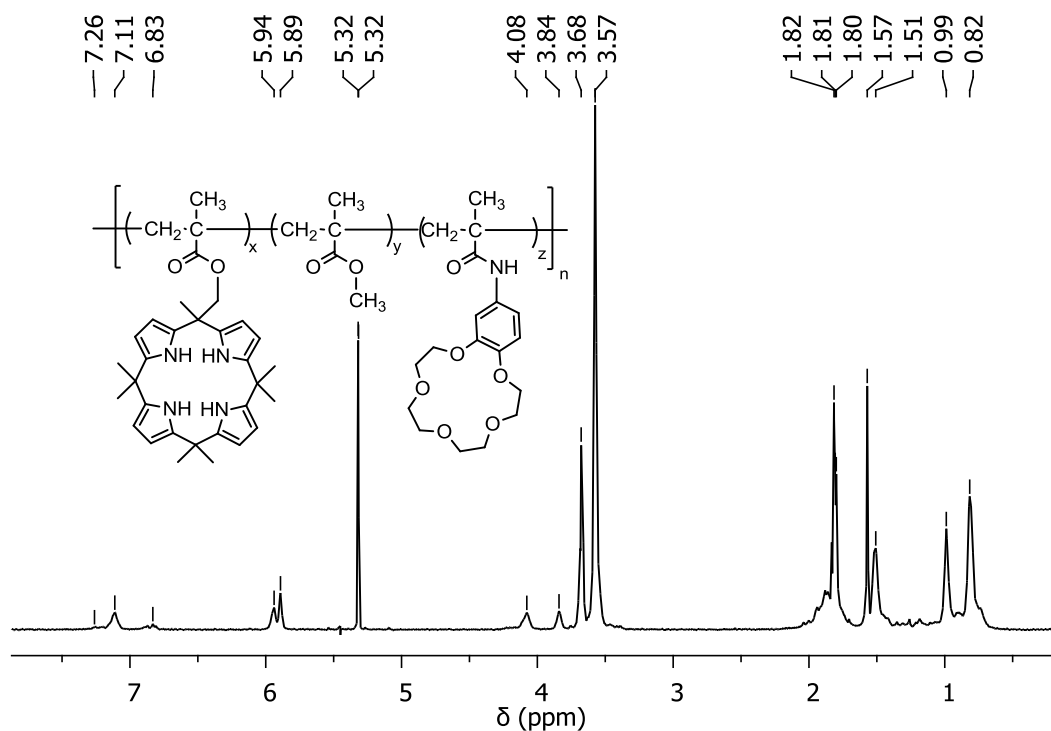


Figure 4.40 : ^1H NMR spectrum of **3.22** recorded in CD_2Cl_2 .

4.3.2.1 Synthesis of calix[4]pyrrole, crown ether, and MMA copolymers

Copolymers **3.22** – **3.24** (Figure 4.39) were prepared from MMA, calix[4]pyrrole **3.18**, and crown ether **4.2** [121] using conventional free radical polymerization techniques. In general, azoisobutyronitrile (1 mol%) was added to THF solutions of these monomers in various ratios. After heating at 70 °C for 17 h, the solutions were independently poured into excess methanol, which caused the polymer to precipitate. After collection by filtration, the resulting materials were characterized by

NMR spectroscopy (CD_2Cl_2) and gel permeation chromatography. The molecular weights (33 – 90 kDa) and polydispersities ($\text{PDI} = 2.1 - 2.5$) of these copolymers were typical of those obtained from free radical polymerizations.

Copolymer **3.22** was prepared in 79% yield by using general reaction conditions described above. ^1H NMR spectroscopic analysis of the copolymer **3.22** revealed pyrrole CH and aromatic crown ether proton signals between 6.83 and 7.26 ppm, pyrrole CH protons at 5.89 ppm, *meso*- CH_2 and crown ether CH_2 protons at 4.08 ppm, crown ether CH_2 protons at 3.84 and 3.68 ppm, PMMA OCH_3 and CH_3 protons at 3.57 and 1.82 ppm, respectively, calixpyrrole *meso*- CH_3 protons at 1.51 ppm, and finally PMMA polymer backbone CH_3 proton signals at 0.82 and 0.89 ppm (Figure 4.40). GPC analysis of the copolymer **3.22** revealed a molecular weight (M_n) of 50.2 kDa and PDI of 2.1.

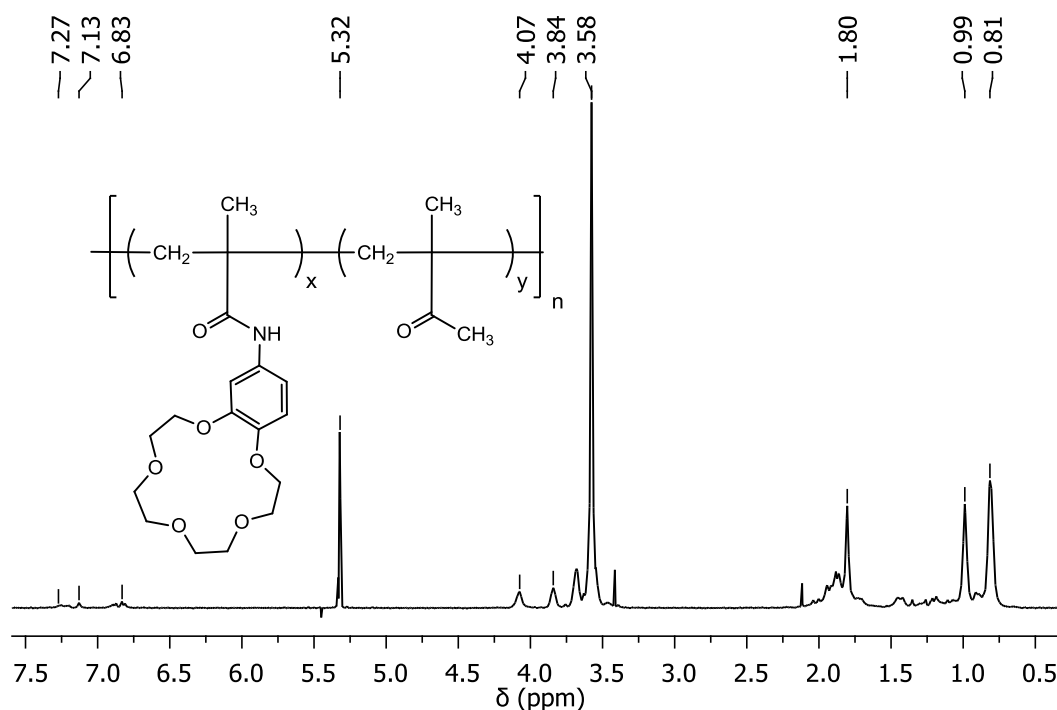


Figure 4.41 : ^1H NMR spectrum of **3.23** recorded in CD_2Cl_2 .

Crown ether and MMA copolymer **3.23** was also synthesized by using conventional free radical polymerization technique described above and found to produce desired polymer in 76% yield as a yellow solid form. Copolymer **3.23** was also subjected to ^1H NMR analysis in CD_2Cl_2 and the results revealed that aromatic proton signals of crown ether moiety arose between 6.81 and 7.26 ppm, crown ether CH_2 protons at 3.84, 4.07, and 3.68 ppm, polymer backbone CH_3 and CH_2 protons at 3.58, 0.99, and 0.81 ppm (Figure 4.41). Copolymer **3.23** was found to have a molecular weight (M_n) of 33.2 kDa and PDI of 2.1 after performing a GPC analysis.

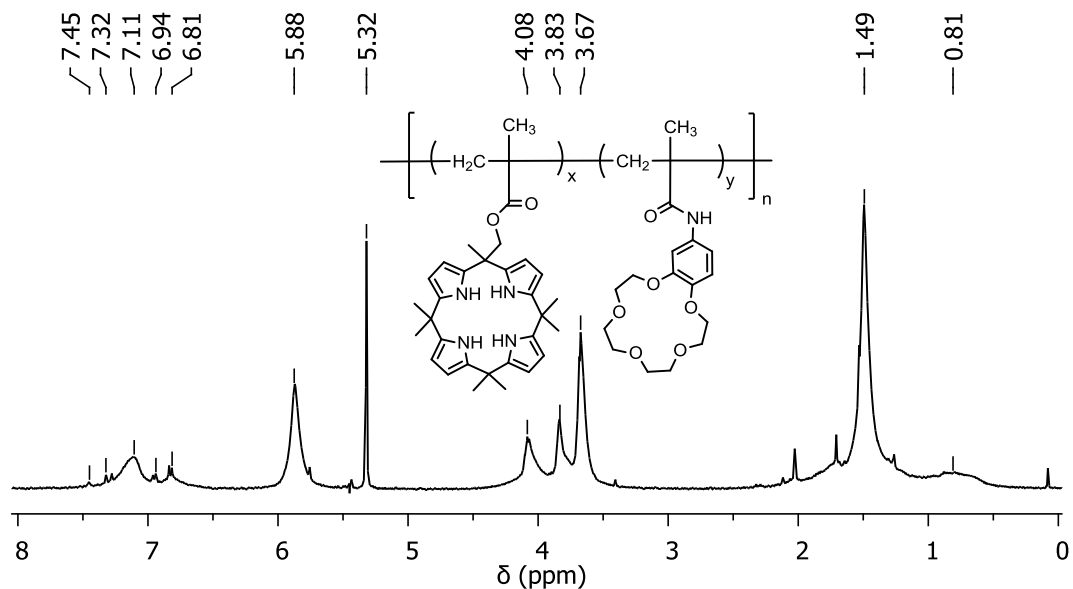


Figure 4.42 : ^1H NMR spectrum of **3.24** recorded in CD_2Cl_2 .

The same free radical polymerization technique used to prepare copolymers **3.22** and **3.23** was utilized to synthesize crown ether and calix[4]pyrrole copolymer. This led to obtain **3.24** in 81% yield in the form of a white solid. Elucidation of the structure of **3.24** using ^1H NMR spectroscopy revealed pyrrolic NH and crown ether aromatic proton signals between 6.82 and 7.32 ppm, and broad pyrrole CH protons at 5.88 ppm, crown ether CH_2 protons between 3.67 and 4.08 ppm, and polymer backbone CH_2 and CH_3 protons at 1.49 ppm (Figure 4.42). GPC analysis of the copolymer **3.24** showed a molecular weight (M_n) of 38.5 kDa and PDI of 2.3.

4.3.2.2 Synthesis of pseudo dimers

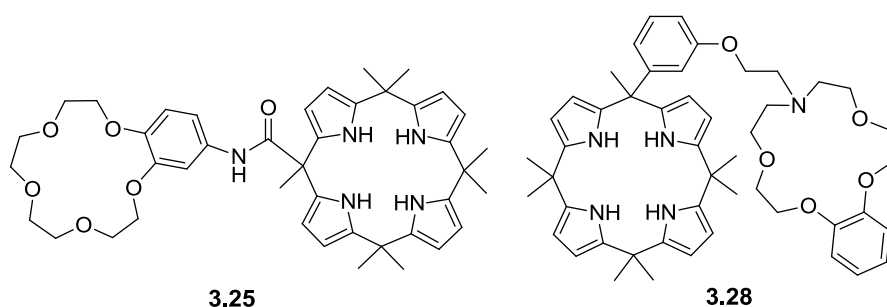


Figure 4.43 : Structures of calix[4]pyrrole – crown ether pseudo dimmers.

After the preparation of copolymers using calix[4]pyrrole (**3.18**), crown ether (**4.2**), and MMA monomers the next effort was focused on the synthesis of pseudo dimers of calixpyrrole and crown ether which were going to be used as control compounds in extraction studies. For this purpose two types of calix[4]pyrrole – crown ether pseudo dimers (**3.25** and **3.28**) were designed and synthesized successfully.

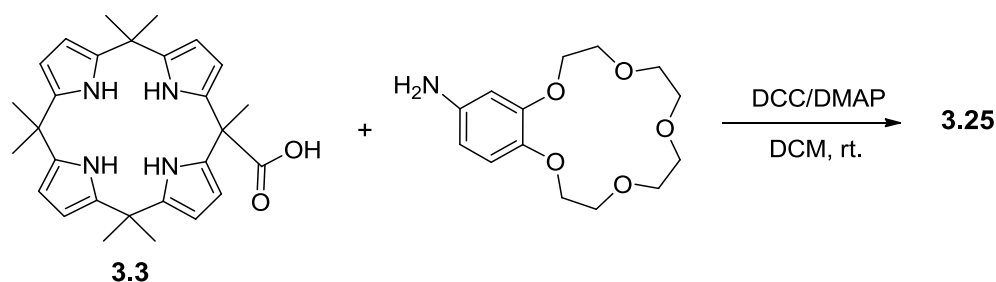


Figure 4.44 : Synthesis of pseudo dimer I (**3.25**).

The first dimer was prepared *via* a direct amide formation reaction of 4'-aminobenzo-15-crown-5 and carboxylic acid functionalized calix[4]pyrrole **3.3** in DCM at room temperature in the presence of DCC/DMAP. Chromatographic purification of the crude product yielded **3.25** in 68% as a yellow solid. ^1H NMR spectrum of the compound **3.25** revealed amide NH, pyrrole NH and crown ether aromatic proton signals between 8.16 and 6.74 ppm, pyrrole CH protons around 5.32 ppm, crown ether CH_2 protons between 4.05 and 3.67 ppm, and finally meso- CH_3 proton signals at 1.83 and 1.50 ppm (Figure 4.45).

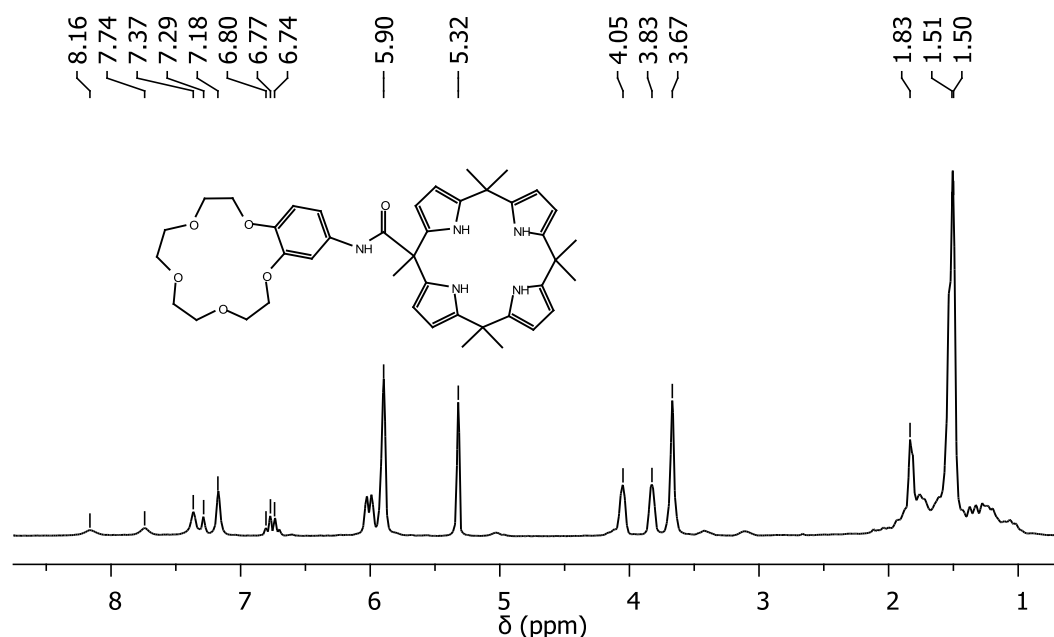


Figure 4.45 : ^1H NMR spectrum of **3.25** recorded in CD_2Cl_2 .

Second calixpyrrole – azacrown ether pseudo dimer (**3.28**) was prepared in a stepwise manner. Towards this end, first, 3'-hydroxyphenyl substituted calix[4]pyrrole **3.26** was prepared via a mixed condensation reaction of pyrrole, acetone, and 3'-hydroxyacetophenone in MeOH in the presence of $\text{CH}_3\text{SO}_3\text{H}$ as an acid catalyst. Then, **3.26** was subjected to a substitution reaction with 1,2-dibromoethane in CH_3CN in the presence of K_2CO_3 . This yielded the product **3.27** in 73% as a white

solid after chromatographic purification. Once 3-(2-Bromoethoxy)phenyl substituted calix[4]pyrrole **3.27** was obtained it was treated with benzoaza-15-crown-5 using the same reaction conditions applied to obtain **3.27**. Purification of the product via column chromatography afforded calix[4]pyrrole – azacrown ether pseudo dimer II (**3.28**) as a white solid in 36% yield. For detailed structural elucidation of the compounds **3.26** – **3.28** see experimental section and for ^1H and ^{13}C NMR spectra see Figure A.16-A.21.

4.3.2.3 Extraction studies

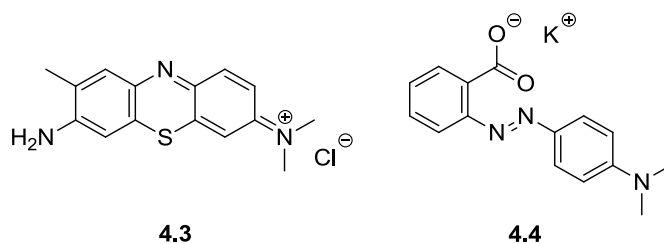


Figure 4.46 : Structures of dyes used in extraction studies.

Initial qualitative evidence that copolymer **3.22**, which contains both calix[4]pyrrole and crown ether subunits, could extract chloride salts into organic media came from a visual test involving **4.3**, a water soluble dye that contains a chloride counter anion. Treatment of an aqueous solution of **4.3** (25.5 μM) with a CH_2Cl_2 solution of copolymer **3.22** (effective concentration of the calix[4]pyrrole and crown ether repeat units = 1.56 and 1.22 mM, respectively) resulted in a colored organic phase (Figure 4.47).

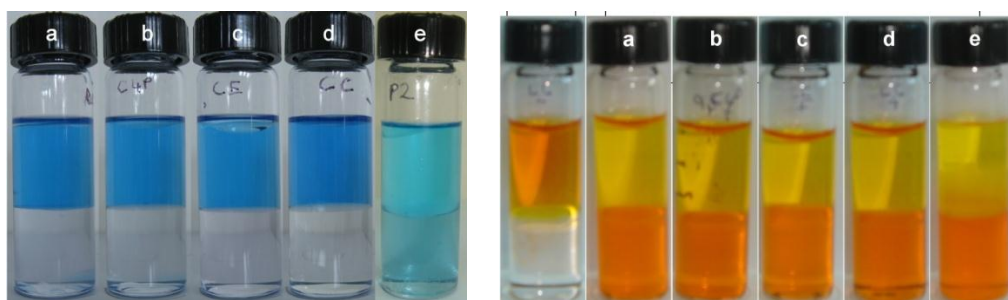


Figure 4.47 : Aqueous solutions (top layers) of **4.3** (left) and **4.4** (right).

Notations in Figure 4.47 correspond to a) After treatment with CH_2Cl_2 (bottom layer). b) After treatment with a CH_2Cl_2 solution of **2.1** (bottom layer). c) After treatment with a CH_2Cl_2 solution of **4.1** (bottom layer). d) After treatment with a CH_2Cl_2 solution of **2.1** and **4.1** (bottom layer). e) After treatment with a CH_2Cl_2 solution of polymer **3.22** (bottom layer). As controls, solutions of the dyes were also exposed to CH_2Cl_2 solutions of **2.1** (1.56 mM), **4.1** (1.22 mM), or a mixture of **2.1** and **4.1** (1.56 and 1.22

mM, respectively), however no transfer of color was observed. These results were quantified using UV-vis spectroscopy as to being presented in Table 4.5.

Table 4.5 : Summary of extraction data of **4.3** and **4.4**.

	Absorbance (630 nm)	Concentration (μM)	Remaining (μM)	Extracted (μM)	Extracted (%)
CH₂Cl₂	0.090	2.06	20.58	4.92	19.29
3.22	0.030	0.65	6.46	19.04	74.68
4.3 2.1	0.092	2.11	21.05	4.45	17.44
4.1	0.089	2.03	20.35	5.15	20.21
2.1+4.1	0.098	2.25	22.46	3.04	11.90
CH₂Cl₂	0.198	10.83	108.31	108.55	50.05
3.22	0.127	6.75	67.53	149.33	68.86
4.4 2.1	0.276	15.31	153.11	63.75	29.40
4.1	0.241	13.30	133.01	83.85	38.67
2.1+4.1	0.252	13.93	139.33	77.53	35.75

As shown in Figure 4.48, analysis of the water phases of these extraction experiments confirmed that **3.22** was able to extract **4.3** into the organic phase more effectively (>54%) than **2.1**, **4.1**, or their mixture. Similar qualitative and quantitative results were observed when aqueous solutions of **4.4** (25.5 μM), a water soluble dye that contains a potassium counter cation, were tested. In this case, copolymer **3.22** (effective concentration of the calix[4]pyrrole and crown ether repeat units = 1.56 and 1.22 mM, respectively) proved more effective as an extractant (>30 %) than **2.1** (1.56 mM), **4.1** (1.22 mM), or the same mixture of **2.1** and **4.1** (1.56 and 1.22 mM, respectively) used above. Table 4.5 summarizes the extraction data of dye **4.4** with copolymer **3.22** and various control compounds.

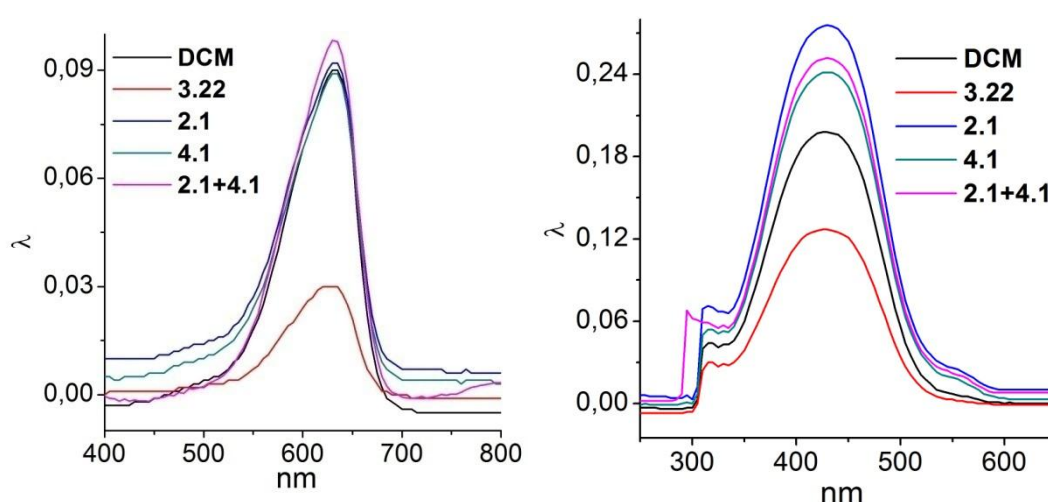


Figure 4.48 : UV-vis spectra of aqueous phases belonging to dye solutions **4.3** (left) and **4.4** (right) exposed to DCM solutions of copolymer **3.22** and the other control systems.

Figure 4.48 shows the UV-vis spectra of aqueous phases (top layer) belonging to dyes **4.2** and **4.4** after treatment with copolymer **3.22** and the other control systems.

Quantification of the dyes **4.3** and **4.4** extracted from the aqueous phase was determined by measuring the amount of the remaining dye using UV-vis spectroscopy. Calibration curves were generated using standardized solutions of **4.3** and **4.4**, independently, in water. The results are summarized in tables and figures below. Using this procedure, the error in the concentrations of **4.3** and **4.4** measured after extraction described is estimated to be less than 0.02 μM . Table 4.7 shows the absorbance values of standardized dye solutions at maximum absorbance values 630 and 430 nm for dyes **4.3** and **4.4**, respectively.

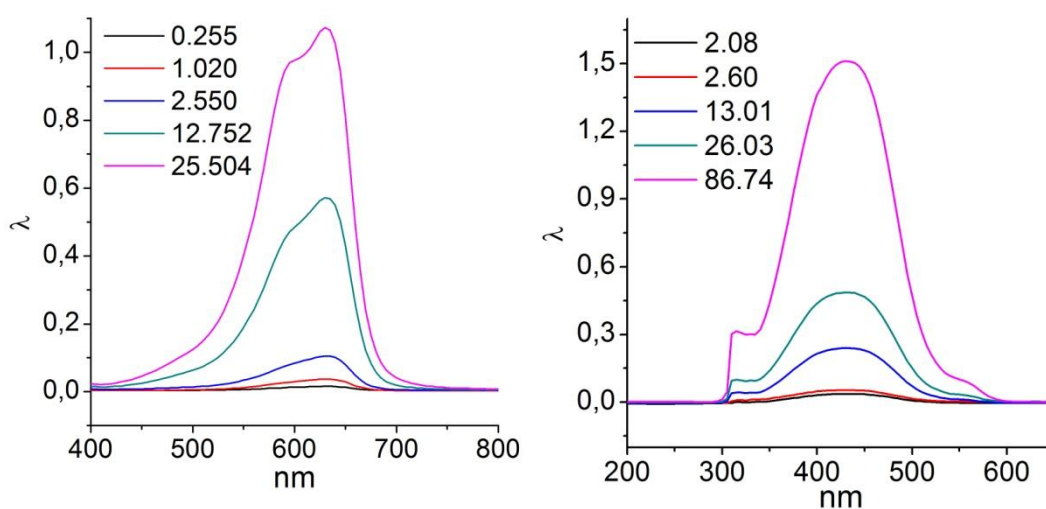


Figure 4.49 : UV-vis spectra of standardized dye solutions of **4.3** (left) and **4.4** (right).

Table 4.6 : Absorbance values (top) and UV-vis spectra (bottom) of standardized dye solutions.

4.3		4.4	
Concentration (μM)	Absorbance (630 nm)	Concentration (μM)	Absorbance (430 nm)
0.000	0.000	0.000	0.000
0.255	0.016	2.082	0.036
1.020	0.037	2.602	0.053
2.550	0.105	13.011	0.240
12.752	0.572	26.023	0.487
25.504	1.073	86.743	1.512
Intercept	Slope	Intercept	Slope
0.00257	0.04248	0.00943	0.01741

Encouraged by these initial results, we next sought to address the question of whether copolymer **3.22** could extract a salt consisting of two hard anions, namely potassium fluoride. In parallel, the extraction properties of **3.20** and **3.23** were

examined. These systems contain either calixpyrrole or crown ether recognition subunits, respectively, and were designed to assess the relative importance of each individual ion recognition unit on the overall extraction properties of **3.22**. As shown in Figure 4.50, addition of a 3.4 M D₂O solution of KF to a CD₂Cl₂ solution of **3.22** (effective concentration of the calix[4]pyrrole and crown ether repeat units = 6.25 and 4.86 mM, respectively) resulted in the appearance of a signal at $\delta = -121.7$ ppm in the ¹⁹F NMR spectrum of the organic phase. A similar signal, but of reduced intensity, was seen in the case of **3.20**, whereas very little signal was observed in the case of **3.23** (for full ¹⁹F NMR spectra of KF see Figure A.25).

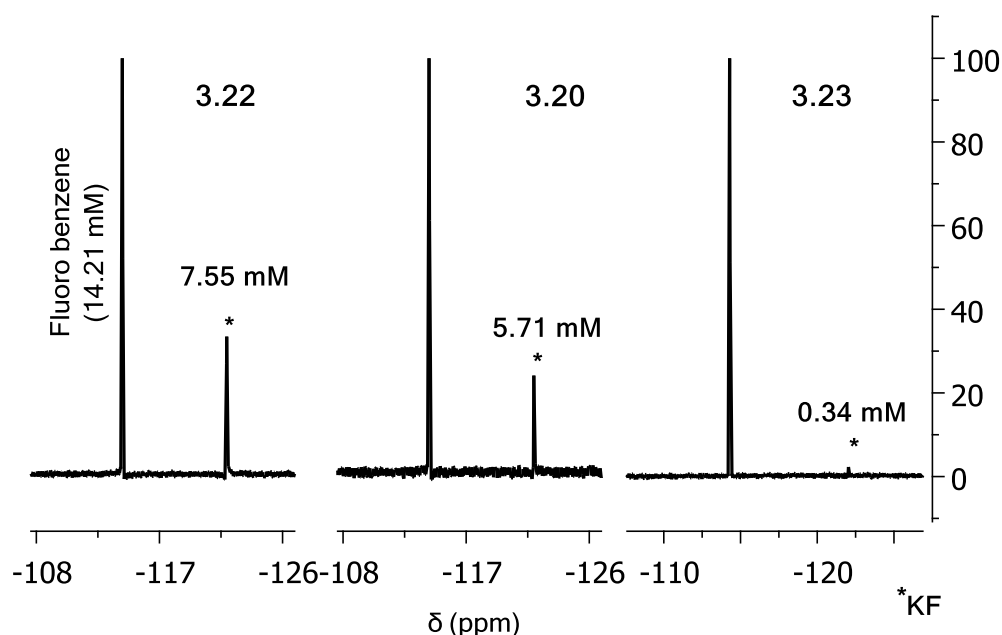


Figure 4.50 : ¹⁹F NMR spectra of CD₂Cl₂ solutions of copolymers **3.22** (effective [calix[4]pyrrole] = 6.25 mM), **3.20** ([calix[4]pyrrole] = 6.50 mM), and **3.23** (no calix[4]pyrrole) after adding D₂O solutions of KF (3.4 M), shaking the tubes vigorously, and then separating the phases with the aid of centrifugation (10 min).

To quantify the amount of fluorine present in the organic phases of the aforementioned extraction experiments, fluorobenzene (final concentration: 14.21 mM) was added to each sample as an internal standard ($\delta = -114.3$ ppm). Based on comparative integrations (i.e., comparing total fluoride content in the CD₂Cl₂ layer relative to this standard), copolymer **3.22** was found to be capable of extracting KF more efficiently (7.55 ± 0.04 mM) than polymer **3.20** (5.71 ± 0.03 mM) under conditions where the effective concentration of the calix[4]pyrrole repeat units in both polymers were essentially the same (6.25 mM versus 6.50 mM for **3.22** and **3.20**, respectively). In addition, both of these polymers were found to extract significantly more fluoride into the organic phase than **3.23** ($[F] = 0.34 \pm 0.03$ mM in the CD₂Cl₂ layer), a copolymer that does not contain any calix[4]pyrrole subunits, as

noted above. As control experiments, extractions were also performed in an analogous manner using **2.1**, **4.1**, MMA homopolymer, an equimolar mixture of calixpyrrole **2.1** and crown ether **4.1**, and the calixpyrrole-crown ether pseudo dimer **3.25**, which was envisioned as a small molecule analogue of **4**. No quantifiable fluorine signal was observed in the organic phase when any of these control systems were used as extractants [122-124].

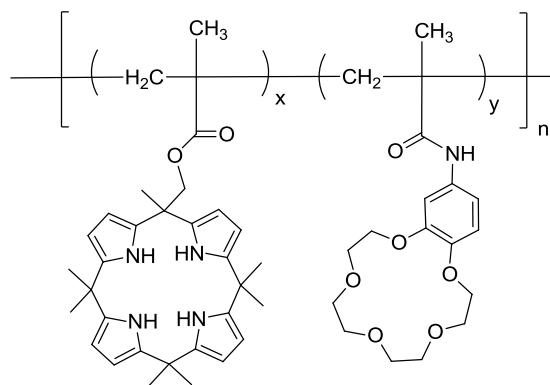


Figure 4.51 : Structure of copolymer **3.24**.

A copolymer of methacrylate functionalized calix[4]pyrrole **3.18** and crown ether **4.2** (i.e., no MMA) was also prepared (**3.24**, Figure 4.51) but found to afford an insoluble white precipitate upon exposure to aqueous solutions of KF or KCl. This result is thought to reflect the formation of strong complexes within the polymer matrix involving either the chloride or fluoride anion and the calix[4]pyrrole subunit, or the potassium cation and the crown ether subunit, perhaps in a cooperative fashion. However, the lack of solubility precluded further analysis of this material. Empirically, the presence of methacrylate units in the backbones of these polymeric extractants (i.e., **3.20**, **3.22**, and **3.23**) appears necessary to retain solubility in dichloromethane.

Table 4.7 : Emission intensities of standardized solutions of potassium tetrakis(2-thienyl)borate.^a

Concentration (ppm)	Emission Intensity
0.0	0.000
0.5	0.330
1.0	0.630
2.0	1.180
Intercept	Slope
-0.03584	1.70251

^a Standard solutions for FES analyses were prepared by dissolving potassium tetrakis(2-thienyl)borate in an ethyl acetate : CH₂Cl₂ (9 : 1 v/v) solution.

Flame emission spectroscopy (FES) was used to confirm the co-extraction of potassium in the above experiments [125], The organic phase obtained after extracting KF with polymer **3.22** afforded an emission intensity (EI) of 0.401 (at

766.5 nm, i.e., the emission wavelength of the excited potassium ion produced by the flame source) after dilution with a known amount of ethyl acetate. By way of comparison, the organic phases produced EI values of 0.277 and 0.038, respectively when polymers **3.20** and **3.23** were used as extractants under otherwise identical conditions. Based on quantification with a series of standards (Table 4.7), extracted potassium concentrations of 6.84, 4.73, and 0.65 ± 0.05 mM were calculated for CH₂Cl₂ solutions of polymers **3.22**, **3.20**, and **3.23**, respectively (at effective crown ether concentrations of 5.60, 0.00, and 5.00 mM, respectively). These values are in good agreement with those obtained from the ¹⁹F NMR data. A summary of the KF extraction data is presented in Table 4.8.

Table 4.8 : Summary of KF extraction efficiencies.^a

Cmpd.	calix : crown ^c	eff. (%) (total) ^{d,e}	eff. (%) (calix) ^{d,f}	eff. (%) (total) ^{e,g}	eff. (%) (crown) ^{g,h}
3.22	1.0 : 0.8	67	121	61	137
3.20	1.0 : 0.0	88	88	73	n.d. ⁱ
3.23	0.0 : 1.0	6	n.d. ⁱ	12	12
4.2	1.0 : 1.0	0	0	0	0

^a Extraction efficiencies (eff.) are reported as the percent (%) of extractant populated with KF upon exposure to a saturated aqueous solution of KF.

^c Relative molar ratios of calixpyrrole (calix) to crown ether (crown) units in the extractant.

^d Calculated from total fluoride extracted.

^e Based on the total number of ion receptors (calixpyrrole plus crown ether) in the extractant.

^f Based on the total number of calixpyrrole units in the extractant.

^g Calculated from total potassium extracted.

^h Based on the total number of crown ether units in the extractant.

ⁱ Not determined.

Next, the ability of polymers **3.22**, **3.20** and **3.23** to extract KCl from aqueous media was evaluated using conditions analogous to those employed for the KF studies described above. In this case, after exposing the polymers to 3.4 M solutions of KCl in D₂O, FES was again used to determine the relative amounts of potassium extracted. Polymer **3.22** proved to be the most effective extractant, displaying an EI value of 0.761, which corresponded to a potassium concentration of 12.97 ± 0.08 mM in the organic phase, with the exact quantification being based on a series of standards (Table 4.7). Polymers **3.20** and **3.23** displayed relatively lower EI values, namely 0.507 and 0.081, respectively, values that corresponded to potassium concentrations of 8.64 and 1.38 ± 0.08 mM, respectively. The higher overall extraction values for KCl compared to KF is consistent with the relative aqueous solvation energies (ΔG_h) of chloride and fluoride anions ($\Delta G_h = -340$ kJ mol⁻¹ for Cl⁻ versus $\Delta G_h = -465$ kJ mol⁻¹ for F⁻).^[15] Specifically, the more hydrophobic anion (Cl⁻) was extracted more effectively than its more hydrophilic analogue (F⁻).

Further support for this conclusion was obtained from ^1H NMR analysis of the pyrrolic NH signal as a function of KF and KCl concentration, under the extraction conditions described in the text. The NH signals shifted downfield and decreased in intensity with increasing concentrations of the potassium salts, KCl and KF (Figure 4.52). In accord with expectations, KCl gave rise to greater downfield shifts in the NH peak shift (δ NH = 7.39 ppm for $[\text{KCl}] \geq 1.04$ mM) than KF ($\delta = 7.35$ ppm for $[\text{KF}] \geq 1.27$ mM). For detailed NMR spectra of **3.22** after treatment with KF and KCl solutions see Figure A.26-A28.

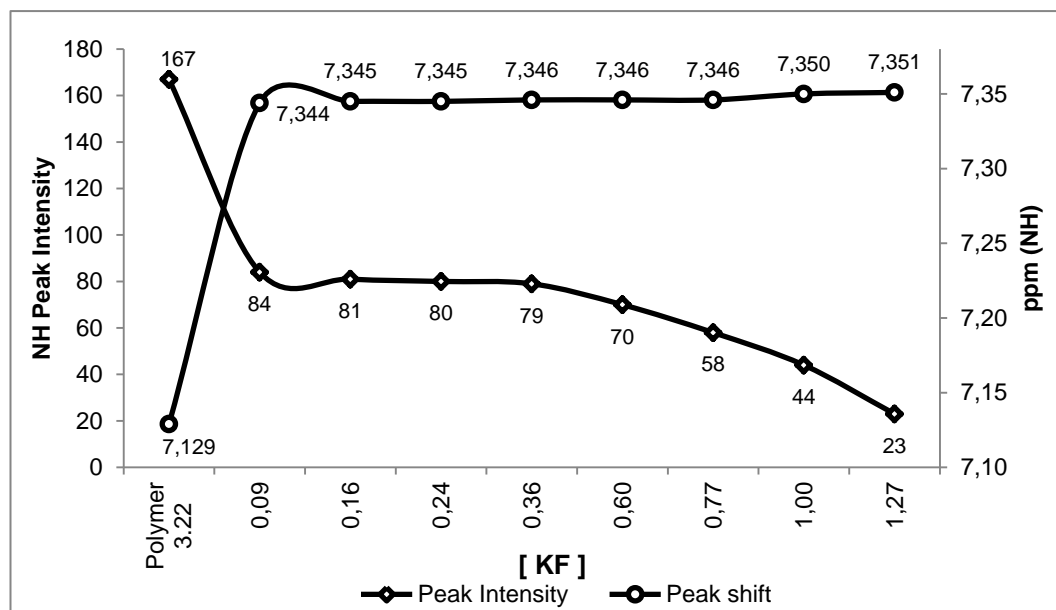


Figure 4.52 : Plot of NH peak intensities and shifts of copolymer **3.22** in CD_2Cl_2 as recorded by ^1H NMR spectroscopy after exposure to different aqueous KF concentrations.

Finally, an effort was made to determine if potassium salts could be selectively extracted in the presence of their sodium analogues. Towards this end, a 0.5 mL H_2O solution of KCl (134.1 mM) and NaNO_3 (1.47 M) was treated with polymer **3.22** (in 0.75 mL CH_2Cl_2) and analyzed using FES. The EI of the signal corresponding to potassium (0.734) was over an order of magnitude greater than the signal corresponding to sodium (0.043). On this basis it was concluded that polymer **3.22** extracts potassium chloride much more effectively than it does sodium chloride. NaCl and NaF extractions were also carried out using the same conditions employed in the case of the corresponding potassium salts. However, no evidence of efficient extraction was observed in the case of any of the polymeric or control systems considered in this report. This finding, which is in accord with the relative hydration energies of K^+ and Na^+ ($\Delta G_h = -295$ kJ mol $^{-1}$ for K^+ and $\Delta G_h = -365$ kJ mol $^{-1}$ for Na^+) [126], suggests to us that these materials may ultimately enable the

selective separation of potassium halide salts from complex aqueous mixtures. This could be especially valuable in specialty medical applications, such as the control of hyperkalemia, where potassium ion exchange resins (e.g., sodium polystyrene sulfate; Kayexalate) have seen widespread use, in spite of being subject to inherent chemical and clinical limitations [127, 128].

In conclusion, the first well-defined and homogenous polymeric systems capable of extracting potassium fluoride and chloride salts from aqueous media have been prepared. These polymers contain pendant calixpyrrole and crown ether subunits, key features that permit the concurrent complexation of both halide and potassium ions. This, in turn, allows the system as a whole to overcome the relatively high hydration energies of KF and KCl and enables their extraction from aqueous media. To the best of our knowledge this has not hitherto proved possible with any other simple polymeric material. Next efforts would be focused on fine-tuning the choice of receptors and investigating the effect of polymer molecular weight and microstructure on the overall extraction performance of these materials.

4.4 Dendrimeric Calix[4]pyrroles

Initially, dendrimer chemistry was concerned with the development of suitable synthetic protocols to produce cascade molecules with a well-defined number of generations and, in particular, with the problems associated with the isolation and characterization of these monodisperse macromolecules. Recently, the discovery of specific functions and novel properties that are a direct consequence of the tree-like dendritic architecture has stimulated spectacular growth in this macromolecular field of chemistry [129]. Dendrimers make unique biological models owing to their three-dimensional nanoscale structures, which can be synthesized in a controllable manner. Dendrimers contain three topologically different regions (core, branches and surface), each of which can be designed to exhibit functional properties including the recognition of guest substrates, catalysis and energy transfer [130]. Calixpyrroles are macrocyclic molecules that can be designed or modified to bind a variety of charged and neutral guest species; however, their integration into dendritic structural frameworks remains unexplored. Interestingly, the physical and chemical properties of such polycalixpyrrole dendritic materials will be dependent upon the nature of calixpyrroles and their anion complexes.

In this part of the thesis design synthesis and characterization of four different calixpyrrole based dendrimeric compounds are being investigated. The target dendrimeric structures have been prepared starting from simple organic compounds

as will be shown in ongoing paragraphs. Although dendrimeric calixpyrrole systems could be accessed via various synthetic strategies so called “click chemistry” would provide an easy and high yield synthetic approach. Therefore, synthesis of final dendrimeric structures has been carried out using click chemistry.

The azide/alkyne ‘click’ reaction [131] (also termed the Sharpless ‘click’ reaction) is a recent re-discovery of a reaction fulfilling many requirements for the formation of 1,2,3-triazole adducts, which include a) often quantitative yields, b) a high tolerance of functional groups, c) an insensitivity of the reaction to solvents, irrespective of their protic/aprotic or polar/non-polar character, and d) reactions at various types of interfaces, such as solid/liquid, liquid/liquid, or even solid/solid interfaces. The basic reaction, which is nowadays summed up under the name ‘Sharpless-type click reaction’, is a variant of the Huisgen 1,3-dipolar cycloaddition reaction [132] between C–C triple, C–N triple bonds, and alkyl-/aryl-/sulfonyl azides.

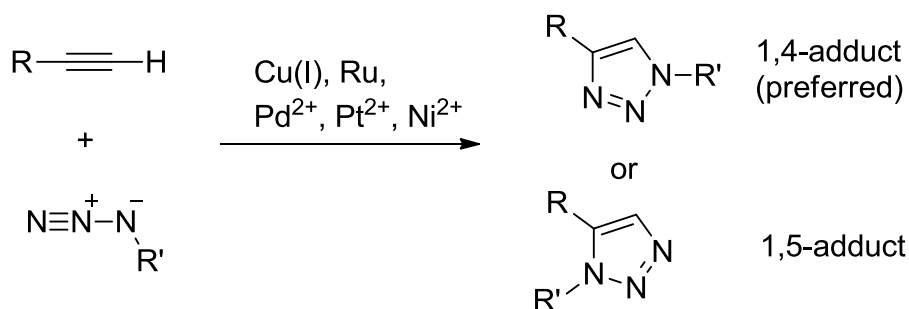


Figure 4.53 : Catalyzed Huisgen 1,3-dipolar cycloaddition.

The basic process of the Huisgen 1,3-dipolar cycloaddition is depicted in Figure 4.53, generating 1,4- and 1,5-triazoles, respectively. Nearly all functional groups are compatible with this process, except those that are a) either self reactive, or b) able to yield stable complexes with the CuI metal under catalyst deactivation. Thus the alkynes, azides, cyclic alkenes, free thiols are not compatible with the azide/alkyne-type click reaction, placing the thermal Huisgen 1,3-dipolar cycloaddition process as the most important side reaction. The main interfering functional groups are strongly activated azides (i.e., acyl- and sulfonyl azides) as well as cyanides, which are able to compete in purely thermal cycloaddition processes.

A mechanistic picture of the copper catalyzed reaction was first proposed by Meldal and co-workers [133] and Sharpless and co-workers [134, 135]. However, the proposed catalytic mechanism (calculated by density functional theory (DFT) calculations) that relied on the initial formation of a Cu acetylide between the Cu(I) species and the terminal alkyne which subsequently proceeded by an initial π -complex formation between the Cu(I) and the alkyne, to lead to a lowering of the pK_a

of the terminal acetylene by up to 9.8 units, thus enabling the attack onto the C–H bond, especially in aqueous systems, has been recently revised in favor of a binuclear mechanism as shown in Figure 4.54 [133].

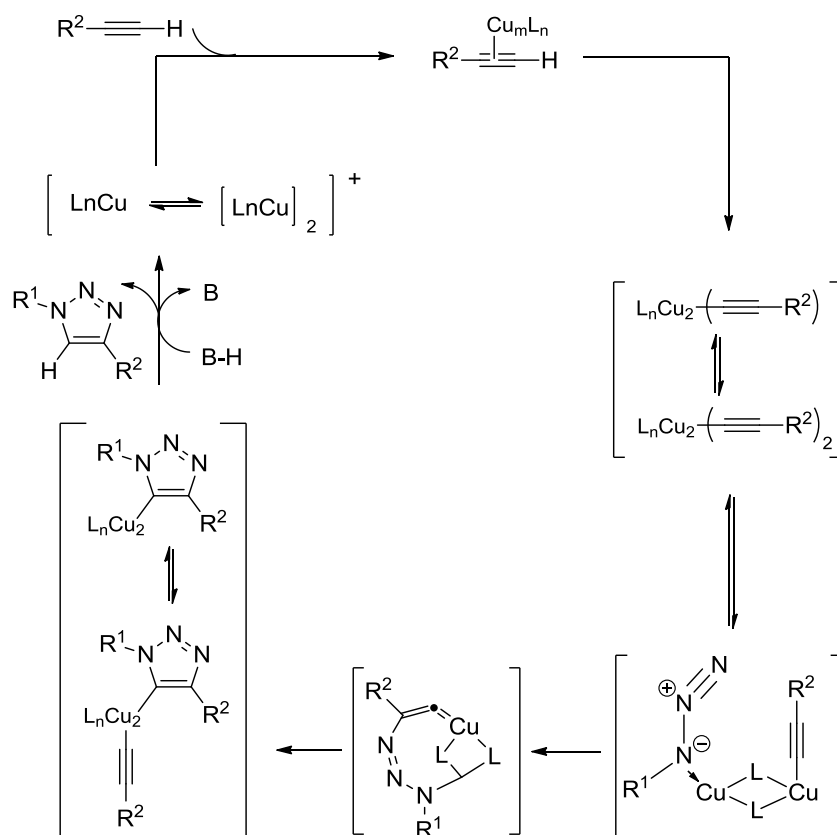


Figure 4.54 : Proposed outline of species involved in the catalytic cycle.

4.4.1 Synthesis of starting materials

As the alkyne and azide functional calix[4]pyrroles needed for the formation of dendrimeric calix[4]pyrroles via click chemistry, initial efforts were devoted to preparation of these calixpyrrole derivatives. A [3+1] mixed condensation method was chosen as it was proven to be used as a convenient strategy.

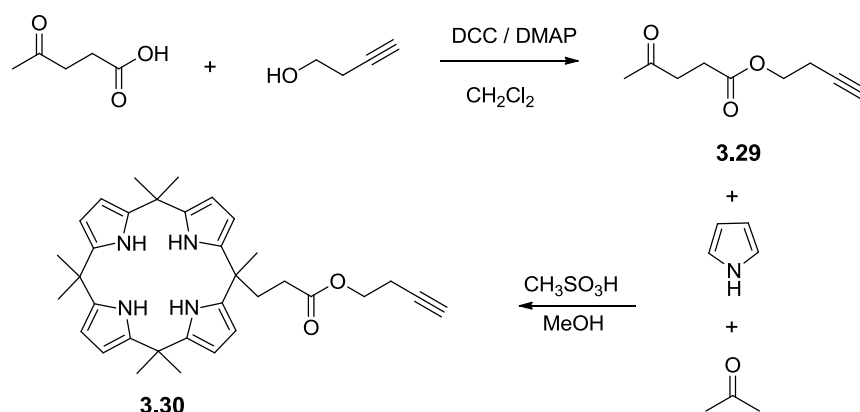


Figure 4.55 : Synthesis of But-3-yn-1-yl 4-oxopentanoate and its calix[4]pyrrole.

First of all, But-3-yn-1-yl 4-oxopentanoate **3.29** has been prepared via esterification of levulinic acid and 3-butyn-1-ol in DCM in the presence of DCC/DMAP. Workup and purification by flash column chromatography afforded **3.29** in 96% yield (Figure 4.55). ^1H NMR spectroscopic analysis of the compound **3.29** revealed ester CH_2 proton signals at 4.17 ppm as a triplet, CH_2 protons between ketone and ester groups at 2.75 and 2.59 ppm as triplet forms, CH_2 proton neighboring to alkyne group at 2.52 ppm as a doublet of triplet, CH_3 protons at 2.18 ppm, and alkyne CH proton at 2.00 ppm as a triplet (Figure 4.56).

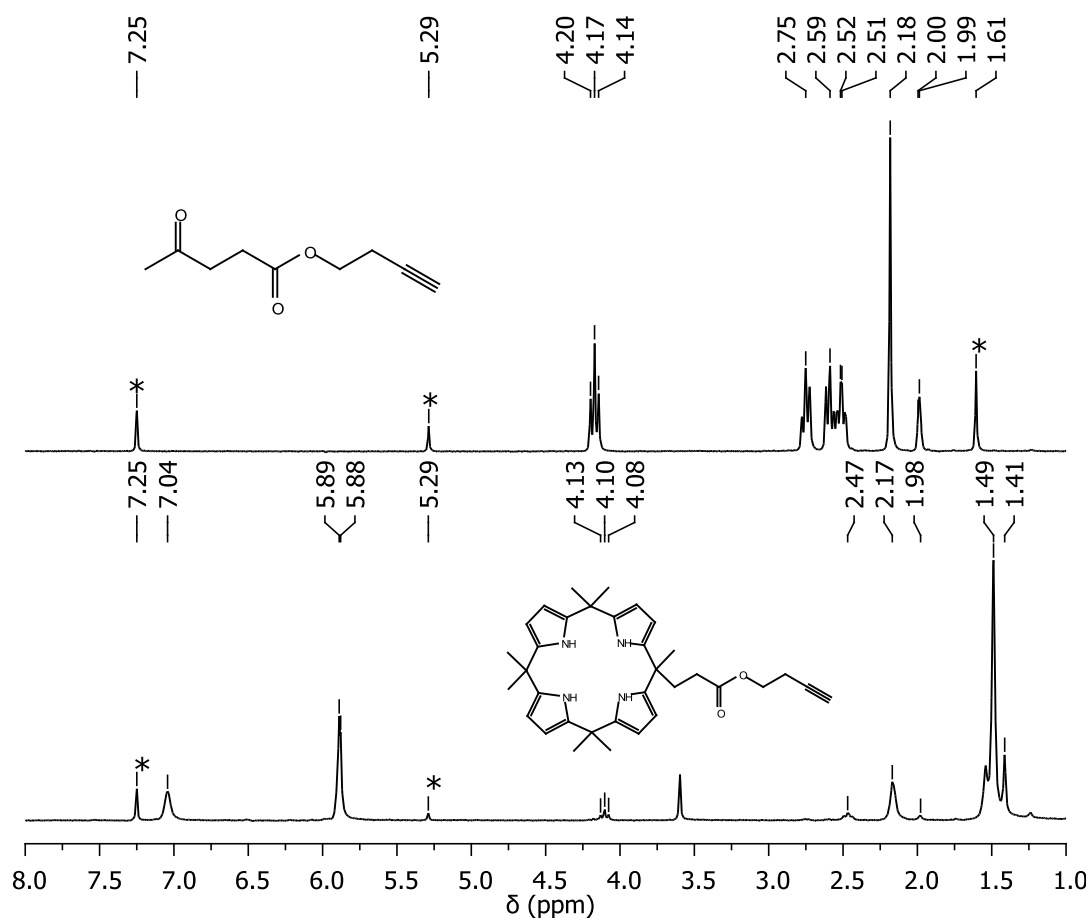


Figure 4.56 : ^1H NMR spectrum of **3.29** and **3.30** recorded in CDCl_3 . Solvent residual and water peaks were indicated by a *.

After the synthesis of starting ketone **3.29** having alkyne functional group, next effort was focused on the establishment of a calix[4]pyrrole using this compound. This would allow obtaining a calixpyrrole that can be used as one of the components of click reaction. For this purpose, **3.29**, acetone, and pyrrole was reacted in MeOH in the presence of methanesulfonic acid. Chromatographic purification of crude product mixture afforded **3.30** in 17% yield as a white solid (Figure 4.55). Structural analysis of **3.30** was also carried out similar to other compounds ^1H NMR

spectroscopy at first. This revealed pyrrole *NH* and *CH* proton signals at 7.04 and 5.89 ppm, respectively. Triplet ester OCH_2 protons were observed at 4.10 ppm, CH_2 protons neighboring to alkyne group at 2.47 ppm as doublet of triplet, *meso-CH*₂ and the other CH_2 protons connected to *meso-CH*₂ carbon, at 2.17 ppm as broad multiplet, alkyne *CH* proton at 1.98 ppm as triplet, and finally remaining *meso-CH*₃ protons at 1.49 ppm (Figure 4.56). ¹³C NMR, LCMS, and FTIR (Figure 4.57) analyses of the compound **3.30** confirmed the expected cyclic structure.

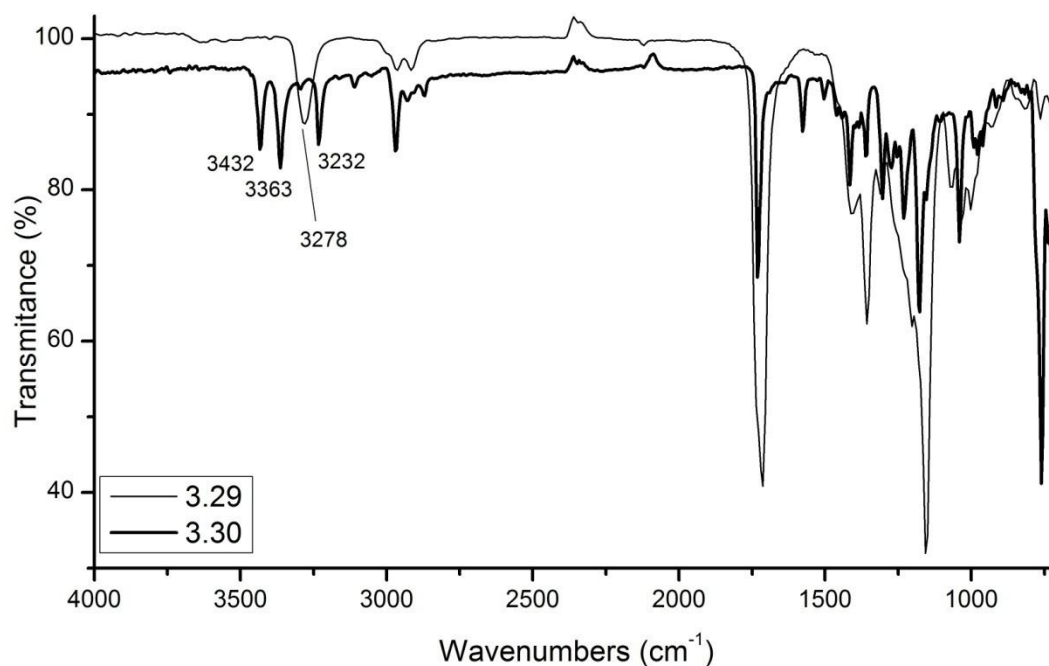


Figure 4.57 : FTIR spectra of **3.29** and **3.30**.

After preparation of alkyne functional calix[4]pyrrole **3.30** another analogue of alkyne functional calixpyrrole **3.34** has been prepared in two steps. This calixpyrrole differs from **3.30** in terms of the connecting alkyne group to core calixpyrrole skeleton. Phenol derivatives are good candidates for attaching alkyne groups via a substitution reaction with propargyl bromide. Therefore, first, a phenol substituted calix[4]pyrrole was synthesized via a mixed condensation of pyrrole with acetone and 4-hydroxyacetophenone in MeOH in the presence of methanesulfonic acid. Chromatographic purification yielded the compound **3.33** in 17% yield as a white solid (Figure 4.58).

Once the compound **3.33** was obtained successfully its structural elucidation was carried out using ¹H NMR spectroscopy. Results revealed that pyrrole *NH* proton signals at 7.17 and 7.07 ppm, pyrrole *CH* protons at 5.88 and 5.65 ppm, aromatic *CH* protons at 6.84 and 6.65 ppm as doublets, phenolic *OH* proton at 4.74 ppm, and *meso-CH*₃ protons at 1.82 and 1.49 ppm (Figure 4.59).

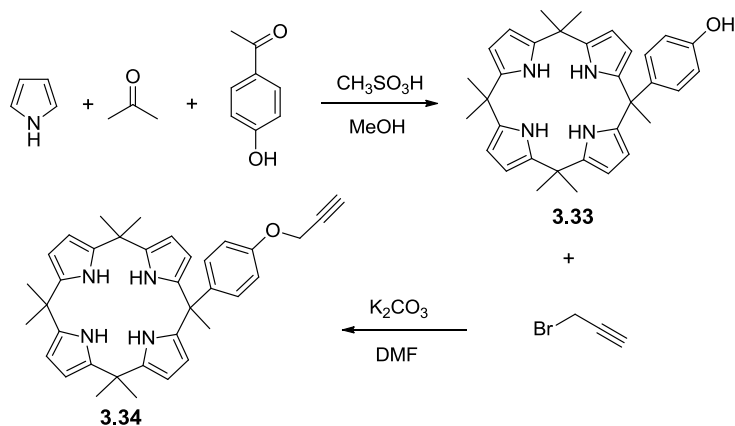


Figure 4.58 : Synthesis of **3.33** and **3.34**.

The synthesis of propargyl attached calix[4]pyrrole was carried out by reacting **3.33** and propargyl bromide in DMF in the presence of K_2CO_3 . 1H NMR spectroscopic analysis of **3.34** revealed pyrrole NH proton signals at 7.18 and 7.07 ppm, aromatic CH protons at 6.92 and 6.82 ppm as doublets, pyrrole CH protons at 5.88 and 5.65 ppm, CH_2 protons connected to alkyne unit at 4.65 ppm, alkyne CH proton at 2.50 ppm, and *meso*- CH_3 protons at 1.84 and 1.50 ppm (Figure 4.59).

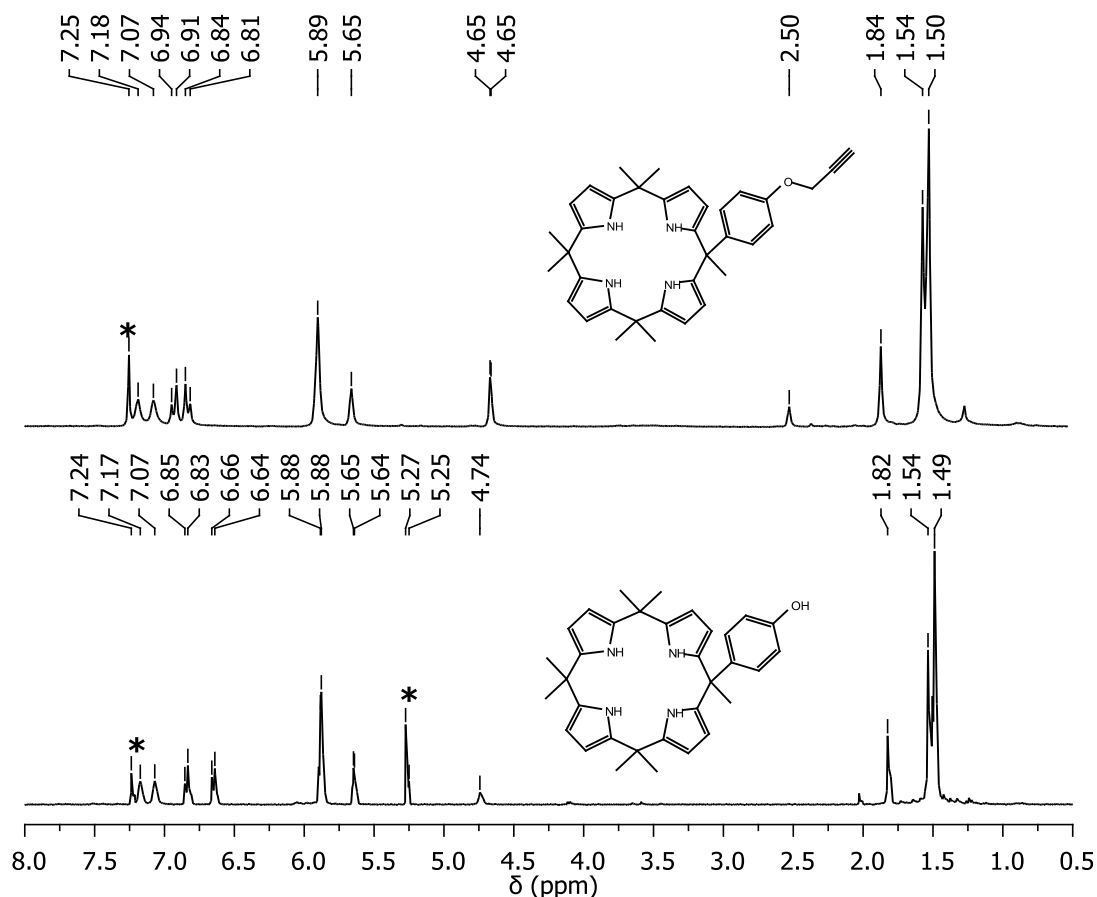


Figure 4.59 : 1H NMR spectrum of **3.33** (down) and **3.34** (up) recorded in $CDCl_3$. Solvent residual peaks were indicated by *.

Azide functional groups are the key constituents of triazol ring formations. Therefore, next effort was shifted to preparation of starting materials having azide functional groups. These starting materials will also be the cores of dendrimeric calixpyrrole compounds. For this purpose, tetraazido functionalized calix[4]pyrrole **3.32** was prepared from tetra(bromopentyl) substituted calix[4]pyrrole **3.31**.

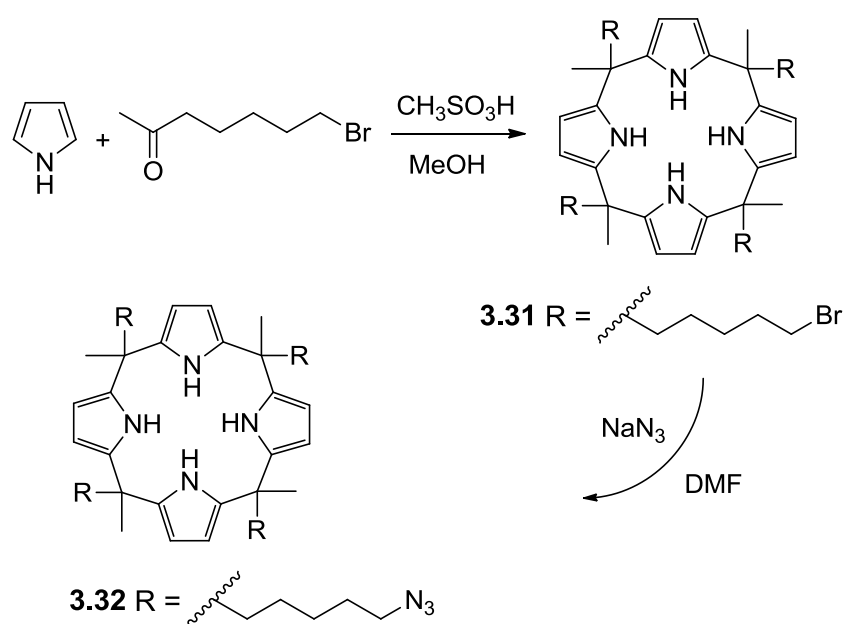


Figure 4.60 : Synthesis of tetra(pentylbromide) (**3.31**) and tetraazido (**3.32**) calix[4]pyrroles.

As shown in Figure 4.60, the synthesis of tetra(1-bromopentyl) substituted calix[4]pyrrole **3.31** was achieved *via* a condensation reaction of pyrrole and 7-bromoheptane-2-one in MeOH in the presence of methanesulfonic acid. The white solid product precipitated out of MeOH and was purified by filtration and washing with excess of MeOH in 78% yield. ¹H NMR spectroscopic analysis of the compound **3.31** revealed NH and CH proton signals at 6.99 and 5.87 ppm respectively, CH₂-Br protons at 3.334 ppm as a multiplet, remaining *meso*-CH₃ and other CH₂ protons between 1.80 and 1.07 ppm (Figure 4.61).

Transformation of tetrabromo functional calix[4]pyrrole to its tetraazido derivative was achieved *via* treatment of **3.31** with sodium azide in DMF at room temperature (Figure 4.60). Removal of the solvent and workup yielded tetraazido calix[4]pyrrole **3.32** in 98%. Structural elucidation of **3.32** using ¹H NMR spectroscopy revealed almost similar results to those of **3.31** but a slightly up field shift (3.20 ppm) on CH₂ protons connected to the azide units (Figure 4.61).

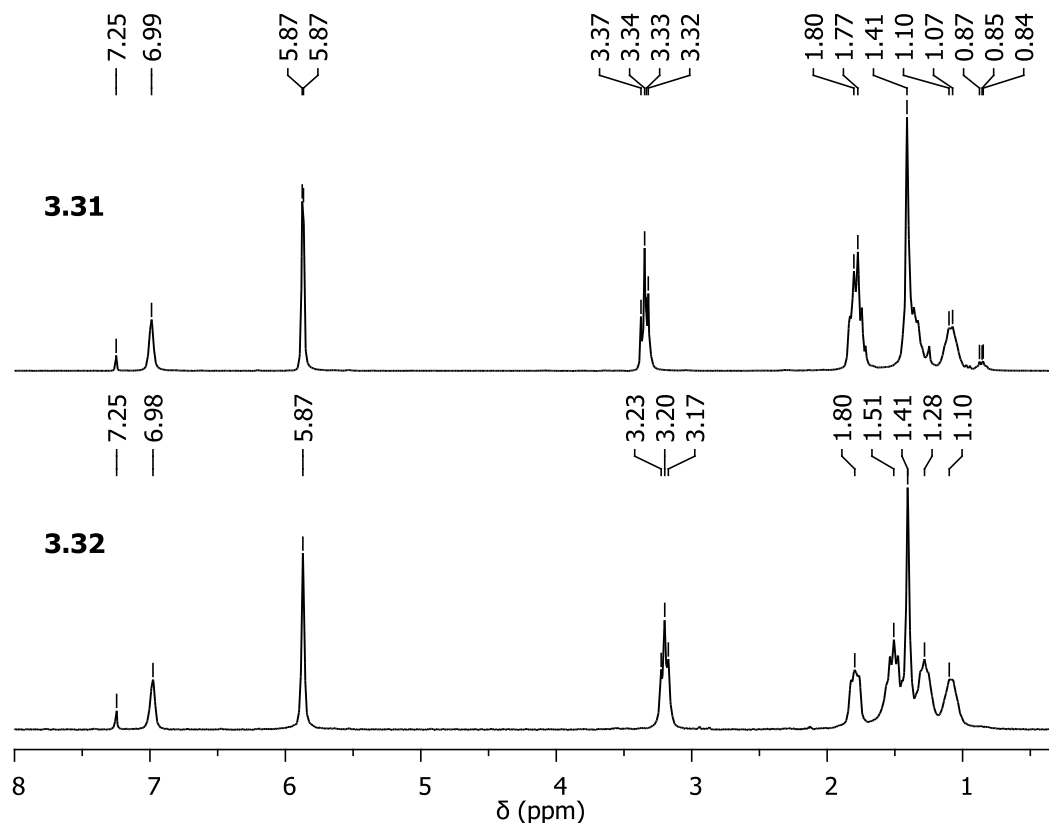


Figure 4.61 : ^1H NMR spectra of **3.31** and **3.32** recorded in CDCl_3 .

FTIR spectroscopic analysis of the compound **3.32** confirmed the expected transformation from bromo to azido derivative. $\text{N}\equiv\text{N}$ triple bond stretching band of **3.32** can be clearly seen at 2082 cm^{-1} (Figure 4.62).

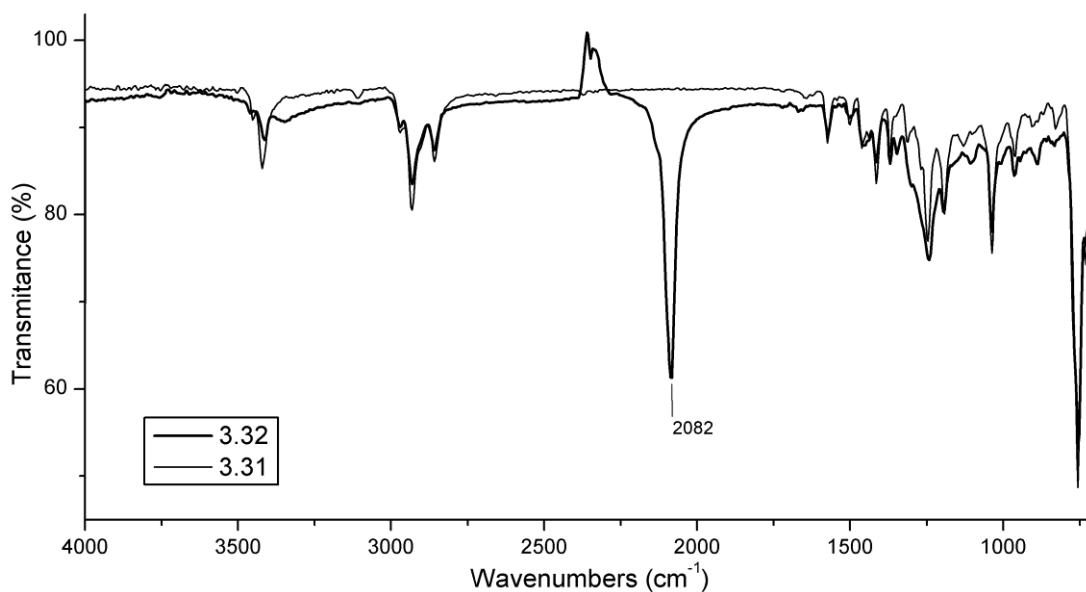


Figure 4.62 : FTIR spectra of tetrabromo and tetrazido substituted calix[4]pyrroles **3.31** and **3.32**.

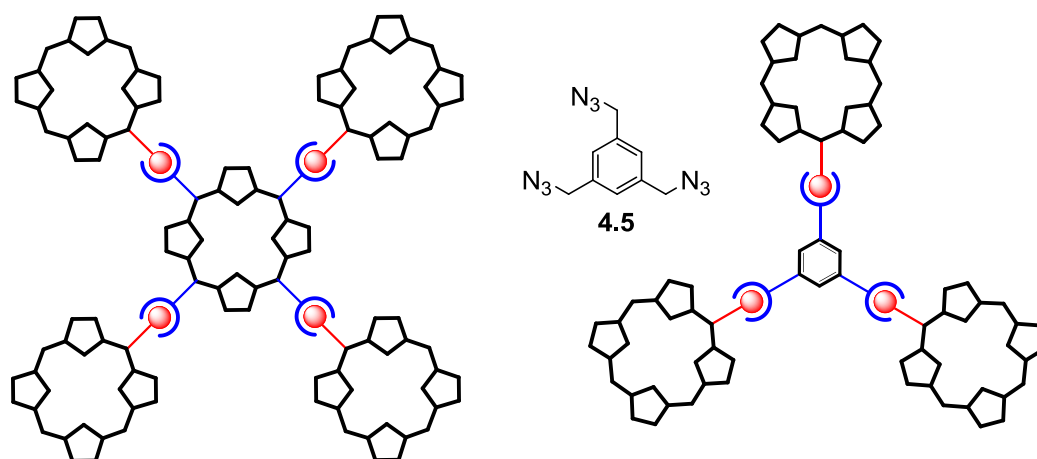
Table 4.9 summarizes some characterization data of starting materials **3.29** – **3.34**.

Table 4.9 : Some characterization data of starting materials.

Compound	Pyr. ^g NH (ppm)	Pyr. CH (ppm)	Func. Group (ppm)	FTIR (cm ⁻¹)	Mass (m/z)
3.29	–	–	2.00 ^a	3278, 1740	168.98
3.30	7.04	5.89	1.98 ^b	3232, 1730	537.29
3.31	6.99	5.87	3.33 ^c	3420, 756	967.05
3.32	6.98	5.87	3.20 ^d	3415, 2082	–
3.33	7.18, 7.07	5.88, 5.65	4.74 ^e	–	506.26
3.34	7.18, 7.07	5.88, 5.65	2.50 ^f	FTIR	543.58

^{a,b} Alkyne CH₂, ^c CH₂-Br, ^d Azide CH₂, ^e Phenol OH, ^f Alkyne CH, ^g Pyr. = Pyrrole.

4.4.2 Synthesis of dendrimeric structures

**Figure 4.63** : Illustration of strategic pathway of obtaining dendrimeric calixpyrrole compounds.

After the synthesis of starting materials, next effort was dedicated to the preparation of dendrimeric calixpyrrole compounds. As illustrated in Figure 4.63, the first strategy is involved to using tetraazido calix[4]pyrrole **3.32** as the core of dendrimers and the second one is involved to using 1,3,5-tris(azidomethyl)benzene (**4.5** can be readily obtained from 1,3,5-tris(bromomethyl)benzene) [72] as the core of dendrimers for enrichment of product versatility.

For this purpose, as a beginning, tetraazido functionalized calix[4]pyrrole **3.32** was reacted with alkyne functionalized calix[4]pyrrole **3.30** (the ratio of **3.32**:**3.30** was 1:4) in a mixture of THF/H₂O in the presence of CuSO₄·5H₂O and sodium ascorbate at room temperature. This reaction conditions afforded the first dendrimeric calixpyrrole compound **3.35** (Figure 4.64) with a perfect yield. Since the product is a huge molecule its chromatographic purification was not possible using common chromatographic techniques. Therefore, another purification method has been sought. The first idea was the purification of the compound **3.35** *via* crystallization but this would not allow us to reach a pure form of product. Precipitation of a

saturated THF solution of **3.35** into hexanes was successfully utilized to purify dendrimeric compound.

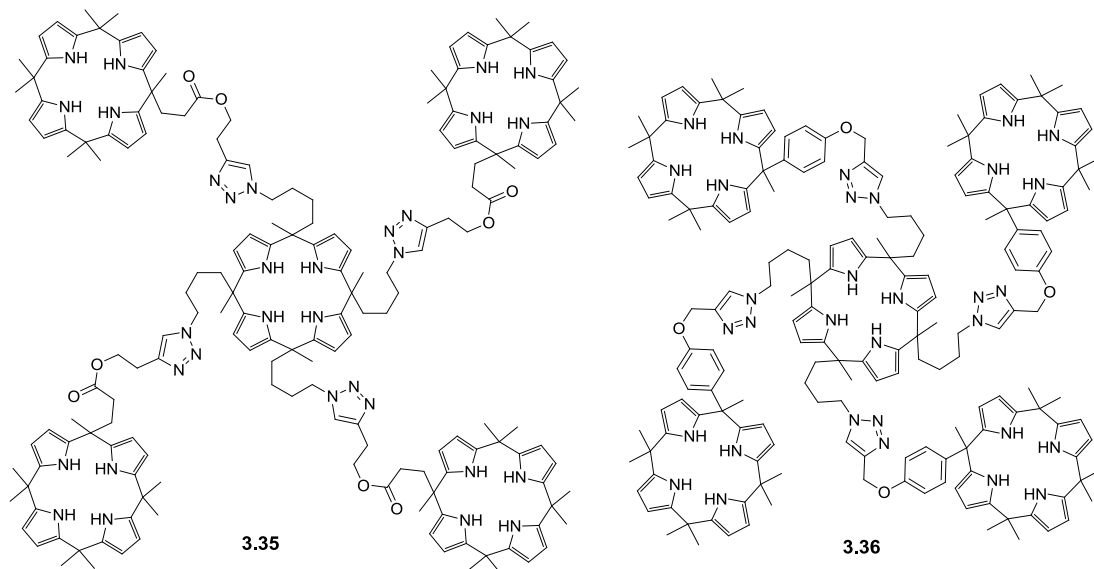


Figure 4.64 : Structure of calixpyrrole based dendrimers **3.35** and **3.36**.

^1H NMR spectroscopic analysis of the compound **3.35** revealed triazole ring CH and pyrrole NH proton signals between 7.39 and 7.03 ppm, pyrrole CH protons at 5.87 ppm, ester CH_2 and NCH_2 protons at 4.24 ppm, NC-CH_2 protons at 2.96, and remaining meso-CH_3 , meso-CH_2 , and other CH_2 protons between 2.15 and 1.11 ppm.

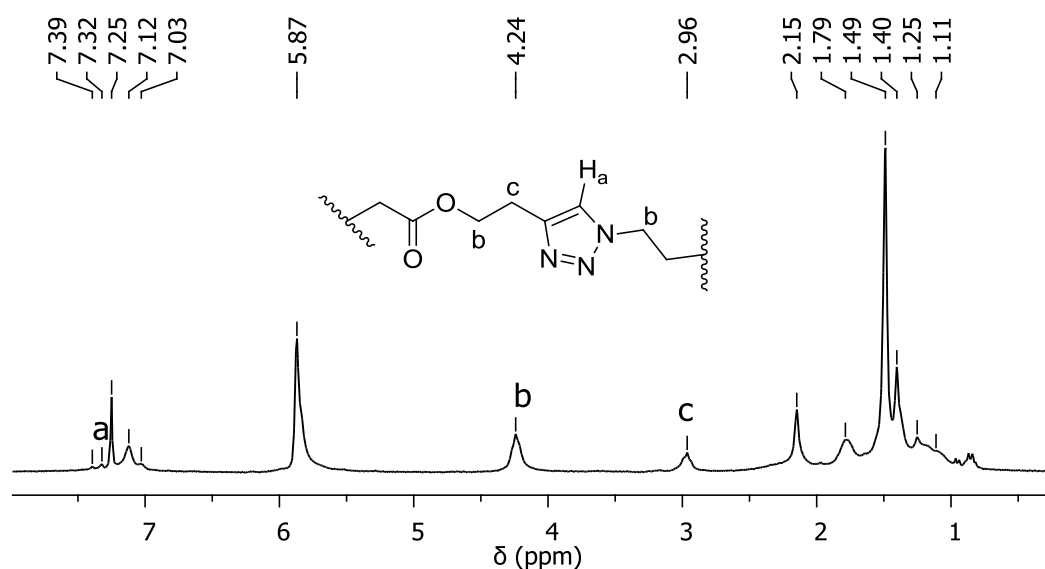


Figure 4.65 : ^1H NMR spectrum of the compound **3.35** recorded in CDCl_3 .

Another support came from comprehensive analysis of the compounds **3.30**, **3.32**, and **3.35** using FTIR spectrophotometer. As it can be seen in Figure 4.66,

disappearance of N=N stretching band at 2086 cm^{-1} and C=O stretching band at 1731 cm^{-1} proves the formation of triazole ring and maintenance of the ester bridges on the final dendrimeric product **3.35**.

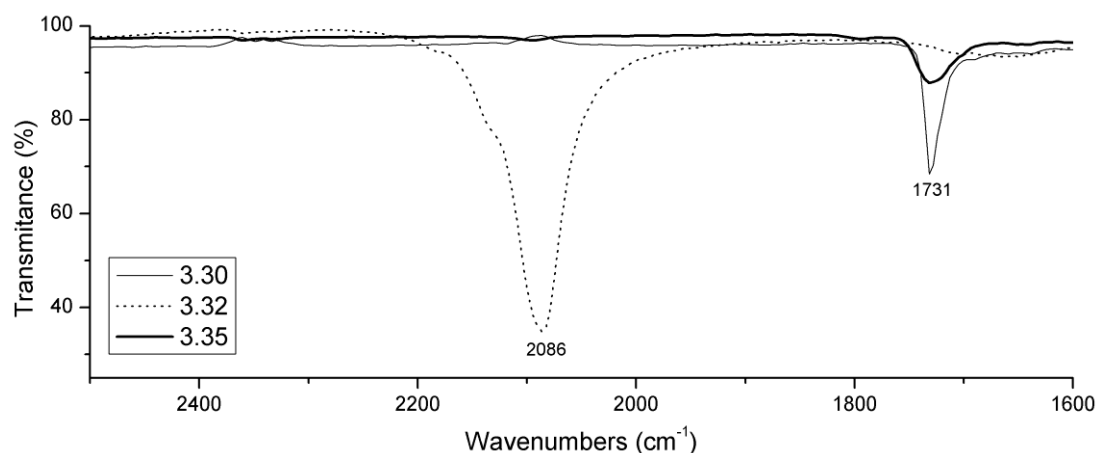


Figure 4.66 : FTIR spectra of calixpyrrole based dendrimer **3.35** and its starting materials.

Once the first calixpyrrole based dendrimer **3.35** (Figure 4.64) was successfully obtained the next effort was shifted to the synthesis of its another analogue using the same core azide functionalized calixpyrrole **3.32** and propargyl ether of phenolic calix[4]pyrrole **3.34**. Calixpyrrole based dendrimer **3.36** was obtained using the same reaction conditions applied to prepare **3.35**. Purification via precipitation into hexanes afforded **3.36** in perfect yield.

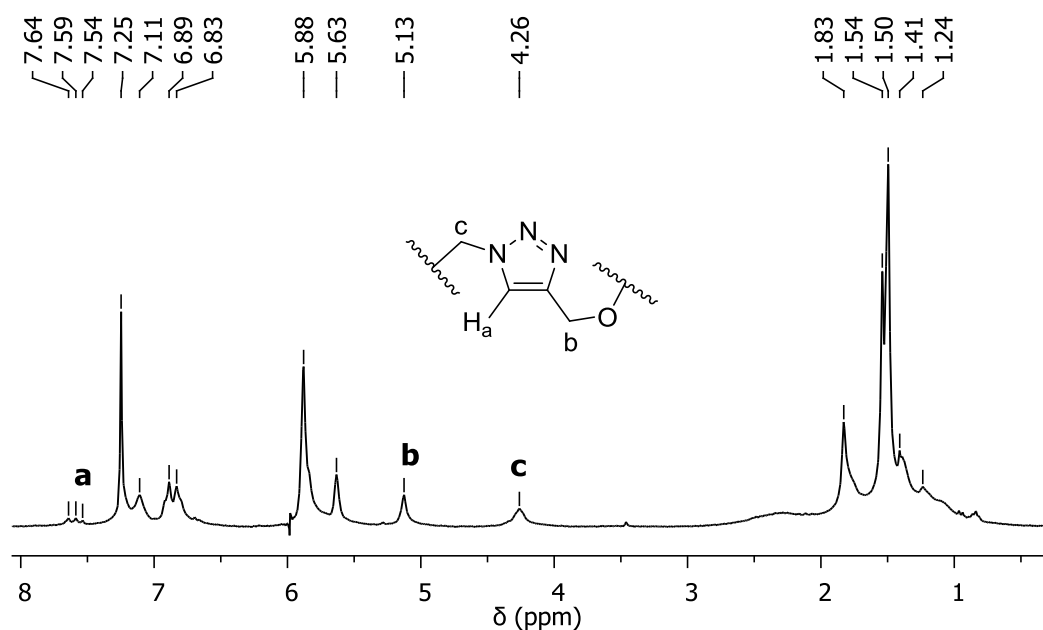


Figure 4.67 : ^1H NMR spectrum of the compound **3.36** recorded in CDCl_3 .

Structural elucidation of the compound **3.36** was carried out using ^1H NMR spectroscopy and revealed triazole ring CH proton signals between 7.64 and 7.54 ppm, pyrrole NH protons at 7.25 (under the solvent peak) and 7.11 ppm, aromatic CH protons at 6.89 and 6.83 ppm, pyrrole CH protons at 5.88 and 5.63 ppm, OCH_2 proton signals at 5.13 ppm, NCH_2 protons at 4.26 ppm, and remaining CH_2 , *meso*- CH_2 , *meso*- CH_3 protons between 1.83 and 1.24 ppm (Figure 4.67).

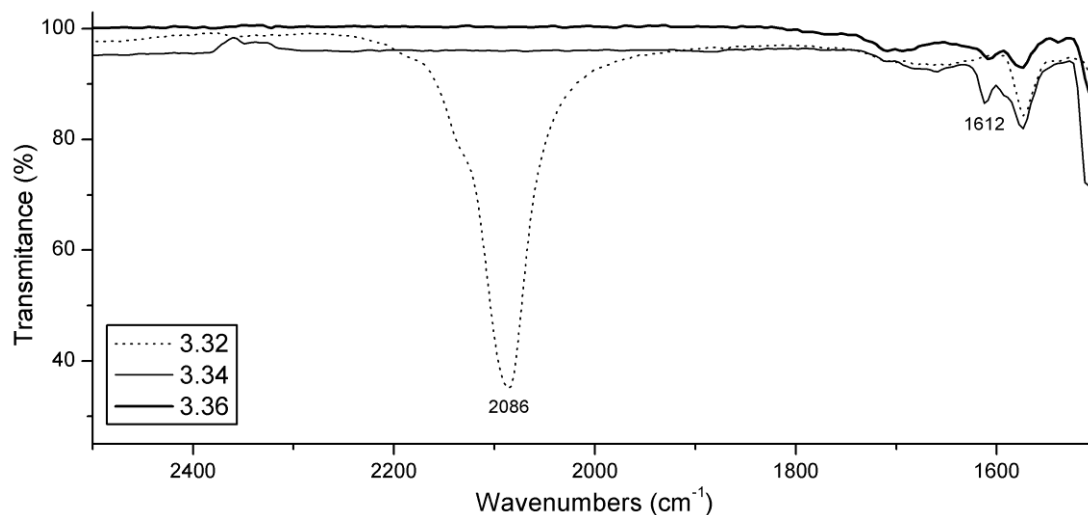


Figure 4.68 : FTIR spectra of calixpyrrole based dendrimer **3.36** and its starting materials.

FTIR spectra of the calixpyrrole based dendrimeric compound **3.36** was found to have a disappearance of azide stretching band at 2086 cm^{-1} that provide information about formation of triazole ring. Another band of both **3.34** and **3.36** at 1612 cm^{-1} shows the presence of aromatic ring in both starting compound and final product.

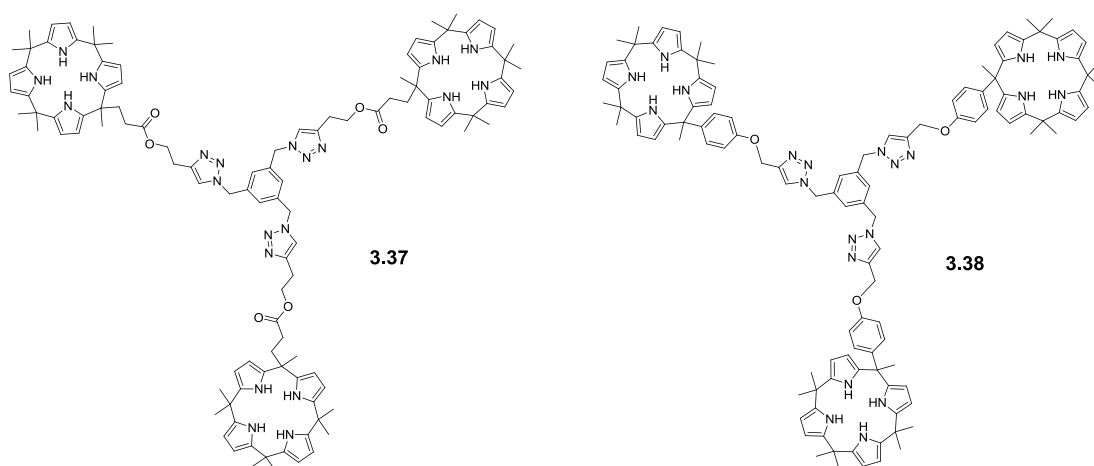


Figure 4.69 : Structures of tripodal dendrimers **3.37** and **3.38**.

Once the calix[4]pyrrole based dendrimeric compounds **3.35** and **3.36** have been successfully prepared focus of the study was directed to synthesis of their analogues having different core structures. For this purpose 1,3,5-trimethyl benzene based calixpyrrole dendrimeric compounds have been prepared using the same conditions applied to synthesize **3.35** and **3.36** (Figure 4.69). 1,3,5-tris(bromomethyl)benzene was reacted with NaN_3 in DMF to obtain 1,3,5-tris(azidomethyl)benzene (**4.5**) which was reacted with alkyne functionalized calix[4]pyrrole **3.30** to afford tripodal dendrimeric compound **3.37**. This compound was also purified via precipitation of its saturated THF solution into hexanes.

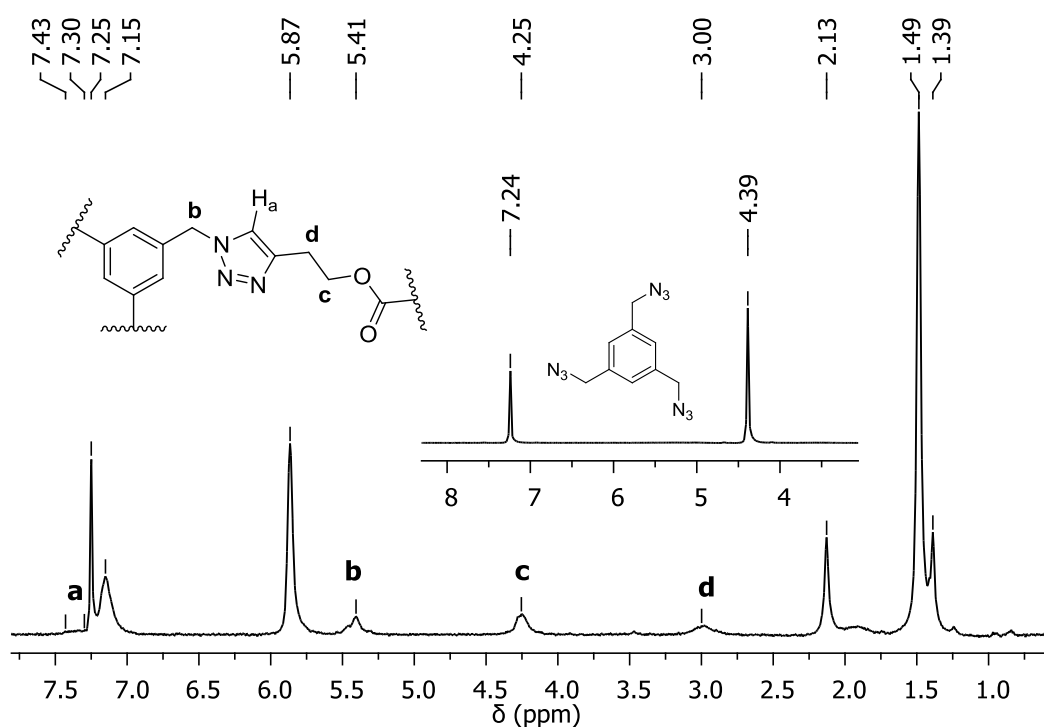


Figure 4.70 : ^1H NMR spectrum of the compound **3.37** recorded in CDCl_3 .

^1H NMR spectroscopic analysis of the compound **3.37** revealed triazole CH proton signals between 7.43 and 7.30 ppm, aromatic CH protons at 7.25 ppm (under the solvent peak, see the ^1H NMR spectrum of **4.5** inset to Figure 4.70), pyrrole NH and CH protons at 7.15 and 5.87 ppm respectively, benzylic CH_2 protons at 5.41 ppm, ester CH_2 protons at 4.25 ppm, CH_2 protons connected to triazole ring through olephin side at 3.00 ppm, and remaining CH_2 and *meso*- CH_3 proton signals 2.13 and 1.39 ppm. FTIR spectrum of the compound **3.37** was found to have a disappearance of azide stretching band 2082 cm^{-1} and keep ester $\text{C}=\text{O}$ bond stretching band at 1731 cm^{-1} . These results are consistent with the expected triazole ring formation between azide units of **4.5** and **3.30** (Figure 4.71).

4.5 was reacted with propargyl ether of phenolic calix[4]pyrrole **3.34** to afford tripodal dendrimeric compound **3.38** (Figure 4.69). This compound was also purified via precipitation of its saturated THF solution into hexanes.

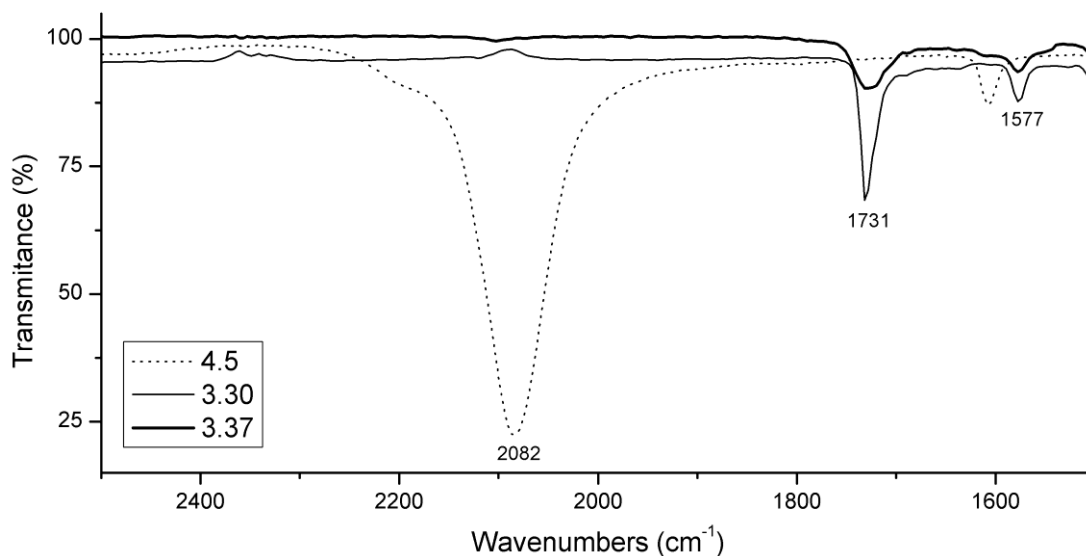


Figure 4.71 : FTIR spectra of calixpyrrole based dendrimer **3.37** and its starting materials.

^1H NMR spectroscopic analysis of the compound **3.38** revealed triazole *CH* proton signal at 7.56 ppm, aromatic *CH* protons at 7.25 ppm, pyrrole *NH* protons at 7.25 and 7.12 ppm respectively, pyrrole *CH* protons at 5.88 and 5.62 ppm, benzylic CH_2 protons at 5.46 ppm, CH_2 protons connected to triazole ring through olephin side at 5.14 ppm, and remaining *meso-CH}_3* proton signals 1.83 and 1.49 ppm (Figure 4.72).

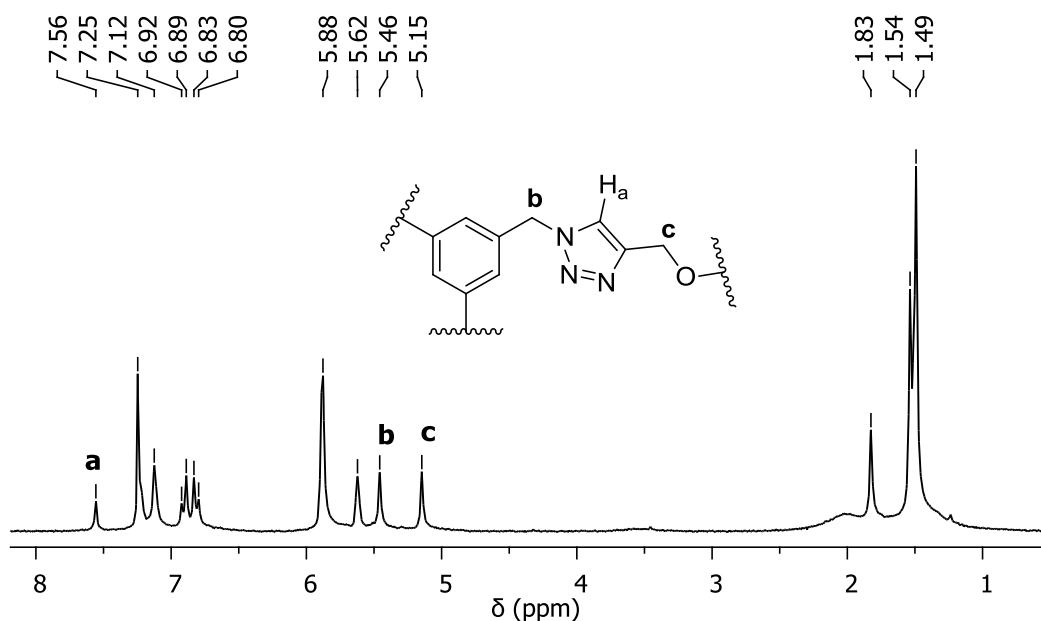


Figure 4.72 : ^1H NMR spectrum of the compound **3.38** recorded in CDCl_3 .

FTIR spectrum of the compound **3.38** was found to have a disappearance of azide stretching band 2082 cm^{-1} and keep aromatic C-H band at 1612 cm^{-1} . These results are consistent with the expected triazole ring formation between azide units of **4.5** and **3.34** (Figure 4.73).

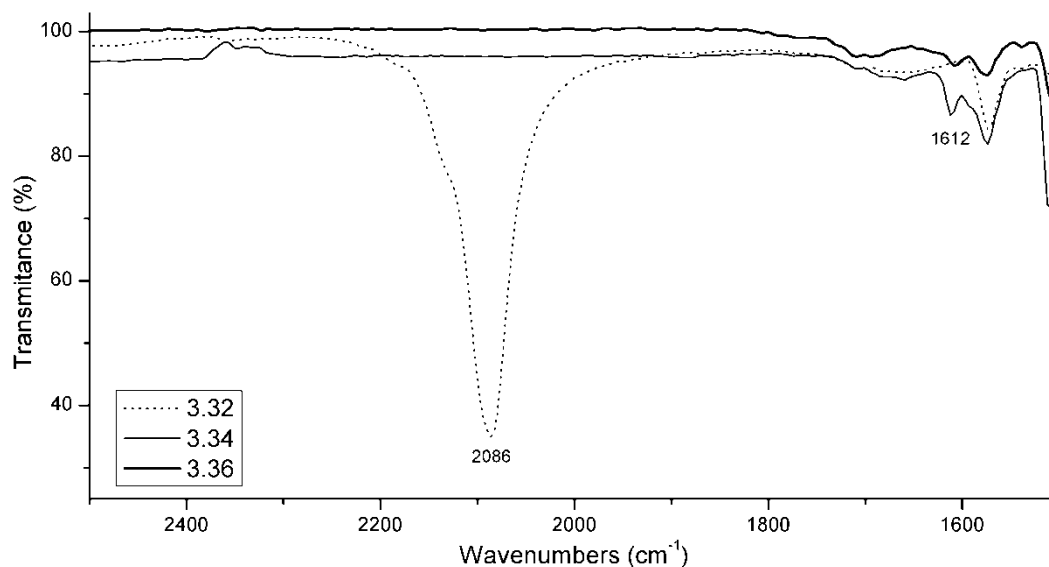


Figure 4.73 : FTIR spectra of calixpyrrole based dendrimer **3.38** and its starting materials.

In conclusion, design, synthesis and characterization of four different calixpyrrole based dendrimeric compounds have been successfully carried out. The target dendrimeric structures have been prepared starting from simple organic compounds having alkyne and azide functional groups. Although dendrimeric calixpyrrole systems could be accessed via various synthetic strategies so called “click chemistry” provided an easy and high yielded synthetic approach. Using this strategy calix[4]pyrrole dendrimers with calix[4]pyrrole and benzene ring cores have been prepared. These novel dendrimeric compounds are potential candidates for extraction of anions, and recognition of polytopic anions such as di-, tri-, and tetra-anions of various organic and inorganic salts.

4.5 Supporting of Calix[4]pyrrole on Silica

Time-honored means of exploring receptor–substrate interactions was provided by the covalent attachment of molecular receptors to solid supports. For instance, azacrown ethers attached to silica gels, have proven useful in the separation of mixtures of metal cations [136]. Another pioneering work reported by Cram and co-workers consists of covalently modified silica gels with chiral crown ethers, that proved capable of resolving enantioselectively various amino acid derivatives [137]. In these works this approach has allowed binding interactions involving a large

number of substrates to be analyzed under identical experimental conditions. As such, it provides a convenient and well validated method of quickly testing the substrate-binding potential of a new receptor or proposed receptor. The above approach has been widely studied in the area of cation recognition and separation; however, it has been less commonly applied in the case of anion binding. One such approach that appears attractive involves the attachment of a metallated porphyrin to either polystyrene or silica gel [42, 138]; these systems have been employed in the separation of quite a number of anionic species including benzoic acid derivatives, iodide, and thiocyanate.

Reports on calix[4]pyrrole modified stationary phase are relatively few. The important one came from Sessler and Gale [45]. They produced calix[4]pyrrole covalently linked silica gels. Under different conditions, they realized the separation of some inorganic and organic anions, such as fluoride, chloride, Cbz-protected amino acids, phosphorylated derivatives of adenine, oligonucleotides, and some small neutral substrates. Through their work, the special separation ability traced to the interactions between calix[4]pyrroles and analytes was revealed.

Most of the above examples relied on the attachment of carboxylic acid functional receptors to a aminopropyl functionalized silica gel [74]. Especially in the field of calixpyrrole chemistry this approach is the only one that have been used. For covalent attachment, this approach requires preparation of a stationary phase with aminopropyl functionality and a receptor having appropriate functional group that can react with the amino group of solid support. When one needs to attach a calixpyrrole receptor to a different solid support, in this case aminopropyl functionalization of this solid support is firstly needed. In this junction, the idea of preparation of a siloxane functionalized seems to be a convenient method for the modification of whatever solid support that can react with siloxane groups. Therefore, in this part of the dissertation, synthesis of siloxane functional calix[4]pyrrole and modification of various silica gels will be presented along with production of silica nanoparticles using this starting material.

Siloxane functionalized calix[4]pyrrole **3.39** was prepared by the reaction of alcohol functionalized calix[4]pyrrole **3.17** with 3-isocyanatotriethoxysilane in dry THF in the presence of catalytic amount of T12 at reflux temperature. Removal of the solvent under reduced pressure and workup followed by washing with hexane afforded **3.39** in 95% yield as a white solid (Figure 4.74). Structural elucidation of the compound **3.39** was carried out using both NMR spectroscopic and X-ray crystallographic methods.

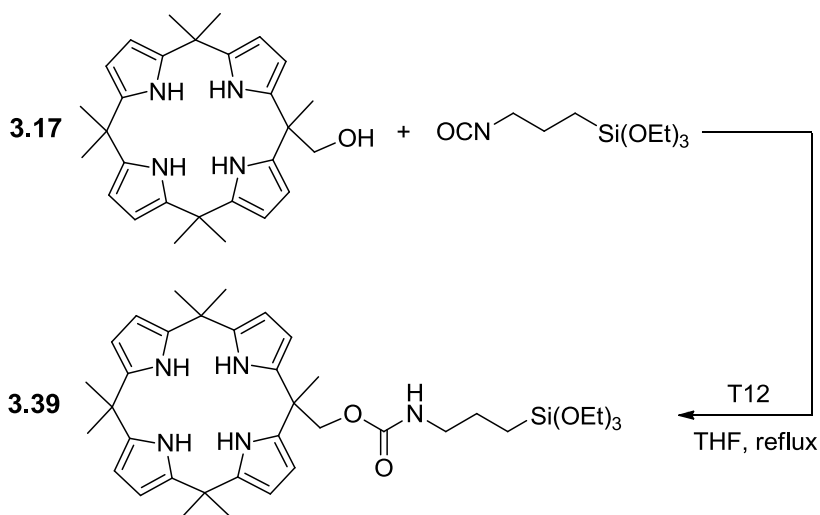


Figure 4.74 : Synthesis of siloxane functionalized calix[4]pyrrole **3.39**.

Figure 4.75 shows ¹H NMR spectroscopic analysis of the compound **3.39** that revealed pyrrole NH proton signals at 7.22 and 7.09 ppm, pyrrole CH proton signals at 5.90 ppm, amide NH proton at 4.83 ppm, *meso*-CH₂ protons at 4.31 ppm, Si-O-CH₂ protons at 3.81 ppm as a quartet, OC-NH-CH₂ protons at 3.12 ppm as a triplet of doublet,

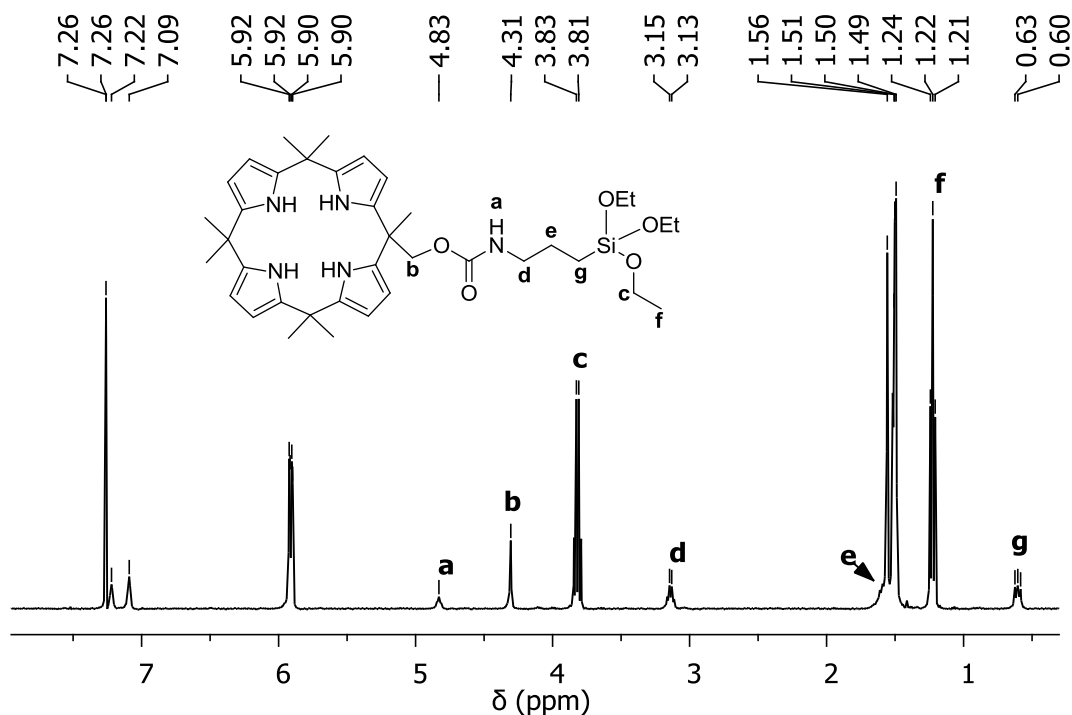


Figure 4.75 : ¹H NMR spectrum of siloxane functionalized calix[4]pyrrole **3.39** recorded in CDCl₃.

Single crystals of **3.39** grew as colorless plates by slow evaporation from DCM/hexane. The data crystal was cut from a cluster of plates and had approximate

dimensions; 0.22 x 0.15 x 0.12 mm. The data were collected on a Nonius Kappa CCD diffractometer using a graphite monochromator with MoK α radiation ($\lambda = 0.71073\text{\AA}$). A total of 204 frames of data were collected using ω -scans with a scan range of 2° and a counting time of 60 seconds per frame. The data were collected at 153 K using an Oxford Cryostream low temperature device. View of **3.39** showing the atom labeling scheme can be seen in Figure 4.76. Displacement ellipsoids are scaled to the 50% probability level. Most hydrogen atoms have been removed for clarity.

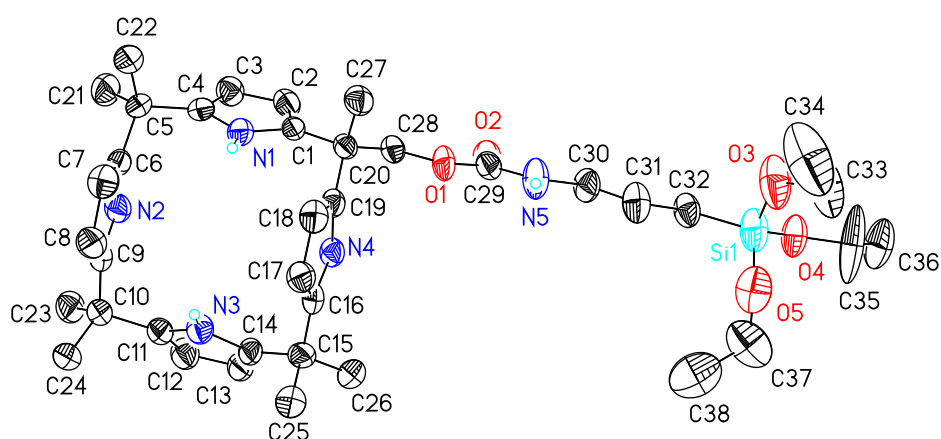


Figure 4.76 : View of **3.39** showing the atom labeling scheme.

Once the siloxane functional compound **3.39** was in hand, the next effort was shifted to modification of various silica gels. Modifications have been carried out following general approach that has been used widely in the literature. For instance, silica gel 60 (a commercially available silica gel that used for column chromatography) was modified with calix[4]pyrrole by reacting this silica gel with the compound **3.39** in dry toluene at room temperature for 24 h. After completion of the reaction the modified silica gel was filtered off and washed with several solvents as described in experimental section. Then, this material was dried under vacuum till no weight change was observed.

When silica gel 60 was modified with siloxane functionalized calix[4]pyrrole **3.39**, FTIR spectrum of modified silica gel revealed carbamate C=O stretching band at 1874 cm^{-1} and aliphatic CH stretching bands at 2977 cm^{-1} . Contrarily, the unmodified silica gel did not reveal any bands in aforementioned wavenumbers (Figure 4.77).

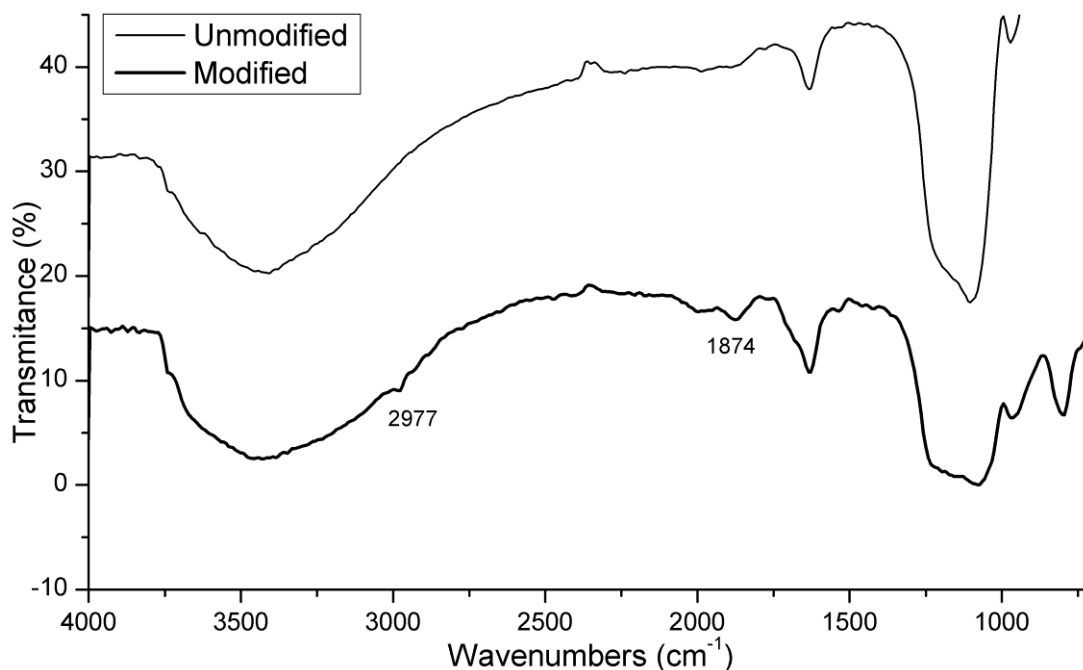


Figure 4.77 : FTIR spectra of modified and unmodified silica gel 60.

Another support about the modification of silica gel 60 came from thermal analysis. Thermogravimetric analyses of both modified and unmodified silica gel 60 showed 5% functionalization upon exposure to siloxane functionalized calix[4]pyrrole **3.39**.

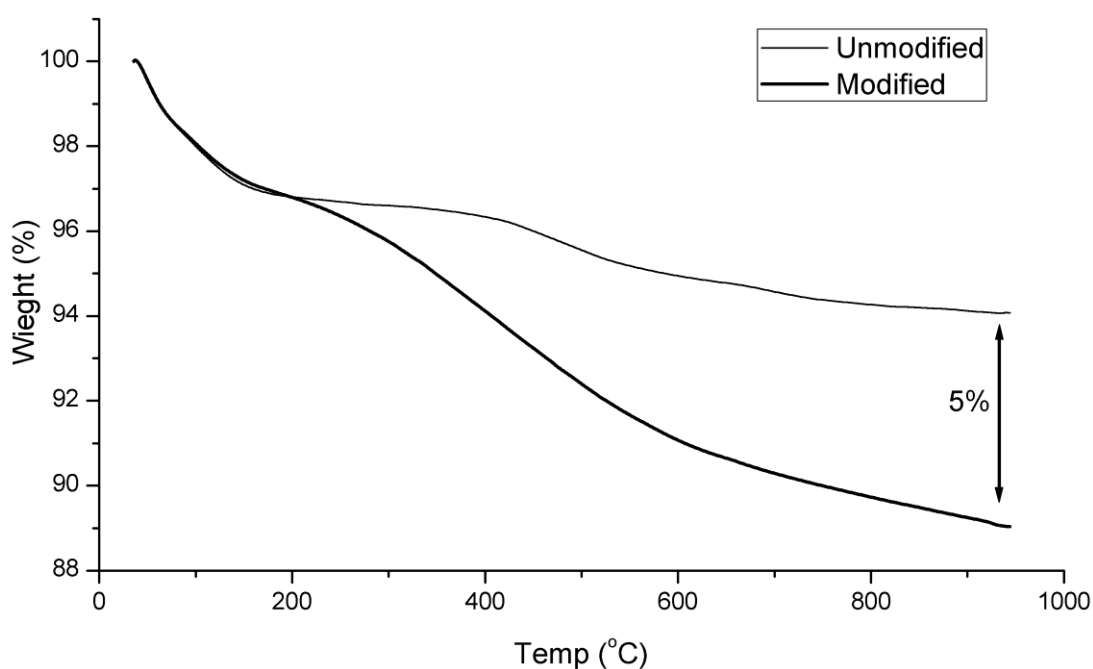


Figure 4.78 : Thermogravigrams of modified and unmodified silica gel 60.

Fume silica was also treated with **3.39** under the similar conditions applied to modify silica gel 60. Modification evidences were obtained by FTIR spectroscopy and thermal analyses. FTIR spectroscopic analyses of the modified and unmodified fume silica revealed carbamate C=O stretching band at 1700 cm^{-1} and aliphatic CH

stretching band at 2981 cm^{-1} . These bands were not observed in the case of unmodified fume silica (Figure 4.79).

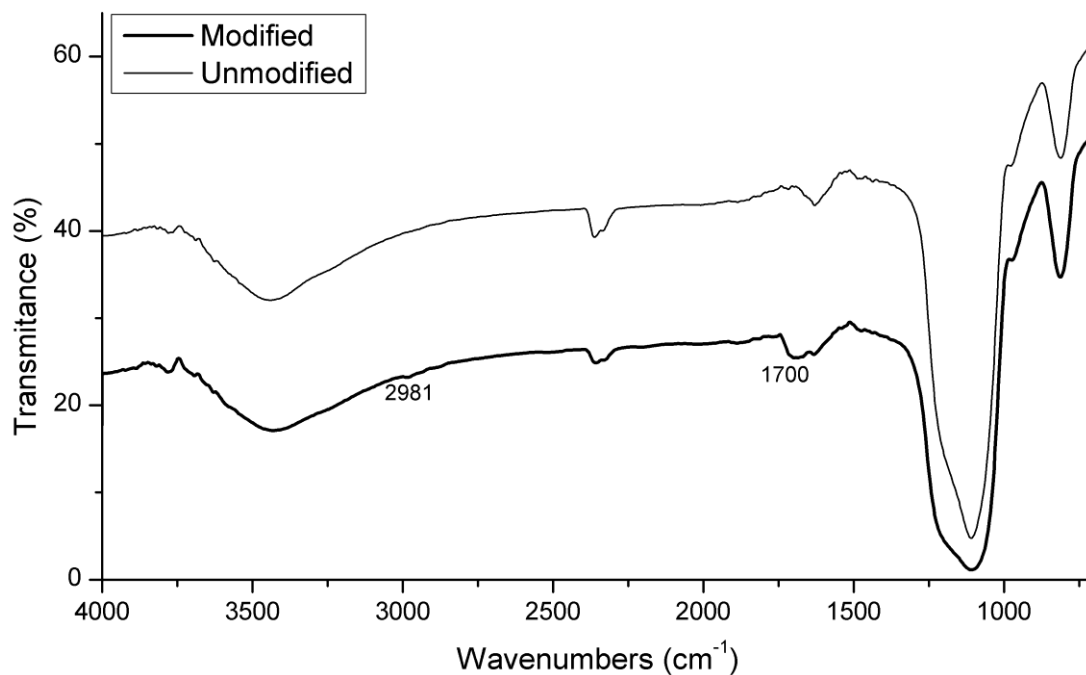


Figure 4.79 : FTIR spectra of modified and unmodified fume silica.

Figure 4.80 indicates that thermogravimetric analyses of both modified and unmodified fume silica showed 16% functionalization upon exposure to siloxane functionalized calix[4]pyrrole **3.39**.

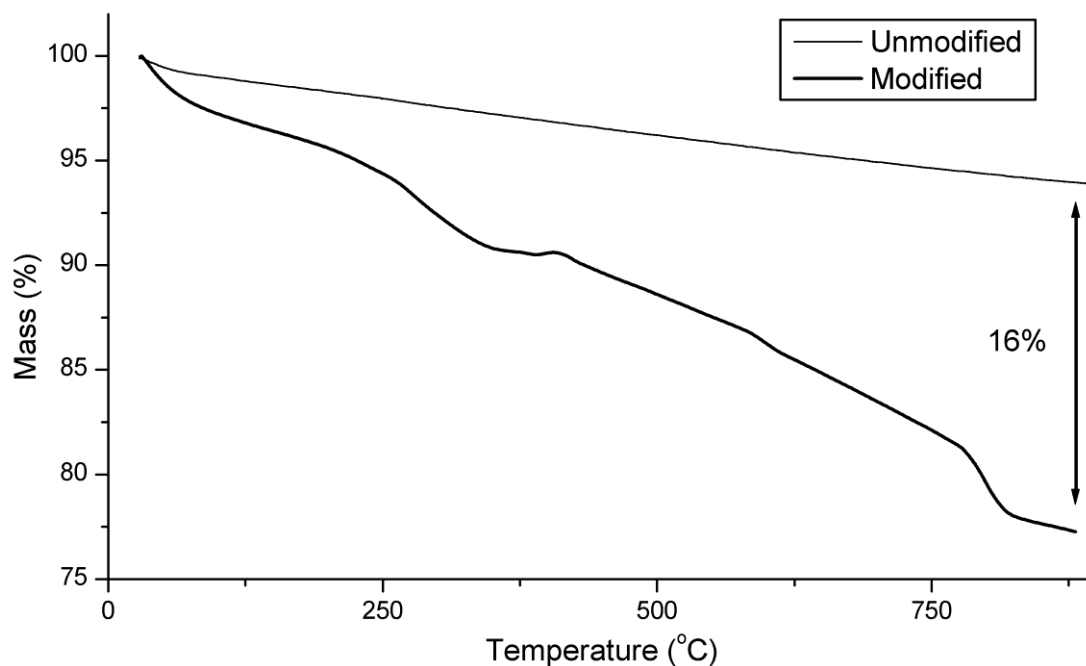


Figure 4.80 : Thermogravigrams of modified and unmodified fume silica.

SiO₂ nanopowder was also modified with siloxane functionalized calix[4]pyrrole **3.39** using a modification strategy analogous to methods described above. At this time, FTIR spectra of fume silica revealed carbamate C=O stretching band at 1689 cm⁻¹ and aliphatic CH stretching band at 2973 cm⁻¹. These bands could not be observed in the case of unmodified fume silica (Figure 4.81).

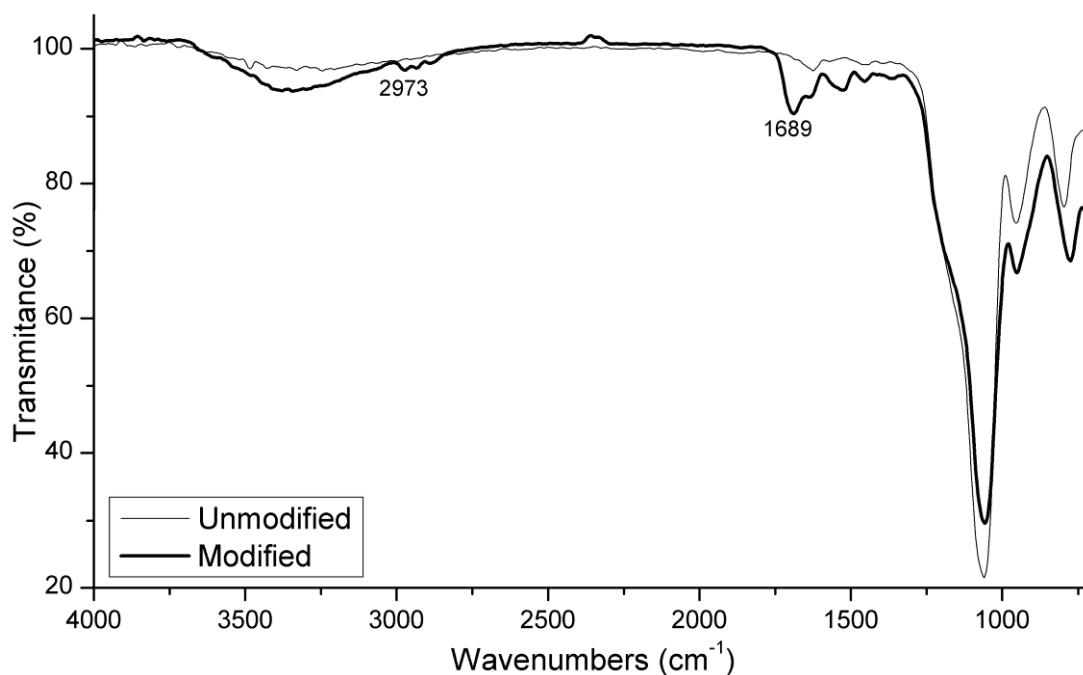


Figure 4.81 : FTIR spectra of modified and unmodified SiO₂ nanopowder.

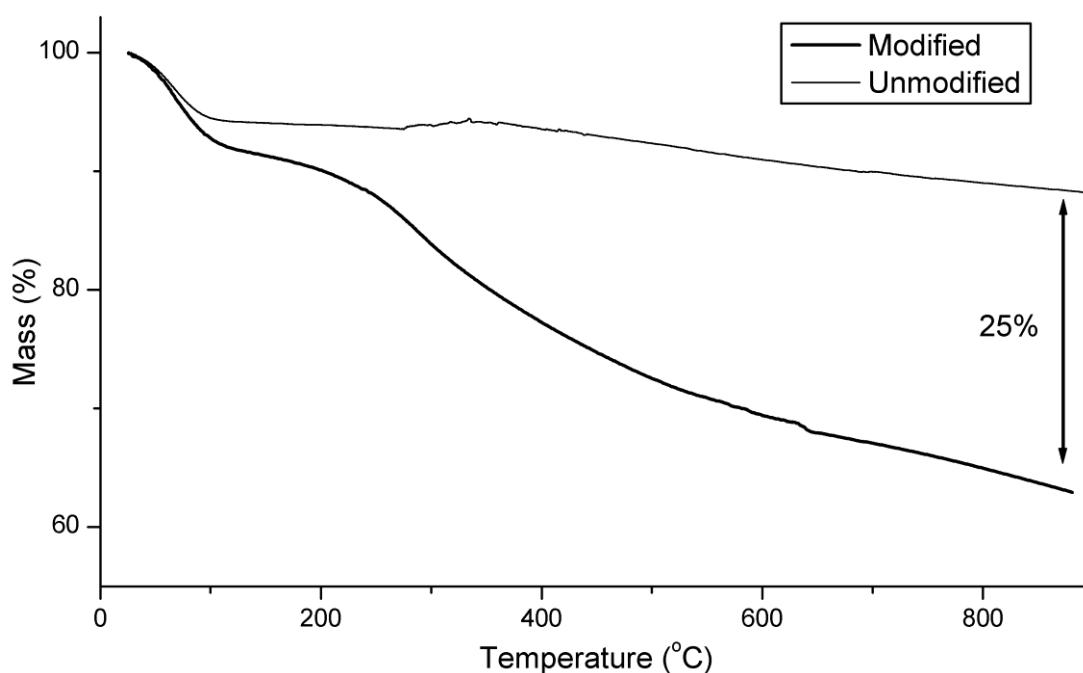


Figure 4.82 : Thermogravigrams of modified and unmodified SiO₂ nanopowders.

Another support about the modification of SiO₂ nanopowder came from thermal analysis. Thermogravimetric analyses of both modified and unmodified SiO₂

nanopowder showed 25% functionalization upon exposure to siloxane functionalized calix[4]pyrrole **3.39**. Table 4.10 summarizes the specifications of modified silica gels studied in this part of the dissertation.

Table 4.10 : Specifications of modified silica gels.

	FTIR (cm ⁻¹)		Organic Content (%)
	Carbamate C=O	Aliphatic CH	
Silica gel 60	1874	2977	5
Fume silica	1700	2981	16
SiO₂ nanopowder	1689	2973	25

Finally an effort was dedicated to preparation of silica nanoparticles via sol-gel reaction. For this purpose siloxane functionalized calix[4]pyrrole **3.39** and TEOS was reacted in EtOH in the presence of NH₄OH at a stirring rate of 250 rpm. After 24 h the white precipitate was filtered off and washed with various solvent to get rid of unwanted organic residues and unreacted starting materials. Drying the final white material afforded calix[4]pyrrole functional silica nanoparticles **3.40** (Figure 4.83).

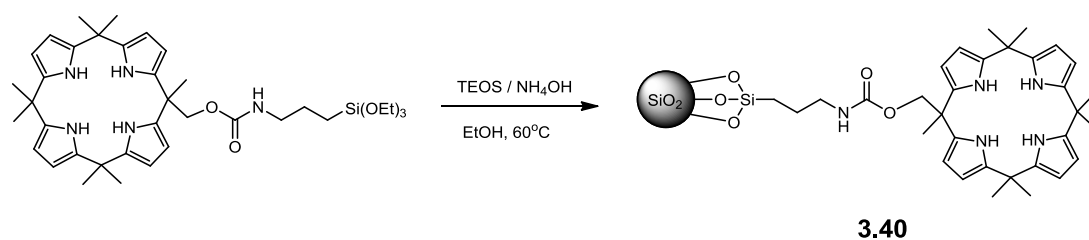


Figure 4.83 : Synthesis of calix[4]pyrrole functional silica nanoparticles.

FTIR spectrum of **3.40** revealed carbamate C=O stretching band at 1855 cm⁻¹ and aliphatic CH stretching band at 2981 cm⁻¹ (Figure 4.84).

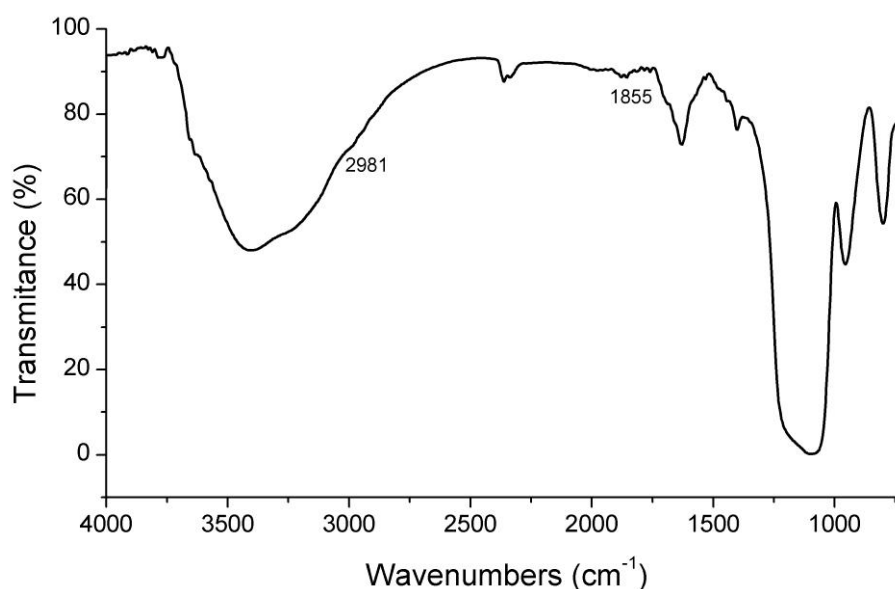


Figure 4.84 : FTIR spectrum of calix[4]pyrrole functional silica nanoparticle.

In conclusion, synthesis of siloxane functionalized calix[4]pyrrole **3.40** have been successfully carried out starting from alcohol functional calixpyrrole **3.17**. Characterization of the compound **3.39** was accomplished by using ^1H NMR spectroscopy and single crystal X-ray crystallography. Modification of silica gel 60, fume silica, and SiO_2 nanopowder was also demonstrated supported by both FTIR spectroscopy and thermogravimetric analysis. These analyses showed that all the materials functionalized with calix[4]pyrrole in a range of 5 – 25% in weight. Further, production of silica nanoparticles with calix[4]pyrrole functionality has been accomplished via sol-gel reaction of siloxane functional calixpyrrole **3.39** and TEOS. Next efforts will be dedicated to increasing the percentage of calix[4]pyrrole units by tuning the ratio of **3.39** and TOES.

5. CONCLUSIONS

In conclusion, new mono carboxylic acid and ester functionalized calix[4]pyrroles bearing both short and long n-alkyl chains on the ester positions have been synthesized. ¹HNMR studies revealed that the brominated derivative **3.2** gives rise to nonobservable *NH* peaks at room temperature (CD₂Cl₂), but that these signals can be readily detected at lower temperatures (i.e., below -20°C). These results are consistent with the brominated calix[4]pyrroles of this study being endowed with more acidic *NH* protons. However, this presumed greater acidity is not reflected in higher chloride or acetate binding affinities relative to the hydrogen atom substituted forms, at least as judged from ITC measurements carried out at room temperature in 1,2-dichloroethane. These same anion binding studies revealed that all the new compounds, including the long n-alkyl esters, display relatively good anion binding affinities, albeit ones that are somewhat reduced compared to those of the parent calix[4]pyrrole (**2.1**). This combination of decent anion affinity and high solubility in nonpolar solvents, such as hexanes, makes the ester systems **3.7**, **3.8**, **3.9**, and **3.10** potentially attractive for use in further applications including anion extraction and transport.

The synthesis of the tetra-bicyclo[2.2.2]-oct-2-ene fused calix[4]pyrrole **3.15** and its partial conversion to the corresponding tetrabenzocalix[4]pyrrole **3.16** were studied. Possible efforts would be improving this latter conversion and studying system **3.15** as a possible ion-pair receptor and deep-walled “molecular container”.

The first well-defined and homogenous polymeric systems capable of extracting potassium fluoride and chloride salts from aqueous media have been prepared. These polymers contain pendant calixpyrrole and crown ether subunits, key features that permit the concurrent complexation of both halide and potassium ions. This, in turn, allows the system as a whole to overcome the relatively high hydration energies of KF and KCl and enables their extraction from aqueous media. To the best of our knowledge this has not hitherto proved possible with any other simple polymeric material. Next efforts would be focused on fine-tuning the choice of receptors and investigating the effect of polymer molecular weight and microstructure on the overall extraction performance of these materials.

Synthesis of siloxane functionalized calix[4]pyrrole **3.39** have been successfully carried out starting from alcohol functional calixpyrrole **3.17**. Characterization of the compound **3.39** was accomplished by using ^1H NMR spectroscopy and single crystal X-ray crystallography. Modification of silica gel 60, fume silica, and SiO_2 nanopowder was also demonstrated supported by both FTIR spectroscopy and thermogravimetric analysis. These analyses showed that all the materials functionalized with calix[4]pyrrole in a range of 5 – 25% in weight. Further, production of silica nanoparticles with calix[4]pyrrole functionality has been accomplished via sol-gel reaction of siloxane functional calixpyrrole **3.39** and TOES. Next efforts will be dedicated to increasing the percentage of calix[4]pyrrole units by tuning the ratio of **3.39** and TOES.

REFERENCES

- [1] **Kavallieratos, K.; Bertao, C. M.; Crabtree, R. H.**, 1999. Hydrogen Bonding in Anion Recognition: A Family of Versatile, Nonpreorganized Neutral and Acyclic Receptors. *Journal of Organic Chemistry*, **64**, (5), 1675-1683.
- [2] **Varo, G.; Brown, L. S.; Needleman, R.; Lanyi, J. K.**, 1996. Proton Transport by Halorhodopsin. *Biochemistry*, **35**, (21), 6604-6611.
- [3] **Schanstra, J. P.; Janssen, D. B.**, 1996. Kinetics of Halide Release of Haloalkane Dehalogenase: Evidence for a Slow Conformational Change. *Biochemistry*, **35**, (18), 5624-5632.
- [4] **Beer, P. D.; Gale, P. A.**, 2001. Anion Recognition and Sensing: The State of the Art and Future Perspectives. *Angewandte Chemie-International Edition*, **40**, (3), 486-516.
- [5] **Sfriso, A.; Pavoni, B.**, 1994. Macroalgae and Phytoplankton Competition in the Central Venice Lagoon. *Environmental Technology*, **15**, (1), 1-14.
- [6] **Kubota, M.**, 1993. Recovery of Technetium from High-Level Liquid Waste Generated in Nuclear-Fuel Reprocessing. *Radiochimica Acta*, **63**, 91-96.
- [7] **Nishiyabu, R.; Anzenbacher, P.**, 2005. Sensing of Antipyretic Carboxylates by Simple Chromogenic Calix[4]Pyrroles. *Journal of the American Chemical Society*, **127**, (23), 8270-8271.
- [8] **Miyaji, H.; Anzenbacher, P.; Sessler, J. L.; Bleasdale, E. R.; Gale, P. A.**, 1999. Anthracene-Linked Calix[4]Pyrroles: Fluorescent Chemosensors for Anions. *Chemical Communications*, (17), 1723-1724.
- [9] **Nielsen, K. A.; Cho, W. S.; Jeppesen, J. O.; Lynch, V. M.; Becher, J.; Sessler, J. L.**, 2004. Tetra-Tf Calix[4]Pyrrole: A Rationally Designed Receptor for Electron-Deficient Neutral Guests. *Journal of the American Chemical Society*, **126**, (50), 16296-16297.
- [10] **Sessler, J. L.; Anzenbacher, P.; Jursikova, K.; Miyaji, H.; Genge, J. W.; Tvermoes, N. A.; Allen, W. E.; Shriver, J. A.; Gale, P. A.; Kral, V.**, 1998. Functionalized Calix[4]Pyrroles. *Pure and Applied Chemistry*, **70**, 2401-2408.
- [11] **Shannon, R. D.**, 1976. Revised Effective Ionic-Radii and Systematic Studies of Interatomic Distances in Halides and Chalcogenides. *Acta Crystallographica Section A*, **32**, (SEP1), 751-767.
- [12] **Chelintzev, V. V.; Tronov, B. V.**, 1916. Process of Condensation of Pyrrole with Acetone. Constitution of the Resulting Products. *Zh. Russ. Fiz.-Khim. O-va.*, **48**, 105-55.

- [13] **Chelintzev, V. V.; Tronov, B. V.; Karmanov, S. G.**, 1916. Simple Condensation of Pyrrole with Cyclohexanone and Other Cyclic Ketones, Mixed Condensation with Acetone and Cyclohexanone, and Conclusions in Respect to the Ability of Different Ketones to Condense with Pyrrole. *J. Russ. Chem. Soc.*, **48**, 1210-21.
- [14] **Rothmund, P.; Gage, C. L.**, 1955. Concerning the Structure of Acetonepyrrole. *Journal of the American Chemical Society*, **77**, (12), 3340-3342.
- [15] **Brown, W. H.; Hutchins.Bj; Mackinno.Mh**, 1971. Condensation of Cyclohexanone with Furan and Pyrrole. *Canadian Journal of Chemistry*, **49**, (24), 4017-&.
- [16] **Floriani, C.**, 1996. The Porphyrinogen-Porphyrin Relationship: The Discovery of Artificial Porphyrins. *Chemical Communications*, (11), 1257-1263.
- [17] **Gale, P. A.; Sessler, J. L.; Kral, V.; Lynch, V.**, 1996. Calix[4]Pyrroles: Old yet New Anion-Binding Agents. *Journal of the American Chemical Society*, **118**, (21), 5140-5141.
- [18] **Bauer, V. J.; Clive, D. L. J.; Dolphin, D.; Paine, J. B.; Harris, F. L.; King, M. M.; Loder, J.; Wang, S. W. C.; Woodward, R. B.**, 1983. Sapphyrins - Novel Aromatic Pentapyrrolic Macrocycles. *Journal of the American Chemical Society*, **105**, (21), 6429-6436.
- [19] **Camiolo, S.; Coles, S. J.; Gale, P. A.; Hursthouse, M. B.; Sessler, J. L.**, 2001. Tetrabutylammonium Meso-Octamethylcalix[4]Pyrrole Fluoride Dichloromethane Solvate. *Acta Crystallographica Section E-Structure Reports Online*, **57**, O816-o818.
- [20] **Anzenbacher, P.; Jursikova, K.; Lynch, V. M.; Gale, P. A.; Sessler, J. L.**, 1999. Calix[4]Pyrroles Containing Deep Cavities and Fixed Walls. Synthesis, Structural Studies, and Anion Binding Properties of the Isomeric Products Derived from the Condensation of P-Hydroxyacetophenone and Pyrrole. *Journal of the American Chemical Society*, **121**, (47), 11020-11021.
- [21] **Camiolo, S.; Gale, P. A.**, 2000. Fluoride Recognition in 'Super-Extended Cavity' Calix[4]Pyrroles. *Chemical Communications*, (13), 1129-1130.
- [22] **Schmidtchen, F. P.**, 2002. Surprises in the Energetics of Host-Guest Anion Binding to Calix[4]Pyrrole. *Organic Letters*, **4**, (3), 431-434.
- [23] **van Hoorn, W. P.; Jorgensen, W. L.**, 1999. Selective Anion Complexation by a Calix[4]Pyrrole Investigated by Monte Carlo Simulations. *Journal of Organic Chemistry*, **64**, (20), 7439-7444.
- [24] **Wu, Y. D.; Wang, D. F.; Sessler, J. L.**, 2001. Conformational Features and Anion-Binding Properties of Calix[4]Pyrrole: A Theoretical Study. *Journal of Organic Chemistry*, **66**, (11), 3739-3746.
- [25] **Akar, A.; Aydogan, A.**, 2005. Synthesis of Meso-Tetra Acid and Ester Functionalized Calix[4]Pyrroles. *Journal of Heterocyclic Chemistry*, **42**, (5), 931-934.
- [26] **Panda, P. K.; Lee, C. H.**, 2005. Metalloporphyrin-Capped Calix[4]Pyrroles: Heteroditopic Receptor Models for Anion Recognition and Ligand Fixation. *Journal of Organic Chemistry*, **70**, (8), 3148-3156.

- [27] **Bucher, C.; Zimmerman, R. S.; Lynch, V.; Sessler, J. L.**, 2001. First Cryptand-Like Calixpyrrole: Synthesis, X-Ray Structure, and Anion Binding Properties of a Bicyclic[3,3,3]Nonapyrrole. *Journal of the American Chemical Society*, **123**, (39), 9716-9717.
- [28] **Anzenbacher, P.; Jursikova, K.; Shriver, J. A.; Miyaji, H.; Lynch, V. M.; Sessler, J. L.; Gale, P. A.**, 2000. Lithiation of Meso-Octamethylcalix[4]Pyrrole: A General Route to C-Rim Monosubstituted Calix[4]Pyrroles. *Journal of Organic Chemistry*, **65**, (22), 7641-7645.
- [29] **Miyaji, H.; Sato, W.; Sessler, J. L.; Lynch, V. M.**, 2000. A 'Building Block' Approach to Functionalized Calix[4]Pyrroles. *Tetrahedron Letters*, **41**, (9), 1369-1373.
- [30] **Gale, P. A.; Sessler, J. L.; Allen, W. E.; Tvermoes, N. A.; Lynch, V.**, 1997. Calix[4]Pyrroles: C-Rim Substitution and Tunability of Anion Binding Strength. *Chemical Communications*, (7), 665-666.
- [31] **Furusho, Y.; Kawasaki, H.; Nakanishi, S.; Aida, T.; Takata, T.**, 1998. Design of Multidentate Pyrrolic Ligands by N-Modification: Synthesis of N-Monomethyl, Monoethyl, Dimethyl, Trimethyl, and Tetramethylporphyrinogens. *Tetrahedron Letters*, **39**, (21), 3537-3540.
- [32] **Cuesta, L.; Gross, D.; Lynch, V. M.; Ou, Z. P.; Kajonkijya, W.; Ohkubo, K.; Fukuzumi, S.; Kadish, K. M.; Sessler, J. L.**, 2007. Design and Synthesis of Polymetallic Complexes Based on Meso-Calix[4]Pyrrole: Platforms for Multielectron Chemistry. *Journal of the American Chemical Society*, **129**, (38), 11696-11697.
- [33] **Sessler, J. L.; Anzenbacher, P.; Miyaji, H.; Jursikova, K.; Bleasdale, E. R.; Gale, P. A.**, 2000. Modified Calix[4]Pyrroles. *Industrial & Engineering Chemistry Research*, **39**, (10), 3471-3478.
- [34] **Dukh, M.; Drasar, P.; Cerny, I.; Pouzar, V.; Shriver, J. A.; Kral, V.; Sessler, J. L.**, 2002. Novel Deep Cavity Calix[4]Pyrroles Derived from Steroidal Ketones. *Supramolecular Chemistry*, **14**, (2-3), 237-244.
- [35] **Sessler, J. L.; Andrievsky, A.; Gale, P. A.; Lynch, V.**, 1996. Anion Binding: Self-Assembly of Polypyrrolic Macrocycles. *Angewandte Chemie-International Edition in English*, **35**, (23-24), 2782-2785.
- [36] **Anzenbacher, P.; Jursikova, K.; Sessler, J. L.**, 2000. Second Generation Calixpyrrole Anion Sensors. *Journal of the American Chemical Society*, **122**, (38), 9350-9351.
- [37] **Turner, B.; Botoshansky, M.; Eichen, Y.**, 1998. Extended Calixpyrroles: Meso-Substituted Calix[6]Pyrroles. *Angewandte Chemie-International Edition*, **37**, (18), 2475-2478.
- [38] **Sessler, J. L.; Cho, W. S.; Gross, D. E.; Shriver, J. A.; Lynch, V. M.; Marquez, M.**, 2005. Anion Binding Studies of Fluorinated Expanded Calixpyrroles. *Journal of Organic Chemistry*, **70**, (15), 5982-5986.
- [39] **Anzenbacher, P.; Try, A. C.; Miyaji, H.; Jursikova, K.; Lynch, V. M.; Marquez, M.; Sessler, J. L.**, 2000. Fluorinated Calix[4]Pyrrole and Dipyrrolylquinoxaline: Neutral Anion Receptors with Augmented Affinities and Enhanced Selectivities. *Journal of the American Chemical Society*, **122**, (42), 10268-10272.

- [40] **Woller, E. K.; Smirnov, V. V.; DiMagno, S. G.**, 1998. A Straightforward Synthesis of 3,4-Difluoropyrrole. *The Journal of Organic Chemistry*, **63**, (16), 5706-5707.
- [41] **Andreas, M.; Roland, S.; Johann, L.**, 1993. 2,3,7,8,12,13,17,18-Octamethoxyporphyrin. *Angewandte Chemie International Edition in English*, **32**, (2), 291-293.
- [42] **Kokufuta, E.; Sodeyama, T.; Takeda, S.**, 1986. Oxochloromolybdenum(V) Tetraphenylporphyrin Complex-Containing Polymer as a Phosphate Ion-Exchanger. *Polymer Bulletin*, **15**, (6), 479-484.
- [43] **Iverson, B. L.; Thomas, R. E.; Kral, V.; Sessler, J. L.**, 1994. Molecular Recognition of Anionic Species by Silica-Gel Bound Sapphyrin. *Journal of the American Chemical Society*, **116**, (6), 2663-2664.
- [44] **Sessler, J. L.; Genge, J. W.; Kral, V.; Iverson, B. L.**, 1996. Separation of Mono-, Di-, and Triphosphate Nucleotides by Cytosine Substituted, Silica-Bound Sapphyrin Solid Supports. *Supramolecular Chemistry*, **8**, (1), 45-52.
- [45] **Sessler, J. L.; Gale, P. A.; Genge, J. W.**, 1998. Calix[4]Pyrroles: New Solid-Phase Hplc Supports for the Separation of Anions. *Chemistry-A European Journal*, **4**, (6), 1095-1099.
- [46] **Zhou, C. Z.; Tang, H.; Shao, S. J.; Jiang, S. X.**, 2006. Calix[4]Pyrrole-Bonded Hplc Stationary Phase for the Separation of Phenols, Benzenecarboxylic Acids, and Medicines. *Journal of Liquid Chromatography & Related Technologies*, **29**, (13), 1961-1978.
- [47] **Gale, P. A.; Anzenbacher, P.; Sessler, J. L.**, 2001. Calixpyrroles II. *Coordination Chemistry Reviews*, **222**, 57-102.
- [48] **Nishiyabu, R.; Anzenbacher, P.**, 2006. 1,3-Indane-Based Chromogenic Calixpyrroles with Push-Pull Chromophores: Synthesis and Anion Sensing. *Organic Letters*, **8**, (3), 359-362.
- [49] **Kim, S. H.; Hong, S. J.; Yoo, J.; Kim, S. K.; Sessler, J. L.; Lee, C. H.**, 2009. Strapped Calix[4]Pyrroles Bearing a 1,3-Indanedione at a Beta-Pyrrolic Position: Chemodosimeters for the Cyanide Anion. *Organic Letters*, **11**, (16), 3626-3629.
- [50] **Allen, W. E.; Gale, P. A.; Brown, C. T.; Lynch, V. M.; Sessler, J. L.**, 1996. Binding of Neutral Substrates by Calix[4]Pyrroles. *Journal of the American Chemical Society*, **118**, (49), 12471-12472.
- [51] **Furusho, Y.; Aida, T.**, 1997. Guest-Responsive Structural Changes of Porphyrinogen Inclusion Crystals: A Long-Range Cooperative Effect on Guest Inclusion. *Chemical Communications*, (22), 2205-2206.
- [52] **Jeppesen, J. O.; Takimiya, K.; Jensen, F.; Becher, J.**, 1999. Pyrrolo Annelated Tetrathiafulvalenes: The Parent Systems. *Organic Letters*, **1**, (8), 1291-1294.
- [53] **Black, C. B.; Andrioletti, B.; Try, A. C.; Ruiperez, C.; Sessler, J. L.**, 1999. Dipyrrolylquinoxalines: Efficient Sensors for Fluoride Anion in Organic Solution. *Journal of the American Chemical Society*, **121**, (44), 10438-10439.

- [54] **Yoo, J. D.; Kim, M. S.; Hong, S. J.; Sessler, J. L.; Lee, C. H.**, 2009. Selective Sensing of Anions with Calix[4]Pyrroles Strapped with Chromogenic Dipyrrolylquinoxalines. *Journal of Organic Chemistry*, **74**, (3), 1065-1069.
- [55] **Piotrowski, T.; Radecka, H.; Radecki, J.; Depraetere, S.; Dehaen, W.**, 2001. Effect of the Symmetry of the Calix[4]Pyrrole Cavity on Sensitivity and Selectivity of Potentiometric Sensors for Neutral Nitrophenols. *Materials Science and Engineering: C*, **18**, (1-2), 223-228.
- [56] **Nishiyabu, R.; Palacios, M. A.; Dehaen, W.; Anzenbacher, P.**, 2006. Synthesis, Structure, Anion Binding, and Sensing by Calix[4] Pyrrole Isomers. *Journal of the American Chemical Society*, **128**, (35), 11496-11504.
- [57] **Sessler, J. L.; Gebauer, A.; Gale, P. A.**, 1997. Anion Binding and Electrochemical Properties of Calix[4]Pyrrole Ferrocene Conjugates. *Gazette Chimica Italy*, 723-726.
- [58] **Gale, P. A.; Hursthouse, M. B.; Light, M. E.; Sessler, J. L.; Warriner, C. N.; Zimmerman, R. S.**, 2001. Ferrocene-Substituted Calix[4]Pyrrole: A New Electrochemical Sensor for Anions Involving Ch Center Dot Center Dot Center Dot Anion Hydrogen Bonds. *Tetrahedron Letters*, **42**, (38), 6759-6762.
- [59] **Hynes, M. J.**, 1993. Eqnmr - a Computer-Program for the Calculation of Stability-Constants from Nuclear-Magnetic-Resonance Chemical-Shift Data. *Journal of the Chemical Society-Dalton Transactions*, (2), 311-312.
- [60] **Gale, P. A.; Bleasdale, E. R.; Chen, G. Z.**, 2001. Synthesis and Electrochemical Polymerisation of Calix[4]Pyrroles Containing N-Substituted Pyrrole Moieties. *Supramolecular Chemistry*, **13**, (4), 557-563.
- [61] **Alunni, S.; Pero, A.; Reichenbach, G.**, 1998. Reactivity of Ions and Ion Pairs in the Nucleophilic Substitution Reaction on Methyl P-Nitrobenzenesulfonate. *Journal of the Chemical Society-Perkin Transactions 2*, (8), 1747-1750.
- [62] **Wilcox, C. S.**, 1991. Synthesis, and Evaluation of an Efficacious Functional Group Dyad. Methods and Limitations in the Use of Nmr for Measuring Host-Guest Interaction, In *Frontiers in Supramolecular Organic Chemistry and Photochemistry*, p.123, Eds. Schneider, H.-J.; Dürr, H., VCH, Michigan.
- [63] **Connors, K. A.**, 1987. *Binding Constants: The Measurement of Molecular Complex Stability*. Wiley.
- [64] **Kortüm, G.**, 1955. *Kolorimetrie, Photometrie Und Spektrometrie*. Springer.
- [65] **Velazquez-Campoy, A.; Ohtaka, H.; Nezami, A.; Muzammil, S.; Freire, E.**, 2004. Isothermal Titration Calorimetry. *Curr Protoc Cell Biol*, **Chapter 17**, Unit 17.8.
- [66] **Job, P.**, 1928. Formation and Stability of Inorganic Complexes in Solution. *Annali di Chimica Applicata*, **9**, 113-203.
- [67] **Okujima, T.; Komobuchi, N.; Uno, H.; Ono, N.**, 2006. A New Synthesis of Acenaphthobenzoporphyrin and Fluoranthobenzoporphyrin. *Heterocycles*, **67**, (1), 255-267.

- [68] **Ito, S.; Ochi, N.; Murashima, T.; Uno, H.; Ono, N.**, 2000. A New Synthesis of Benzoporphyrins Using 4,7-Dihydro-4,7-Ethano-2h-Isoindole as an Isoindole Equivalent. *Heterocycles*, **52**, (1), 399-411.
- [69] **Ito, S.; Murashima, T.; Uno, H.; Ono, N.**, 1998. A New Synthesis of Benzoporphyrins Using 4,7-Dihydro-4,7-Ethano-2h-Isoindole as a Synthone of Isoindole. *Chemical Communications*, (16), 1661-1662.
- [70] **Ito, S.; Murashima, T.; Ono, N.**, 1997. A New Synthesis of Pyrroles Fused with Polycyclic Skeletons. *Journal of the Chemical Society-Perkin Transactions 1*, (21), 3161-3165.
- [71] **Zhang, W. C.; Li, C. J.**, 2000. A Direct Retro-Barbier Fragmentation. *Journal of Organic Chemistry*, **65**, (18), 5831-5833.
- [72] **Cecioni, S.; Argintaru, O.-A.; Docsa, T.; Gergely, P.; Praly, J.-P.; Vidal, S.**, 2009. Probing Multivalency for the Inhibition of an Enzyme: Glycogen Phosphorylase as a Case Study. *New Journal of Chemistry*, **33**, (1).
- [73] **Cecioni, S.; Argintaru, O. A.; Docsa, T.; Gergely, P.; Praly, J. P.; Vidal, S.**, 2009. Probing Multivalency for the Inhibition of an Enzyme: Glycogen Phosphorylase as a Case Study. *New Journal of Chemistry*, **33**, (1), 148-156.
- [74] **Angeletti, E.; Canepa, C.; Martinetti, G.; Venturello, P.**, 1989. Amino Groups Immobilized on Silica Gel: An Efficient and Reusable Heterogeneous Catalyst for the Knoevenagel Condensation. *Journal of the Chemical Society, Perkin Transactions 1*, (1), 105-107.
- [75] **Xu, H.; Strater, N.; Schroder, W.; Bottcher, C.; Ludwig, K.; Saenger, W.**, 2003. Structure of DNA Helicase Repa in Complex with Sulfate at 1.95 Angstrom Resolution Implicates Structural Changes to an 'Open' Form. *Acta Crystallographica Section D-Biological Crystallography*, **59**, 815-822.
- [76] **Anderson, M. P.; Gregory, R. J.; Thompson, S.; Souza, D. W.; Paul, S.; Mulligan, R. C.; Smith, A. E.; Welsh, M. J.**, 1991. Demonstration That Cfr Is a Chloride Channel by Alteration of Its Anion Selectivity. *Science*, **253**, (5016), 202-205.
- [77] **Devuyst, O.; Christie, P. T.; Courtoy, P. J.; Beauwens, R.; Thakker, R. V.**, 1999. Intra-Renal and Subcellular Distribution of the Human Chloride Channel, Clc-5, Reveals a Pathophysiological Basis for Dent's Disease. *Human Molecular Genetics*, **8**, (2), 247-257.
- [78] **Kornak, U.; Kasper, D.; Bosl, M. R.; Kaiser, E.; Schweizer, M.; Schulz, A.; Friedrich, W.; Dellling, G.; Jentsch, T. J.**, 2001. Loss of the Clc-7 Chloride Channel Leads to Osteopetrosis in Mice and Man. *Cell*, **104**, (2), 205-215.
- [79] **Scott, D. A.; Wang, R.; Kreman, T. M.; Sheffield, V. C.; Karniski, L. P.**, 1999. The Pendred Syndrome Gene Encodes a Chloride-Iodide Transport Protein. *Nature Genetics*, **21**, (4), 440-443.

- [80] **Simon, D. B.; Bindra, R. S.; Mansfield, T. A.; NelsonWilliams, C.; Mendonca, E.; Stone, R.; Schurman, S.; Nayir, A.; Alpay, H.; Bakkaloglu, A.; RodriguezSoriano, J.; Morales, J. M.; Sanjad, S. A.; Taylor, C. M.; Pilz, D.; Brem, A.; Trachtman, H.; Griswold, W.; Richard, G. A.; John, E.; Lifton, R. P.**, 1997. Mutations in the Chloride Channel Gene, *Clcnkb*, Cause Bartter's Syndrome Type III. *Nature Genetics*, **17**, (2), 171-178.
- [81] **Levitskaia, T. G.; Marquez, M.; Sessler, J. L.; Shriver, J. A.; Vercouter, T.; Moyer, B. A.**, 2003. Fluorinated Calixpyrroles: Anion-Binding Extractants That Reduce the Hofmeister Bias. *Chemical Communications*, (17), 2248-2249.
- [82] **Moyer, B. A.; Bonnesen, P. V.; Custelcean, R.; Delmau, L. H.; Gorbunova, M. G.; Haverlock, T. J.; Kang, H.-A.; Hay, B. P.; Levitskaia, T. G.; Sessler, J. L.; Cho, W.-S.; Shriver, J. A.; Bowman-James, K.; Llinares, J. M.; Hossain, M. A.**, 2004. Using Coordination Chemistry to Selectively Separate Anions, *228th ACS National Meeting*, Philadelphia,
- [83] **Custelcean, R.; Delmau, L. H.; Moyer, B. A.; Sessler, J. L.; Cho, W. S.; Gross, D.; Bates, G. W.; Brooks, S. J.; Light, M. E.; Gale, P. A.**, 2005. Calix[4]Pyrrole: An Old yet New Ion-Pair Receptor. *Angewandte Chemie-International Edition*, **44**, (17), 2537-2542.
- [84] **Moss, B.**, 1996. A Land Awash with Nutrients - the Problem of Eutrophication. *Chemistry & Industry*, (11), 407-411.
- [85] **EIEtri, M.; Cuppoletti, J.**, 1996. Metalloporphyrin Chloride Ionophores: Induction of Increased Anion Permeability in Lung Epithelial Cells. *Am. J. Physiol. Lung Cell Mol. Physiol.*, **14**, (3), L386-L392.
- [86] **Perry, S. F.; Rivero-Lopez, L.; McNeill, B.; Wilson, J.**, 2006. Fooling a Freshwater Fish: How Dietary Salt Transforms the Rainbow Trout Gill into a Seawater Gill Phenotype. *Journal of Experimental Biology*, **209**, (23), 4591-4596.
- [87] **Gale, P. A.; Allen, W. E.; Genge, J.; Tvermoes, N.; Lynch, V.; Sessler, J. L.**, 1997. Beta-Substituted Calix[4]Pyrroles: New Chemistry at the C-Rim. *Abstracts of Papers of the American Chemical Society*, **213**, 522.
- [88] **Sessler, J. L.; Gross, D. E.; Cho, W. S.; Lynch, V. M.; Schmidtchen, F. P.; Bates, G. W.; Light, M. E.; Gale, P. A.**, 2006. Calix[4]Pyrrole as a Chloride Anion Receptor: Solvent and Counteraction Effects. *Journal of the American Chemical Society*, **128**, (37), 12281-12288.
- [89] **Sessler, J. L.; An, D. Q.; Cho, W. S.; Lynch, V.; Yoon, D. W.; Hong, S. J.; Lee, C. H.**, 2005. Anion-Binding Behavior of Hybrid Calixpyrroles. *Journal of Organic Chemistry*, **70**, (5), 1511-1517.
- [90] **Aydogan, A.; Coady, D. J.; Lynch, V. M.; Akar, A.; Marquez, M.; Bielawski, C. W.; Sessler, J. L.**, 2008. Poly(Methyl Methacrylate)S with Pendant Calixpyrroles: Polymeric Extractants for Halide Anion Salts. *Chemical Communications*, (12), 1455-1457.
- [91] **Aydogan, A.; Coady, D. J.; Kim, S. K.; Akar, A.; Bielawski, C. W.; Marquez, M.; Sessler, J. L.**, 2008. Poly(Methyl Methacrylate)S with Pendant Calixpyrroles and Crown Ethers: Polymeric Extractants for Potassium Halides. *Angewandte Chemie-International Edition*, **47**, (50), 9648-9652.

- [92] **De, L. O.; Modena, G.**, 1982. Cis-1,2-Bis(Phenylsulfonyl)Ethylene: A Novel, Convenient Acetylene Synthon in Diels-Alder Reactions. *Journal of the Chemical Society, Chemical Communications*, (16), 914-15.
- [93] **Shishkanova, T. V.; Sykora, D.; Sessler, J. L.; Kral, V.**, 2007. Potentiometric Response and Mechanism of Anionic Recognition of Heterocalixarene-Based Ion Selective Electrodes. *Analytica Chimica Acta*, **587**, (2), 247-253.
- [94] **Kral, V.; Sessler, J. L.; Shishkanova, T. V.; Gale, P. A.; Volf, R.**, 1999. Molecular Recognition at an Organic-Aqueous Interface: Heterocalixarenes as Anion Binding Agents in Liquid Polymeric Membrane Ion-Selective Electrodes. *Journal of the American Chemical Society*, **121**, (38), 8771-8775.
- [95] **Zyryanov, G. V.; Kinstle, T. H.; Anzenbacher, P.**, 2008. Synthesis of Calix[4]Pyrrole-Based Acrylate and Acrylamide Monomers: Precursors for Preparation of Anion-Selective Polymer Membranes. *Synlett*, (8), 1171-1174.
- [96] **Schofield, K.**, 2003. A New Method to Minimize High-Temperature Corrosion Resulting from Alkali Sulfate and Chloride Deposition in Combustion Systems. I. Tungsten Salts. *Energy & Fuels*, **17**, (1), 191-203.
- [97] **Eller, L. R.; Stpieri, M.; Fowler, C. J.; Lee, J. T.; Sessler, J. L.; Moyer, B. A.**, 2007. Octamethyl-Octaundecylcyclo[8]Pyrrole: A Promising Sulfate Anion Extractant (Vol 129, Pg 11020, 2007). *Journal of the American Chemical Society*, **129**, (46), 14523-14523.
- [98] **Moyer, B. A.; Delmau, L. H.; Fowler, C. J.; Ruas, A.; Bostick, D. A.; Sessler, J. L.; Katayev, E.; Pantos, G. D.; Llinares, J. M.; Hossain, A.; Kang, S. O.; Bowman-James, K.**, 2007. Supramolecular Chemistry of Environmentally Relevant Anions, In *Advances in Inorganic Chemistry: Including Bioinorganic Studies*, Vol. 59, pp.175-204, Eds. Eldik, R.; Bowman-James, K., Academic Press,
- [99] **Bhattacharya, P. K.**, 2005. *Metal Ions in Biochemistry*. Alpha Science International Ltd.: Harrow, U.K.
- [100] **Kirk, K. L.**, 1991. *Biochemistry of the Elemental Halogens and Inorganic Halides*. Plenum Press: New York, U.S.A.
- [101] **Block, G.; Port, F. K.**, 2003. Calcium Phosphate Metabolism and Cardiovascular Disease in Patients with Chronic Kidney Disease. *Seminars in Dialysis*, **16**, (2), 140-147.
- [102] **Kaledkowski, A.; Trochimczuk, A. W.**, 2006. Performance of Chelating Resins Containing Calixpyrroles in Sorption of Anions. *Separation Science and Technology*, **41**, (15), 3431-3447.
- [103] **Kaledkowski, A.; Trochimczuk, A. W.**, 2006. Chelating Resin Containing Hybrid Calixpyrroles: New Sorbent Metal Cations. *Reactive & Functional Polymers*, **66**, (9), 957-966.
- [104] **Aldakov, D.; Anzenbacher, P.**, 2004. Sensing of Aqueous Phosphates by Polymers with Dual Modes of Signal Transduction. *Journal of the American Chemical Society*, **126**, (15), 4752-4753.
- [105] **Kaledkowski, A.; Trochimczuk, A. W.**, 2006. Novel Chelating Resins Containing Calix[4]Pyrroles: Synthesis and Sorptive Properties. *Reactive & Functional Polymers*, **66**, (7), 740-746.

- [106] **Wu, C. Y.; Chen, M. S.; Lin, C. A.; Lin, S. C.; Sun, S. S.**, 2006. Photophysical Studies of Anion-Induced Colorimetric Response and Amplified Fluorescence Quenching in Dipyrrolylquinoxaline-Containing Conjugated Polymers. *Chemistry-A European Journal*, **12**, (8), 2263-2269.
- [107] **Odian, G. G.**, 2004. Radical Chain Polymerization, In *Principles of Polymerization*, pp.198-238, Eds. John Wiley and Sons,
- [108] **Custelcean, R.; Moyer, B. A.**, 2007. Anion Separation with Metal-Organic Frameworks. *European Journal of Inorganic Chemistry*, (10), 1321-1340.
- [109] Hydration energies were taken from Table 1.1 of B. A. Moyer and P. V. Bonnensen "Physical Factors in Anion Separations" in *Supramolecular Chemistry of Anions*, A. Bianchi, K. Bowman-James, and E. García-España, Eds., Wiley-VCH, New York, 1997.
- [110] **Mansour, A. R.; Takroui, K. J.**, 2007. A New Technology for the Crystallization of Dead Sea Potassium Chloride. *Chemical Engineering Communications*, **194**, (6), 803 - 810.
- [111] **Krumgalz, B. S.; Millero, F. J.**, 1989. Halite Solubility in Dead Sea Waters. *Marine Chemistry*, **27**, (3-4), 219-233.
- [112] **Carpenter, A.**, 1978. Geochemistry of Bromide-Rich Brines of the Dead Sea and Southern Arkansas. *Circular - Oklahoma Geological Survey* **79**, 78-88.
- [113] **Park, K. H.; Hernandez, L.; Cai, S.-Q.; Wang, Y.; Sesti, F.**, 2005. A Family of K^+ Channel Ancillary Subunits Regulate Taste Sensitivity in *Caenorhabditis Elegans*. *Journal of Biological Chemistry*, **280**, (23), 21893-21899.
- [114] **Bobkov, Y. V.; Kolesnikov, S. S.**, 1999. Extracellular Protons Activate K^+ Current in a Subpopulation of Frog Taste Receptor Cells. *Neuroscience Letters*, **264**, (1-3), 25-28.
- [115] **Sweeney, G.; Klip, A.**, 2001. Mechanisms and Consequences of Na^+, K^+ -Pump Regulation by Insulin and Leptin. *Cellular and Molecular Biology*, **47**, (2), 363-372.
- [116] **Morris, S.; Edwards, T.**, 1995. Control of Osmoregulation Via Regulation of Na^+/K^+ -Atpase Activity in the Amphibious Purple Shore Crab *Leptograpsus Variegatus*. *Comparative Biochemistry and Physiology Part C: Comparative Pharmacology and Toxicology*, **112**, (2), 129-136.
- [117] **Pedersen, C. J.**, 1967. Cyclic Polyethers and Their Complexes with Metal Salts. *Journal of the American Chemical Society*, **89**, 7017-7036.
- [118] **Albanese, D.; Landini, D.; Maia, A.; Penso, M.**, 1999. Phase Transfer Catalysis: Some Recent Applications in Organic Synthesis. *Journal of Molecular Catalysis a-Chemical*, **150**, (1-2), 113-131.
- [119] **Makosza, M.; Fedorynski, M.**, 2003. Phase Transfer Catalysis (Reprinted from *Interfacial Catalysis*, Pg 159-201, 2003). *Catalysis Reviews-Science and Engineering*, **45**, (3-4), 321-367.

- [120] **Albanese, D.**, 2003. Liquid-Liquid Phase Transfer Catalysis: Basic Principles and Synthetic Applications (Reprinted from *Interfacial Catalysis*, Pg 203-226, 2003). *Catalysis Reviews-Science and Engineering*, **45**, (3-4), 369-395.
- [121] **Yagi, K.; Sanchez, M. C.**, 1984. *Polymer Science and Technology*. Plenum Press: Vol. 24, p 345-357.
- [122] **Mammen, M.; Choi, S.-K.; Whitesides, G. M.**, 1998. Polyvalent Interactions in Biological Systems: Implications for Design and Use of Multivalent Ligands and Inhibitors. *Angewandte Chemie International Edition*, **37**, (20), 2754-2794.
- [123] **Mammen, M.; Choi, S.-K.; Whitesides, G. M.**, 1998. Polyvalente Wechselwirkungen in Biologischen Systemen: Auswirkungen Auf Das Design Und Die Verwendung Multivalenter Liganden Und Inhibitoren. *Angewandte Chemie*, **110**, (20), 2908-2953.
- [124] **Kim, I. B.; Dunkhorst, A.; Gilbert, J.; Bunz, U. H. F.**, 2005. Sensing of Lead Ions by a Carboxylate-Substituted Ppe: Multivalency Effects. *Macromolecules*, **38**, (11), 4560-4562.
- [125] **Jackson, K. W.; Lu, S. J.**, 1998. Atomic Absorption, Atomic Emission, and Flame Emission Spectrometry. *Analytical Chemistry*, **70**, (12), 363R-383R.
- [126] **Marcus, Y.**, 1991. Thermodynamics of Solvation of Ions. Part 5.—Gibbs Free Energy of Hydration at 298.15 K. *Journal of the Chemical Society, Faraday Transactions*, **87**, 2995 - 2999.
- [127] **Palmer, B. F.**, 2004. Managing Hyperkalemia Caused by Inhibitors of the Renin-Angiotensin-Aldosterone System. *New England Journal of Medicine*, **351**, (6), 585-592.
- [128] **Putcha, N.; Allon, M.**, 2007. Management of Hyperkalemia in Dialysis Patients. *Seminars in Dialysis*, **20**, (5), 431-439.
- [129] **Chow, H.-F.; Mong, T. K. K.; Nongrum, M. F.; Wan, C.-W.**, 1998. The Synthesis and Properties of Novel Functional Dendritic Molecules. *Tetrahedron*, **54**, (30), 8543-8660.
- [130] **David, K. S.; François, D.**, 1998. Functional Dendrimers: Unique Biological Mimics. *Chemistry - A European Journal*, **4**, (8), 1353-1361.
- [131] **Kolb, H. C.; Finn, M. G.; Sharpless, K. B.**, 2001. Click Chemistry: Diverse Chemical Function from a Few Good Reactions. *Angewandte Chemie-International Edition*, **40**, (11), 2004.
- [132] **Gothelf, K. V.; Jorgensen, K. A.**, 1998. Asymmetric 1,3-Dipolar Cycloaddition Reactions. *Chemical Reviews*, **98**, (2), 863-909.
- [133] **Tornøe, C. W.; Christensen, C.; Meldal, M.**, 2002. Peptidotriazoles on Solid Phase:[1,2,3]-Triazoles by Regiospecific Copper(I)-Catalyzed 1,3-Dipolar Cycloadditions of Terminal Alkynes to Azides. *The Journal of Organic Chemistry*, **67**, (9), 3057-3064.
- [134] **Demko, Z. P.; Sharpless, K. B.**, 2002. A Click Chemistry Approach to Tetrazoles by Huisgen 1,3-Dipolar Cycloaddition: Synthesis of 5-Acyltetrazoles from Azides and Acyl Cyanides. *Angewandte Chemie-International Edition*, **41**, (12), 2113-2116.

- [135] **Lewis, W. G.; Green, L. G.; Grynszpan, F.; Radic, Z.; Carlier, P. R.; Taylor, P.; Finn, M. G.; Sharpless, K. B.**, 2002. Click Chemistry in Situ: Acetylcholinesterase as a Reaction Vessel for the Selective Assembly of a Femtomolar Inhibitor from an Array of Building Blocks. *Angewandte Chemie-International Edition*, **41**, (6), 1053-+.
- [136] **Izatt, R. M.; Bruening, R. L.; Tarbet, B. J.; Griffin, L. D.; Bruening, M. L.; Krakowiak, K. E.; Bradshaw, J. S.**, 1990. Macrocycle Metal Cation Interactions Involving Polyaza Macrocycles Bonded to Silica-Gel Via a Nitrogen Donor Atom. *Pure and Applied Chemistry*, **62**, (6), 1115-1118.
- [137] **Sogah, G. D. Y.; Cram, D. J.**, 1976. Total Chromatographic Optical Resolutions of Alpha-Amino-Acid and Ester Salts through Chiral Recognition by a Host Covalently Bound to Polystyrene Resin. *Journal of the American Chemical Society*, **98**, (10), 3038-3041.
- [138] **Kibbey, C. E.; Meyerhoff, M. E.**, 1993. Preparation and Characterization of Covalently Bound Tetraphenylporphyrin Silica-Gel Stationary Phases for Reversed-Phase and Anion-Exchange Chromatography. *Analytical Chemistry*, **65**, (17), 2189-2196.

APPENDICES

APPENDIX A : ^1H , ^{13}C NMR spectra, ITC curves, X-ray crystal structures and TGA graphics of the compounds.

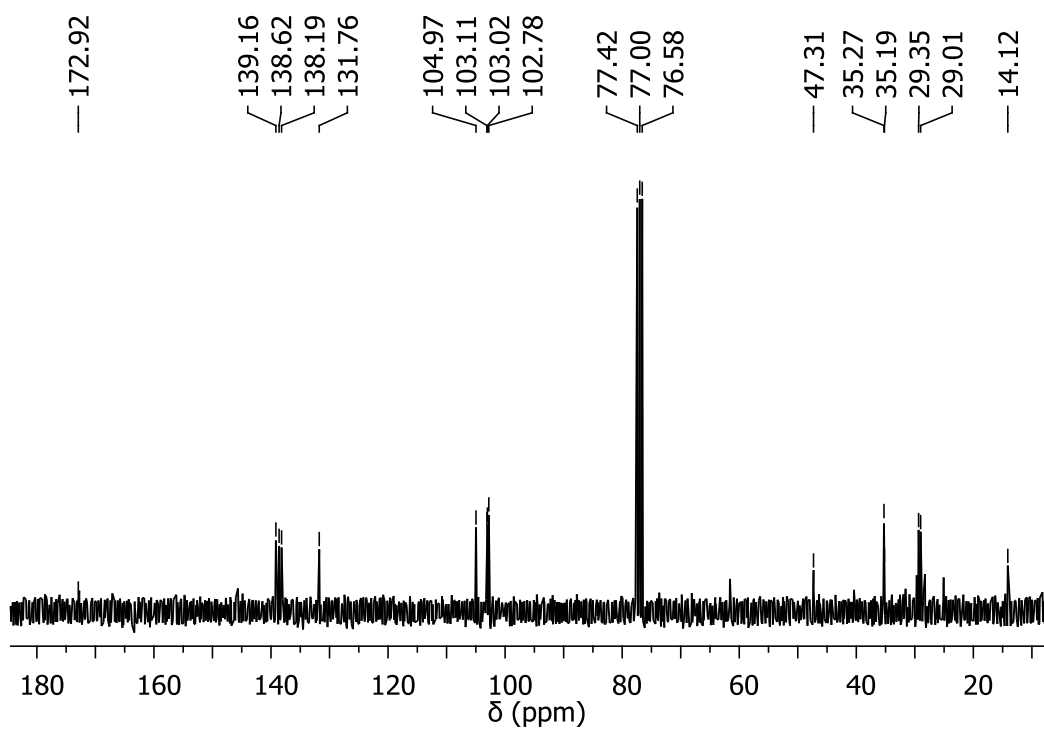


Figure A.1 : ^{13}C NMR spectrum of **3.1** recorded in CDCl_3 .

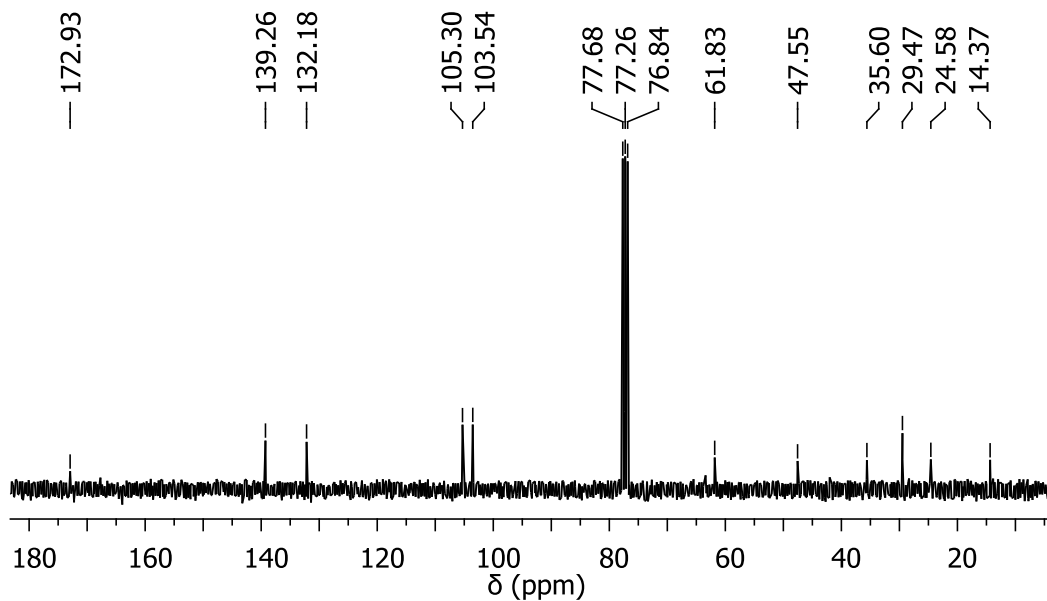


Figure A.2 : ^{13}C NMR spectrum of **3.2** recorded in CDCl_3 .

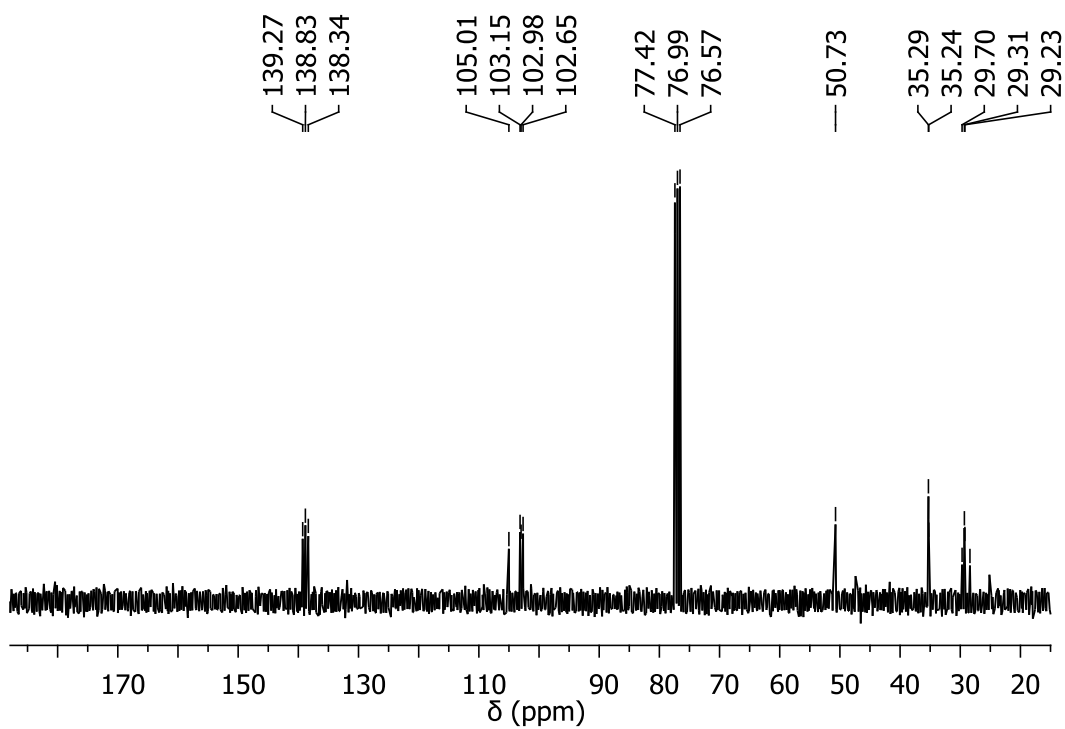


Figure A.3 : ^{13}C NMR spectrum of **3.3** recorded in CDCl_3 .

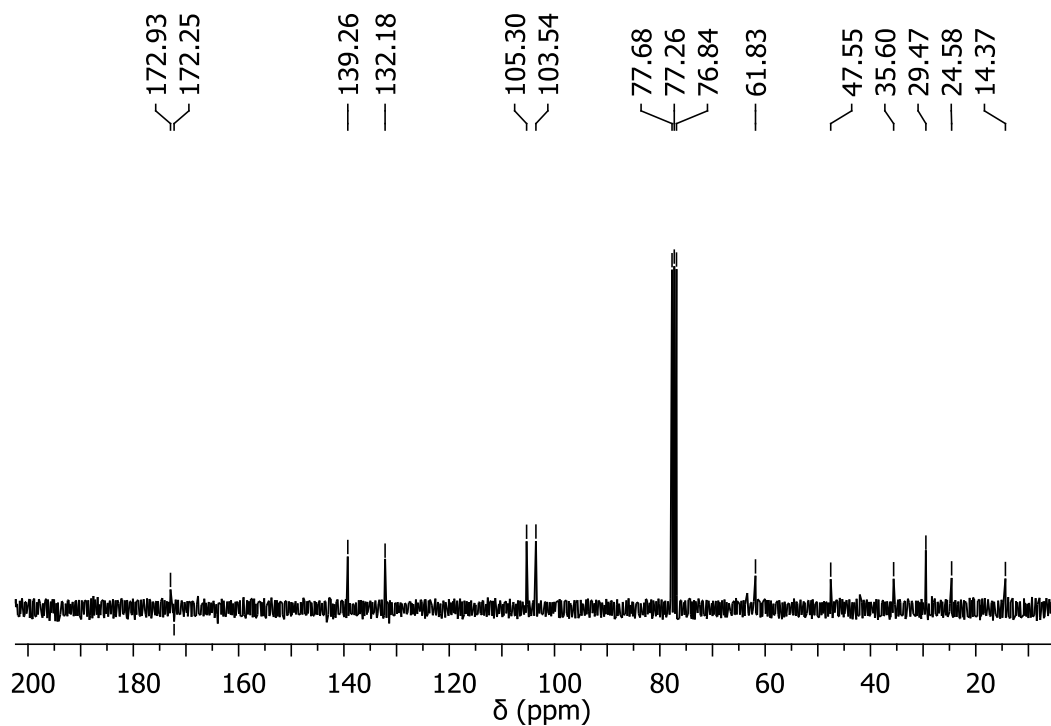


Figure A.4 : ^{13}C NMR spectrum of **3.4** recorded in CDCl_3 .

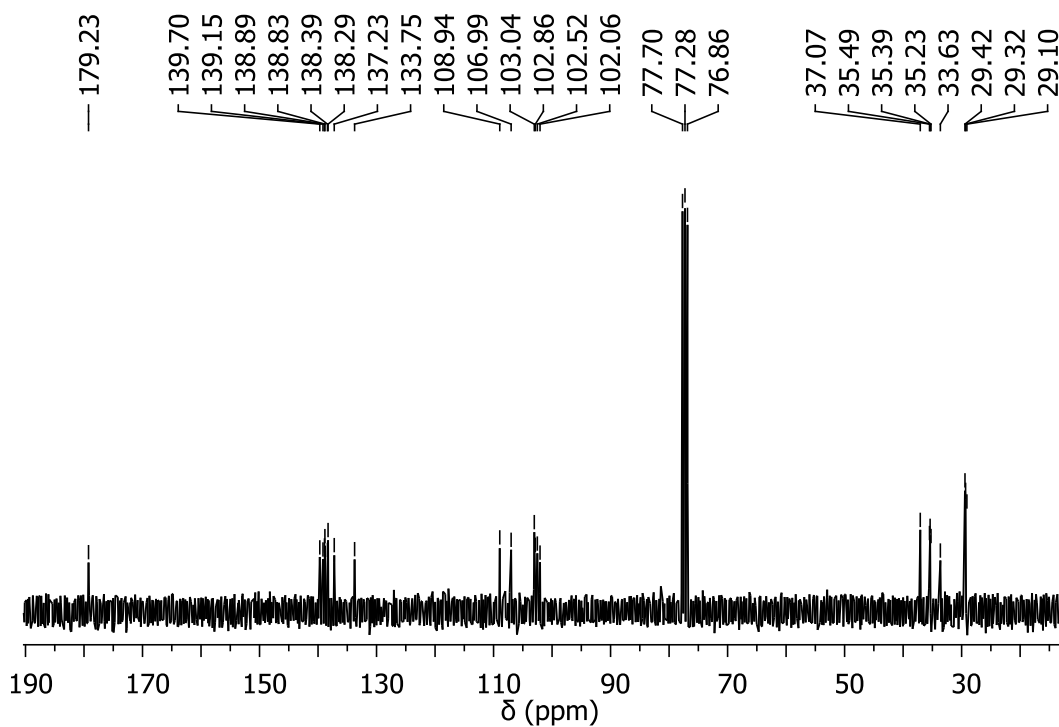


Figure A.5 : ^{13}C NMR spectrum of **3.5** recorded in CDCl_3 .

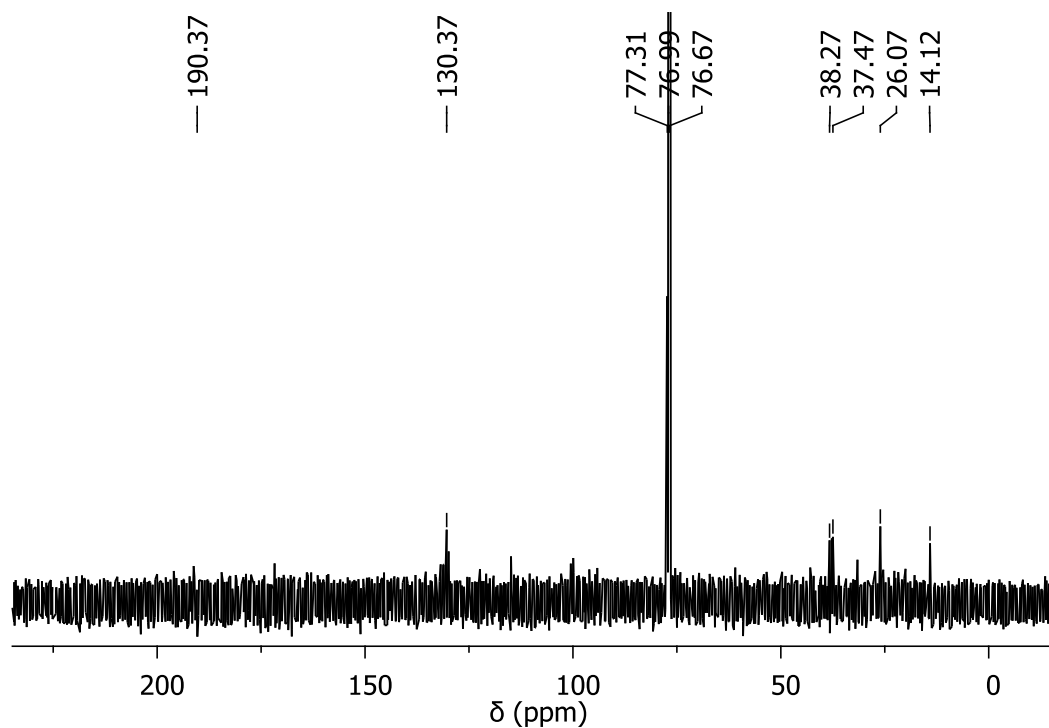


Figure A.6 : ^{13}C NMR spectrum of **3.6** recorded in CDCl_3 .

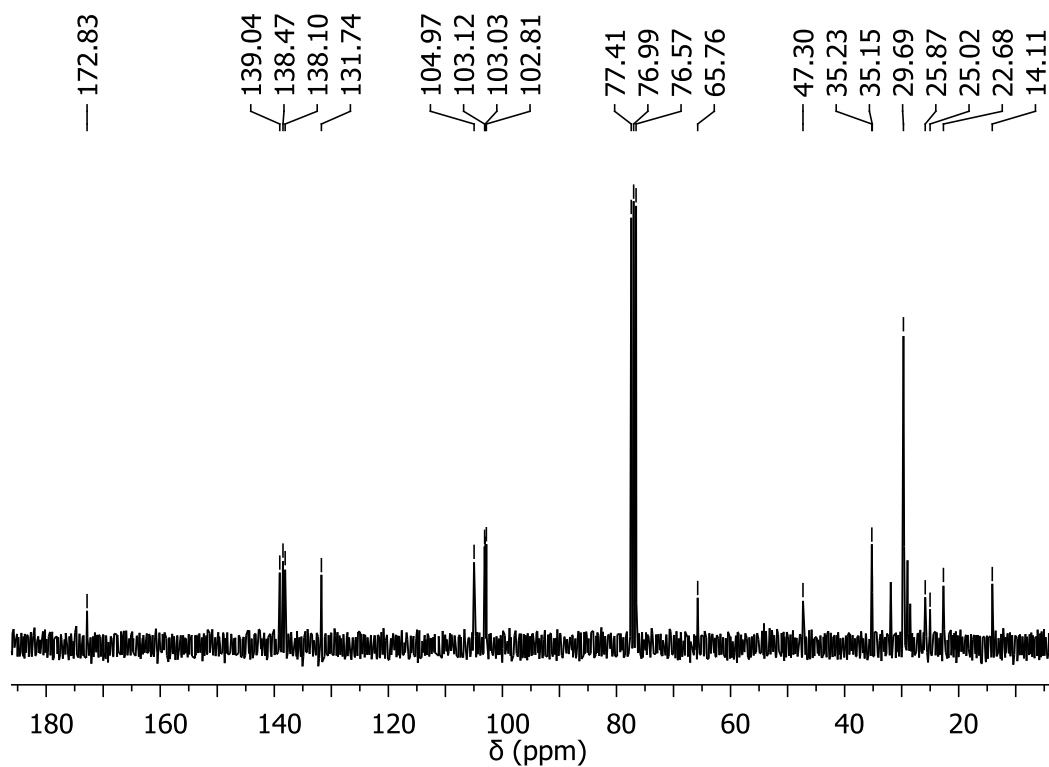


Figure A.7 : ^{13}C NMR spectrum of **3.7** recorded in CDCl_3 .

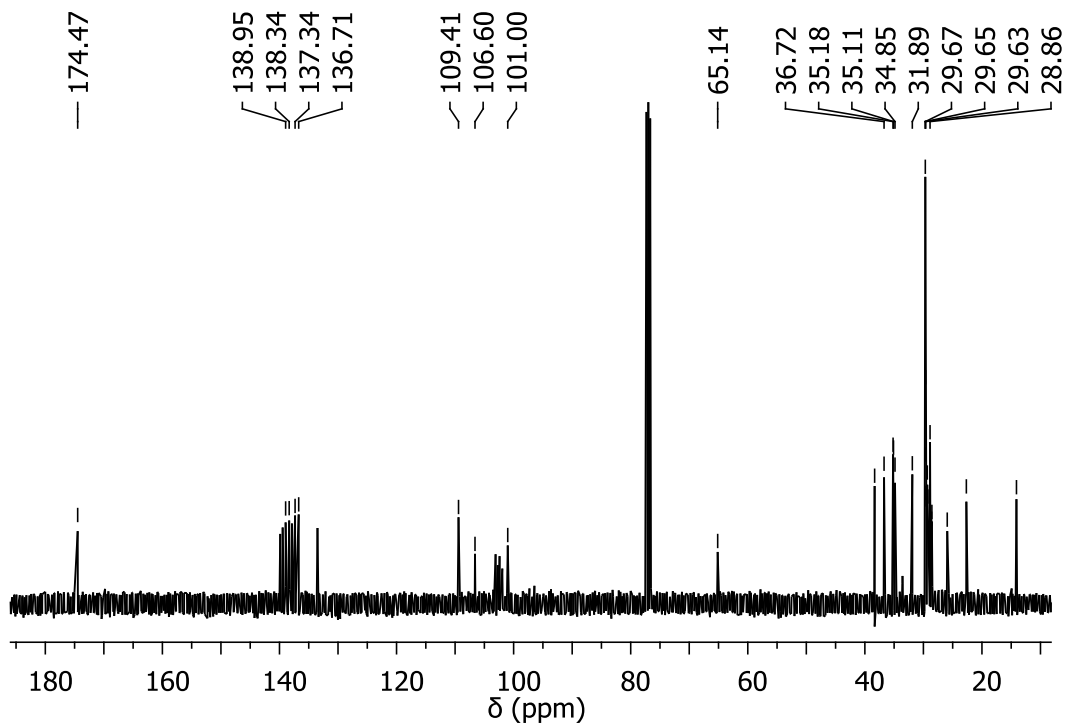


Figure A.8 : ^{13}C NMR spectrum of **3.9** recorded in CDCl_3 .

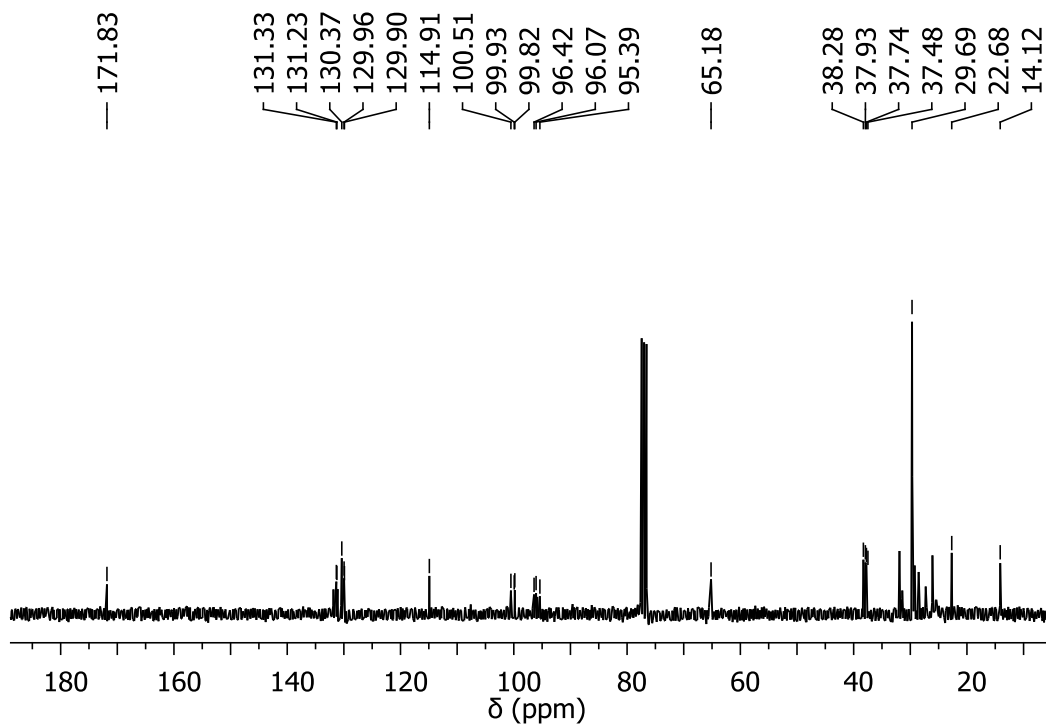


Figure A.9 : ^{13}C NMR spectrum of **3.10** recorded in CDCl_3 .

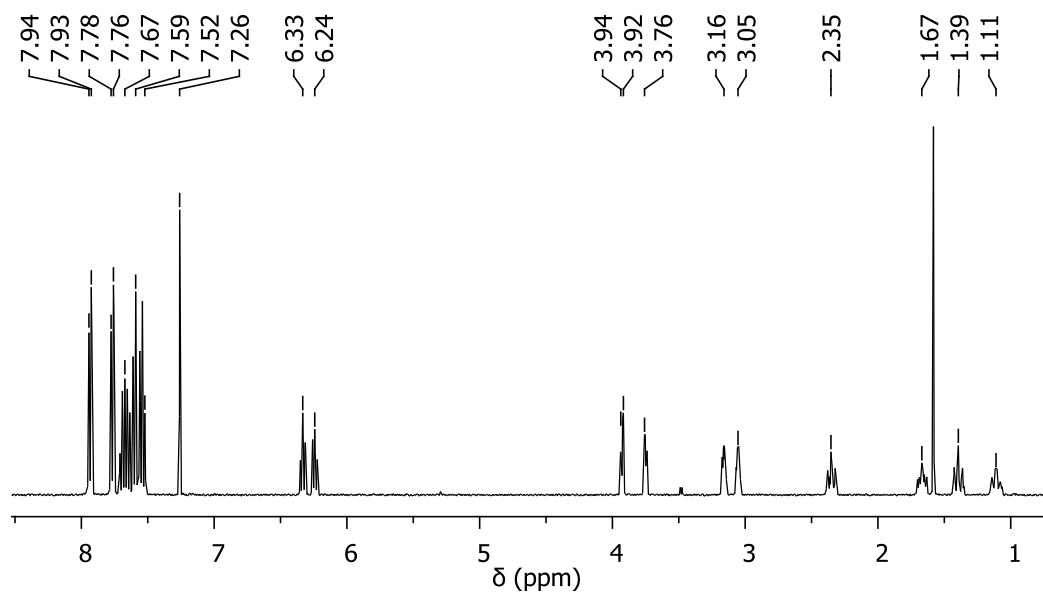


Figure A.10 : ^1H NMR spectrum of **3.11** recorded in CDCl_3 .

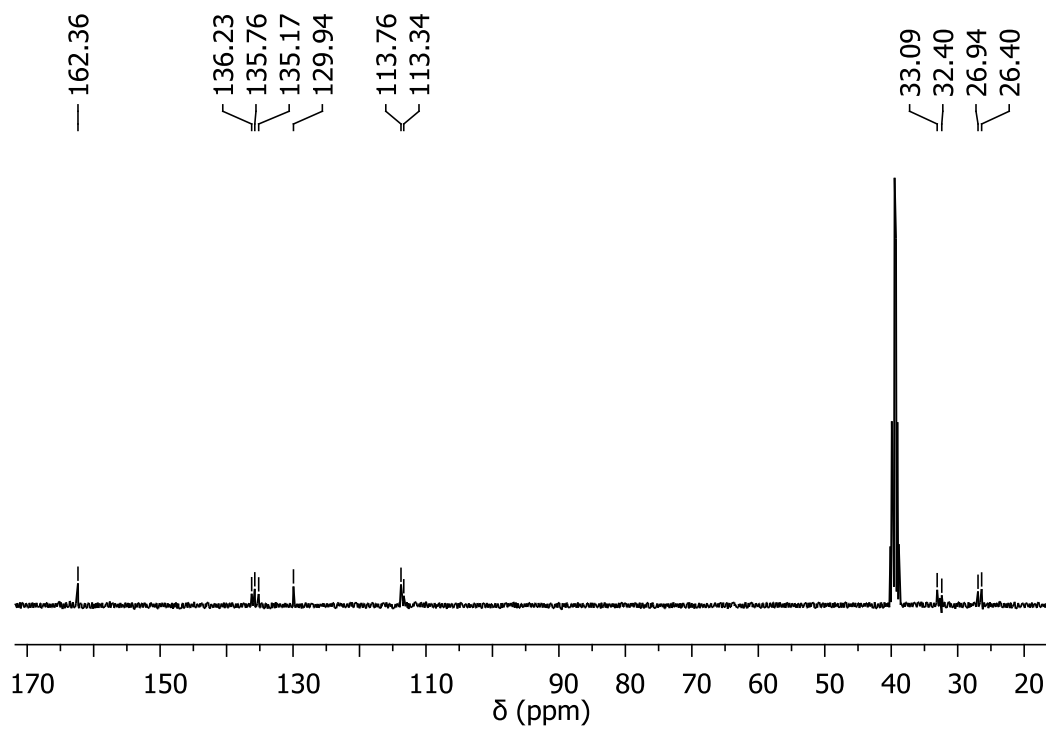


Figure A.11 : ^{13}C NMR spectrum of **3.13** recorded in $\text{DMSO}-d_6$.

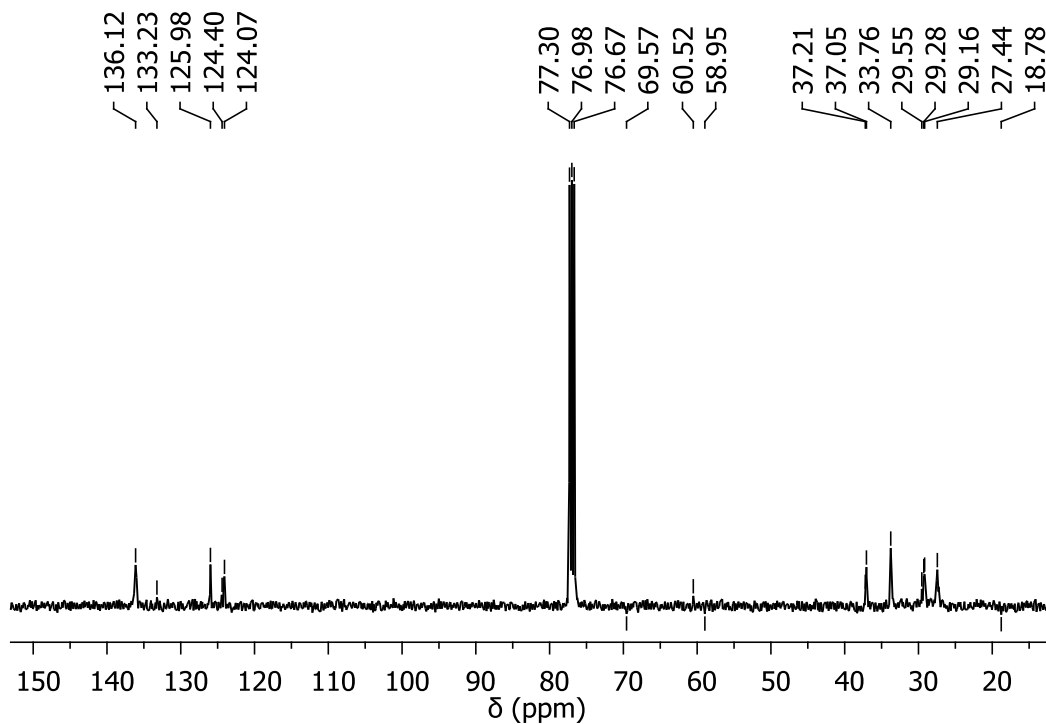


Figure A.12 : ^{13}C NMR spectrum of **3.15** recorded in CDCl_3 .

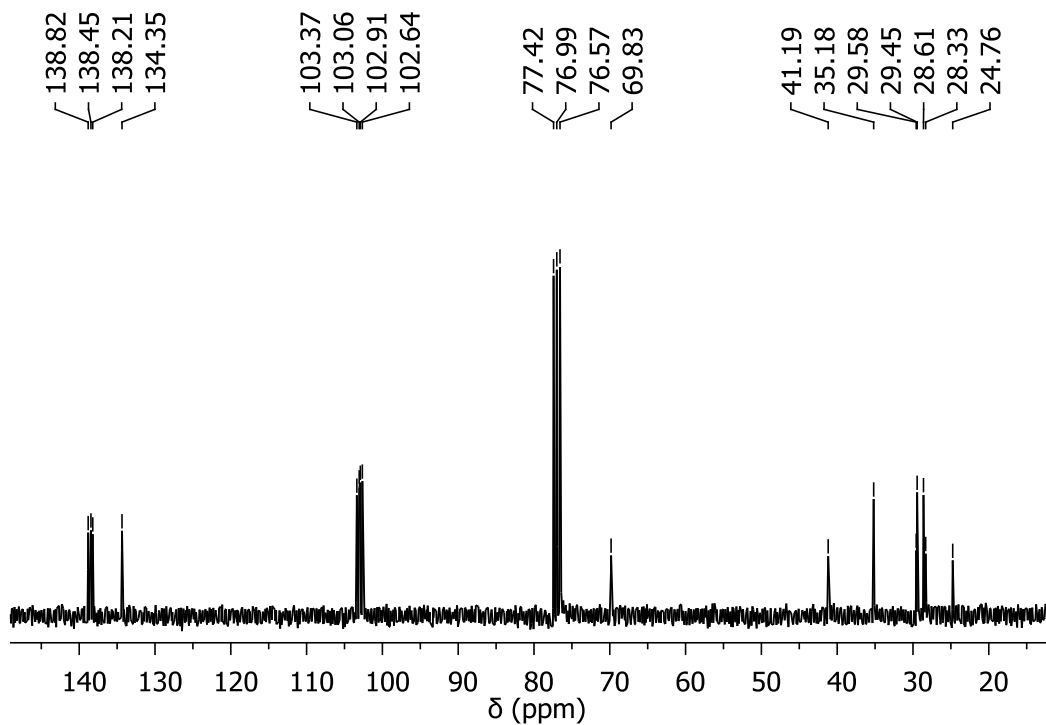


Figure A.13 : ^{13}C NMR spectrum of **3.17** recorded in CDCl_3 .

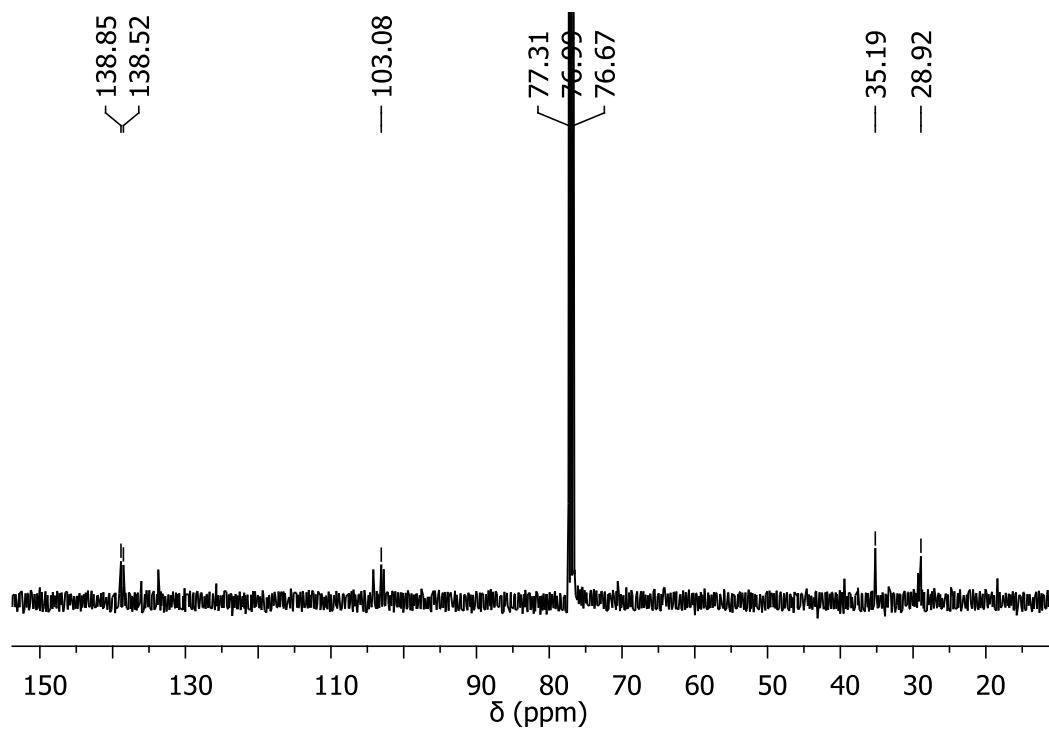


Figure A.14 : ^{13}C NMR spectrum of **3.18** recorded in CDCl_3 .

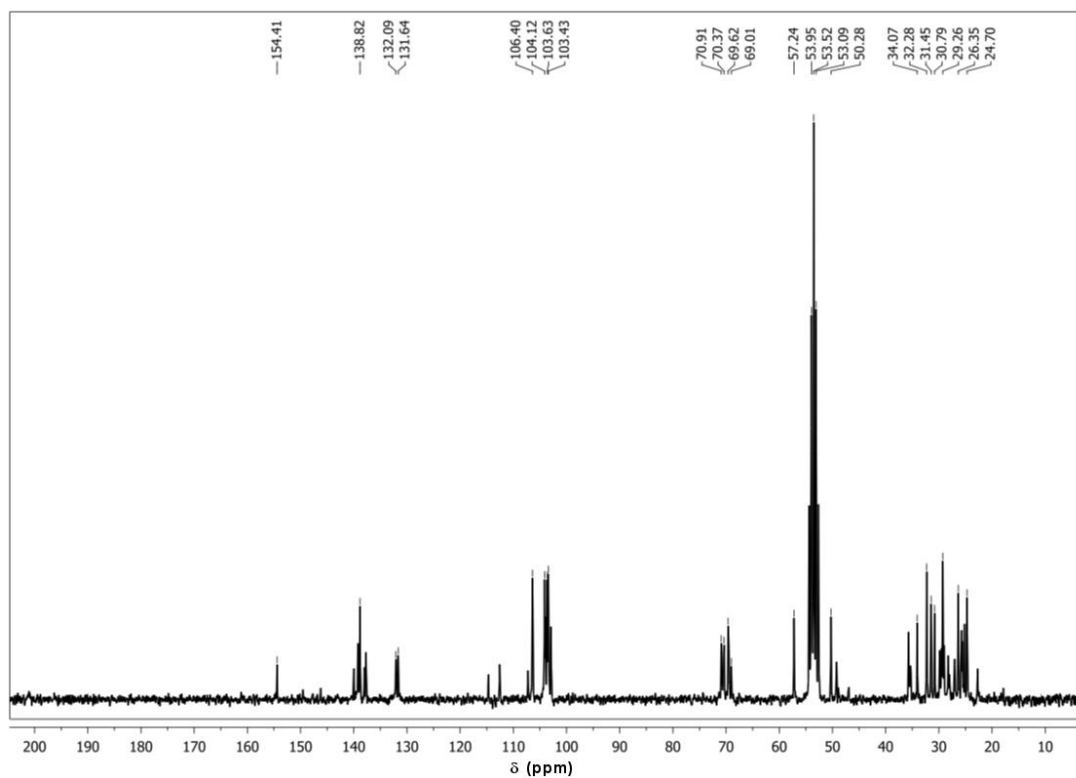


Figure A.15 : ^{13}C NMR spectrum of **3.25** recorded in CD_2Cl_2 .

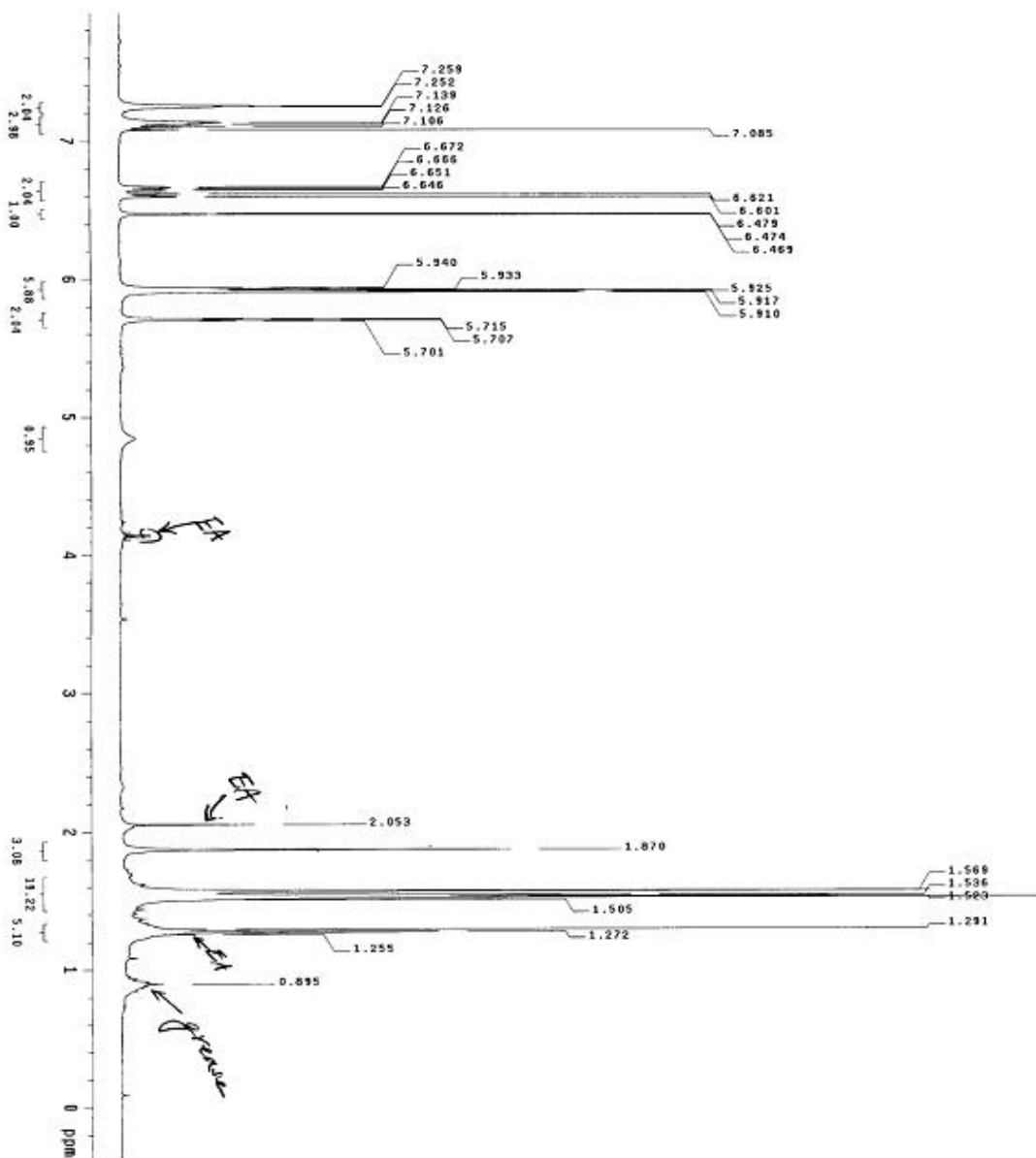


Figure A.16 : ¹H NMR spectrum of 3.26 recorded in CDCl₃.

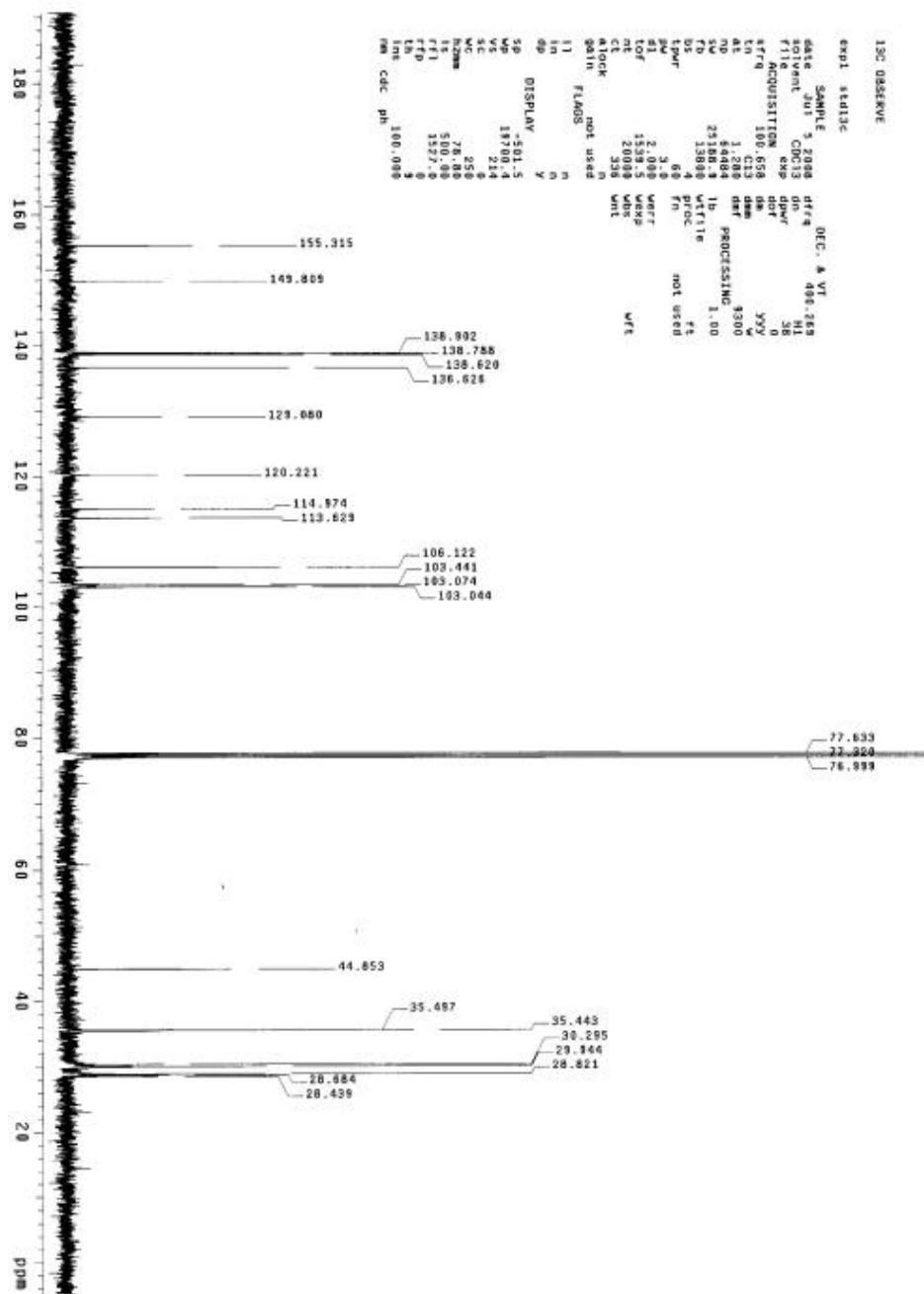


Figure A.17 : ^{13}C NMR spectrum of **3.26** recorded in CDCl_3 .

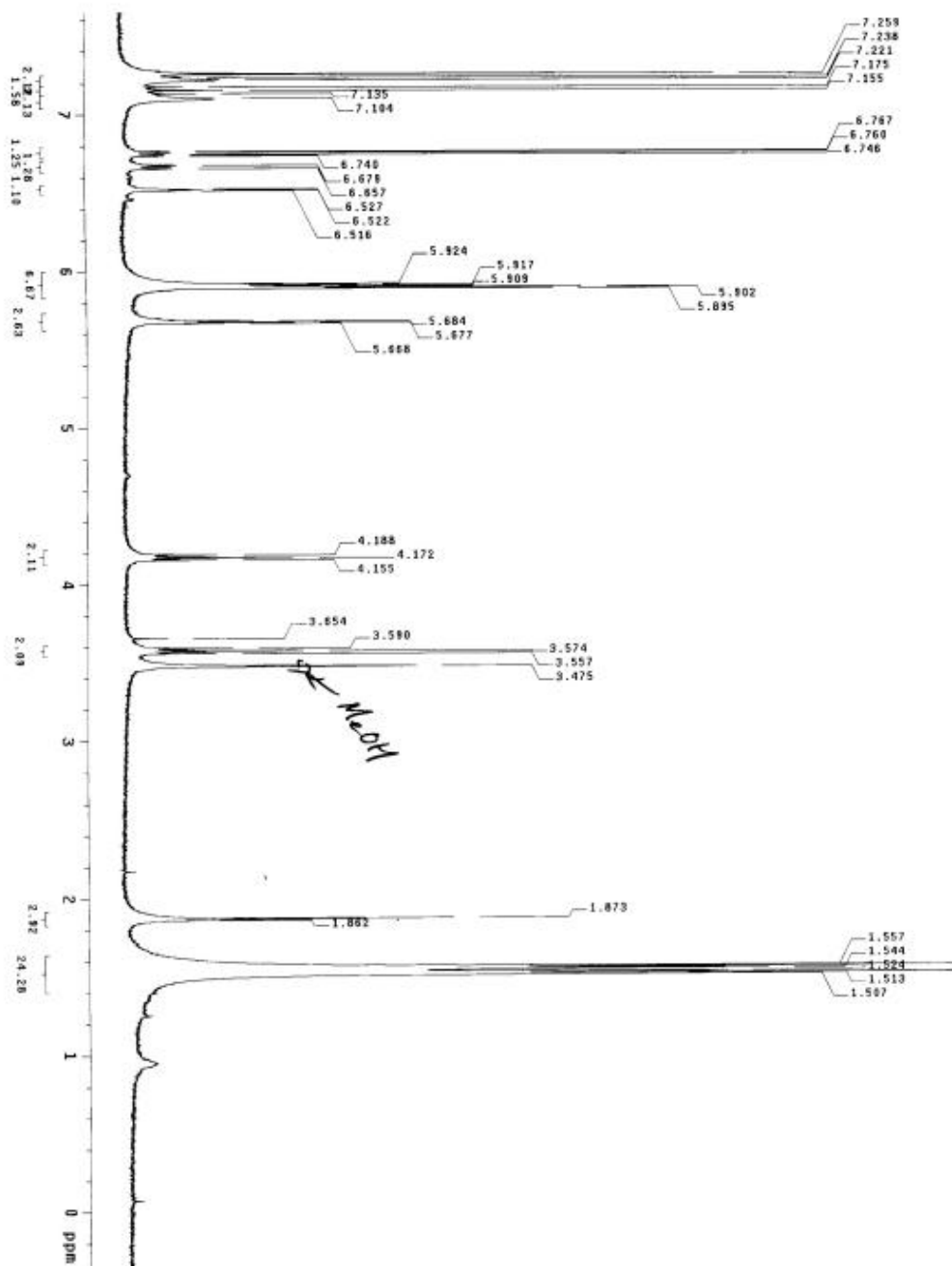


Figure A.18 : ^1H NMR spectrum of **3.27** recorded in CDCl_3 .

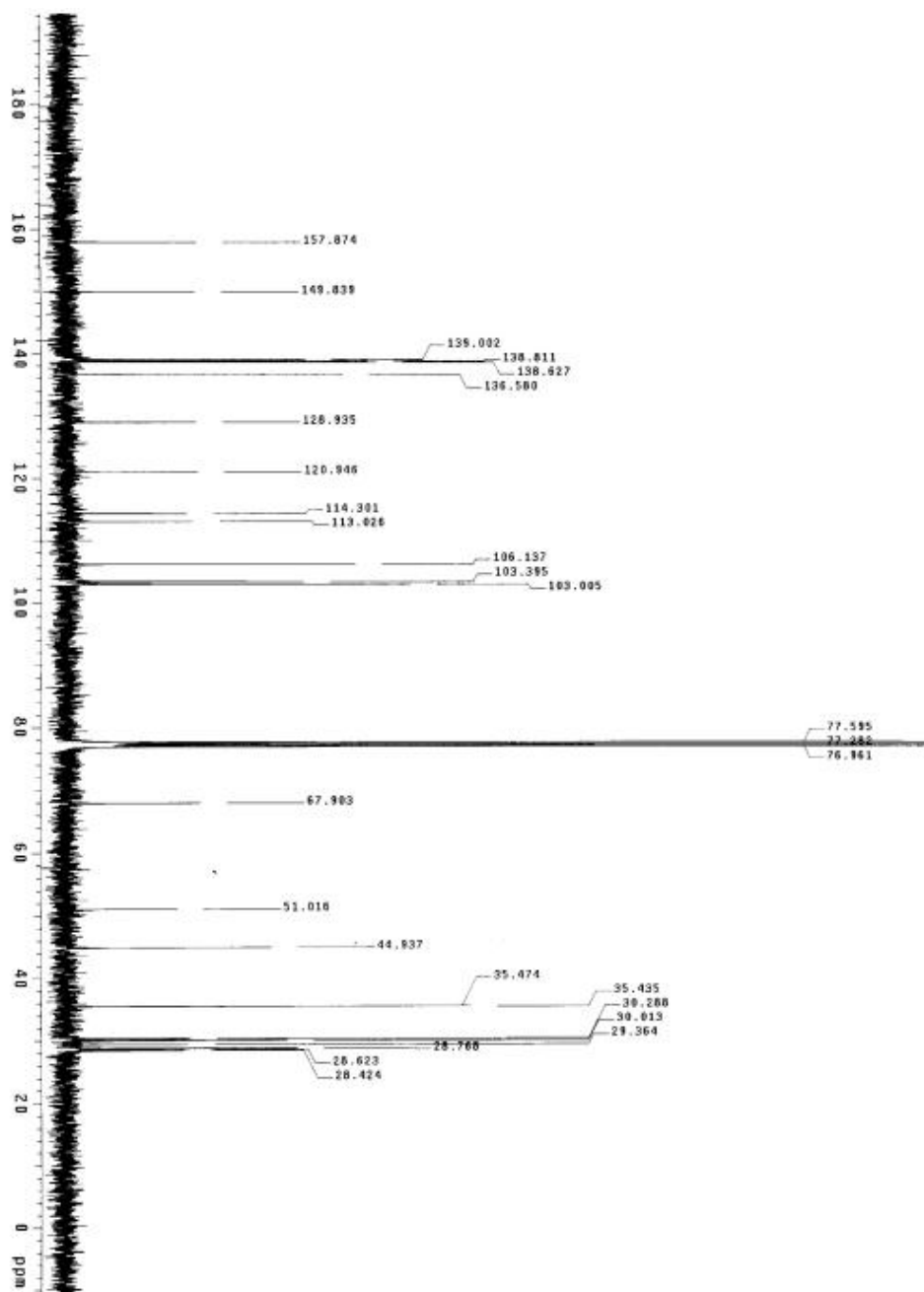


Figure A.19 : ^{13}C NMR spectrum of **3.27** recorded in CDCl_3 .

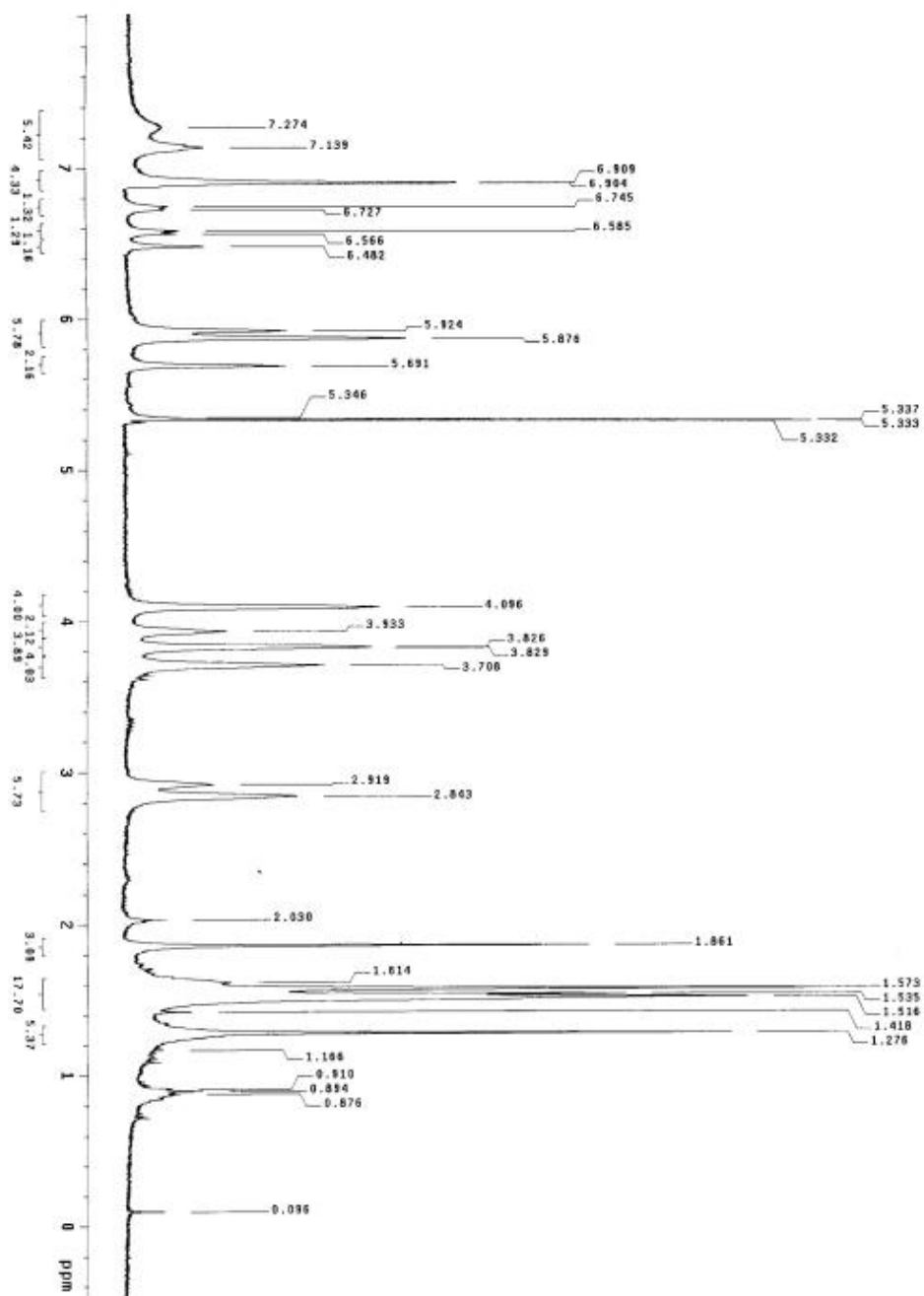


Figure A.20 : ^1H NMR spectrum of **3.28** recorded in CDCl_3 .

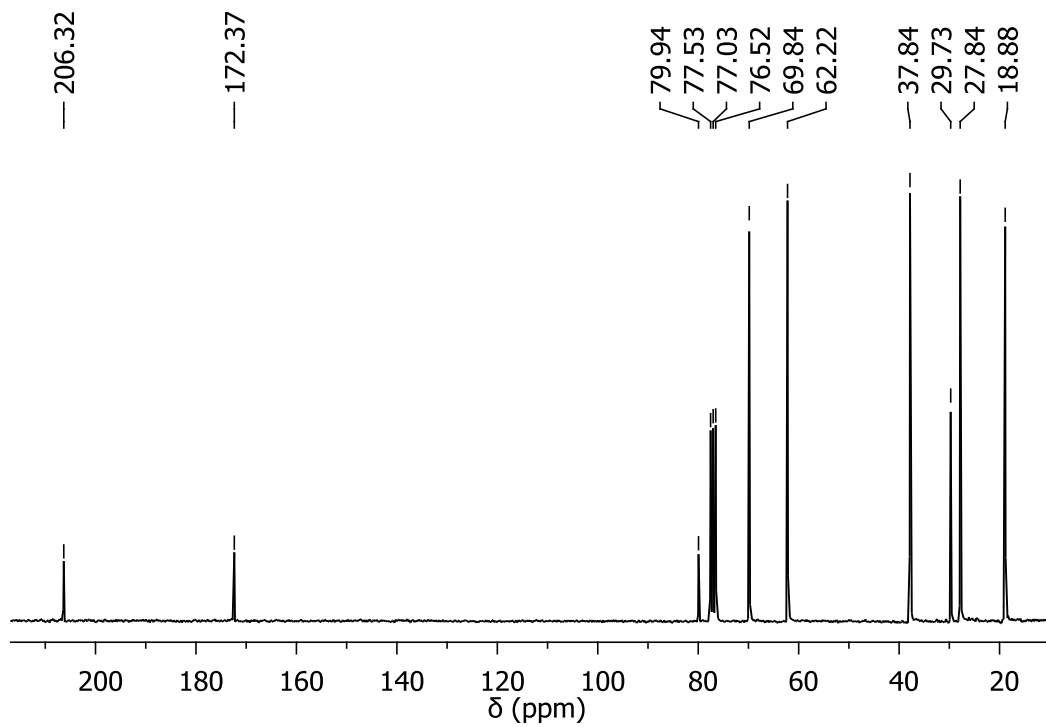


Figure A.22 : ^{13}C NMR spectrum of **3.29** recorded in CDCl_3 .

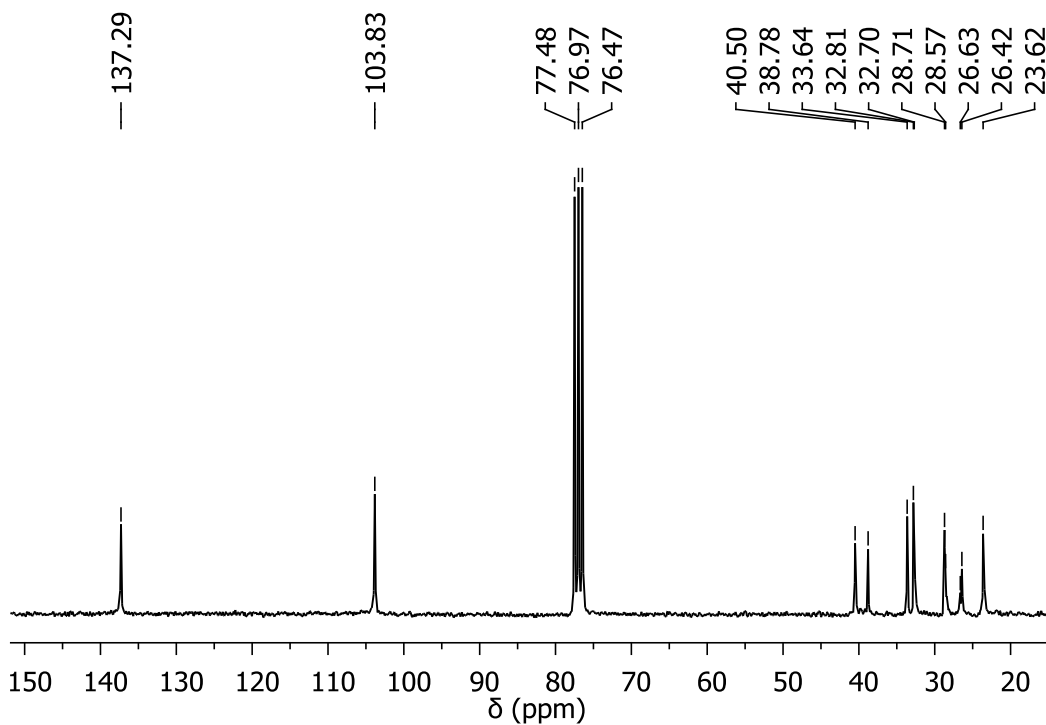


Figure A.23 : ^{13}C NMR spectrum of **3.31** recorded in CDCl_3 .

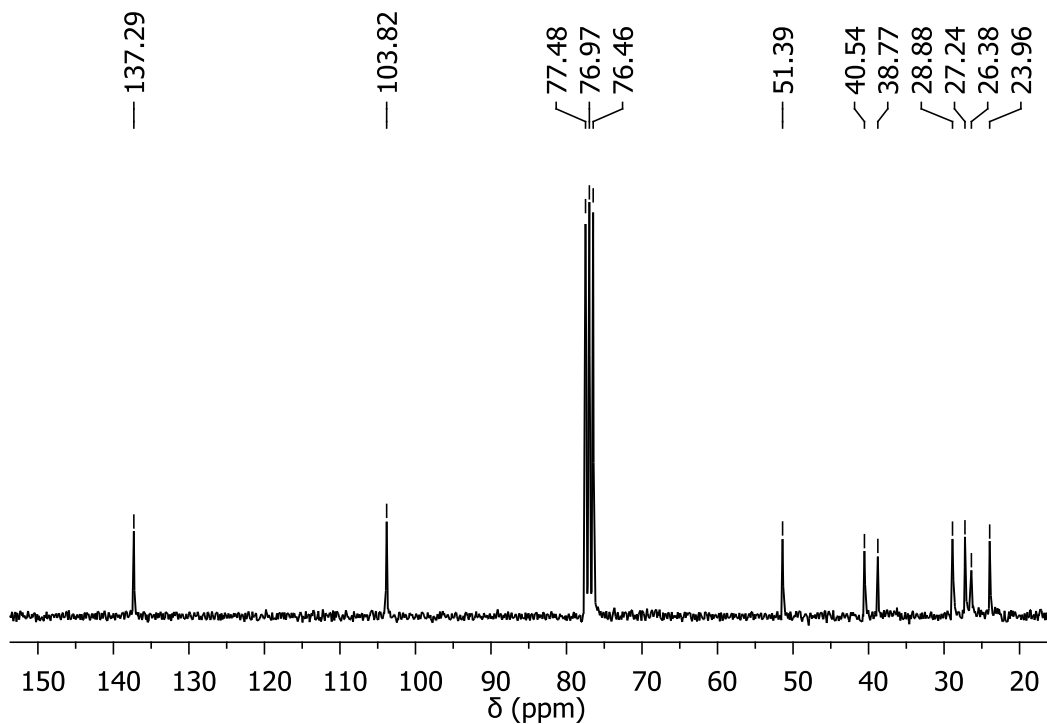


Figure A.24 : ^{13}C NMR spectrum of **3.32** recorded in CDCl_3 .

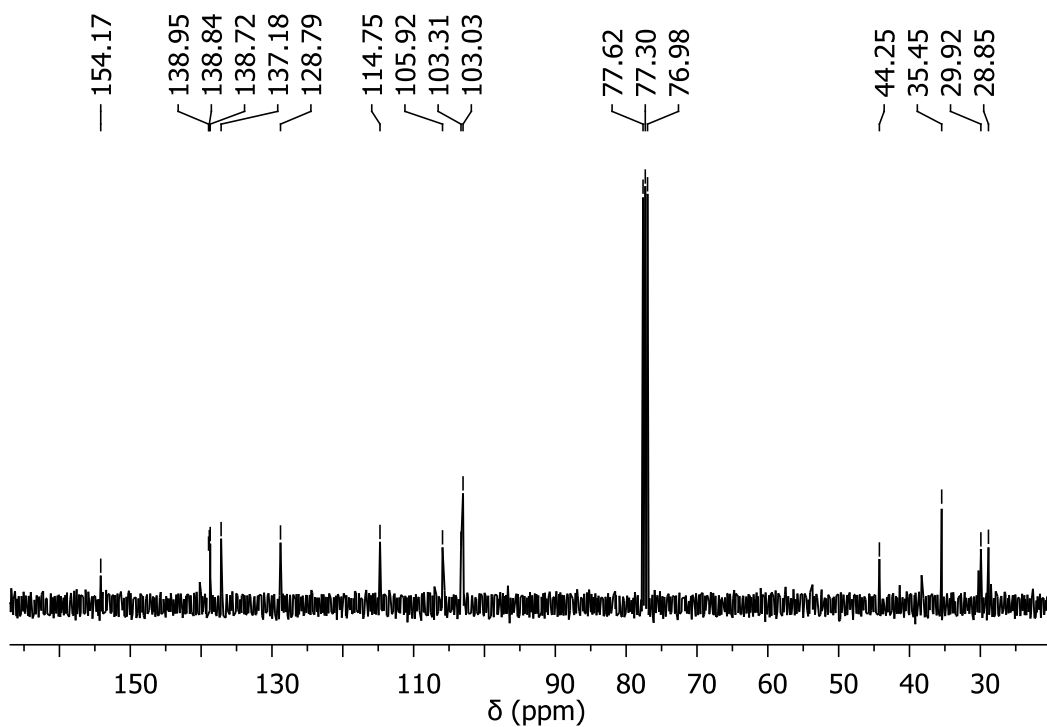


Figure A.25 : ^{13}C NMR spectrum of **3.33** recorded in CDCl_3 .

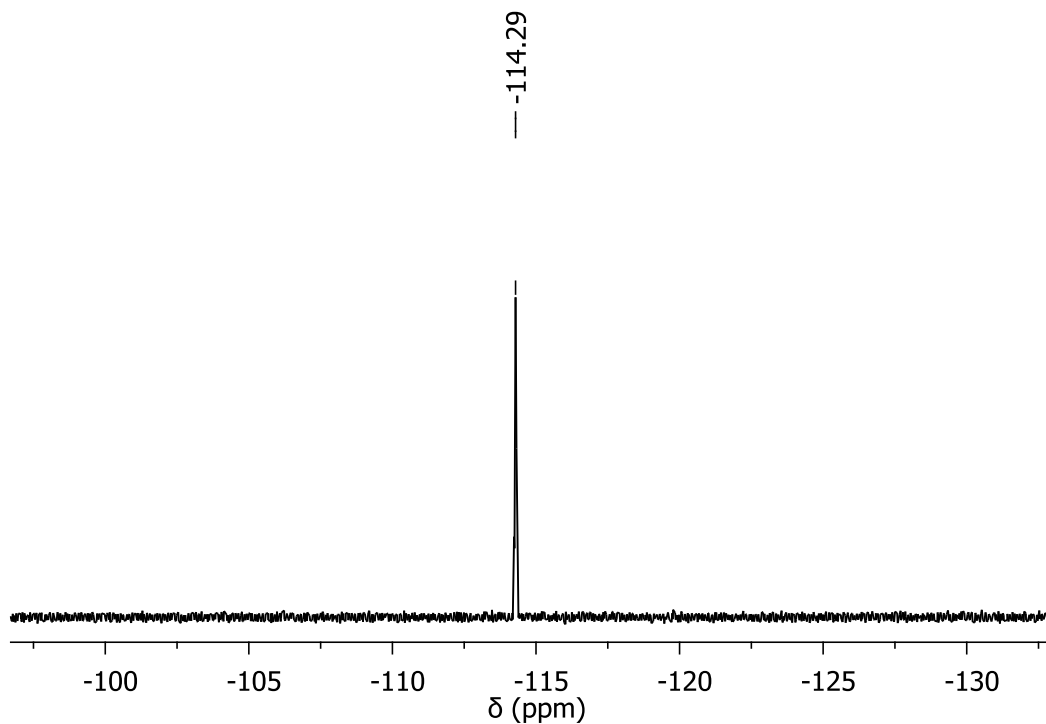


Figure A.26 : ^{19}F NMR spectrum of fluorobenzene in CD_2Cl_2 .

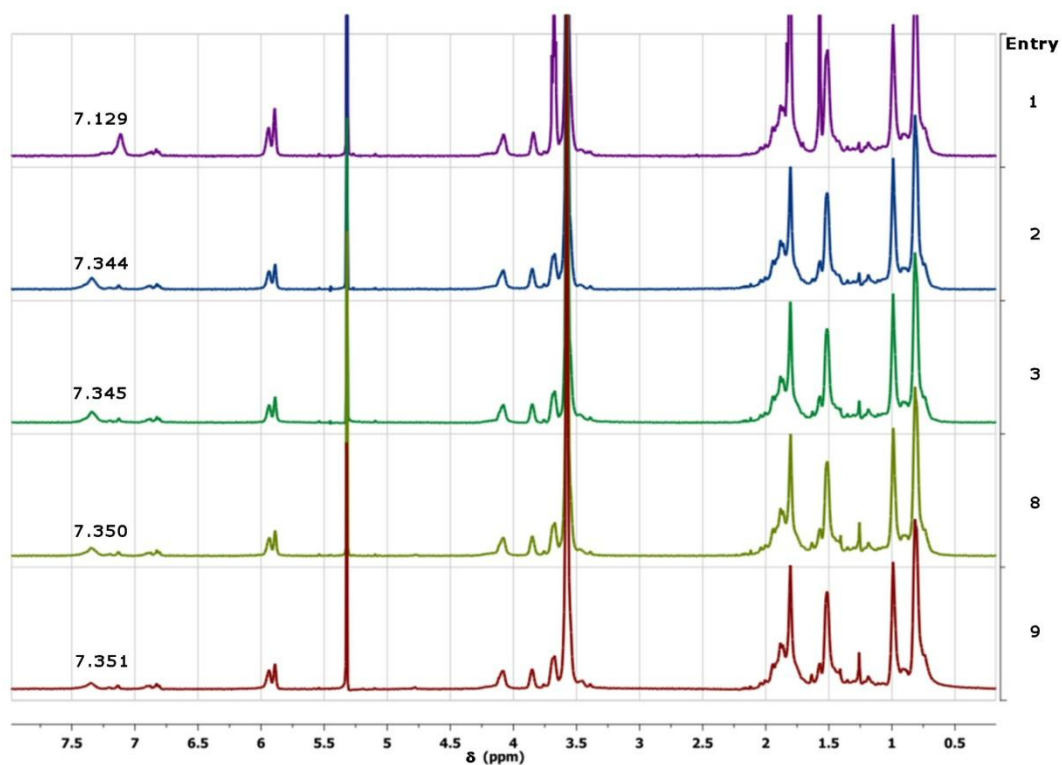


Figure A.27 : ^1H NMR spectra of copolymer **3.22** in CD_2Cl_2 recorded after exposure to different aqueous KF concentrations.

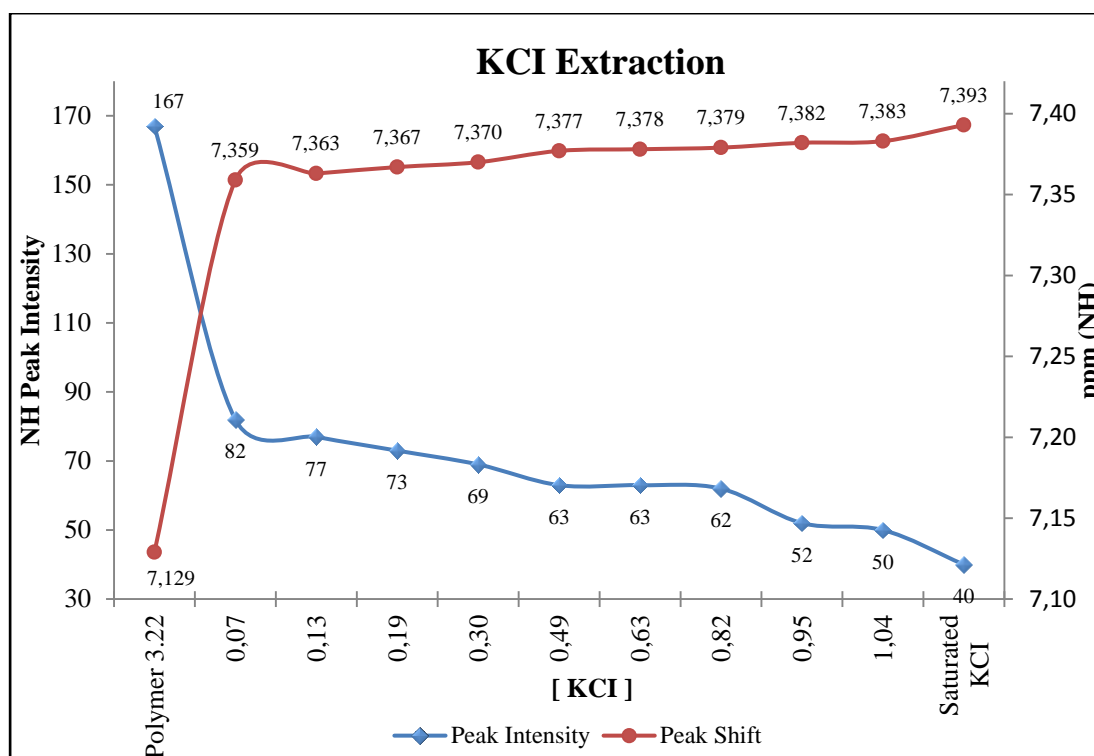


Figure A.28 : NH peak intensity and shifts of copolymer **3.22** in CD_2Cl_2 as recorded by ^1H NMR spectroscopy after exposure to different aqueous KCl concentrations (mM).

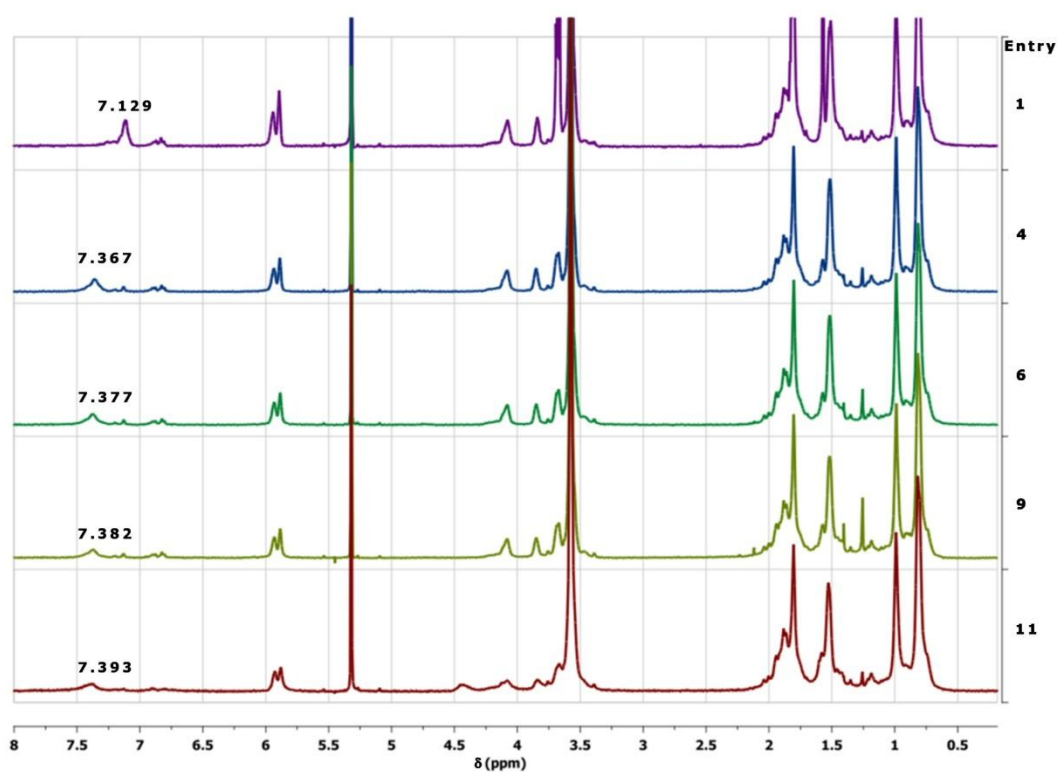


Figure A.29 : ^1H NMR spectra of copolymer **3.22** in CD_2Cl_2 recorded after exposure to different aqueous KCl concentrations.

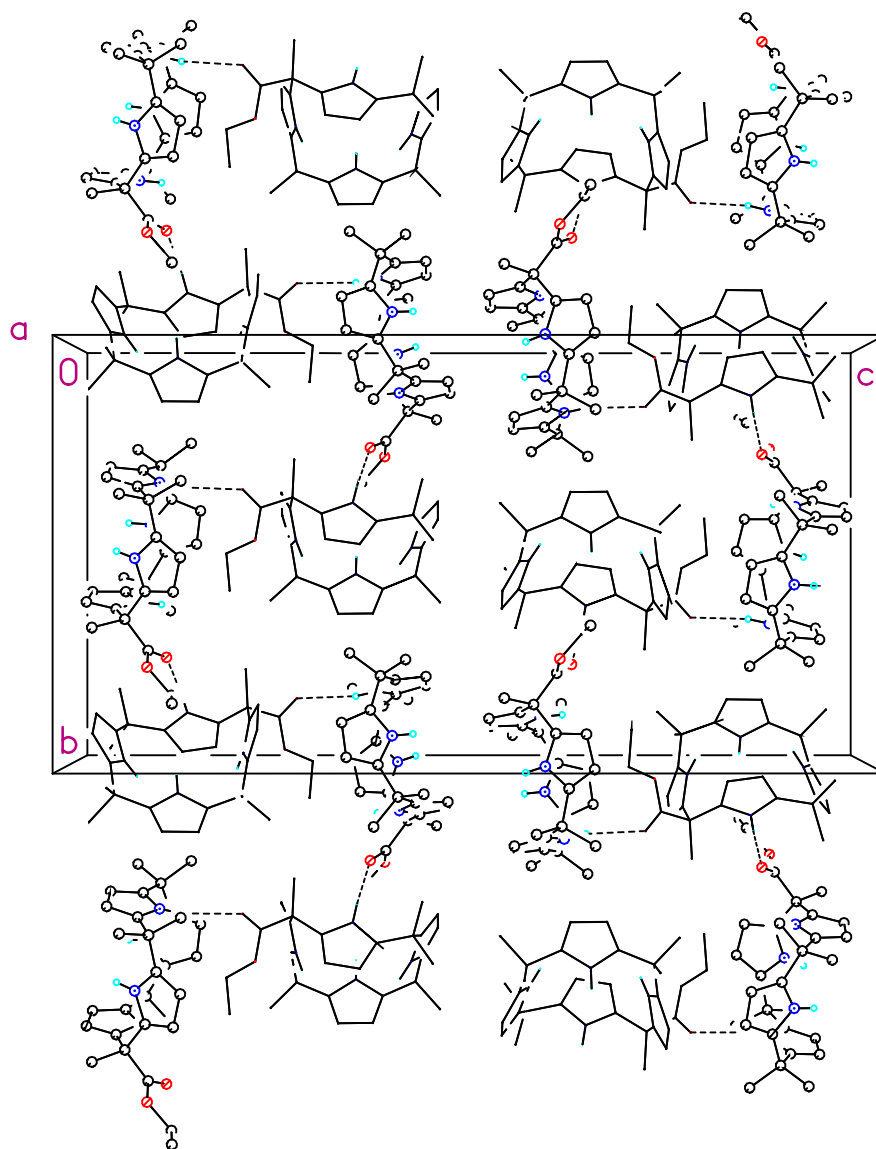


Figure A.30 : Unit cell packing diagram for **3.1**. The view is approximately down the *a* axis. Molecules **3.1a** are shown in ball-and-stick format while molecules **3.1b** are in wireframe display format. Dashed lines are indicative of H-bonding interactions.

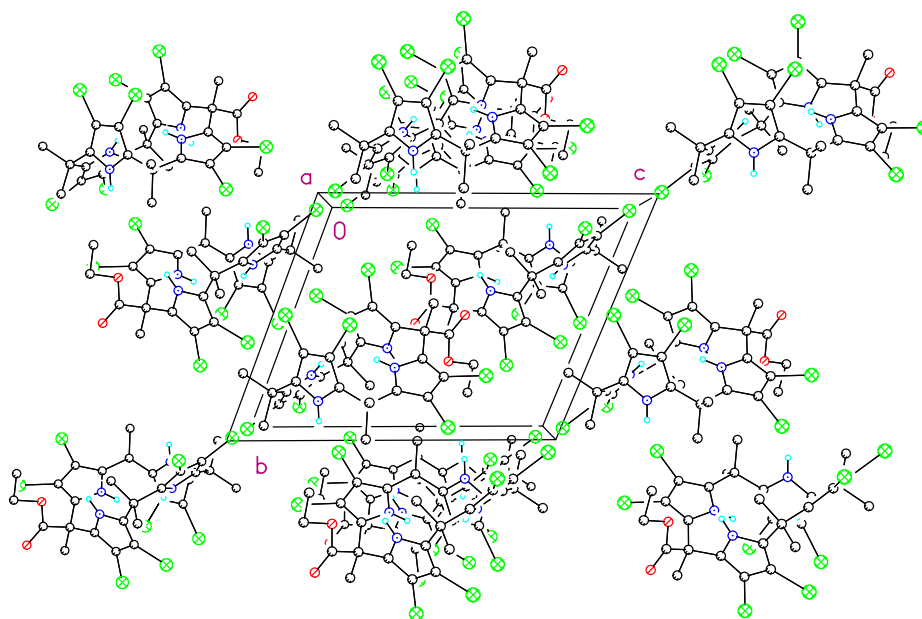


Figure A.31 : Unit cell packing diagram for **3.2**. The view is approximately down the *a* axis.

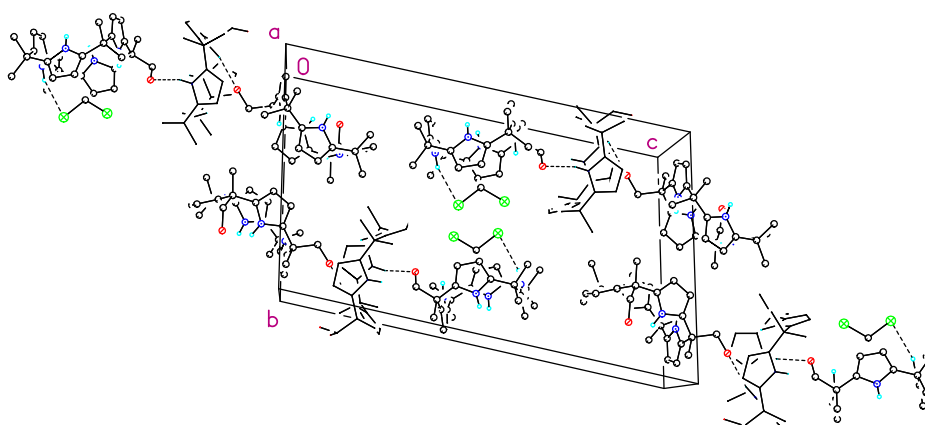


Figure A.32 : Unit cell packing diagram for **3.17**. The view is approximately down the *a* axis.

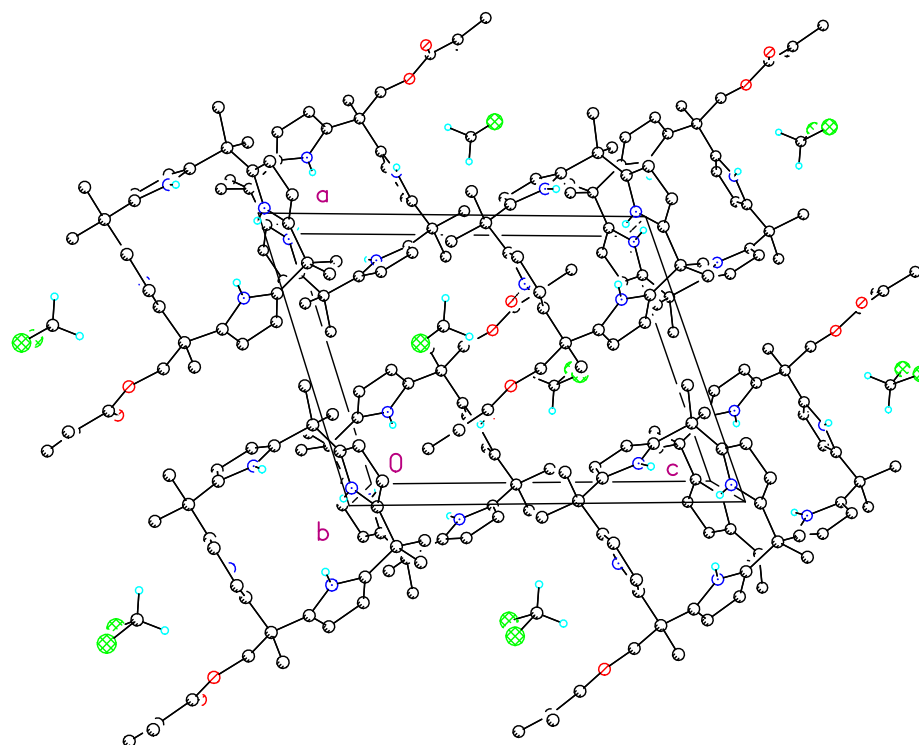


Figure A.33 : Unit cell packing diagram for **3.8**. The view is approximately down the *b* axis.

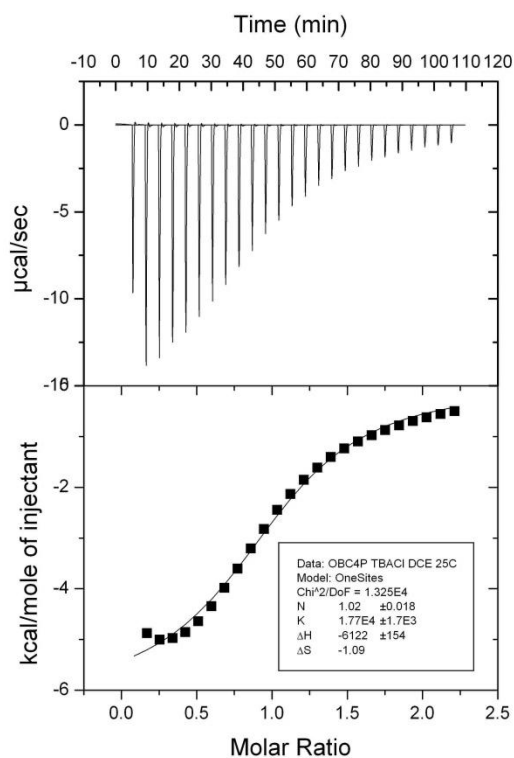


Figure A.34 : ITC titration curves obtained from the titration of compound **2.20** (0.4 mM) with chloride anion (8 mM) in CH_2Cl_2 at 25 °C. The curve shows the fit of the experimental data to 1:1 binding profile.

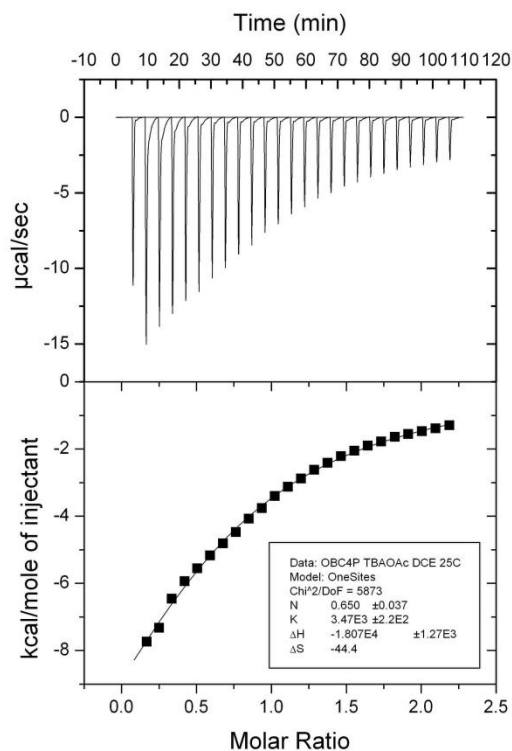


Figure A.35 : ITC titration curves obtained from the titration of compound **2.20** (0.40 mM) with acetate anion (7.91 mM) in CH₂Cl₂ at 25 °C. The curve shows the fit of the experimental data to 1:1 binding profile.

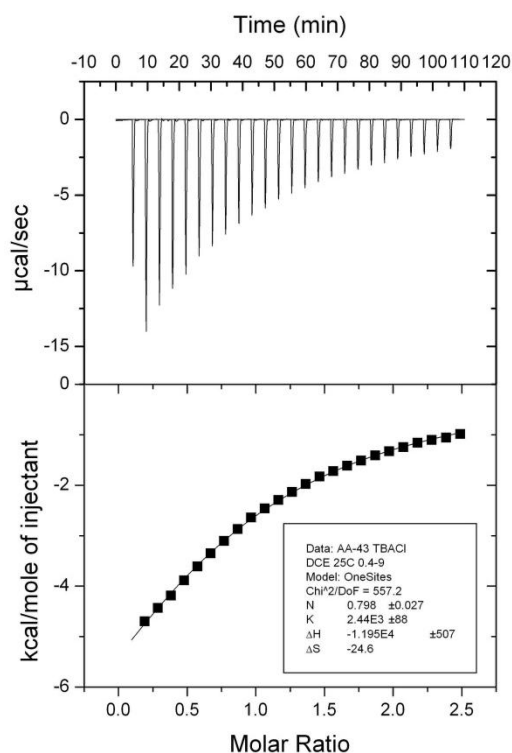


Figure A.36 : ITC titration curves obtained from the titration of compound **2.14** (0.4 mM) with chloride anion (9 mM) in CH₂Cl₂ at 25 °C. The curve shows the fit of the experimental data to 1:1 binding profile.

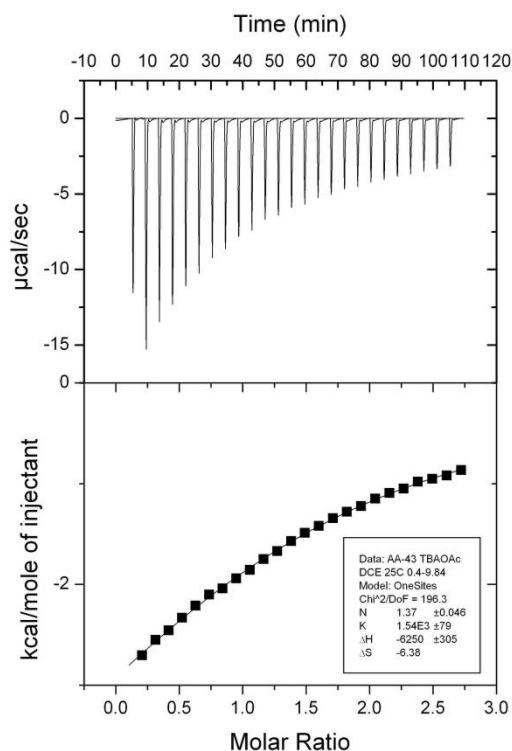


Figure A.37 : ITC titration curves obtained from the titration of compound **2.14** (0.40 mM) with acetate anion (9.84 mM) in CH_2Cl_2 at 25 °C. The curve shows the fit of the experimental data to 1:1 binding profile.

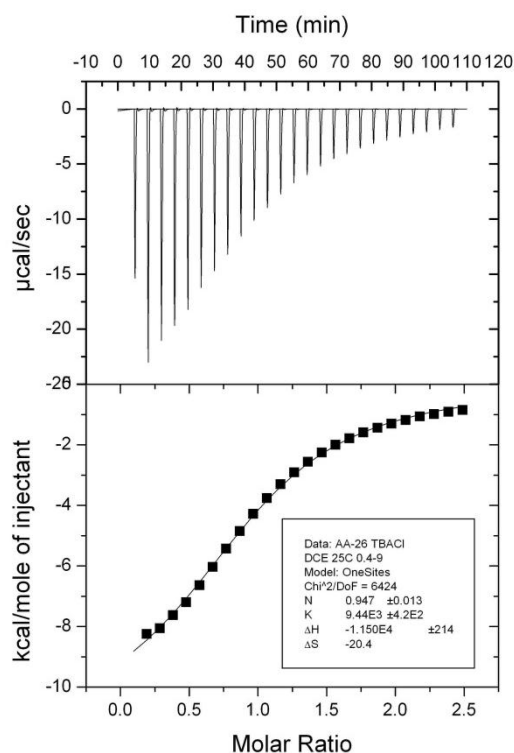


Figure A.38 : ITC titration curves obtained from the titration of compound **3.1** (0.412 mM) with chloride anion (9 mM) in CH_2Cl_2 at 25 °C. The curve shows the fit of the experimental data to 1:1 binding profile.

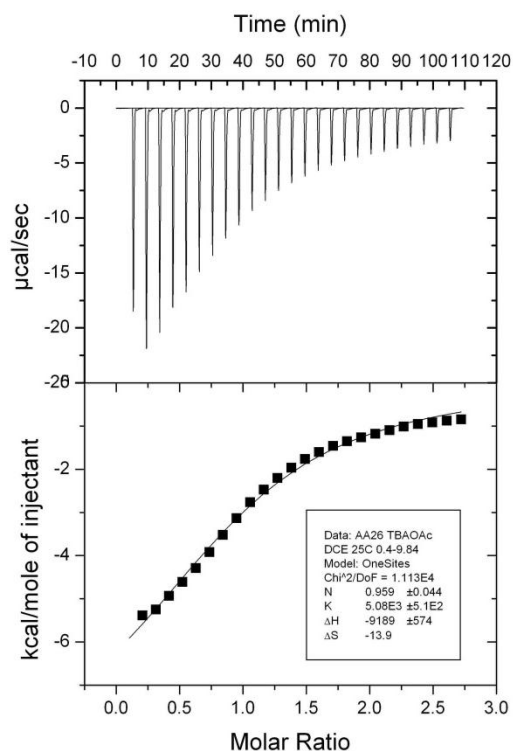


Figure A.39 : ITC titration curves obtained from the titration of compound **3.1** (0.403 mM) with acetate anion (9.840 mM) in CH_2Cl_2 at 25 °C. The curve shows the fit of the experimental data to 1:1 binding profile.

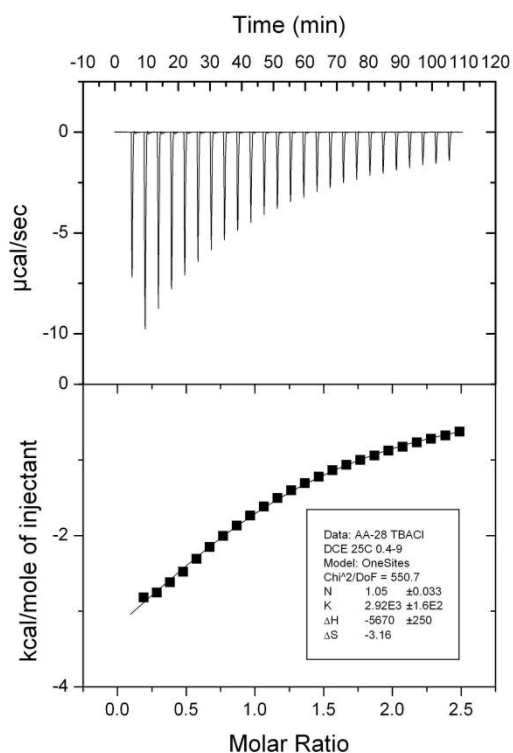


Figure A.40 : ITC titration curves obtained from the titration of compound **3.2** (0.4 mM) with chloride anion (9 mM) in CH_2Cl_2 at 25 °C. The curve shows the fit of the experimental data to 1:1 binding profile.

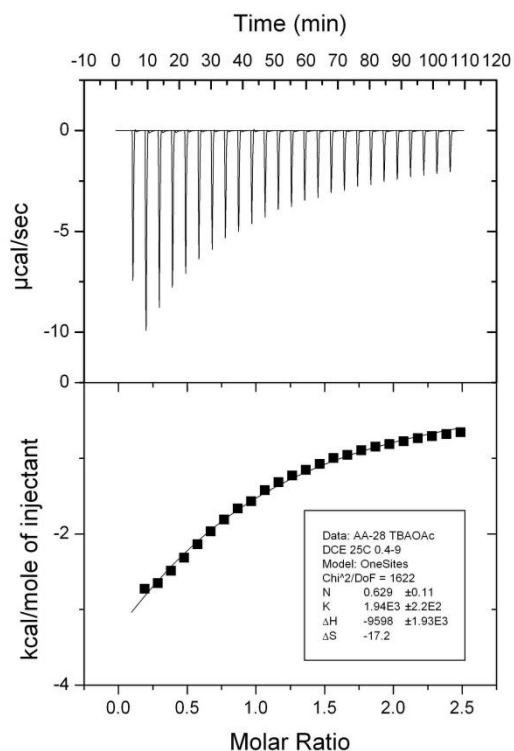


Figure A.41 : ITC titration curves obtained from the titration of compound **3.2** (0.4 mM) with acetate anion (9 mM) in CH_2Cl_2 at 25 °C. The curve shows the fit of the experimental data to 1:1 binding profile.

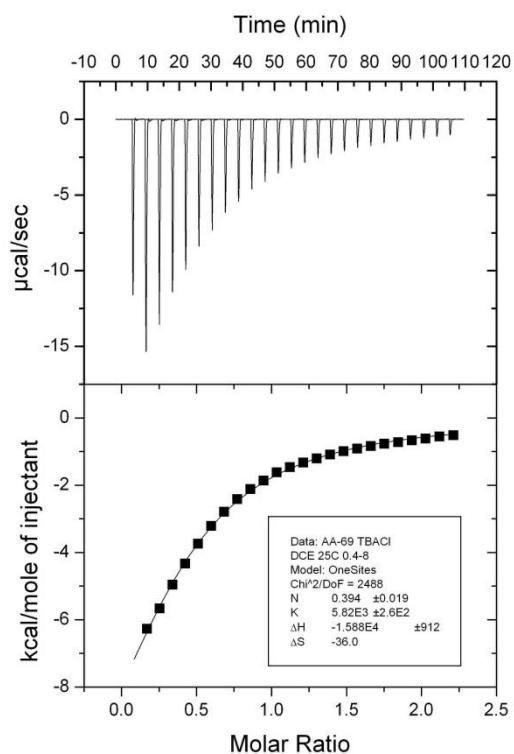


Figure A.42 : ITC titration curves obtained from the titration of compound **3.7** (0.4 mM) with chloride anion (8 mM) in CH_2Cl_2 at 25 °C. The curve shows the fit of the experimental data to 1:1 binding profile.

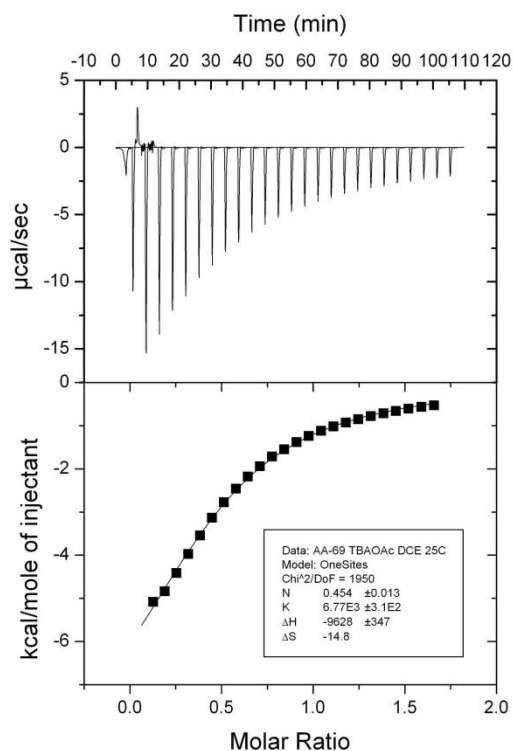


Figure A.43 : ITC titration curves obtained from the titration of compound **3.7** (0.5 mM) with acetate anion (7.5 mM) in CH_2Cl_2 at 25 °C. The curve shows the fit of the experimental data to 1:1 binding profile.

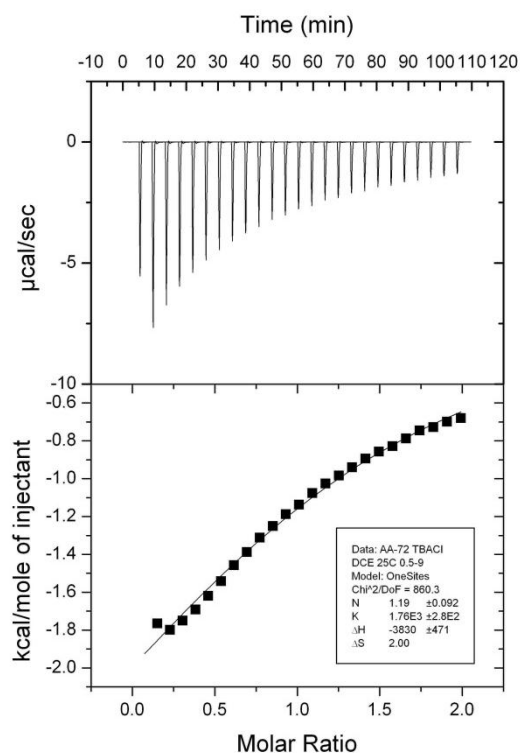


Figure A.44 : ITC titration curves obtained from the titration of compound **3.8** (0.5 mM) with chloride anion (9 mM) in CH_2Cl_2 at 25 °C. The curve shows the fit of the experimental data to 1:1 binding profile.

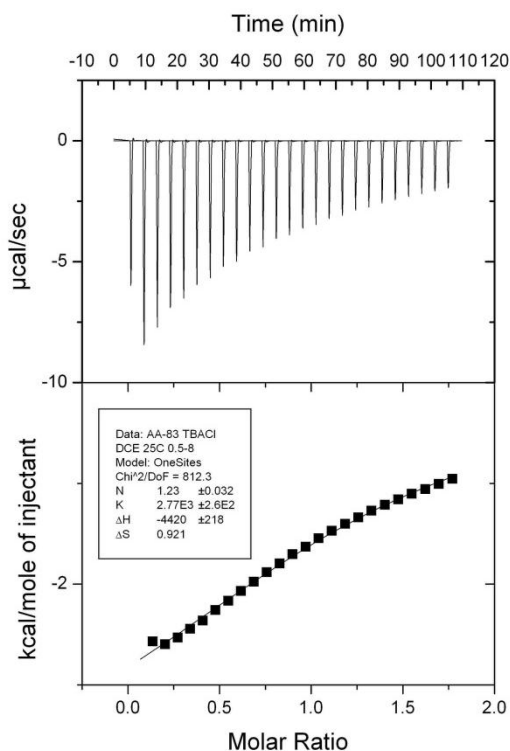


Figure A.45 : ITC titration curves obtained from the titration of compound **3.6** (0.5 mM) with chloride anion (8 mM) in CH_2Cl_2 at 25 °C. The curve shows the fit of the experimental data to 1:1 binding profile.

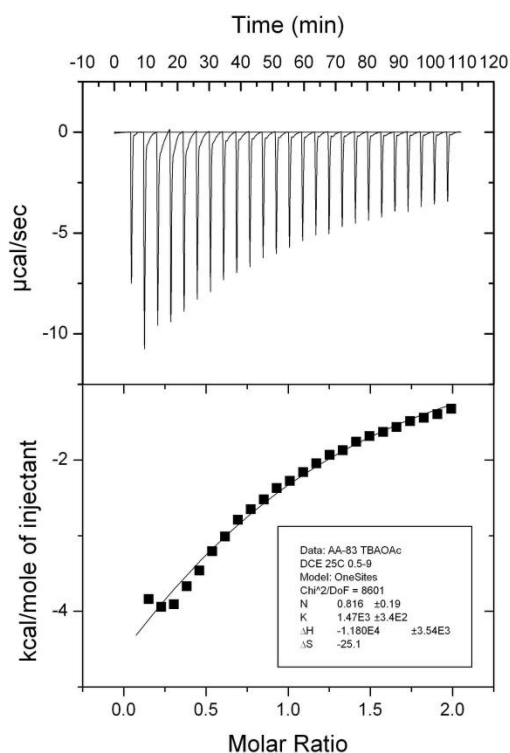


Figure A.46 : ITC titration curves obtained from the titration of compound **3.6** (0.5 mM) with acetate anion (9 mM) in CH_2Cl_2 at 25 °C. The curve shows the fit of the experimental data to 1:1 binding profile.

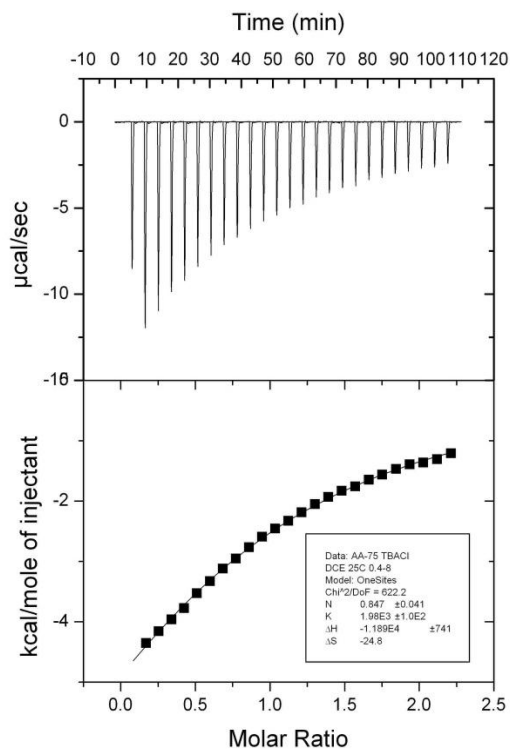


Figure A.47 : ITC titration curves obtained from the titration of compound **3.9** (0.4 mM) with chloride anion (8 mM) in CH_2Cl_2 at 25 °C. The curve shows the fit of the experimental data to 1:1 binding profile.

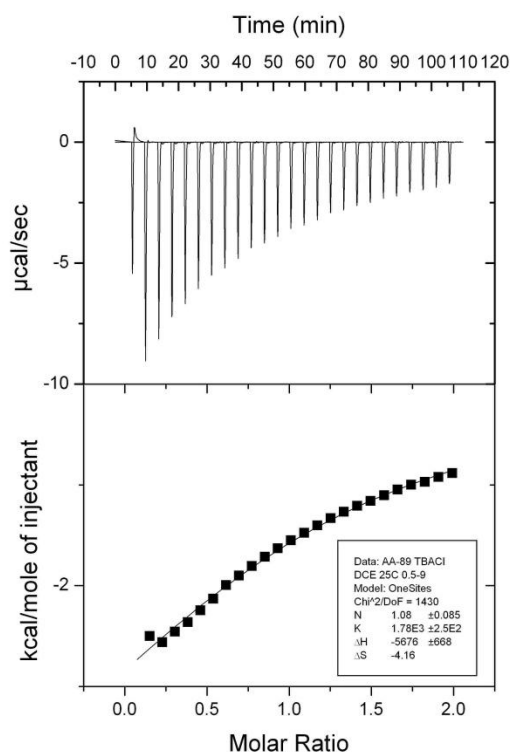


Figure A.48 : ITC titration curves obtained from the titration of compound **3.10** (0.5 mM) with chloride anion (9 mM) in CH_2Cl_2 at 25 °C. The curve shows the fit of the experimental data to 1:1 binding profile.

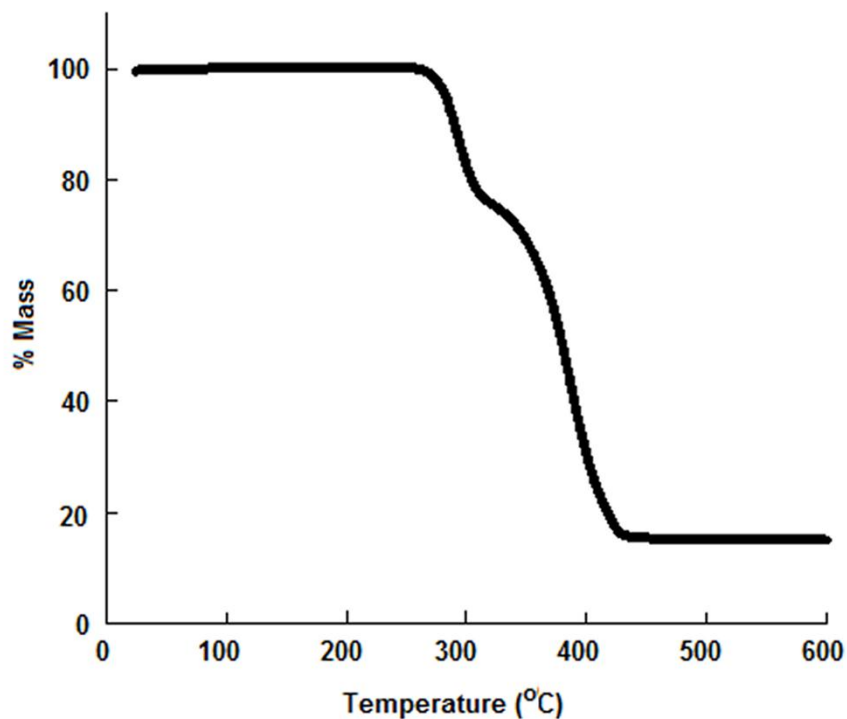


Figure A.49 : Thermogravigram of a PMMA homopolymer taken under an atmosphere of nitrogen at a scan rate = 10 °C/min.

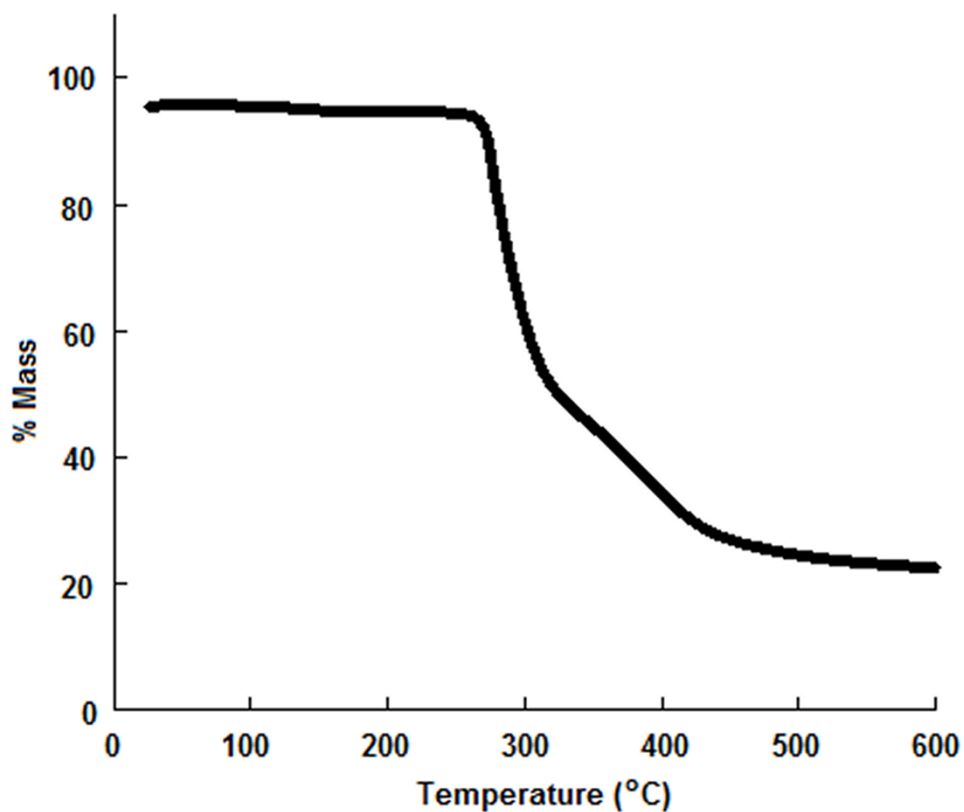


Figure A.50 : Thermogravigram of a polymer 3.19 taken under an atmosphere of nitrogen at a scan rate = 10 °C/min.

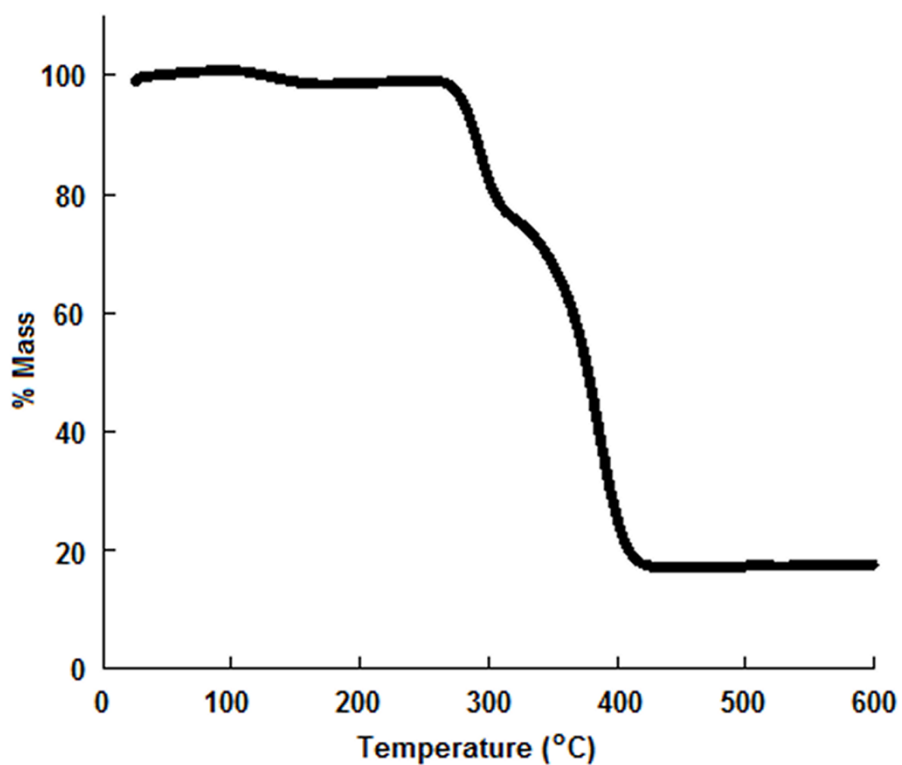


Figure A.51 : Thermogravigram of a PMMA homopolymer (control), after being exposed to TBAF as described in the text, taken under an atmosphere of nitrogen at a scan rate = 10 °C/min.

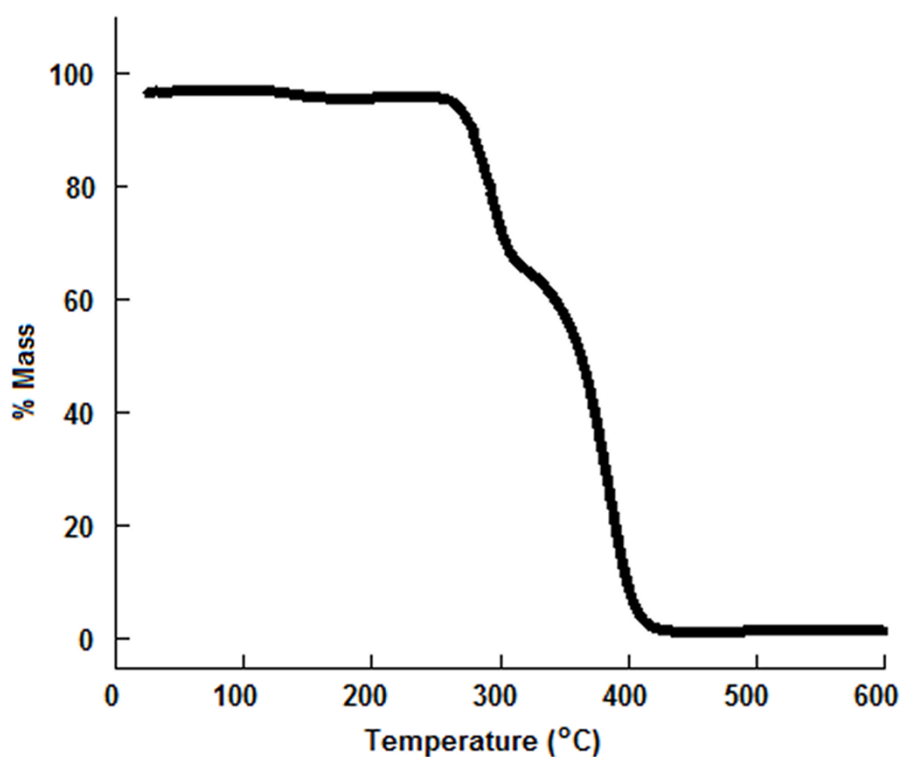


Figure A.52 : Thermogravigram of a PMMA homopolymer (control), after being exposed to TBACl as described in the text, taken under an atmosphere of nitrogen at a scan rate = 10 °C/min.

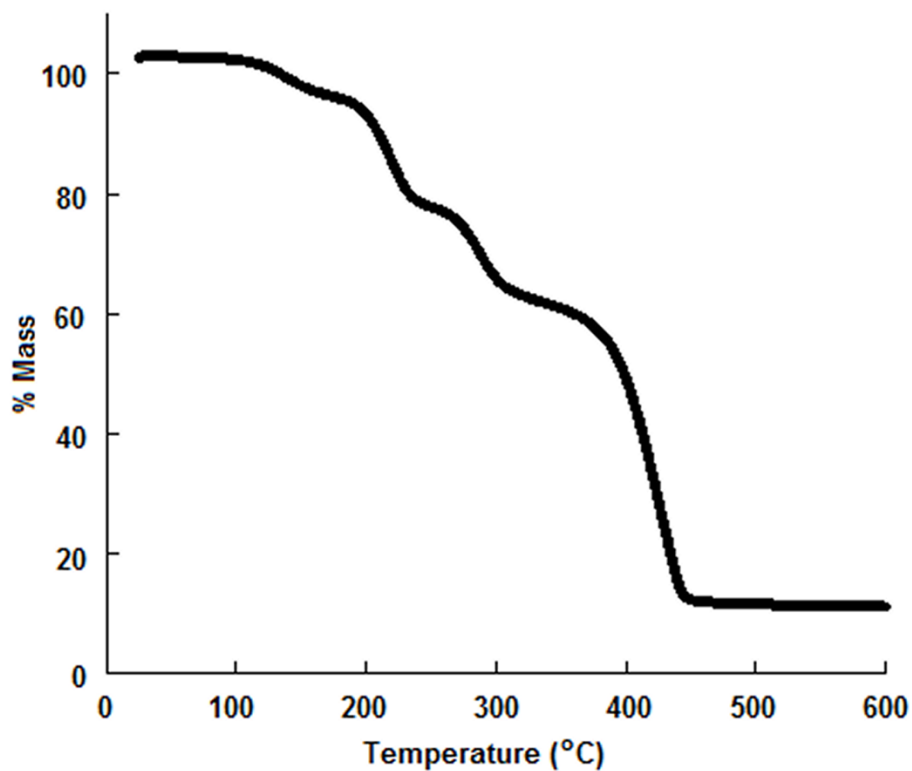


Figure A.53 : Thermogravigram of copolymer **3.20**, after being exposed to TBACl as described in the text, taken under an atmosphere of nitrogen at a scan rate = 10 °C/min.

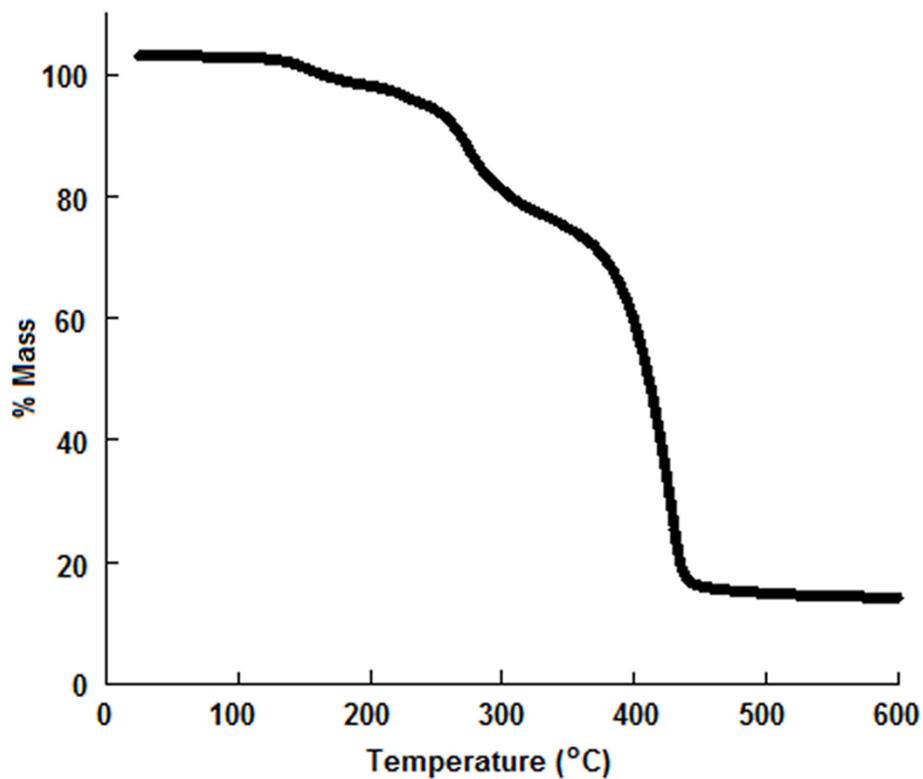


Figure A.54 : Thermogravigram of copolymer **3.20**, after being exposed to TBAF as described in the text, taken under an atmosphere of nitrogen at a scan rate = 10 °C/min.

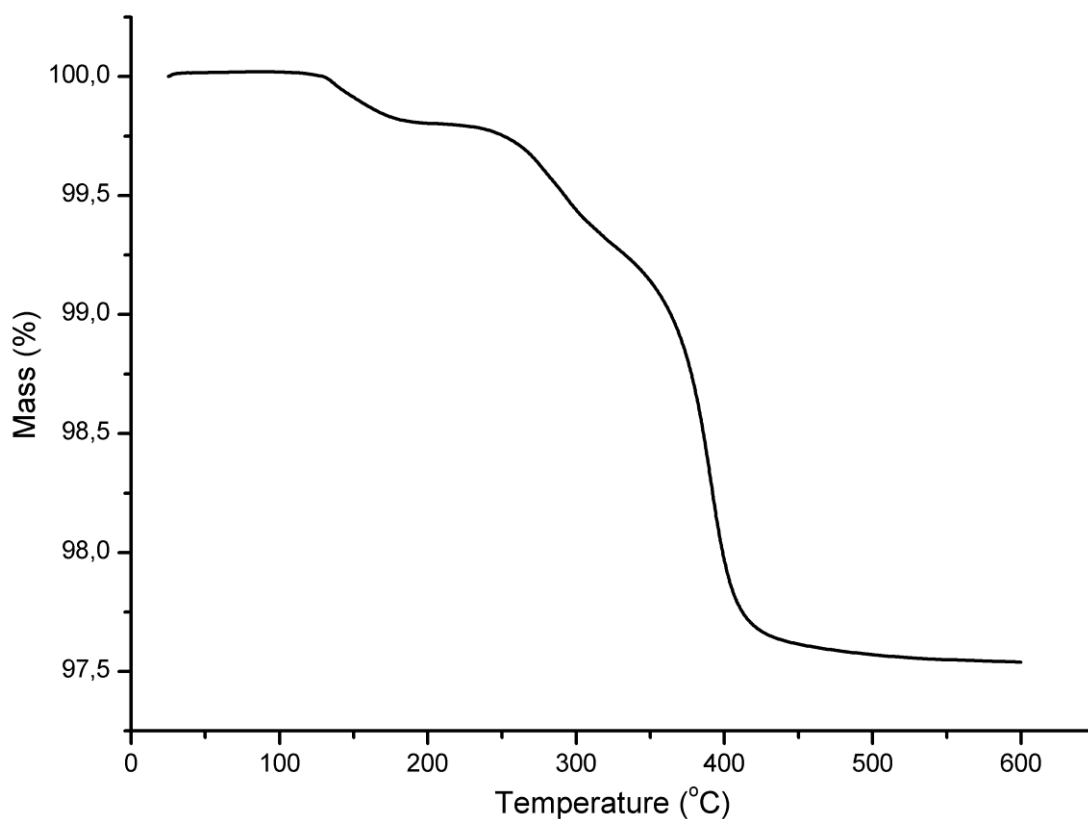


Figure A.55 : Thermogravigram of polymer **3.20** taken under an atmosphere of nitrogen at a scan rate = 10 °C/min after exposing to KCl.

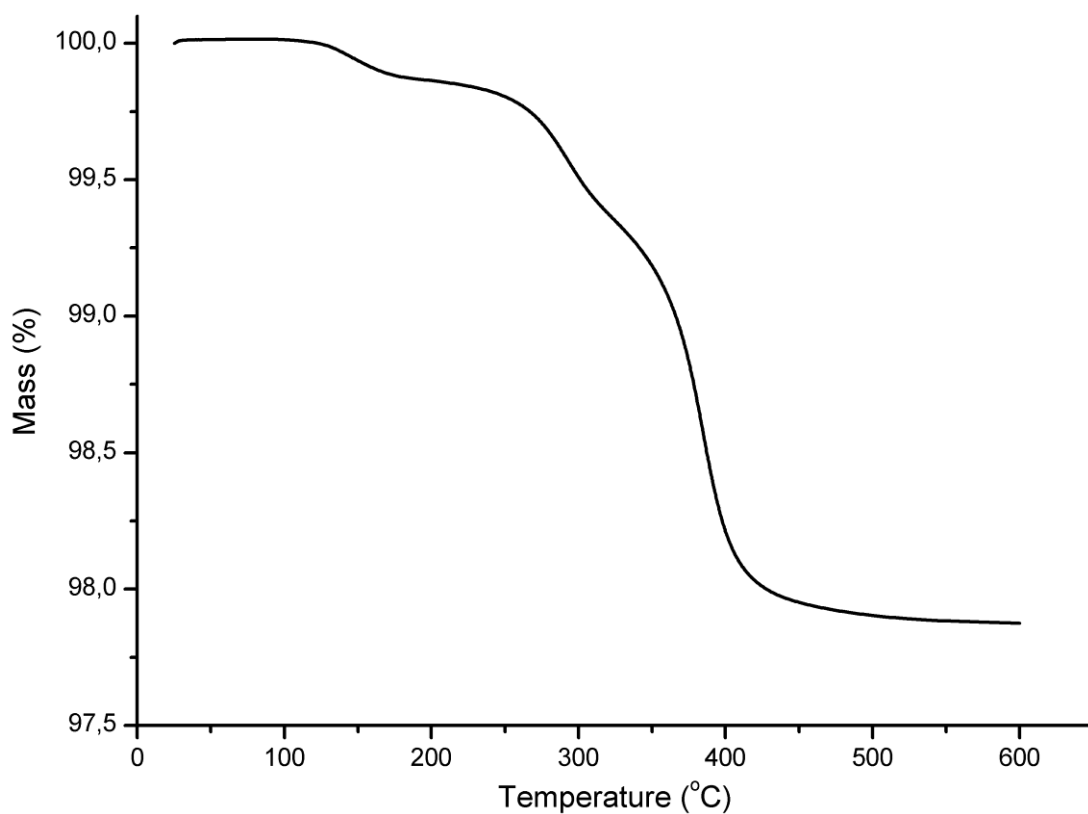


Figure A.56 : Thermogravigram of polymer **3.20** taken under an atmosphere of nitrogen at a scan rate = 10 °C/min after exposing to KF.

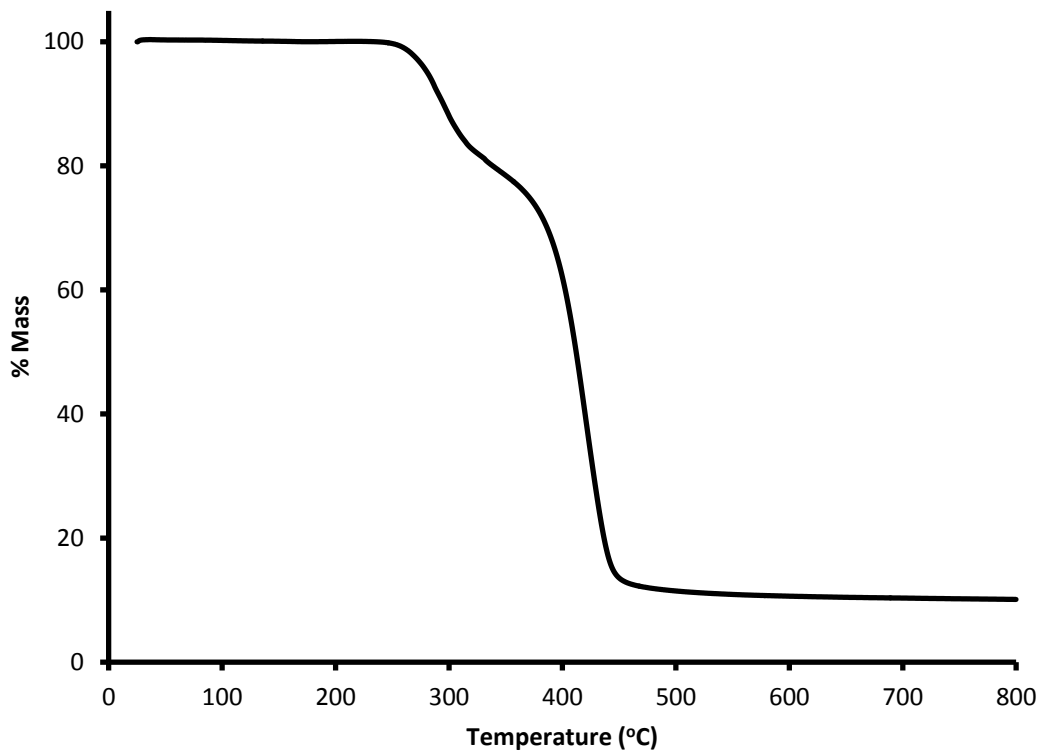


Figure A.57 : Thermogravigram of polymer **3.22** taken under an atmosphere of nitrogen at a scan rate = 10 °C/min.

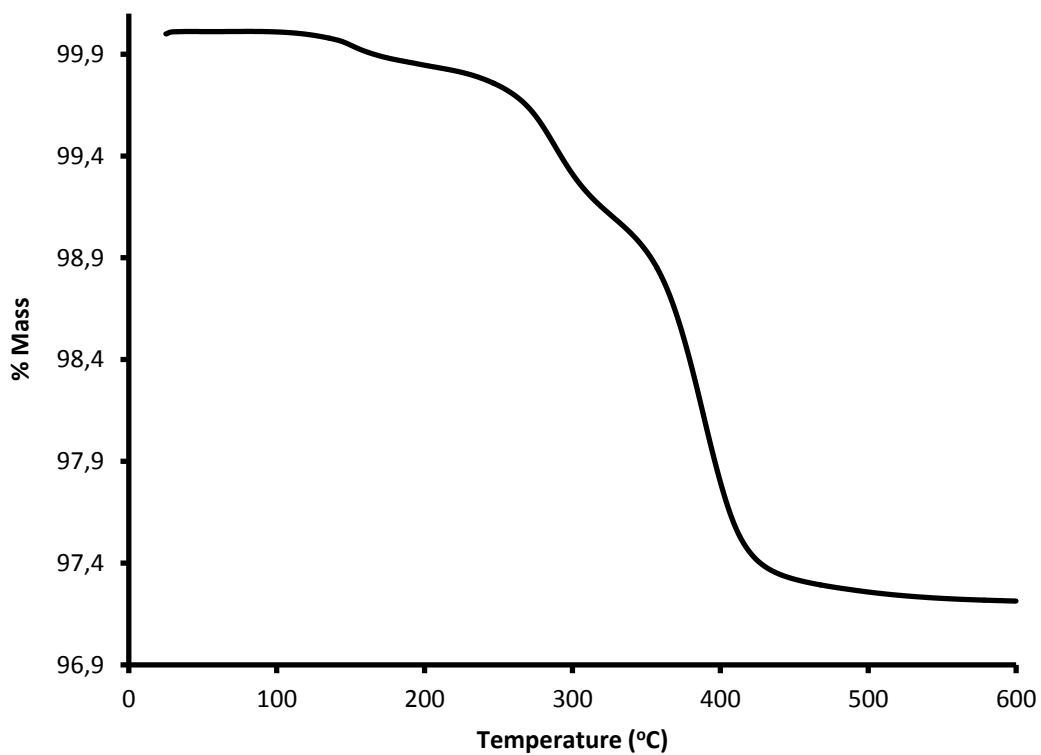


Figure A.58 : Thermogravigram of polymer **3.22** taken under an atmosphere of nitrogen at a scan rate = 10 °C/min after exposing to KCl.

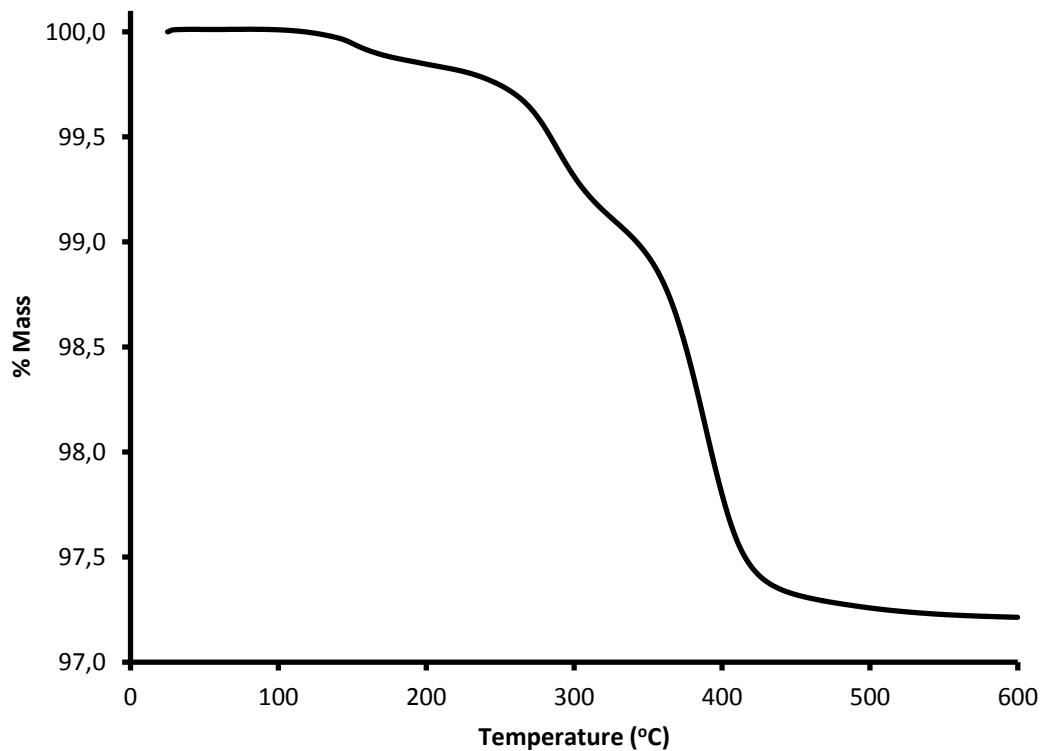


Figure A.59 : Thermogravigram of polymer **3.22** taken under an atmosphere of nitrogen at a scan rate = 10 °C/min after exposing to KF.

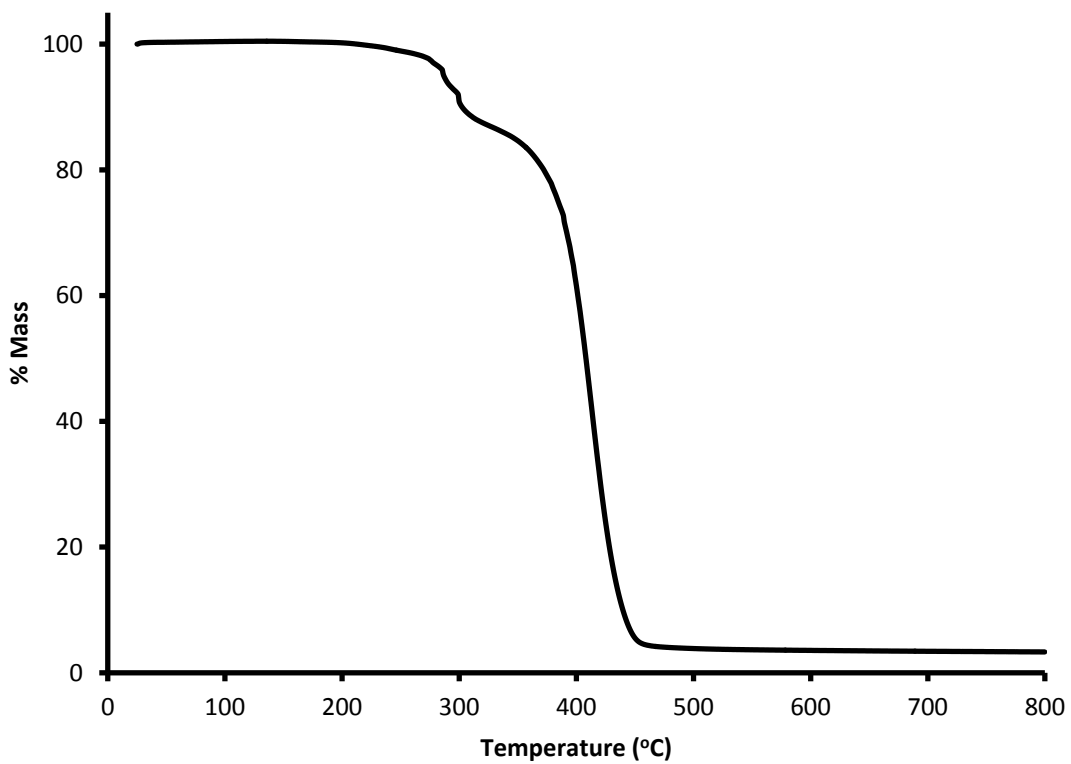


Figure A.60 : Thermogravigram of polymer **3.23** taken under an atmosphere of nitrogen at a scan rate = 10 °C/min.

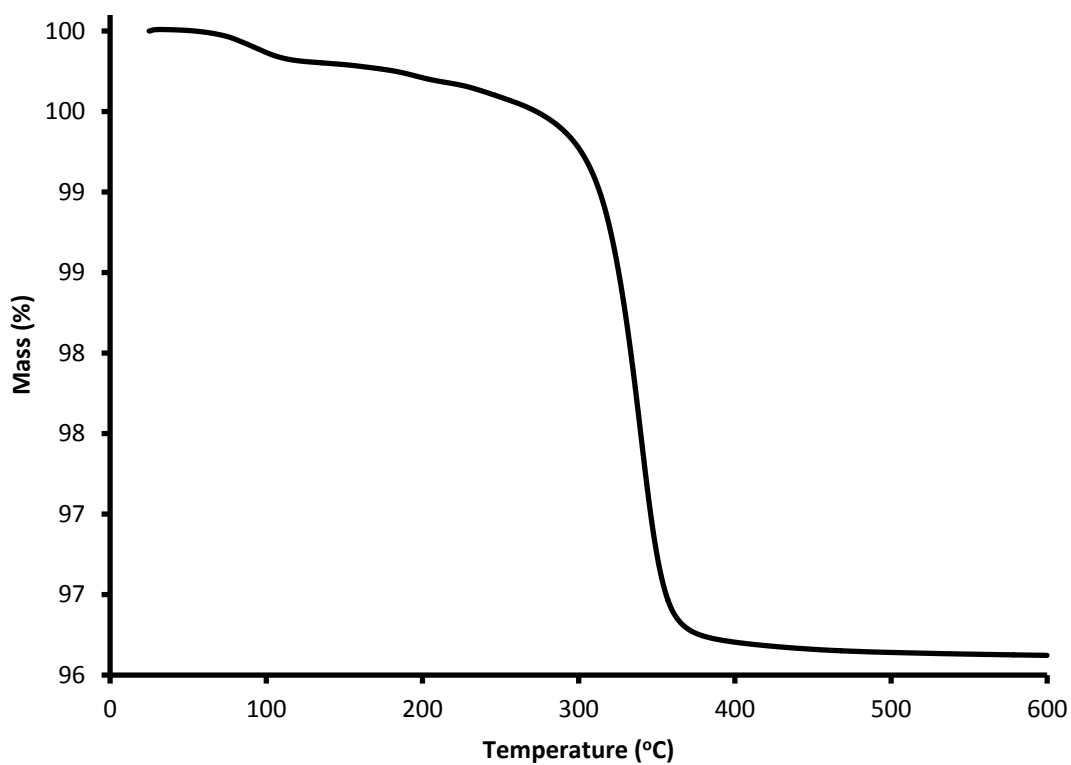


Figure A.61 : Thermogravigram of polymer **3.23** taken under an atmosphere of nitrogen at a scan rate = 10 °C/min after exposing to KCl.

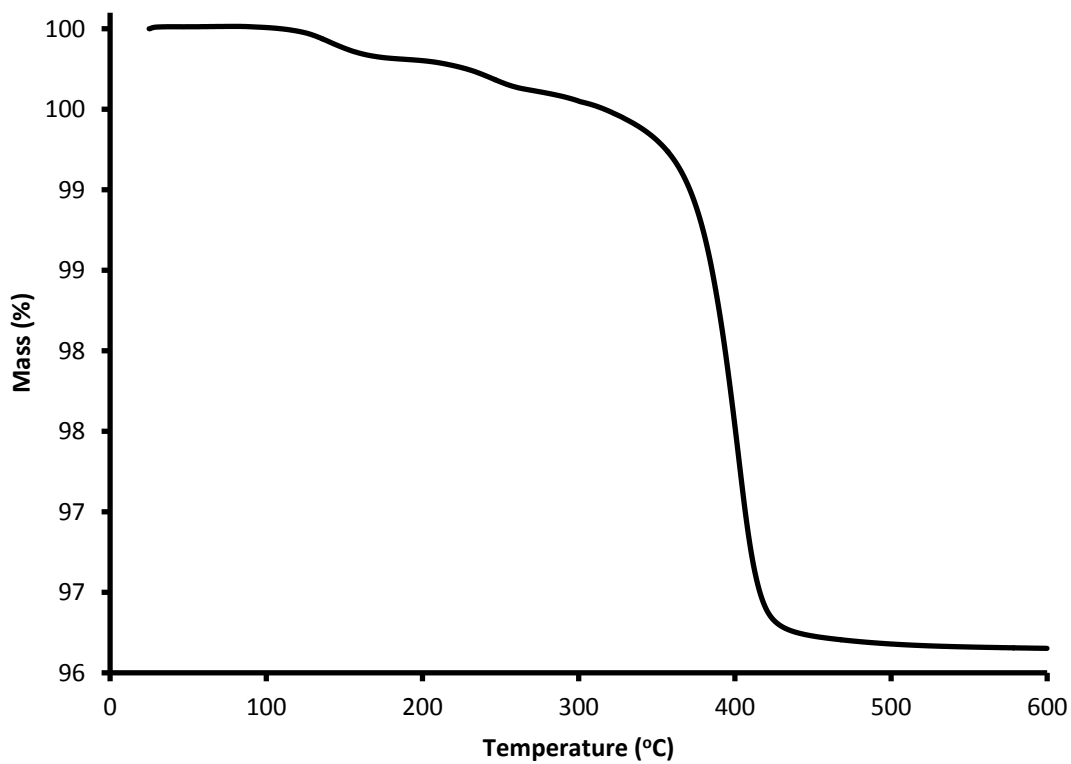


Figure A.62 : Thermogravivogram of polymer **3.23** taken under an atmosphere of nitrogen at a scan rate = 10 °C/min after exposing to KF.

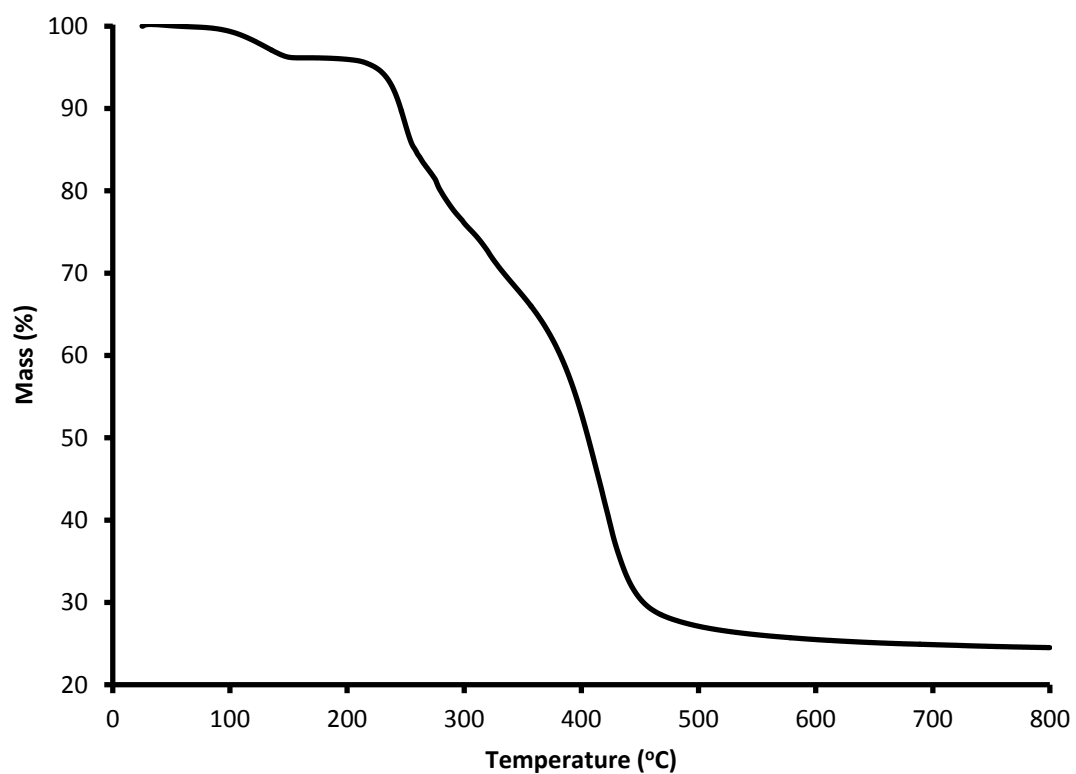


Figure A.63 : Thermogravigram of polymer **3.24** taken under an atmosphere of nitrogen at a scan rate = 10 °C/min.

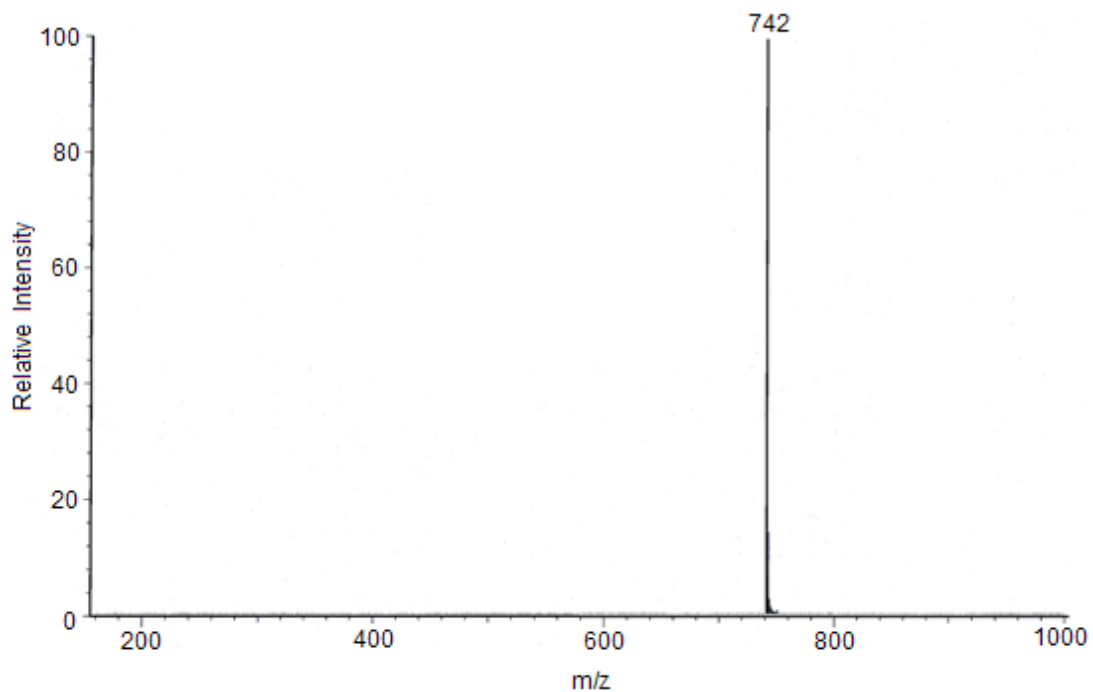


Figure A.64 : FAB-MS spectrum of **3.16**.

CURRICULUM VITAE



Name Surname : Abdullah Aydoğan
Place and Date of Birth : NIĞDE / 01.03.1978
Address : Istanbul Technical University, Faculty of Science
and Letters, Department of Chemistry, Maslak,
Istanbul/TURKEY
BC Degree : ITU, Chemistry Department, 2000
MSc Degree : ITU, Chemistry Department, 2003

Publications:

- **Akar, A.; Aydoğan, A.**, 2005. Synthesis of Meso-Tetra Acid and Ester Functionalized Calix[4]Pyrroles, *J. Heterocycl. Chem.*, **42**, (5), 931-934.
- **Aydoğan, A.; Coady, D. J.; Kim, S. K.; Akar, A.; Bielawski, C. W.; Marquez, M.; Sessler, J. L.**, 2008. Poly(Methyl Methacrylate)S with Pendant Calixpyrroles and Crown Ethers: Polymeric Extractants for Potassium Halides, *Angew. Chem., Int. Ed.*, **47**, (50), 9648-9652.
- **Aydoğan, A.; Coady, D. J.; Lynch, V. M.; Akar, A.; Marquez, M.; Bielawski, C. W.; Sessler, J. L.**, 2008. Poly(Methyl Methacrylate)S with Pendant Calixpyrroles: Polymeric Extractants for Halide Anion Salts, *Chem. Commun. (Cambridge, U. K.)*, (12), 1455-1457.
- **Aydoğan, A.; Akar, A.**, 2009. 5,10,10,15,20,20-Hexamethylcalix[4]Pyrrole 5,15-Diethyl Diester, *Acta Crystallogr., Sect. E: Struct. Rep. Online*, **E65**, (12), o3157.
- **Rambo, B. M.; Bill, N. L.; Aydoğan, A.; Coady, D. J.; Kim, D.-S.; Bielawski, C. W.; Sessler, J. L.** In *Polymeric Systems Containing Macrocyclic Structures for the Extraction of Ionic Species from Aqueous Environments*, 2009; American Chemical Society: 2009; pp PMSE-392.
- **Rambo, B. M.; Bill, N. L.; Aydoğan, A.; Coady, D. J.; Kim, D.-S.; Bielawski, C. W.; Sessler, J. L.**, 2009. Polymeric Systems Containing Macrocyclic Structures for the Extraction of Ionic Species from Aqueous Environments, *PMSE Prepr.*, **100**, 441-442.
- **Sessler, J. L.; Bielawski, C. W.; Aydoğan, A.; Coady, D. J.**, Polymers Functionalized with Ion-Specific Recognition Elements, 2010, U.S. Patent Application, US 2010 129308 A1 20100527

